Sumoylation activates the transcriptional activity of Pax-6, an important transcription factor for eye and brain development

Qin Yan[a,1,2], Lili Gong[a,1], Mi Deng[a,1], Lan Zhang[b,1], Shuming Sun[a,b], Jiao Liu[a,b], Haili Ma[a], Dan Yuan[a], Pei-Chao Chen[b], Xiaohui Hu[b], Jinping Liu[a], Jichao Qin[a,3], Ling Xiao[a,b], Xiao-Qin Huang[c], Jian Zhang[b], and David Wan-Cheng Li[a,b,d,4]

Departments of [a]Biochemistry and Molecular Biology and [d]Ophthalmology and Visual Sciences, University of Nebraska Medical Center, Omaha, NE 68198; [b]Key Laboratory of Protein Chemistry and Developmental Biology of Education Ministry of China, College of Life Sciences, Hunan Normal University, Changsha, Hunan 410081, China; and [c]Biomedicine Engineering Center, Hunan University, Changsha, Hunan 410081, China

Edited* by Michael Karin, University of California, San Diego School of Medicine, La Jolla, CA, and approved October 20, 2010 (received for review June 3, 2010)

Pax-6 is an evolutionarily conserved transcription factor regulating brain and eye development. Four Pax-6 isoforms have been reported previously. Although the longer Pax-6 isoforms (p46 and p48) bear two DNA-binding domains, the paired domain (PD) and the homeodomain (HD), the shorter Pax-6 isoform p32 contains only the HD for DNA binding. Although a third domain, the proline-, serine- and threonine-enriched activation (PST) domain, in the C termini of all Pax-6 isoforms mediates their transcriptional modulation via phosphorylation, how p32 Pax-6 could regulate target genes remains to be elucidated. In the present study, we show that sumoylation at K91 is required for p32 Pax-6 to bind to a HD-specific site and regulate expression of target genes. First, in vitro-synthesized p32 Pax-6 alone cannot bind the P3 sequence, which contains the HD recognition site, unless it is preincubated with nuclear extracts precleared by anti–Pax-6 but not by anti-small ubiquitin-related modifier 1 (anti-SUMO1) antibody. Second, in vitro-synthesized p32 Pax-6 can be sumoylated by SUMO1, and the sumoylated p32 Pax-6 then can bind to the P3 sequence. Third, Pax-6 and SUMO1 are colocalized in the embryonic optic and lens vesicles and can be coimmunoprecipitated. Finally, SUMO1-conjugated p32 Pax-6 exists in both the nucleus and cytoplasm, and sumoylation significantly enhances the DNA-binding ability of p32 Pax-6 and positively regulates gene expression. Together, our results demonstrate that sumoylation activates p32 Pax-6 in both DNA-binding and transcriptional activities. In addition, our studies demonstrate that p32 and p46 Pax-6 possess differential DNA-binding and regulatory activities.

retina | lens | cataract | small eye mutation | pancreas

Pax-6 belongs to the Pax transcription factor family, which contains nine members that share a conserved paired domain (PD) and a homeodomain (HD) (1, 2). This evolutionarily conserved transcription factor acts high in the regulatory hierarchy, controlling eye and brain development in humans, mice, zebrafish, and *Drosophila* (1–6). The highly conserved amino acid sequence of Pax-6 proteins in different species suggests its critical function in regulating development of these organisms. Indeed, targeted expression of Pax-6 from a general promoter in *Drosophila* induces formation of ectopic compound eyes (7). Furthermore, haploinsufficiency or deletion of the Pax-6 gene causes many ocular diseases including aniridia, cataracts, and glaucoma. A homozygous mutation in Pax-6 is lethal at birth, with severe brain defects and absence of eyes and nose in humans and mice (4, 5).

At the molecular level, Pax-6 functions primarily to mediate the commitment of the ectoderm above the optic vesicle into the lens ectoderm and also to promote formation of the lens vesicle (6). Pax-6 controls transcriptional expression of genes encoding both transcription factors responsible for lens development, such as musculoaponeurotic fibrosarcoma (*L-maf*), SRY-box containing gene 1 (*Sox-1*), prospero homeobox 1 (*Prox-1*), and also lens structural proteins, such as α-, β-, and γ-crystallins (8–11). Previous studies have demonstrated the presence of at least four forms of Pax-6 in quail cellular extracts with molecular masses of 48, 46, 43, and 32 kDa, which were named "p48," "p46," "p43," and "p32," respectively (12). These isoforms vary from each other in their N-terminal structures. The common p46 isoform has a 128-amino acid PD at the N terminus and a 56-amino acid HD in the central region which bind specifically to different DNA sequences, P6CON and P3 (TAAT/ATTA), respectively (12–14). At the C terminus, a conserved domain rich in proline (P), serine (S), and threonine (T) residues exists in all Pax-6 isoforms and thus is named the "PST" domain (Fig. S1*A*). This domain mediates activation of Pax-6 through phosphorylation by p38 MAP kinase and homeodomain-interacting protein kinase 2 (15, 16). Several phosphorylation sites have been identified in the PST domain of human and zebrafish Pax-6. Our recent studies have shown that both p32 and p46 Pax-6 isoforms are subjected to negative regulation by protein serine/threonine phosphatase-1 (PP-1) in vitro and in vivo (17). However, the obvious absence of a PD domain in the N terminus might endow p32 Pax-6 with a DNA-binding specificity different from that of p46 Pax-6; hence, it may modulate different downstream genes. In this investigation, we have explored how p32 Pax-6 can bind to the HD-specific P3 sequence and exert its regulatory function.

The small ubiquitin-related modifier (SUMO) family of proteins is an important class of ubiquitin-like proteins that share a common ancestry, structural fold, and a core conjugation pathway but have distinct sequences and functional properties (18, 19). SUMO is structurally related to ubiquitin and also is ligated to lysine residues within its target proteins. In sumoylation, the target lysine generally falls within a recognizable consensus, namely ψ-Lys-X-Glu/Asp (where ψ is a large hydrophobic amino acid, most commonly isoleucine or valine, and X is any residue). The enzymatic machinery that adds and removes SUMO includes SUMO E1-activating enzyme AOS1/UBA2, SUMO E2 conjugation enzyme UBC9, and SUMO E3 ligase (18, 19). Sumoylation of target proteins is implicated in protein–protein interactions, subcellular localization, protein–DNA interactions, transcriptional activation and repression, and enzyme activity (18, 19). Three SUMO family members, SUMO1, -2, and -3, have been identified

Author contributions: Q.Y., L.G., M.D., L.Z., and D.W.-C.L. designed research; Q.Y., L.G., M.D., L.Z., S.S., J.L., H.M., D.Y., P.-C.C., X.H., J.L., J.Q., L.X., and X.-Q.H. performed research; J.Z. contributed new reagents/analytic tools; Q.Y., L.G., M.D., L.Z., S.S., J.L., H.M., D.Y., P.-C.C., X.H., J.L., J.Q., L.X., X.-Q.H., J.Z., and D.W.-C.L. analyzed data; and D.W.-C.L. wrote the paper.

The authors declare no conflict of interest.

*This Direct Submission article had a prearranged editor.

[1]Q.Y., L.G., M.D., and L.Z. contributed equally to this work.

[2]Present Address: Department of Pathology and Laboratory Medicine, School of Medicine, University of Pennsylvania, Philadelphia, PA 19104.

[3]Present address: Department of Surgery, Tongji Medical College, Huazhong University of Science and Technology, Wuhan, Hubei 430030, China.

[4]To whom correspondence should be addressed. E-mail: dwli1688@hotmail.com.

This article contains supporting information online at www.pnas.org/lookup/suppl/doi:10.1073/pnas.1007866107/-/DCSupplemental.

in mammals. Like ubiquitin, SUMO2 and SUMO3 can form polymeric chains. In contrast, SUMO1 is a 97-amino acid polypeptide of 11.5 kDa that is covalently monoconjugated to proteins at lysine residues, thereby playing a critical role in many cellular processes, as mentioned earlier, through rapidly reversible changes in sumoylation status (18, 19).

In the present study, we provide evidence showing that sumoylation acts as a posttranslational modification that activates p32 Pax-6 and that sumoylated p32 Pax-6 positively regulates expression of the target genes. Moreover, we demonstrate that sumoylation of p32 Pax-6 occurs in vivo mainly at embryonic day (ED) 9.5 and ED 11.5, possibly playing an important role in controlling eye and brain development of vertebrates. Finally, we show that the p32 and p46 Pax-6 isoforms display differential DNA-binding and regulatory activities and thus can regulate different downstream target genes.

Results

Various Pax-6 Isoforms Are Present in Mouse Eye Tissues and Human Ocular Cell Lines. Previous studies have shown that four different Pax-6 isoforms (p48, p46, p43, and p32) are present in quail (12) (Fig. S1*A*). To determine if these Pax-6 isoforms are also present in mammals, we examined their expression in developing and adult mouse eyes and human ocular cell lines with three different antibodies (Fig. S1*B*). The eye tissues of newborn mice contain all four Pax-6 isoforms (Fig. 1*A*). Although p46 and p32 Pax-6 are the major isoforms, a considerable amount of p48 was detected also. Among the four isoforms, p43 was the least abundant and was detectable only in the immunoprecipitated Pax-6 mixture (Fig. 1*A*). RT-PCR revealed that p43 in mice and humans was not derived from alternative splicing (Fig. S2). In eye tissues from adult mice, significant amounts of p46 and p32 Pax-6 were present in the retina and cornea (Fig. S1*C*). In contrast, a much reduced level of p43 was observed in these tissues. In the lens epithelium, p46 Pax-6 was relatively abundant, but p32 and p43 Pax-6 isoforms were barely detectable (Fig. S1*C*). A thorough analysis of Pax-6 in four human ocular cell lines (20, 21) revealed that p46, p43, and p32 were all present in these cells (Fig. S1*D*).

Among different eye tissues and cell lines, p32 and p46 Pax-6 are the two major Pax-6 isoforms. Therefore, we tested the transcriptional activities of these two isoforms on the αB-crystallin promoter (−427 to +44) containing four copies of Pax-6 binding sites (22). As shown in Fig. 1*B*, both p32 and p46 displayed significant amounts of transcriptional activity on the αB-crystallin gene promoter.

In Vitro-Translated Pax-6 Proteins Lack P3 Recognition Ability. Next, we studied the DNA-binding activities of p46 and p32 Pax-6. To do so, we synthesized wild-type p32 and p46 using a cell-free system (Fig. 1*C*). In addition, to examine whether phosphorylation at the five identified sites (Fig. S1*E*) modulates the DNA-binding ability of the two major Pax-6 isoforms, we also synthesized p32-5A and p46-5A Pax-6 (mimicking constant dephosphorylation) and p32-5D and p46-5D Pax-6 (mimicking constant phosphorylation) (Fig. 1*C*, *Upper*). Western blot analysis revealed that the wild-type and mutant proteins displayed some differences in their electrophoretic mobility (Fig. 1*C*, *Lower*). In addition, two bands (p46 and p32) were always generated when the cDNA encoding p46 Pax-6 was translated (Fig. 1*C*). Subsequently, we tested the DNA-binding activities of the two major Pax-6 isoforms, in either wild-type or mutated status, using EMSA. Nuclear extracts from fetal human lens epithelial (FHL-124) cells, telomerase-transfected human lens epithelial (T-HLE) cells, and human lens epithelial (HLE) cells were included for comparison. As shown in Fig. 1*D*, although the nuclear extracts bound the P3 sequence, presumably because of the presence of endogenous Pax-6, none of the in vitro-synthesized proteins displayed P3-binding activity. This result suggests that in vitro-synthesized Pax-6 needs to be modified further to recognize the P3 sequence. Because neither 5A nor 5D displayed P3-binding activity, the modification is unlikely to be a result of phosphorylation or dephosphorylation.

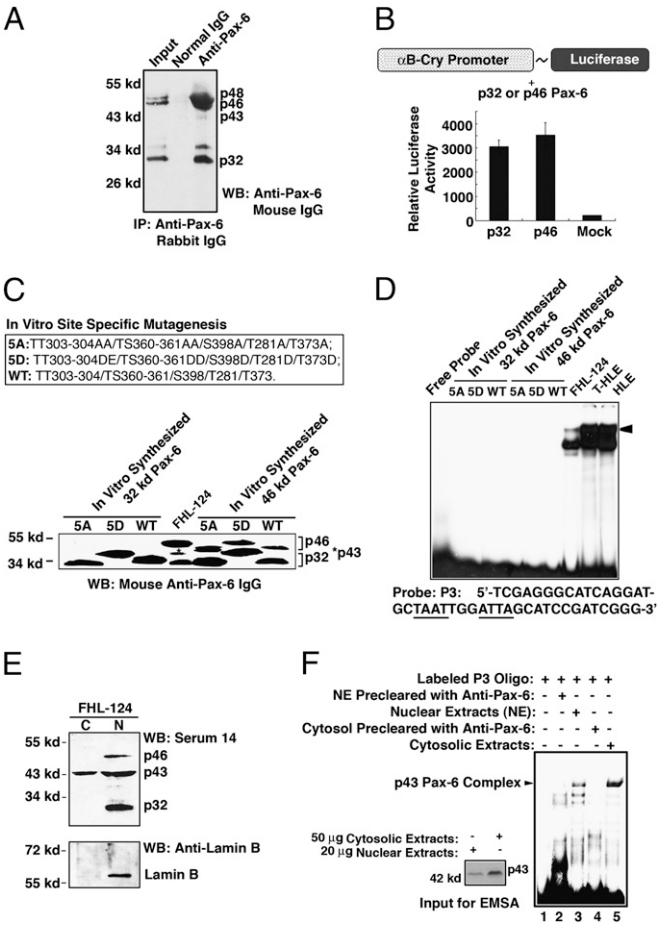

Fig. 1. Detection of four Pax-6 isoforms and exploration of DNA-binding and transcriptional activities of p32 and p46 Pax-6. (*A*) Detection of different Pax-6 isoforms in newborn mouse eyes. Note that p46 and p32 are present in relatively high levels. In contrast, p43 is much reduced. (*B*) Both p46 and p32 Pax-6 isoforms positively regulate the expression of αB-crystallin as tested in FHL-124 cells. (*C*) (*Upper*) In vitro site-specific mutagenesis-generated mutants mimicking constant dephosphorylation (5A) or phosphorylation (5D) in human Pax-6 (WT). (*Lower*) Western blot analysis of in vitro-generated mutant or wild-type p32 and p46 Pax-6 proteins; note their differential electrophoretic mobilities. In addition, the mutant and wild-type 46-kDa Pax-6 plasmids generate both p46 and p32 because of the activation of an internal ATG initiator. (*D*) In vitro-synthesized p32 and p46 Pax-6 cannot bind to the P3 sequence. In contrast, nuclear extracts from HLE cells and the P3 sequence form three DNA–protein interacting complexes. The arrowhead designates the complex derived from Pax-6 and the P3 sequence (see legend of Fig. 2 for explanation). (*E*) Western blot analysis of different Pax-6 isoforms in cytosolic (C) and nuclear (N) extracts of FHL-124 cells. (*F*) EMSA demonstrating that p43 Pax-6 from FHL-124 cytosol and the P3 sequence form a strong interacting complex. The relative amounts of nuclear and cytosolic p43 Pax-6 are shown in the Western blot.

The Cellular 43-kDa Pax-6 Isoform Can Bind to the P3 Sequence. To understand the binding patterns exhibited by the nuclear extracts of HLE cells and to explore what kind of modification is necessary for binding to the P3 sequence, we further examined the Pax-6 expression profile in the nucleus and cytoplasm of FHL-124 cells. As shown in Fig. 1*E*, although FHL-124 nuclear extracts contained three Pax-6 isoforms, p46, p43, and p32, the cytoplasm contained only a single isoform, p43. When we conducted EMSA with nuclear extracts of FHL-124 cells and the P3 sequence (Fig. S3*A*), three DNA–protein complexes were detected (Fig. S3*B*, lane 2). Furthermore, when mouse Pax-6 antibody was used to remove the endogenous Pax-6 from FHL-124 nuclear extracts, the only band depleted was the one with the slowest mobility and weakest P3

binding (Fig. S3*B*, lane 3). These experiments suggest that the other two complexes were derived from non–Pax-6 proteins.

To identify which Pax-6 isoform was responsible for binding to the P3 sequence, we conducted EMSA using cytosolic extracts of FHL-124 cells. As shown in lane 5 of Fig. 1*F*, the p43 Pax-6 in the FHL-124 cytosol exhibited strong binding to the P3 sequence. This complex displayed similar mobility to that of the top complex formed by the nuclear extracts and the P3 sequence (compare lane 3 and lane 5, Fig. 1*F*), which was inhibited by preclearing with the mouse anti–Pax-6 antibody (Fig. 1*F*, lane 2). Together, these experiments strongly suggest that p43 Pax-6 is responsible for binding to the P3 sequence.

In Vitro-Translated p32 Pax-6 Binds to P3 After Preincubation with Pax-6–Depleted Nuclear Extracts. To further explore what kind of modification is necessary for the in vitro-synthesized Pax-6 to bind to the P3 sequence, we combined in vitro-translated wild-type p32 Pax-6 protein with Pax-6–depleted FHL-124 nuclear extracts. After incubation for 1 h at 30 °C, the mixture was analyzed by EMSA. As shown in lane 5 of Fig. 2*A*, the mixture exhibited a strong interaction with the P3 sequence, forming a DNA–protein complex with the same migration position as the complex formed by the FHL-124 nuclear extracts and the P3 sequence (Fig. 2*A*, lane 2). Thus, a modification of the in vitro-synthesized p32 Pax-6 by the Pax-6–depleted FHL124 nuclear extracts most likely conferred the ability to bind to the P3 sequence.

We then examined whether phosphorylation/dephosphorylation would modulate the binding of p32 Pax-6 to the P3 sequence using synthesized p32 mutant proteins mimicking constant dephosphorylation (5A) or constant phosphorylation (5D) (Figs. 1*C* and 2*B*) to conduct EMSA. As shown in Fig. 2*C*, after incubation with the Pax-6–depleted nuclear extracts, the 5A mutant demonstrated a reduced (27% less) P3-binding ability compared with wild-type (WT) p32 Pax-6. In contrast, the 5D mutant exhibited enhanced (63% more) P3-binding ability. As mentioned earlier (Fig. 1*D*), none of the in vitro-translated proteins could bind to the P3 sequence on their own. Thus, phosphorylation/dephosphorylation may further modulate binding to the P3 sequence after the proteins are modified and enabled to bind P3 by the nuclear extracts.

In Vitro-Translated p46 Pax-6 Cannot Bind to the P3 Sequence even After Mixing with the Pax-6–Depleted FHL124 Nuclear Extract. To test whether in vitro-generated p46 Pax-6 also can gain the ability to bind P3 after mixing with Pax-6–depleted FHL-124 nuclear extracts, we combined in vitro-translated p46 and p32 Pax-6 proteins with the Pax-6–depleted FHL-124 nuclear extracts. After incubation for 1 h at 30 °C, the mixture was analyzed by EMSA with the P3 sequence. As shown in lanes 2–4 of Fig. S3*C*, the mixture of p46 and p32 Pax-6 yielded a strong P3-binding complex after incubation with the Pax-6–depleted nuclear extracts. This complex migrated to a position similar to that of the top complex generated by the FHL-124 nuclear extracts and the P3 sequence (Fig. S3*C*, lane 6). This binding activity was inhibited by immunoprecipitation of the in vitro-translated protein with serum 14 but not serum 11 (Fig. 2*D*). As shown in Fig. 2*E*, serum 11 precipitated only p46, whereas serum 14 precipitation depleted both p46 and p32. Thus, only p32 can bind to the P3 sequence after incubation with the Pax-6–depleted nuclear extracts.

Sumoylation Converts p32 Pax-6 into p43 Pax-6 and Endows It with P3-Binding Ability. The fact that p43 Pax-6 from either the cytosol or the nucleus of FHL-124 cells can bind to P3 oligo, whereas p32

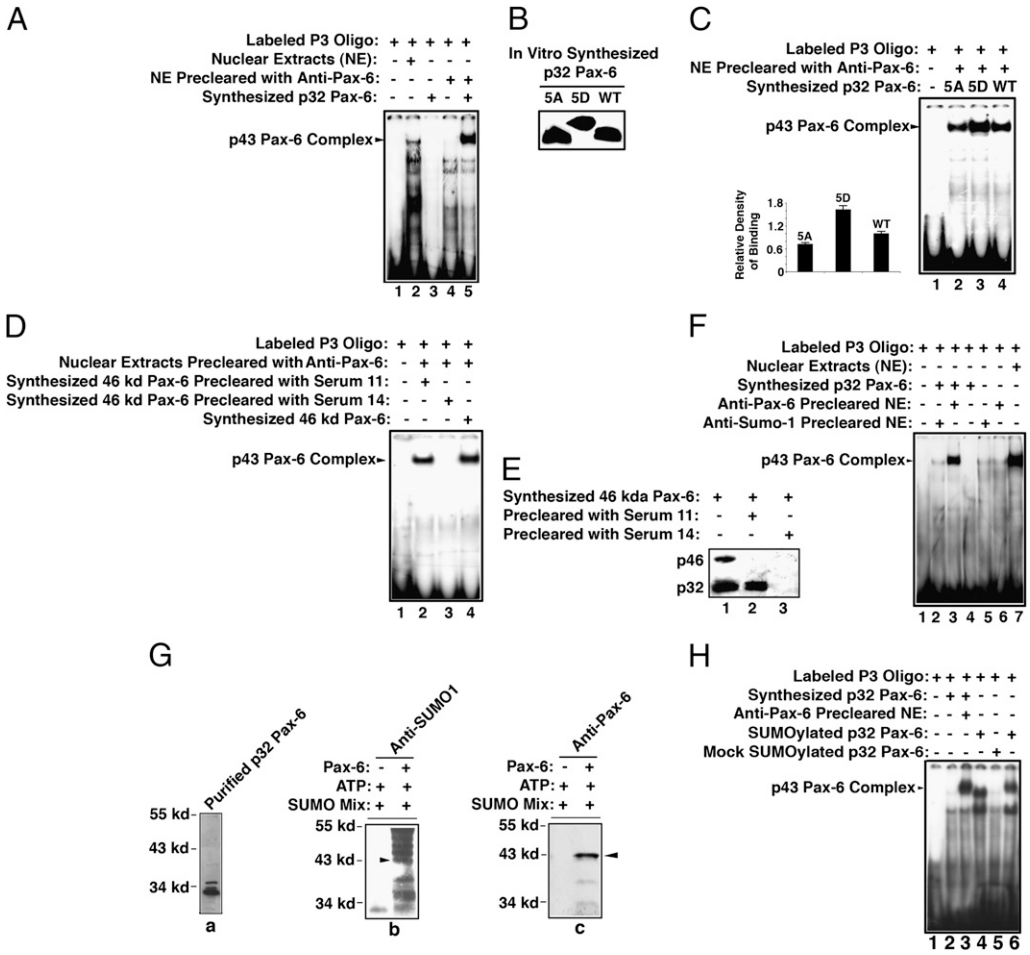

Fig. 2. Demonstration that sumoylation of the p32 Pax-6 activates its DNA-binding activity. (*A*) Gel mobility-shifting assay showing that in vitro-translated p32 Pax-6 can bind to the P3 sequence only after preincubation with Pax-6–depleted FHL-124 nuclear extract. (*B*) Western blot analysis indicating the amounts of in vitro-synthesized mutant and wild-type p32 Pax-6 used for EMSA described in *C*. (*C*) EMSA demonstrating that phosphorylation and dephosphorylation modulate DNA binding of p32 Pax-6 to the P3 sequence. (*D*) EMSA demonstrating that p32 but not p46 Pax-6 binds to the P3 sequence. (*E*) Western blot analysis of in vitro-synthesized p46 and p32 proteins from Pax-6 full-length cDNA without (lane 1) or with preclearance by serum 11 (lane 2) or by serum 14 (lane 3). (*F*) EMSA demonstrating that sumoylation is necessary for p32 Pax-6 to bind to the P3 sequence. (*G*) Demonstration that p32 Pax-6 can be sumoylated by SUMO1 in vitro. (*a*) The in vitro-generated GST–p32 Pax-6 fusion protein was purified by thrombin cleavage and GST column. (*b* and *c*) Purified p32 Pax-6 was subjected to sumoylation with a kit from Biomol (UW8955). After sumoylation, the reaction products were identified by anti-SUMO1 (*b*) or anti–Pax-6 antibodies (*c*). Arrowheads indicate p43 Pax-6. (*H*) EMSA demonstrating that sumoylation of p32 Pax-6 in vitro activates its DNA binding to the P3 sequence.

Pax-6 can bind to the P3 sequence only if it is preincubated with the Pax-6–depleted nuclear extract, suggests that p32 Pax-6 may be converted to p43 Pax-6 by the extract. Among different protein modifications, sumoylation could add a peptide of about 11 kDa to p32 Pax-6 and generate a 43-kDa Pax-6. To explore this possibility, we searched the putative SUMO acceptor sites in p32 Pax-6 and identified K91 as a putative site (Fig. S4*A*). Western blot analysis of the total FHL-124 proteins by anti-SUMO1 or anti–Pax-6 antibodies identified the same 43-kDa Pax-6 band (Fig. S4*B*). Moreover, the strong binding complex generated by in vitro-synthesized p32 and the P3 sequence in the presence of the Pax-6–depleted FHL124 nuclear extracts was diminished when the mixtures were precleared with a SUMO1 antibody (Fig. 2*F*, lane 2). Together, these results suggest that sumoylation converts p32 Pax-6 into p43 Pax-6 and endows p32 Pax-6 with P3-binding ability.

In Vitro-Synthesized p32 Pax-6 Can Be Sumoylated into p43 Pax-6. To confirm that p32 indeed can be sumoylated into p43 Pax-6, we conducted an in vitro sumoylation reaction with purified p32 Pax-6 (Fig. 2*Ga*). As shown in Fig. 2*G b* and *c*, the sumoylated mixture contained a 43-kDa protein, which was detected by both anti-SUMO1 (except for p43, other bands detected in Fig. 2*Gb* seem to be derived from oligomerization of SUMO1 itself; see ref. 23) and anti–Pax-6 antibodies, suggesting that sumoylation indeed converts p32 Pax-6 into p43 Pax-6. Next, we confirmed that sumoylated p32 can bind to the P3 sequence. As shown in lanes 4 and 6 of Fig. 2*H*, the in vitro-sumoylated p32 Pax-6 exhibited strong P3-binding activity, but the mock sumoylation without ATP did not yield any P3 binding (Fig. 2*H*, lane 5).

Sumoylation Enhances p32 Pax-6 DNA-Binding and Transcription Activities. To examine the importance of sumoylation of p32 Pax-6 by SUMO1, we conducted several lines of experiments. First, we tested if a mutation in the sumoylation site (K91R) would change its P3-binding ability. As shown in lanes 3 and 4 of Fig. 3*A*, compared with wild-type p32 Pax-6, the K91R mutation significantly reduced binding to the P3 sequence in the presence of the Pax-6–depleted nuclear extracts. The presence of some DNA binding in the K91R mutant p32 suggests the possible existence of other sumoylation sites. However, mutation of the only other putative sumoylation site, K110, had no effect on p32 Pax-6 DNA binding (Fig. 3*B*, lane 8). EMSA results with K91R p32 Pax-6 and P3 oligo alone also ruled out the possibility that the K91R mutation itself may activate its DNA binding (Fig. S5). Thus, the small amount of DNA binding by K91R could be from background, because it is not always present (Fig. S5), or from sumoylation in an unknown nonconsensus site. In addition, we found that the N terminus of p32 Pax-6 is necessary for its DNA binding (Fig. 3*B* and Fig. S5). Second, we explored sumoylated p32 regulation on the exogenous gene. Transfection of the wild-type p32 significantly increased the reporter gene activity driven by a minipromoter containing three copies of the P3 sequence (Fig. 3*C*). Cotransfection of SUMO1 further enhanced the reporter gene activity (Fig. 3*C*). In contrast, transfection of the K91R p32 without or with cotransfection of

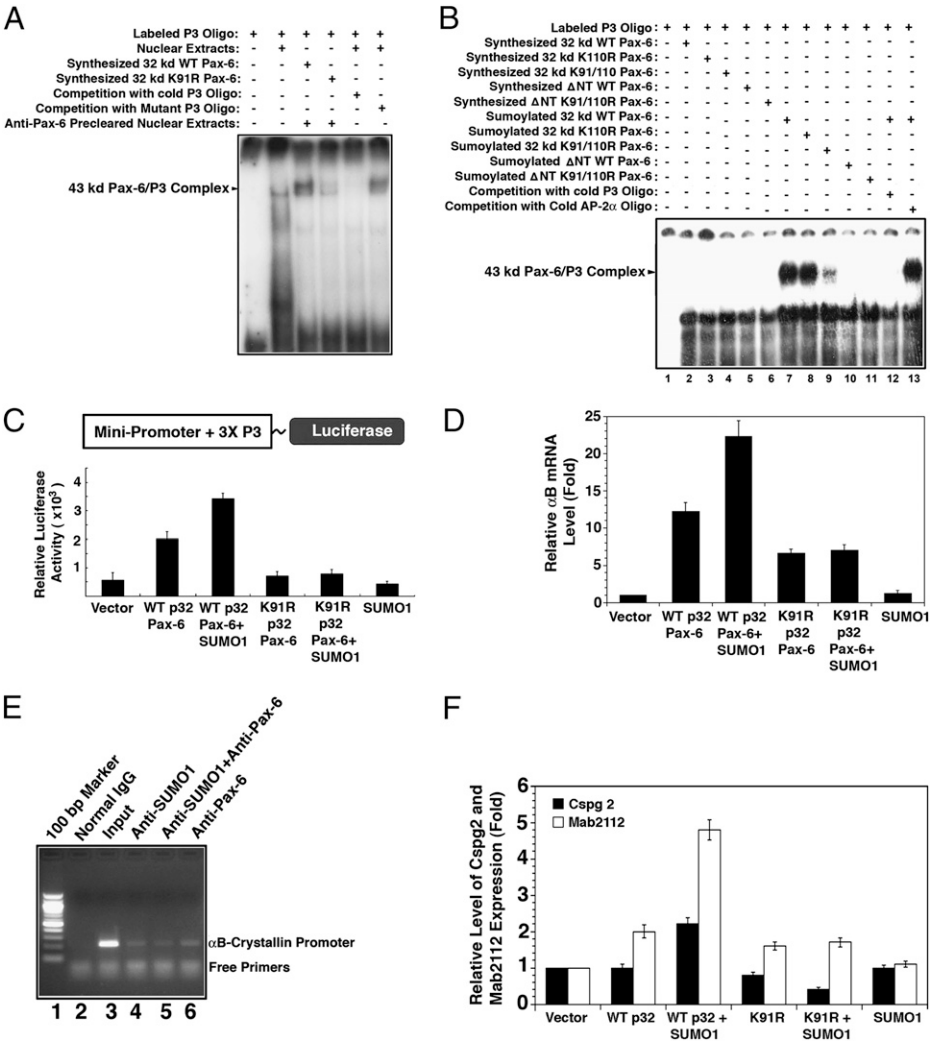

Fig. 3. Demonstration that sumoylation of p32 Pax-6 at K91 activates its DNA-binding and transcriptional activities. (*A*) EMSA showing that sumoylation at K91 activates p32 Pax-6 DNA-binding activity. (*B*) EMSA showing that deletion of the N terminus of p32 Pax-6 abolishes its DNA-binding activity (lanes 5 and 10). In contrast, mutation in the other putative sumoylation site, K110, has no effect on the DNA binding of p32 Pax-6 (lane 8). (*C*) Sumoylation of p32 Pax-6 activates its transactivity on the luciferase reporter gene as tested in FHL-124 cells. (*D*) Sumoylation of p32 Pax-6 up-regulates expression of the endogenous αB-crystallin gene in ARPE cells. ARPE-19 cells were transfected with vector alone or with wild-type or K91R p32 Pax-6 with or without SUMO1 as indicated. After 36 h, the transfected cells were harvested for preparation of total RNAs, which were used for quantitative real-time PCR as described in *Methods*. Note that αB-crystallin mRNA from vector-transfected cells is considered as 1.0. Transfection of wild-type p32 Pax-6 yielded a 12-fold increase in αB-crystallin mRNA expression. Cotransfection of the wild-type p32 Pax-6 with SUMO1 leads to an additional 11-fold enhancement of the αB-crystallin mRNA expression. The K91R mutant substantially decreased its transactivity. (*E*) ChIP assay demonstrating that Pax-6 sumoylated by SUMO1 binds directly to the αB-crystallin gene promoter in ARPE-19 cells. Lane 5 indicates ChIP result from sequential precipitations, first by anti-SUMO1 and then by anti–Pax-6 antibodies. (*F*) Sumoylation of p32 Pax-6 up-regulates expression of the endogenous *Cspg2* and *Mab2112* genes in αTN4-1 cells. αTN4-1 cells were transfected and processed as described in Fig. 3*D*. Cotransfection of the wild-type p32 Pax-6 with SUMO1 leads to a 2.2-fold enhancement of *Cspg2* mRNA expression and a 5.1-fold increase of *Mab2112* mRNA expression in αTN4-1 cells. The p32 K91R mutant substantially decreased its transactivity.

SUMO1 yielded only a weak increase in the reporter gene activity (Fig. 3*C*). Next, we cotransfected wild-type or K91R p32 with or without SUMO1 into human retinal pigment epithelial (ARPE-19) cells and measured the mRNA expression level of the endogenous αB-crystallin gene in the transfected cells using quantitative real-time PCR. As shown in Fig. 3*D*, transfection of the wild-type p32 Pax-6 into ARPE cells significantly increased the mRNA expression level of the αB-crystallin gene. Furthermore, cotransfection of SUMO1 cDNA with wild-type p32 Pax-6 cDNA led to further up-regulation of αB-crystallin mRNA. In contrast, mutation at K91 caused a substantial decrease in p32 Pax-6 transactivity. A ChIP assay further confirmed that sumoylated Pax-6 binds directly to the αB-crystallin gene promoter in ARPE-19 cells (Fig. 3*E*). Finally, we cotransfected wild-type or K91R p32 with or without SUMO1 into mouse lens αTN4-1 cells and measured the mRNA expression levels of two additional Pax-6 target genes, *Cspg2* and *Mab21l2*. Sumoylation of p32 Pax-6 significantly increased the mRNA expression levels of both genes. This up-regulation was largely inhibited in the cotransfection of K91R p32 with SUMO1 (Fig. 3*F*). Thus, sumoylation of K91 by SUMO1 within the DNA-binding domain (HD) significantly enhances both DNA-binding activity and transactivity of the p32 Pax-6.

SUMO1 and Pax-6 Are Colocalized in Embryonic Mouse Eyes. To confirm further that Pax-6 sumoylation takes place in vivo, we examined the expression of SUMO1 and Pax-6 in the embryonic eye from ED 9.5 to ED 19.5. As shown in Figs. S6 and S7, both SUMO1 and Pax-6 were expressed at ED 9.5, and their expression became much stronger at ED 11.5. At these two stages, colocalization of SUMO1 and Pax-6 was detected in neural tube (Fig. S7) and optic and lens vesicles (Fig. 4 *A* and *B*). Expression of both SUMO1 and Pax-6 was down-regulated by ED 12.5 (Figs. S6 and S7) and became significantly decreased from ED 14.5 to ED 18.5. At birth (ED 19.5), the SUMO1 signal was diminished (Figs. S6 and S7).

The observed colocalization reflects the specific interaction between p32 Pax-6 and SUMO1, because p43 Pax-6 was detected only in the cotransfected cells by wild-type p32 and SUMO1 but not with K91R p32 and SUMO1 (Fig. S8). This specific interaction also exists in vivo, as revealed by coimmunoprecipitation-linked Western blot analysis (Fig. 4 *C* and *D*). Together, our results demonstrated that during the early stages of mouse eye development, sumoylation activation of p32 Pax-6 occurs in vivo.

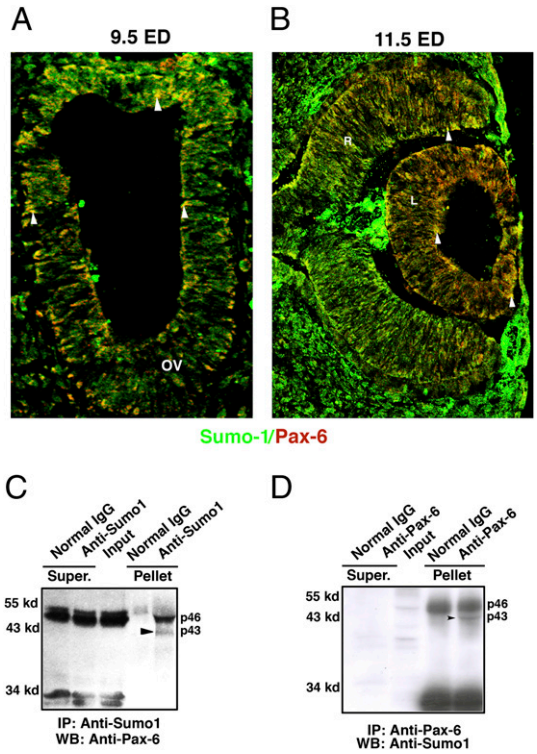

Fig. 4. Presence of p32 Pax-6 sumoylation in the developing mouse embryonic eye. (*A* and *B*) Immunohistochemistry analysis of Pax-6 and SUMO1 in the optic vesicle and lens vesicle of a mouse embryonic eye. Note that both Pax-6 and SUMO1 are clearly detected in the optical vesicle at ED 9.5 (*A*) and in the lens vesicle and retina tissues at ED 11.5 (*B*). In most cases, Pax-6 and SUMO1 overlap each other to generate the yellow fluorescence (arrowheads) (*C* and *D*) Total proteins were extracted from ED 11.5 embryonic eyes and were used for immunoprecipitation-linked Western blot analysis. Note that p43 Pax-6 (arrowhead in *C*) immunoprecipitated by anti-SUMO1 can be detected by anti–Pax-6 antibody. Similarly, p43 Pax-6 (arrowhead in *D*) immunoprecipitated by anti–Pax-6 can be detected by anti-SUMO1 antibody. L, lens; OV, optic vesicle; R, retina.

Discussion

Various Pax-6 Isoforms Are Generated Through Different Mechanisms of Gene Expression. The early results that quail cells contain four Pax-6 isoforms (12) are confirmed here in mice (Fig. 1*A* and Fig. S1*C*) and humans (Fig. S1*D*). The presence of various Pax-6 isoforms in different vertebrate species suggests the existence of common regulatory mechanisms for Pax-6 expression, which are essential to govern brain and eye development in these organisms.

Among the four different isoforms of Pax-6, p48 is derived from alternative splicing (24) with an additional 14 amino acids inserted into the PD. This insertion interrupts the N-subdomain (PAI) of the PD but leaves the C-subdomain (RED) of the PD intact (25). Thus, compared with p46 Pax-6, p48 Pax-6 is restricted in both DNA binding and regulation of downstream genes (26). Overexpression of p48 Pax-6 driven by a lens-specific promoter changes the gene-expression profile and leads to lens pathology (11). The p32 Pax-6 is derived from alternative translation of an internal ATG codon in full-length Pax-6 mRNA (12). Proteins generated through usage of the internal ATG codon have been observed in other genes, and such proteins sometimes act as repressors of the activities of full-length proteins (26). In the present study, we observed that p32 Pax-6 generated from an internal ATG codon of the full-length Pax-6 mRNA may or may not repress the full-length p46 Pax-6 function, depending on the target genes. Both p32 and p46 Pax-6 isoforms show positive regulation on the αB-crystallin gene (Fig. 1*B*). However, the two Pax-6 isoforms display differential controls on *Cspg2* and *Mab21l2*. In the Pax6$^{+/-}$ lens, the expression levels of *Cspg2* and *Mab21l2* are increased, suggesting that p46 Pax-6 represses these genes (27). In contrast, cotransfection of p32 Pax-6 and SUMO1 positively regulates their expression (Fig. 3*F*). Thus, p32 and p46 Pax-6 isoforms display differential regulations on the same target genes.

Our results also detected the presence of p43 Pax-6 in both newborn and adult mouse eyes. Where does p43 Pax-6 come from? In quail cells, one source for p43 Pax-6 is the alternative splicing (12). In mice and humans, however, we could not detect the alternative splicing products (Fig. S2). Thus, the origin of p43 Pax-6 must be different. In our study, we noticed that in eye tissue from both newborn and adult mice, p43 Pax-6 is present at a very low level (about 5% compared with the total p32), suggesting that its presence may be transitory. Indeed, our study reveals that p43 Pax-6 in mice and humans is derived from SUMO1-conjugated sumoylation of p32 Pax-6 (see discussion below). Thus, four different Pax-6 isoforms reflect differential expression mechanisms of the Pax-6 gene at transcriptional (p46), splicing (p48), translational (p32), and posttranslational (p43) levels.

Sumoylation of p32 Pax-6 Activates Its DNA-Binding and Transcriptional Activities. In the present study, we demonstrated that in vitro-synthesized p32 Pax-6, although containing the HD for DNA binding, cannot bind directly to the P3 sequence. This result is surprising, because the P3 sequence contains the conserved HD recognition site. Knowing that p43 Pax-6 is present at a very low level in newborn and adult mouse eye tissues and that the cytosolic p43 Pax-6 can bind to the P3 sequence, we predicted that in vitro-

synthesized p32 Pax-6 needs to be modified to bind to the P3 sequence. Indeed, when in vitro-synthesized p32 Pax-6 is mixed with Pax-6–depleted FHL-124 nuclear extracts, it displays strong binding affinity to the P3 sequence. However, when FHL-124 nuclear extracts are precleared with anti-SUMO1 antibody, in vitro-synthesized p32 Pax-6 loses the ability to bind to the P3 sequence. These results led us to conclude that p32 Pax-6 is sumoylated by SUMO1 before it can bind to the P3 sequence. Additional experiments further confirmed our conclusion. First, purified synthetic p32 from a cell-free system can be sumoylated in vitro with SUMO1, yielding a 43-kDa protein that can be recognized by anti-SUMO1 and anti–Pax-6 antibodies. Second, bioinformatics and in vitro mutagenesis identify K91 as a SUMO1 acceptor site, an analysis that is confirmed by EMSA and ex vivo functional assays. Finally, in the developing mouse embryo at ED 9.5 and ED 11.5, immunocytochemistry demonstrates the colocalization of endogenous SUMO1 and Pax-6. This result is confirmed further by the in vitro cotransfection study and in vivo immunoprecipitation-linked Western blot analysis, which identify the same p43 Pax-6 by anti-SUMO1 and mouse anti–Pax-6 antibody. Together, our data show that p32 Pax-6 is converted to p43 Pax-6 through sumoylation and elucidate the in vivo source of p43 Pax-6 in mice and humans.

Protein sumoylation, in addition to regulating many cellular processes (18, 19), seems to be especially important for the regulation of gene expression (28). Although most studies have revealed that sumoylation of various transcriptional factors leads to repression of gene expression (28), considerably less is known about sumoylation promoting transcription activation (29). In the present study, our results demonstrate that sumoylation of p32 Pax-6 at K91 activates its ability to bind to the P3 sequence, which contains the HD recognition site. How could sumoylation activate the DNA-binding activity of p32 Pax-6? It is possible that sumoylation may remove the intramolecular inhibition on the HD domain. However, our finding that deletion of the N terminus abolishes its DNA binding (Fig. 3*B* and Fig. S5) rules out this possibility. Alternatively, sumoylation may stabilize p32 Pax-6 in a configuration favoring DNA binding. In any case, the N terminus of the p32 Pax-6 is essential for sumoylation-activated DNA binding.

Our results also show that sumoylation of p32 Pax-6 enhances its transactivity to regulate the expression of either the exogenous or the endogenous genes. ChIP assay reveals that the sumoylated p32 Pax-6 can bind directly to the target gene promoter. Our results are consistent with several recent studies that found that sumoylation activates other transcription factors (29, 30). Because chondroitin sulfate proteoglycan 2 (*Cspg2*), Mab-21-like-2 (*Mab2112*), and αB-crystallin are actively involved in cell proliferation or differentiation, regulation of these genes by the sumoylated p32 Pax-6 likely produces profound effects on early brain and eye development. These effects are consistent with our observations that the interactions between SUMO1 and Pax-6 occur in mouse embryonic neural tube, optic vesicles, and lens vesicles (Fig. 4 and Figs. S6 and S7).

p46 Pax-6 contains the same homeodomain as p32 Pax-6. However, our results show that p46 Pax-6 cannot bind to the P3 sequence even after incubation with Pax-6–depleted FHL-124 nuclear extract. This result suggests several possibilities. First, the tertiary structure of p46 Pax-6 protein may prevent its homeodomain from being sumoylated. Alternatively, sumoylation of p46 Pax-6 may occur, but the presence of the PD in p46 Pax-6 may prevent its binding to the P3 sequence. In any case, our results reveal that p32 and p46 Pax-6 isoforms also display differential DNA-binding activities, and thus probably regulate different target genes.

Methods

Animals. Mice used in this study were handled in compliance with the *Guide for the Care and Use of Laboratory Animals* (National Academy Press, Washington, DC). Embryonic mice of different stages (ED 9.5 to ED 19.5), neonatal mice, and 4-wk-old adult mice were obtained from the University of Nebraska Medical Center breeding facility.

Other analytical methods used in this study are detailed in *SI Methods*. Oligo primers used in the generation of 5A and 5D mutants are listed in Table S1.

ACKNOWLEDGMENTS. We thank Dr. Joram Piatigorsky (National Eye Institute, Rockville, MD) for the αB-CAT construct, Dr. Anastassia Stoykova (Max-Planck-Institute for Biophysical Chemistry, Goettingen, Germany) for 5X P3 construct, Dr. Simon Saule (Institut Pasteur, Lillie, France) for sera 11 and 14, Dr. Venkat Reddy (University of Michigan, Ann Arbor, MI) for HLE cells, Dr. John Reddan (Oakland University, Rochester, MI) for FHL-124 cells, Dr. Melinda Duncan (University of Delaware, Newark, DE) for mouse Pax-6 cDNA, and Ms. Kari Nelson (University of Nebraska Medical Center, Omaha, NE) for critical reading of the manuscript. This work is supported in part by National Institutes of Health Grants 1R01 EY015765 and 1R01 EY018380 and by the Lotus Scholar Program.

1. Mansouri A, Hallonet M, Gruss P (1996) Pax genes and their roles in cell differentiation and development. *Curr Opin Cell Biol* 8:851–857.
2. Callaerts P, Halder G, Gehring WJ (1997) PAX-6 in development and evolution. *Annu Rev Neurosci* 20:483–532.
3. Ton CC, et al. (1991) Positional cloning and characterization of a paired box- and homeobox-containing gene from the aniridia region. *Cell* 67:1059–1074.
4. Glaser T, Walton DS, Maas RL (1992) Genomic structure, evolutionary conservation and aniridia mutations in the human PAX6 gene. *Nat Genet* 2:232–239.
5. Wilson D, Sheng G, Lecuit T, Dostatni N, Desplan C (1993) Cooperative dimerization of paired class homeo domains on DNA. *Genes Dev* 7:2120–2134.
6. Li HS, Yang JM, Jacobson RD, Pasko D, Sundin O (1994) Pax-6 is first expressed in a region of ectoderm anterior to the early neural plate: Implications for stepwise determination of the lens. *Dev Biol* 162:181–194.
7. Halder G, Callaerts P, Gehring WJ (1995) Induction of ectopic eyes by targeted expression of the eyeless gene in Drosophila. *Science* 267:1788–1792.
8. Cvekl A, Sax CM, Li X, McDermott JB, Piatigorsky J (1995) Pax-6 and lens-specific transcription of the chicken delta 1-crystallin gene. *Proc Natl Acad Sci USA* 92:4681–4685.
9. Chauhan BK, et al. (2002) Identification of genes downstream of Pax6 in the mouse lens using cDNA microarrays. *J Biol Chem* 277:11539–11548.
10. Richardson J, Cvekl A, Wistow G (1995) Pax-6 is essential for lens-specific expression of zeta-crystallin. *Proc Natl Acad Sci USA* 92:4676–4680.
11. Duncan MK, Kozmik Z, Cveklova K, Piatigorsky J, Cvekl A (2000) Overexpression of PAX6(5a) in lens fiber cells results in cataract and upregulation of (alpha)5(beta)1 integrin expression. *J Cell Sci* 113:3173–3185.
12. Carriere C, et al. (1993) Characterization of quail Pax-6 (Pax-QNR) proteins expressed in the neuroretina. *Mol Cell Biol* 13:7257–7266.
13. Epstein J, Cai J, Glaser T, Jepeal L, Maas R (1994) Identification of a Pax paired domain recognition sequence and evidence for DNA-dependent conformational changes. *J Biol Chem* 269:8355–8361.
14. Tuoc TC, Stoykova A (2008) Trim11 modulates the function of neurogenic transcription factor Pax6 through ubiquitin-proteosome system. *Genes Dev* 22:1972–1986.
15. Mikkola I, Bruun JA, Bjorkoy G, Holm T, Johansen T (1999) Phosphorylation of the transactivation domain of Pax6 by extracellular signal-regulated kinase and p38 mitogen-activated protein kinase. *J Biol Chem* 274:15115–15126.
16. Kim EA, et al. (2006) Phosphorylation and transactivation of Pax6 by homeodomain-interacting protein kinase 2. *J Biol Chem* 281:7489–7497.
17. Yan Q, et al. (2007) Protein phosphatase-1 modulates the function of Pax-6, a transcription factor controlling brain and eye development. *J Biol Chem* 282:13954–13965.
18. Johnson ES (2004) Protein modification by SUMO. *Annu Rev Biochem* 73:355–382.
19. Geiss-Friedlander R, Melchior F (2007) Concepts in sumoylation: A decade on. *Nat Rev Mol Cell Biol* 8:947–956.
20. Xiang H, et al. (2002) Human telomerase accelerates growth of lens epithelial cells through regulation of the genes mediating RB/E2F pathway. *Oncogene* 21:3784–3791.
21. Xiao L, et al. (2010) Protein phosphatase-1 regulates Akt1 signal transduction pathway to control gene expression, cell survival and differentiation. *Cell Death Differ* 17:1448–1462.
22. Dubin RA, Gopal-Srivastava R, Wawrousek EF, Piatigorsky J (1991) Expression of the murine α B-crystallin gene in lens and skeletal muscle: Identification of a muscle-preferred enhancer. *Mol Cell Biol* 11:4340–4349.
23. Pichler A, Gast A, Seeler JS, Dejean A, Melchior F (2002) The nucleoporin RanBP2 has SUMO1 E3 ligase activity. *Cell* 108:109–120.
24. Epstein JA, et al. (1994b) Two independent and interactive DNA-binding subdomains of the Pax6 paired domain are regulated by alternative splicing. *Genes Dev* 8: 2022–2034.
25. Kozmik Z, Czerny T, Busslinger M (1997) Alternatively spliced insertions in the paired domain restrict the DNA sequence specificity of Pax6 and Pax8. *EMBO J* 16:6793–6803.
26. Descombes P, Schibler U (1991) A liver-enriched transcriptional activator protein, LAP, and a transcriptional inhibitory protein, LIP, are translated from the same mRNA. *Cell* 67:569–579.
27. Yamada R, Mizutani-Koseki Y, Koseki H, Takahashi N (2004) Requirement for Mab21l2 during development of murine retina and ventral body wall. *Dev Biol* 274: 295–307.
28. Garcia-Dominguez M, Reyes JC (2009) SUMO association with repressor complexes, emerging routes for transcriptional control. *Biochim Biophys Acta* 1789:451–459.
29. Lyst MJ, Stancheva I (2007) A role for SUMO modification in transcriptional repression and activation. *Biochem Soc Trans* 35:1389–1392.
30. Cardone L, et al. (2005) Circadian clock control by SUMOylation of BMAL1. *Science* 309:1390–1394.

Author's personal copy

Biochimica et Biophysica Acta 1802 (2010) 621–631

Contents lists available at ScienceDirect

Biochimica et Biophysica Acta

journal homepage: www.elsevier.com/locate/bbadis

The small heat shock protein αA-crystallin is expressed in pancreas and acts as a negative regulator of carcinogenesis

Mi Deng [a,1], Pei-Chao Chen [b,1], Sisi Xie [b], Junqiong Zhao [b], Lili Gong [a], Jinping Liu [a], Lan Zhang [a,b], Shuming Sun [a,b], Jiao Liu [a,b], Haili Ma [a], Surinder K. Batra [a], David Wan-Cheng Li [a,b,c,*]

[a] Department of Biochemistry and Molecular Biology, University of Nebraska Medical Center, Omaha, NE 68198-5870, USA
[b] Key Laboratory of Protein Chemistry and Developmental Biology of National Education Ministry of China, College of Life Sciences, Hunan Normal University, Changsha, Hunan 410081, China
[c] Department of Ophthalmology and Visual Sciences, University of Nebraska Medical Center, Omaha, NE 68198-5870, USA

ARTICLE INFO

Article history:
Received 16 January 2010
Received in revised form 14 April 2010
Accepted 16 April 2010
Available online 29 April 2010

Keywords:
Small heat shock protein
αA
Pancreas
AP-1
Smad2/3/5
TGFβ
Pancreatic cancer
Cell migration
Lens

ABSTRACT

The small heat shock protein αA-crystallin is a structural protein in the ocular lens. In addition, recent studies have also revealed that it is a molecular chaperone, an autokinase and a strong anti-apoptotic regulator. Besides its lenticular distribution, a previous study demonstrates that a detectable level of αA-crystallin is found in other tissues including thymus and spleen. In the present study, we have re-examined the distribution of αA-crystallin in various normal human and mouse tissues and found that the normal pancreas expresses a moderate level of αA-crystallin. Moreover, αA-crystallin is found significantly downregulated in 60 cases of pancreatic carcinoma of different types than it is in 11 normal human pancreas samples. In addition, we demonstrate that αA-crystallin can enhance the activity of the activating protein-1 (AP-1) through modulating the function of the MAP kinase, and also upregulates components of TGFβ pathway. Finally, expression of αA-crystallin in a pancreatic cancer cell line, MiaPaCa, results in retarded cell migration. Together, these results suggest that αA-crystallin seems to negatively regulate pancreatic carcinogenesis.

© 2010 Elsevier B.V. All rights reserved.

1. Introduction

Heat shock proteins (HSPs) are implicated in multiple cellular functions including signaling transduction, protein degradation, survival promotion, exocytosis and endocytosis [1–5]. Recent studies have revealed that HSPs also play an important role in tumorigenesis [6–8]. The lens structural proteins, αA- and αB-crystallins are characterized as HSPs [9]. Besides their robust expression in mammalian lens [10,11], the two α-crystallins are also expressed in non-lenticular tissues. αB-crystallin is significantly expressed in the retina, muscle, heart and brain, and acts to prevent neural degradation, and heart failure, but promote carcinogenesis [4,5,12–15]. αA-crystallin is also expressed in some non-lenticular tissues, such as the retina, spleen and thymus [16]. However, the function of non-lenticular αA-crystallin remains unknown.

Pancreatic cancer in human poses clinical challenges in diagnosis and treatment [17,18]. Among the various types of pancreatic malignancies, pancreatic duct adenocarcinoma is dominant and in addition, the mucinous adenocarcinoma, islet adenocarcinoma and acinic cell carcinoma are also observed with less frequency of occurrence [19,20]. At the molecular level, development of pancreatic malignancies is associated with canonical oncogenes and tumor suppressor genes, such as Ki-Ras, p16, p53, Smad4 and BRCA2, which are involved in several cross-talking cellular signaling pathways including TGFβ/SMAD, PI3K/AKT, and MAPK pathways [20–22].

In the present study, we present evidence to show that αA-crystallin is expressed in the normal human and mouse pancreas at a moderate level. Moreover, analysis of αA-crystallin in the tissue samples from normal human pancreas and 60 cases of pancreatic carcinoma reveals significant difference. αA-crystallin is downregulated more than 10-fold in the pancreatic carcinoma of various types than that in normal pancreas. To explore the possible role of αA-crystallin in pancreatic carcinoma, we demonstrate here for the first time that αA-crystallin positively regulates the DNA binding and transactivity of the activating protein-1 (AP-1). This upregulation of AP-1 activity is derived from changed MAPK activity, which can positively regulate c-Jun and c-Fos. Moreover, expression of αA-crystallin in pancreatic cells enhances

* Corresponding author. Department of Biochemistry and Molecular Biology, University of Nebraska Medical Center, 985870 Nebraska Medical Center, Omaha, NE 68198-5870, USA. Tel.: +1 402 559 5073; fax: +1 402 559 6650.
E-mail address: dwli1688@hotmail.com (D.W.-C. Li).
[1] These authors made equal contribution.

0925-4439/$ – see front matter © 2010 Elsevier B.V. All rights reserved.
doi:10.1016/j.bbadis.2010.04.004

Author's personal copy

TGFβ signaling pathway. Finally, expression of αA-crystallin in pancreatic cancer cells leads to retarded cell migration. Together, these results suggest that αA-crystallin appears to suppress pancreatic carcinogenesis.

2. Materials and methods

2.1. Reagents and antibodies

Anti-αA/B-crystallin antibodies were described before [23]. ERK2 kinase assay kit, and anti-phosphorylated Elk antibody were purchased from Cell Signaling, Inc. Anti-c-Jun antibody was a kind gift from Dr. Tom Curran's Laboratory. Anti-c-Fos, anti-Lamin B, and anti-β-actin antibodies were purchased from Santa Cruz Biotechnology. Human normal pancreas and pancreatic carcinoma tissue samples were obtained from US Biomax, Inc.

2.2. Immunohistochemistry analysis of αA-crystallin, measure of fluorescence intensity and HE staining

Immunohistochemistry analysis was conducted as recently described [24]. Briefly, the sections were rehydrated in graded alcohols, heated up to boiling for 5 min in citrate buffer at pH 6. The sections were washed three times with PBS. For non-specific blocking, each section was incubated in 500 μl of 5% normal goat serum (Sigma-Aldrich, CA) in PBS for 1 h at room temperature and then incubated overnight in 400 μl of diluted anti-αA-crystallin antibody (1:100) in a humidified chamber at 4 °C. The sections were then washed with PBS three times (5 min each) followed by incubation with 400 μl of FITC-linked secondary antibody and DAPI (Vector Laboratories, CA) in blocking solution for 1 h in the absence of visible light. After incubation, sections were washed with PBS at room temperature 6 times (5 min each) and then observed under a Carl Zeiss Laser Scanning Confocal microscope. For negative controls, the sections were treated in the same way except that the primary antibody was replaced with normal serum IgG.

A quantitative measure of fluorescence intensity was conducted using confocal microscopy for assessment of the level of αA-crystallin expression. During analysis of the obtained results, the designated values of 0 to 10, 10 to 100, 100 to 1000 and more than 1000 represent negative background, weak, moderate and strong expression of αA-crystallin, respectively. The same immunohistochemical quantitative system was used for tissue microarray analysis by others [25]. Each core was measured individually. If more than one core was evaluated from each tissue the mean intensity and standard deviation were calculated and shown as mean ± SD.

For histology analysis, hematoxylin and eosin (HE) staining was conducted as recently described [26].

2.3. Cell culture and cell fraction extraction

The preparation of the pEGFP-C3 and pEGFP-C3-αA/αB-crystallin expression constructs, and establishment of stable transfected cell lines were conducted as previously described [23,24]. The pEGFP-αTN4-1, pEGFP-αA-αTN4-1, pEGFP-αB-αTN4-1, pEGFP-MiaPaCa, pEGFP-αA-MiaPaCa and pEGFP-αB-MiaPaCa stable clones were grown in Dulbecco's Modified Eagle's Minimal Essential Medium (DMEM) containing 10% fetal bovine serum, 50 U/ml penicillin and streptomycin and 400 μg/ml neomycin as described before [23,24]. All cells were kept at 37 °C and 5% CO_2 gas phase. Cell fractions were extracted by differential sucrose gradient as previously described [23]. The cytoplasmic and nuclear extracts of vector (pEGFP)-, αA-crystallin (pEGFP-αA)- or αB-crystallin (pEGFP-αB)-transfected cells were used for Western blot analysis. The nuclear extracts from parent, vector (pEGFP)-, αA-crystallin (pEGFP-αA)- or αB-crystallin (pEGFP-αB)-transfected cells were used for gel mobility shifting assays.

2.4. Reverse transcription-linked polymerase chain reaction (RT-PCR)

Total RNA samples were extracted from αA-crystallin-transfected cells (pEGFP-αA-MiaPaCa), αB-crystallin-transfected cells (pEGFP-αB-MiaPaCa), vector-transfected cells (pEGFP-MiaPaCa) and control parent pancreatic cancer cells (MiaPaCa) using TRIZOL reagent. Five μg of total RNA from each sample was used for cDNA synthesis. Several components of TGFβ signaling pathway were examined by RT-PCR using specific primer pairs listed in Table 1. The PCR reaction is: 94 °C for 5 min; 94 °C for 30 s, 55 °C for 30 s, and 72 °C for 40 s, in 30 cycles; 72 °C for 5 min; kept at 4 °C. The PCR products were examined by agarose gel electrophoresis and visualized under UV illumination.

2.5. Gel mobility shifting assay

Gel mobility shifting assays were conducted as previously described [27–29]. The following oligos were used: 5′-GTCCTTCATTACGTCACG-CATAG-3′ for conserved AP-1 binding site, 5′-GTCCTTCATTCATTCACG-CATAG-3′ for mutated AP-1 binding site; 20 μg of nuclear extracts or cytoplasmic extracts prepared from the pEGFP-αTN4-1, pEGFP-αA-αTN4-1, pEGFP-MiaPaCa, and pEGFP-αA-MiaPaCa cells was incubated with 1×10^5 cpm of ^{32}P-labeled double-stranded synthetic oligonucleotides for 30 min at 37 °C in binding shifting buffer [27–29]. For competition experiments, 50-fold of the non-labeled wild type or mutant double-stranded synthetic oligonucleotides was pre-incubated with the nuclear extracts for 30 min before the labeled probe was added into the reaction. For the pre-cleared experiments, 20 μg of nuclear extract prepared from pEGFP-αTN4-1, pEGFP-αA-αTN4-1, pEGFP-MiaPaCa, and pEGFP-αA-MiaPaCa cells was pre-incubated with 10 μg antibody against c-Jun or/and c-Fos for 1 h on ice, then mixed with protein A/G agarose and rotated for additional 1 h at 4 °C, and then the supernatant was recovered for incubation with 1×10^5 cpm of ^{32}P-labeled double-stranded synthetic AP-1 oligonucleotides for 30 min at 37 °C in a binding shifting buffer. After the binding reactions, the mixtures were loaded onto 6% native PAGE and detected by autoradiography.

2.6. Kinase activity assay

Substrate Elk protein was incubated with different doses of ERK2 kinase, 0.1, 1, 5 or 10 ng or mock kinase, GSK3β in the kinase buffer for 30 min at 37 °C in the presence of ATP. For the effect of αA-crystallin on ERK kinase, differential concentrations (0, 1 and 10 μg) of purified bovine αA-crystallin were added to the kinase assay reactions. After reaction, the mixtures were loaded to SDS-PAGE and detected by Western blot analysis using anti-phosphorylated-Elk antibody.

Table 1
Oligos used to detect expression of the related genes.

Gene	Primers
β-actin	5′-GTGGGGCGCCCCAGGCACCA-3′
	5′-CTCCTTAATGTCACGCACGATTTC-3′
αA-crystallin	5′-GGCTGTTCGACCAGTTTTTC-3′
	5′-CAGACAGGGAGCAAGAGAGG-3′
αB-crystallin	5′-TTCTTCGGAGAGCACCTGTT-3′
	5′-GCCAGAGACCTGTTTCCTTG-3′
TGFβ	5′-GGGACTATCCACCTGCAAGA-3′
	5′-CGGAGCTCTGATGTGTTGAA-3′
TGFβR1	5′-GAGCATGGATCCCTTTTTGA-3′
	5′-AACATCGTCGAGCAATTTCC-3′
TGFβR2	5′-GGGGAAACAATACTGGCTGA-3′
	5′-TCACACAGGCAGCAGGTTAG-3′
TGFβR3	5′-CAGTCCACATCCACCACAAG-3′
	5′-ACACACCCTTCTGCTGCTTT-3′

Author's personal copy

2.7. Western blot analysis

Preparation of total proteins from mouse tissues and various transfected cells and Western blot analysis of different protein samples were conducted as previously described [30–32].

2.8. Wound healing assay

The three types of stable clones of pEGFP-MiaPaCa, pEGFP-αA-MiaPaCa and pEGFP-αB-MiaPaCa cells were seeded in 6-well plates and cultured until 100% confluent. A straight scratch was made by using a 1 ml blue pipette tip to simulate the wound in each well. After PBS washing for 2 times, new DMEM medium was added for a continuous growth of another 48 h. The wound healing process was recorded daily using the Leica Inverted Phase Contrast Fluorescence Microscopy with a 10× objective.

2.9. Statistical analysis

The Student *t*-test was used to compare the medians of two unpaired groups. $p<0.05$ was considered significant [31].

3. Results

3.1. Expression of αA-crystallin in human non-lenticular tissues

Recent studies have shown that αB-crystallin is implicated in promotion of carcinogenesis [6,15,33]. Whether αA-crystallin has similar functions remains to be explored. For this reason, we have re-examined the tissue-specific expression of αA-crystallin in human non-lenticular tissues using immunohistochemistry analysis of human multi-organ tissue array samples and confocal microscope measurement of the relative fluorescence density derived from immunohistochemistry staining. As shown in Fig. 1A, a strong lenticular expression of αA-crystallin in the developing mouse eye was observed, which is consistent with a previously reported result [10]. In addition, we observed a moderate level of αA-crystallin expression in human pancreas and to a less degree, in human liver (Fig. 1A). Similar pancreatic level of αA-crystallin was observed in 7 out of 11 human samples examined (Fig. 1B). In pancreas, αA-crystallin was specifically expressed in islets, acinus and interlobular tubes (Fig. 1A). In other non-lenticular ocular tissues, αA-crystallin was also expressed at a moderate level in the retina and ciliary processes (data not shown). The relative mean values of fluorescence intensities in various non-lenticular tissues were measured with confocal microscope coupled with related software and were presented in Fig. 1B.

3.2. Expression of αA-crystallin in mouse tissues

To validate the observed results of αA-crystallin expression in human samples, we next dissected 10 different tissues from adult mouse: lens, heart, thymus, kidney, brain, spleen, pancreas, lung, liver and testis, and analyzed the expression level of αA-crystallin in these tissues. As shown in the top panel of Fig. 2, Western blot analysis revealed that besides its robust expression in the ocular lens (lane 1 contains only 0.5 μg protein, the rest of the lanes 100 μg proteins), αA-crystallin was detected in the thymus and pancreas at a relatively strong level, then to a less degree in the brain. The αA-crystallin level in the heart, kidney, spleen and liver was much lower than that in the thymus and pancreas. Finally, a trace of αA-crystallin was also observed in testis. No αA-crystallin was detected in the lung. As a comparison, we also examined the tissue distribution of αB-crystallin in mouse. Besides the strongest expression in lens, αB-crystallin was highly expressed in the heart, thymus and brain, and moderately expressed in the kidney and lung. However, different from the tissue-specific expression patterns of αA-crystallin, αB-crystallin was barely detectable in the pancreas and spleen, and absent in the liver and testis examined. Thus, our results confirm that the pancreas expresses a moderate level of αA-crystallin. In addition, we also show that several other non-lenticular tissues also express a low level of αA-crystallin. These results are slightly different from the pattern of αA-crystallin detected in different tissues from rat [16,34].

3.3. Downregulation of αA-crystallin in pancreatic tumors

Since both Hsp27 and αB-crystallin are implicated in carcinogenesis [6–8,15,33,36,37], we reason that αA-crystallin may be also involved in regulation of carcinogenesis. To test this possibility, we compared the expression pattern of αA-crystallin in human normal pancreatic tissues and various types of pancreatic carcinoma using the tissue array samples. As shown in Fig. 3A, the expression of αA-crystallin in human pancreatic cancer tissues was lower than that in human normal pancreas. Among the 11 normal pancreas samples examined, 7 samples displayed moderate expression level of αA-crystallin (normal pancreas A in Fig. 3A) and 4 samples relatively weak expression (normal pancreas B in Fig. 3A). In contrast, among the 60 cases of pancreatic cancer samples, 4 had weak expression of αA-crystallin signal (shown as pancreatic cancer #A of Fig. 3A), 17 displayed barely detectable αA-crystallin signal and the remaining 39 samples displayed no detectable signals (shown as pancreatic cancer #B of Fig. 3A).

To further characterize the expression of αA-crystallin in different human pancreatic cancer, we divided the pancreatic cancer samples into 4 different types: duct adenocarcinoma ($n=48$), mucinous adenocarcinoma ($n=3$), islet adenocarcinoma ($n=6$) and acinic cell carcinoma ($n=3$). The fluorescence signal in each individual sample and the statistic data with the mean value of fluorescence intensity of αA-crystallin expression in each type of pancreatic carcinoma were presented in Fig. 3B. The expression level of each normal pancreas and the statistical data derived from the normal pancreas were also included for comparison (Fig. 3B). Together, our results reveal that αA-crystallin is significantly downregulated in human pancreatic carcinoma compared with normal pancreas.

3.4. Expression of αA-crystallin in MiaPaCa cells upregulates expression of c-Jun and c-Fos

It is well established that the transcriptional factor complex, activating protein-1 (AP-1) plays a significant role in tumorigenesis [38–42]. AP-1 is either a homodimer containing two Jun family members (c-Jun, Jun-B or Jun D) or a heterodimer containing one member from the Jun family and another from the Fos family (C-Fos, Fra-1 and Fra-2) [38,43]. To explore the possible function of αA-crystallin in human pancreatic cancer, we overexpressed αA-crystallin in both pancreatic cancer cells, MiaPaCa and non-cancer cells, αTN4-1, a SV40 large-T-transformed mouse lens epithelial cell line expressing very little endogenous αA-crystallin. Then, we examined the AP-1 expression and activity in these transfected cells. As shown in Fig. 4, expression and phosphorylation of c-Jun were significantly upregulated in the nucleus of the MiaPaCa cells expressing αA-crystallin than in the nucleus of the vector-transfected cells, expression of c-Fos was also upregulated, though to a much less degree, in both nucleus and cytoplasm of the MiaPaCa cells expressing αA-crystallin than in the same fractions of the vector-transfected cells. Similar results were also obtained in the nucleus of the αTN4-1 cells expressing αA-crystallin (Supplementary Fig. 1).

3.5. Expression of αA-crystallin in MiaPaCa cells upregulates AP-1 activity

To determine whether the upregulated c-Jun and c-Fos actually led to increased AP-1 activity, we first conducted DNA binding assays using the oligos containing either the conserved AP-1 binding site

Author's personal copy

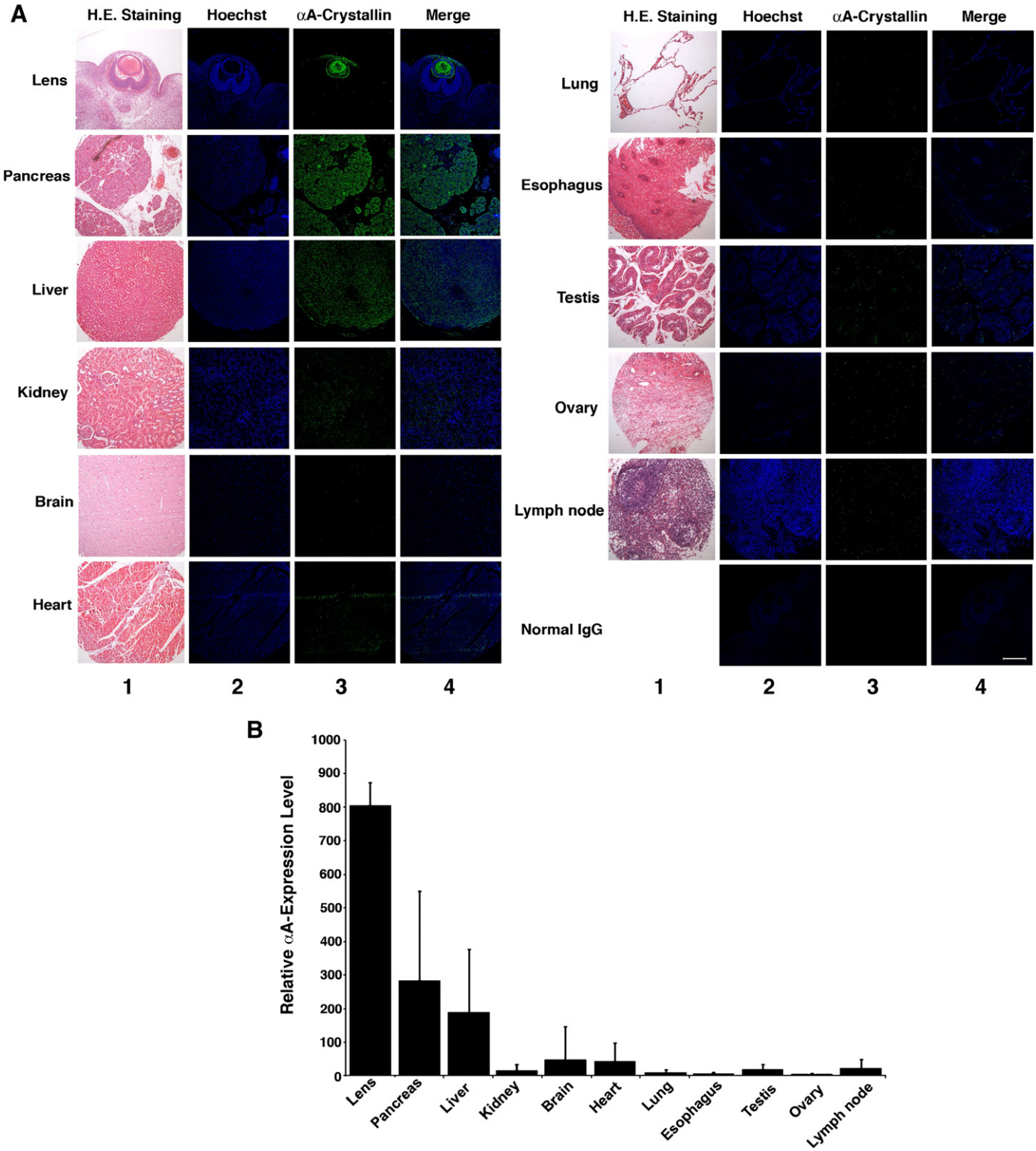

Fig. 1. Expression of αA-crystallin in human normal tissues. (A) Immunohistochemistry of αA-crystallin in the human lens, pancreas, liver, kidney, brain, heart, lung, esophagus, testis, ovary, and lymph node. Hematoxylin–eosin staining (HE staining) results of various tissues were included for comparison (column 1). Nuclei were visualized by Hoechst staining (blue color in column 2). αA-crystallin stained in green was derived from FITC (column 3). Merge showed combination of Hoechst in blue and αA-crystallin in green (column 4). Mouse lens section from embryonic day 11.5 was stained as positive control for αA-crystallin expression. Primary antibody was replaced by normal IgG in negative control (last row). Note that normal human pancreas displays moderate level of αA-crystallin signal. Liver also displays αA-crystallin signal but the intensity is less (see B for other tissues). Scale bar: 200 μm. (B) Quantification of fluorescence intensity. The mean intensity of fluorescence was measured by Carl Zeiss Laser Scanning System LSM 510.

(TGAGTCA) or the mutated site (ATCGGTA). As shown in Fig. 5A, the nuclear extract prepared from either parent MiaPaCa cells (lane 13) or vector pEGFP transfected MiaPaCa cells can bind to the wild type AP-1 oligo (lane 2) which was competed off by cold wild type oligo (lane 3) but much less by the mutated oligo (lane 4). The nuclear extracts pre-cleared by antibodies against c-Jun (lane 5), c-Fos (lane 6) or both antibodies (lane 7) lost most of the AP-1 activity so that the formed AP-1 complex was either lost or appeared very weak. In contrast, the

Author's personal copy

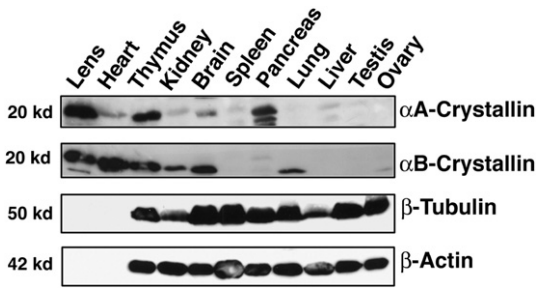

Fig. 2. Western blot analysis of αA- and αB-crystallins in 11 tissues from normal adult mouse (4 weeks). Various tissues were dissected and total proteins were extracted from the 11 tissues indicated. For the lens sample, 0.5 μg of total protein was used for Western blot analysis. For other samples, 100 μg of total protein was used. The blot was probed with specific antibodies against αA-crystallin, αB-crystallin antibody, β-tubulin or β-Actin at a dilution of 1:1000 for the primary antibody and at a dilution of 1:1500 for the secondary antibody. Note that the mouse pancreas expresses a distinct level of αA-crystallin but only a trace of αB-crystallin. Both β-actin and β-tubulin are absent in lane 1 (lens) and lane 2 (heart) due to limited sample loaded (only 0.5 μg lens protein in lane 1) or due to tissue characteristics (lacking β-actin and β-tubulin).

nuclear extracts pre-cleared by normal IgG only slightly attenuated the AP-1 complex (lane 8). These results suggest that the specific band we detected between the nuclear extract from pEGFP-MiaPaCa cells and the wild type oligo is the AP-1/DNA complex. Next, we compared the AP-1 DNA binding activity in vector- and αA-crystallin-transfected cells. As shown in lanes 9 and 11 of Fig. 5A, MiaPaCa cells expressing αA-crystallin display significant upregulation of AP-1 activity. Similar results were obtained with the lens epithelial cells, αTN4-1 expressing either only EGFP or EGFP-αA-crystallin (Supplementary Fig. 2). As a control for the specific binding to the AP-1 site, we conducted the reaction using purified p53 protein and AP-1 oligo, lane 12 of Fig. 5A clearly showed that p53 did not bind to AP-1 oligo. To further confirm that the transactivity of AP-1 was indeed upregulated in MiaPaCa cells expressing αA-crystallin, we introduced two reporter genes into the two types of stable transfectants: pEGFP-MiaPaCa and pEGFP-αA-MiaPaCa. As shown in Fig. 5B, assayed with either pJun-Luc (the luciferase gene was driven by the Jun promoter), or pProlactin-1xAP-1-Luc (the luciferase gene was driven by a mini-prolactin gene promoter containing a copy of AP-1 binding site), the MiaPaCa cells expressing αA-crystallin showed statistically significant upregulation of luciferase activity, indicating the upregulation of AP-1 activity in αA-crystallin expression MiaPaCa cells (Fig. 5B). Thus,

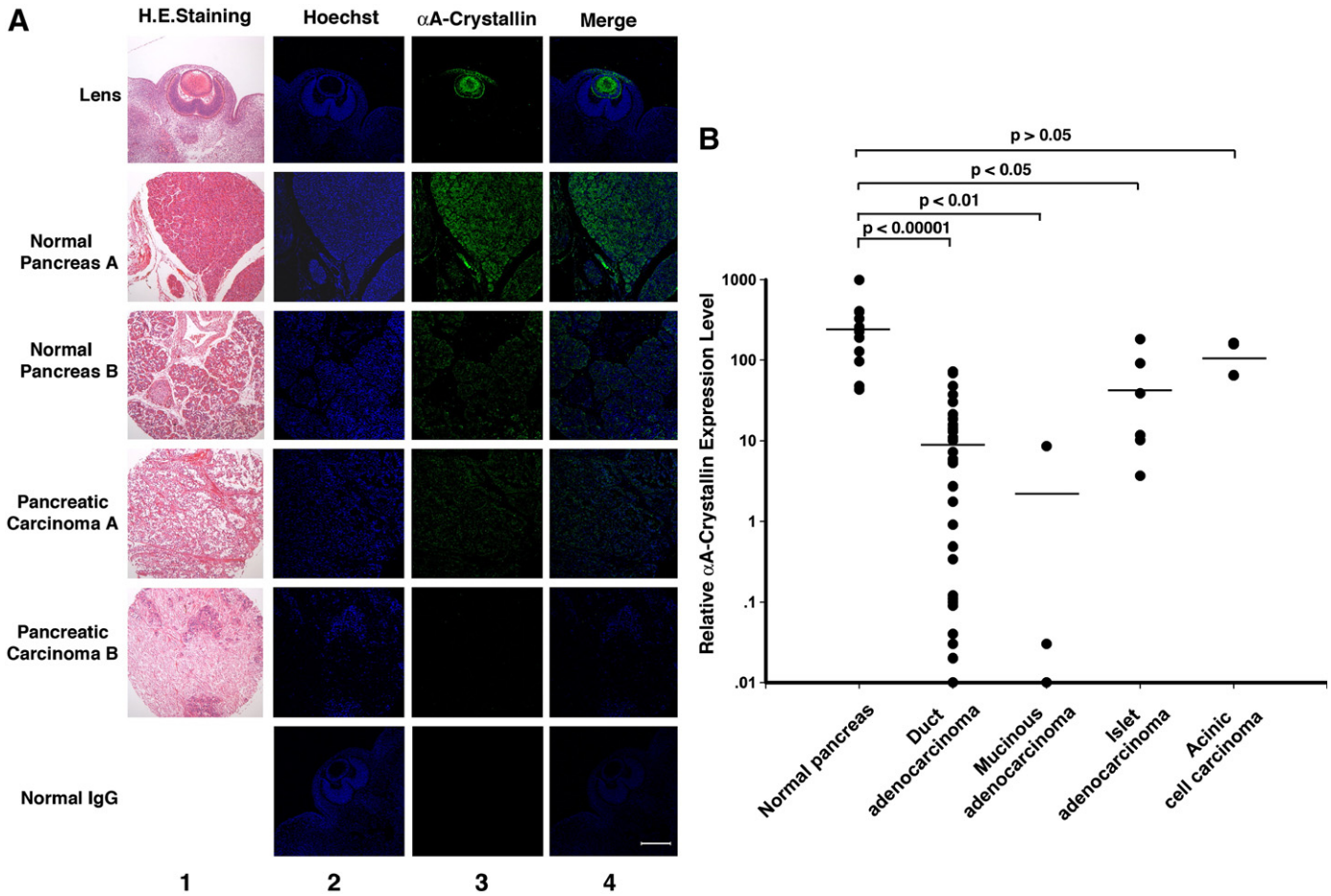

Fig. 3. Expression of αA-crystallin in human pancreatic cancer tissues. (A) Immunohistochemistry results of αA-crystallin in human pancreatic cancer. As comparison, immunohistochemistry results of αA-crystallin in two human normal pancreas samples were included. Hematoxylin–eosin staining (HE staining) results of two normal and two cancerous pancreatic sections were included for comparison (column 1). Nuclei were visualized by Hoechst staining (blue color in column 2). αA-crystallin stained in green was derived from FITC (column 3). Merge showed combination of Hoechst in blue and αA-crystallin in green (column 4). Mouse lens section from embryonic day 11.5 was stained as positive control for αA-crystallin expression. Primary antibody was replaced by normal IgG in negative control (last row). Scale bar: 200 μm. Note that normal human pancreas sample A displays moderate level of αA-crystallin signal, and normal human pancreas sample B shows weaker signals than the sample A. In the cancerous sample A, the level of αA-crystallin signal was much weaker than that in normal human sample A and also slightly weaker than that in normal human sample B. (B) Quantification of fluorescence intensity. The fluorescence intensity was measured by Carl Zeiss Laser Scanning System LSM 510. Each spot indicates the value of fluorescence intensity from a single tissue sample. Each short solid line indicates mean value of fluorescence intensity of one type of pancreatic cancer. Specifically, mean intensity of normal pancreas is 283 ± 267 ($n = 11$ among which 3 samples have a value less than 100 and 8 samples have a value more than 200); mean intensity of pancreatic duct adenocarcinoma is 9 ± 16 ($n = 48$); mean intensity of pancreatic mucinous adenocarcinoma is 3 ± 5 ($n = 3$); mean intensity of pancreatic islet adenocarcinoma is 56 ± 69 ($n = 6$) and mean intensity of pancreatic acinic cell carcinoma is 128 ± 55 ($n = 3$).

Author's personal copy

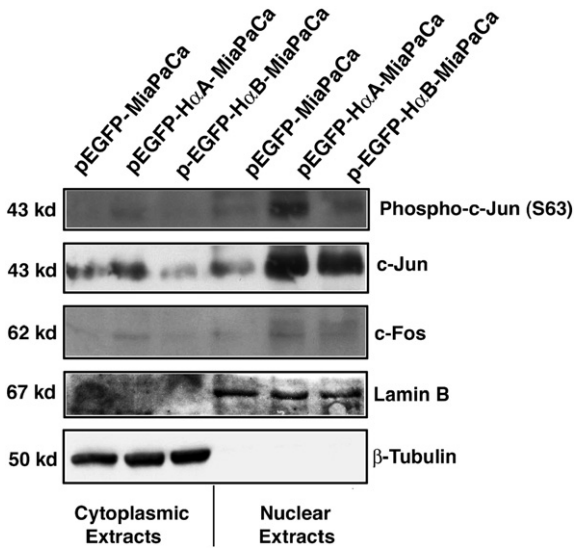

Fig. 4. Expression of αA-crystallin in pancreatic cancer cell line, MiaPaCa, upregulates expression of c-Jun and c-Fos. The stable clones of MiaPaCa cells expressing pEGFP, pEGFP-HαA or pEGFP-HαB were grown to 95% confluence in MEM with 10% FBS and 400 μg/ml G418, and then harvested for extraction of total proteins which were subjected to Western blot analysis for AP-1 components, c-Jun and c-Fos, in two different cellular fractions: cytoplasmic and nuclear portions. Note that MiaPaCa cells expressing αA-crystallin display upregulated levels of c-Jun and c-Fos protein. In addition, the phospho-c-Jun level was also enhanced in pEGFP-HαA-MiaPaCa cells.

expression of αA-crystallin in pancreatic cancer cells positively regulates AP-1 activity.

3.6. αA-crystallin positively regulates ERK2 MAPK

It has been shown that AP-1 expression and activity can be enhanced by MAP kinases [44–48]. To explore how might αA-crystallin regulate AP-1, we examined the possible modulation of ERK kinase activity by αA-crystallin since ERK is a major MAP kinase regulating AP-1 components in both expression and activation [44–48]. As shown in Fig. 6A, we found that Elk was dose-dependently phosphorylated by ERK2 in vitro. Moreover, in the presence of αA-crystallin, phosphorylation of Elk by 0.1 or 1 ng ERK2 was significantly enhanced. Addition of 1 μg of αA-crystallin into the ERK2 kinase reaction with low level of ERK2 (1 ng) enhanced more than 10-fold Elk phosphorylation, reflecting the corresponding enhancement of ERK2 activity. Together, these results reveal that αA-crystallin can positively regulate AP-1 activity through modulation of ERK activity. To further confirm that αA-crystallin enhances ERK2 kinase activity, we analyzed the ERK1/2 expression and activity in vector- and αA-crystallin-transfected stable lines of cells. As shown in Fig. 6C, both expression and activity of ERK2 were clearly upregulated in MiaPaCa cells expressing αA-crystallin than vector-transfected cells.

3.7. αA-crystallin regulates TGFβ signaling pathway

To determine whether αA-crystallin actively regulates TGFβ signaling pathway which plays a key role in pancreatic carcinogenesis [20], we first examined expression of several genes in the TGFβ signaling pathway at the mRNA level. As shown in Fig. 7, TGFβ was increased about 2-fold when αA-crystallin was overexpressed in MiaPaCa (Fig. 7A and B, similar result was observed in αA-crystallin-transfected Capan-1 cells, data not shown). For the receptor, TGFβ receptors 1 and 2 are not detected and TGFβ receptor 3 displayed little change in the three types of cells (Fig. 7A and C). To further confirm the modulation of TGFβ signaling pathway by αA-crystallin, we examined the protein expression levels of TGFβ and the downstream smads, as well as the phosphorylation status of the smads. As shown in Fig. 8, Western blot analysis revealed that TGFβ was also upregulated at the protein level. In addition, expression and phosphorylation of Smad 3 and Smad 5 were significantly upregulated. Thus, αA-crystallin actively enhances TGFβ signaling pathway.

3.8. Retardation of cell migration in αA-crystallin-overexpressed cells

To explore how αA-crystallin may regulate carcinogenesis, we conducted wound healing assay using the established stable cell lines: pEGFP-MiaPaCa, pEGFP-αA-MiaPaCa and pEGFP-αB-MiaPaCa. When these cells with similar expression levels were selected to conduct wound healing assays (Fig. 9), it was found that MiaPaCa cells expressing αA-crystallin displayed statistically significant retardation in cell migration. In contrast, the same cells expressing either the vector or αB-crystallin did not show such effect. Thus, αA-crystallin retards migration of pancreatic cancer cells, which is consistent with its downregulation in various types of pancreatic carcinoma (Fig. 3).

4. Discussion

In the present study, we have demonstrated the following: 1) αA-crystallin is expressed at moderate level in pancreas from human and mouse, a non-ocular tissue previously not documented; 2) αA-crystallin is significantly downregulated in the pancreatic tumors than in the normal human pancreas; 3) expression of αA-crystallin in pancreatic carcinoma cells induces significant upregulation of the AP-1 components and activity, 4) αA-crystallin can enhance activity of ERK2 MAP kinase, through which it can regulate AP-1 expression and activity; 5) expression of αA-crystallin in pancreatic carcinoma cells significantly enhanced the TGFβ signaling pathways; and 6) expression of αA-crystallin in pancreatic cells led to obvious retardation of the cell migration. Together, our results suggest that αA-crystallin appears to negatively regulate pancreatic carcinogenesis, which is in contrast to the function of αB-crystallin in breast cancer.

4.1. αA-crystallin is expressed in normal pancreas besides other non-lenticular tissues

αA-crystallin is first known as a lens structural protein [10,11]. It shares about 60% identity in amino acid sequence with αB-crystallin, another lens structure protein [10,11]. Several lines of evidence have shown that although the two genes encoding αA- and αB-crystallins may arise from gene duplication, they have diverged significantly. First, during murine development, the initial turning on of the two genes occurs at different time. While αB mRNA is first becoming detectable at E9.5, expression of αA mRNA appears at E10.5 [10]. Such differential turning on time reflects the different control mechanisms in the promoters of the two α-crystallin genes. Second, the two genes display distinct tissue-specific expression patterns. While αA is highly restricted to lens during mouse embryonic developmental process, αB-crystallin is expressed in the developing heart, nasal epithelium, and retinal pigment epithelium [10]. In the adult vertebrates, although both αA and αB are abundantly expressed in the lens, they display significant difference in non-lenticular tissue expressions. αB is strongly expressed in the heart, skeletal muscle, kidney and brain [11–13]. In contrast, αA is reported to be expressed at a very low level in some non-lenticular tissues including the spleen, thymus, heart, brain and liver [16,34]. In the present study, our results not only confirm the presence of a low level of αA-crystallin in the kidney and liver, but also reveal a moderate level of αA-crystallin expression in a novel non-lenticular tissue, the normal human pancreas. Among the 11 normal human pancreas samples examined, 7 samples display consistently moderate level of αA-crystallin expression and the remaining 4 samples also showed a low level of αA-crystallin expression (Fig. 1). The pancreatic distribution of αA-crystallin is further confirmed from analysis of mouse tissue samples (Fig. 2).

Author's personal copy

In a previous study, Kato et al. [16] compared the relative abundance αA-crystallin in both lens and non-lenticular tissues (ng αA-crystallin/per mg total protein in organ). These authors found that in the adult rat (8–16 weeks), the lens contains 244 μg αA-crystallin/per mg total lens protein, and the spleen contains 16.6 ng αA-crystallin/per mg total spleen protein, so the relative abundance of lens αA-crystallin is about 14,698-fold. Using confocal fluorescence microscopy, we quantitated the relative abundance of αA-

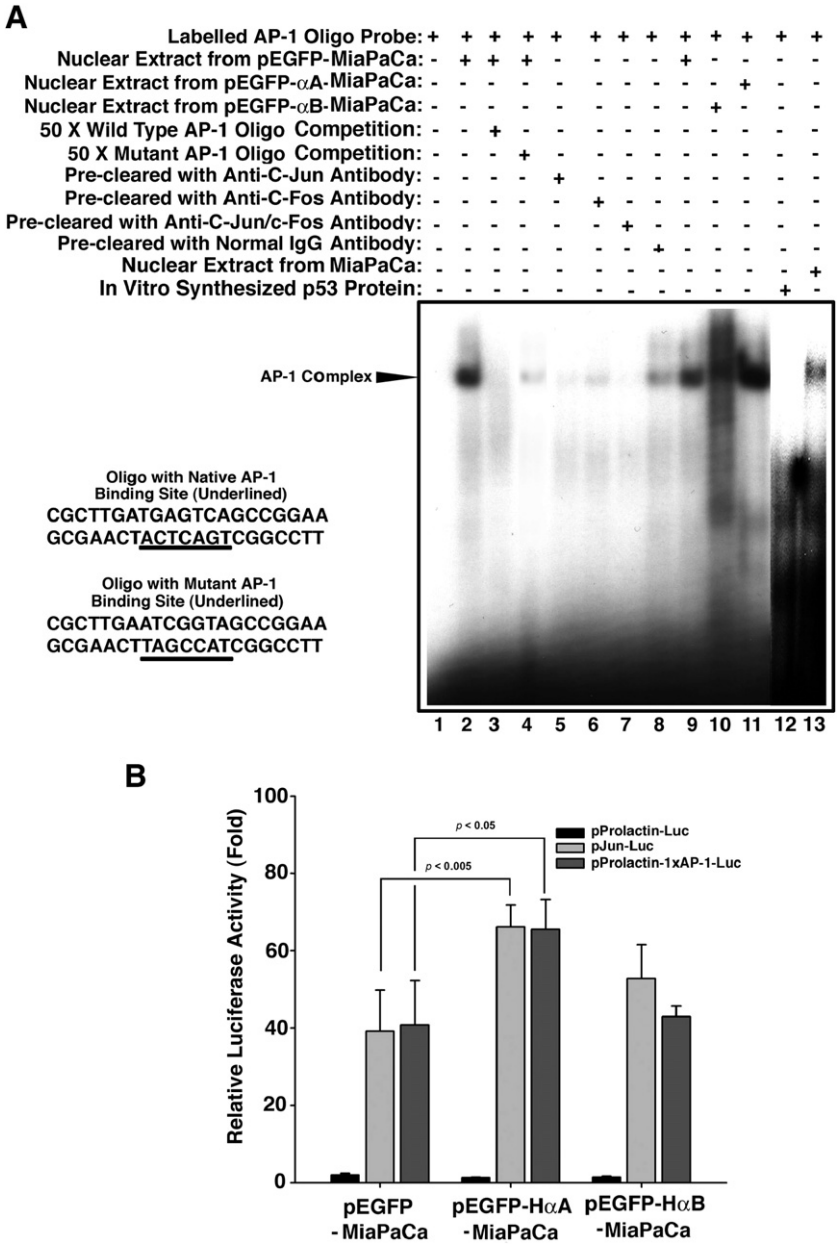

Fig. 5. Expression of αA-crystallin in pancreatic cancer cell line, MiaPaCa, upregulates AP-1 DNA binding activity (A) and transactivity (B). A. Gel mobility shifting assay demonstrates the existence of AP-1 DNA binding activity in parent MiaPaCa cell nuclear extract (lane 13), pEGFP-MiaPaCa cell nuclear extracts (lanes 2 to 9), which was much lower than that in MiaPaCa cell nuclear extracts expressing αA-crystallin (lane 11) or αB-crystallin (lane 10). Nuclear extracts prepared from three types of cells were incubated with γ-^{32}P-ATP-labeled oligos containing wild type AP-1 binding site (up panel of A left part) under various conditions shown in the figure. Lane 1, gel mobility shifting assay with labeled wild type AP-1 oligo. Lane 2, gel mobility shifting assay with labeled wild type AP-1 oligo and pEGFP-MiaPaCa nuclear extract. Lane 3, the same assay as in lane 2 except that 50-fold of non-labeled wild type AP-1 oligos was added into the reaction. Lane 4, the same assay as in lane 3 except that the non-labeled competing oligo contains a mutated AP-1 binding site (bottom panel of Fig. 5A left part). Lane 5, gel mobility shifting assay with labeled wild type AP-1 oligo and pEGFP-MiaPaCa nuclear extract pre-cleared by anti-c-Jun antibody. Lane 6, gel mobility shifting assay with labeled wild type AP-1 oligo and pEGFP-MiaPaCa nuclear extract pre-cleared by anti-c-Fos antibody. Lane 7, gel mobility shifting assay with labeled wild type AP-1 oligo and pEGFP-MiaPaCa nuclear extract pre-cleared by anti-c-Jun antibody and anti-c-Fos antibody. Lane 8, gel mobility shifting assay with labeled wild type AP-1 oligo and pEGFP-MiaPaCa nuclear extract pre-cleared by normal IgG. Lane 9, the same assay as in lane 2. Lane 10, the same assay as in lane 2 except that the nuclear extracts were from the pEGFP-HαB-MiaPaCa cells. Lane 11, the same assay as in lane 2 except that the nuclear extracts were from the pEGFP-HαA-MiaPaCa cells. Lane 12 (mock for AP-1 site specificity), the same assay as in lane 2 except that the nuclear extract was replaced with in vitro synthesized p53 protein. Note that p53 does not bind to AP-1 site. B. Luciferase assays to demonstrate that the AP-1 transactivity in pEGFP-HαA-MiaPaCa cells was significantly higher than that in pEGFP-MiaPaCa cells. The luciferase reporter gene driven by a mini-prolactin gene promoter without enhancer (pProlactin-Luc), or with 1 copy of AP-1 binding site (pProlactin-1xAP-1-Luc), or driven by the c-Jun promoter (pJun-Luc), together with a reference plasmid were separately transfected into pEGFP-MiaPaCa cells, pEGFP-HαA-MiaPaCa cells, or pEGFP-HαB-MiaPaCa cells. After 48 h, the transfected cells were harvested for the assaying of luciferase activity. After calibration with the luciferase activity from the reference plasmid, the transactivity of AP-1 in each type of cells was presented. Note that as assayed by both constructs, pProlactin-1xAP-1-Luc and pJun-Luc, the AP-1 activity in pEGFP-MiaPaCa cells were significantly lower than that in pEGFP-HαA-MiaPaCa cells ($p<0.005$ for pJun-Luc construct, and $p<0.05$ for pProlactin-1xAP-1-Luc construct). In contrast, the AP-1 activity in pEGFP-MiaPaCa cells is only slightly lower than that in pEGFP-HαB-MiaPaCa cells ($p>0.05$ in both cases).

Author's personal copy

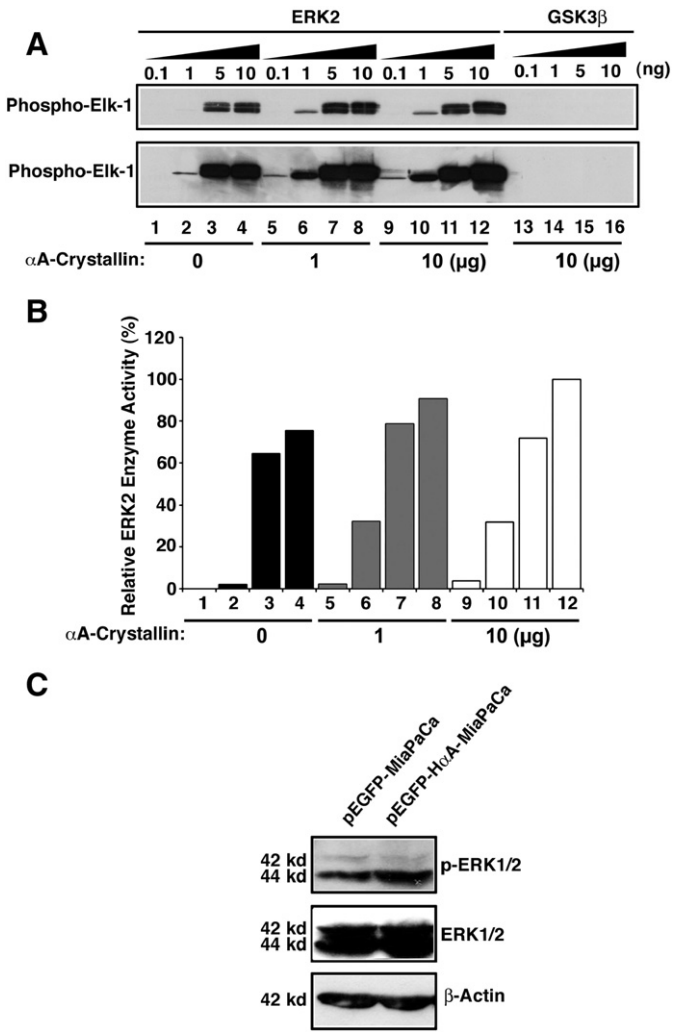

Fig. 6. αA-crystallin enhances MAPK (ERK2) activity in the in vitro kinase assay. A. The substrate of Elk-1 protein was phosphorylated by ERK2 kinase in the in vitro assay in the presence of ATP. Phosphorylation of Elk was detected by Western blot analysis as described above. Results of two different exposures were shown. The kinase reaction with GSK3β was included as control for ERK2. B. Quantitative results of the Elk phosphorylation under different conditions. The relative pixel of each band was quantitated using the software from Silk Scientific Inc. Note that at the concentration of 0.1 and 1 ng ERK2 kinase conditions, addition of 1 or 10 μg of αA-crystallin significantly enhances the ERK2 activity as reflected by the differential intensity of Elk phosphorylation. C. Western blot analysis of expression and activities of ERK1/2 in vector- or αA-transfected MiaPaCa cells. Western blot analysis was conducted as described in Fig. 2. Note that both expression and activity of ERK2 was upregulated in MiaPaCa cells expressing αA-crystallin than vector-transfected cells.

crystallin in the developing mouse lens and the pancreatic tissue, and found that the corresponding values are 807 ± 48 and 283 ± 67, respectively. Therefore, the human adult pancreatic signal of αA-crystallin is about 1/3 of the developing mouse eye lens (Fig. 1). In mouse tissue, we estimate that αA-crystallin in lens is about 500-fold higher than that in the pancreas (see Fig. 2, 200-fold difference in sample load × 2.5-fold difference in αA-crystallin band in the lens versus in the pancreas). Together, our results demonstrate that the pancreas expresses a moderate level of αA-crystallin.

4.2. αA-crystallin is implicated in carcinogenesis

It is well established that small heat shock proteins are implicated in carcinogenesis [8]. One of the most studied members is Hsp27, which is involved in carcinogenesis of many different types of tissues [35,49–57]. Another member of the HSP family implicated in carcinogenesis is αB-crystallin. Iwaki and Tateishi [58] first demonstrated the existence of αB-crystallin in hamartomas of tuberous sclerosis. Then, it was found that concentrations of αB-crystallin in prostatic carcinoma tissues were significantly higher than in benign prostatic hyperplasia [59]. In breast cancer cells, αB-crystallin was found expressing constitutively in certain breast carcinoma cell lines, and increased intensity of αB-crystallin expression was correlated with shorter survival [33]. Moreover, expression of αB-crystallin results in transformation of immortalized human mammary epithelial cells, induction of EGF- and anchorage-independent growth, and enhancement of cell migration

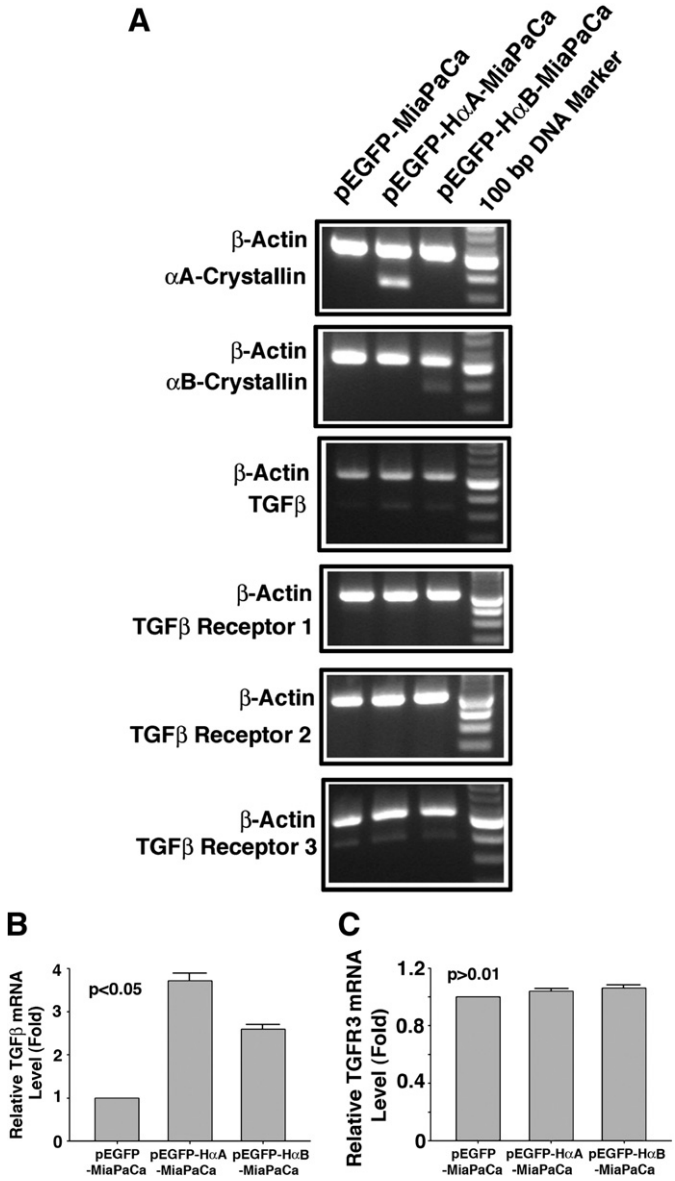

Fig. 7. αA-crystallin modulates expression of TGFβ as demonstrated by RT-PCR analysis. A. RT-PCR. Total cellular RNAs were extracted from vector-, HαA- or HαB-crystallin-transfected cells, then were used for RT-PCR assays as described in the Materials and methods. B. Quantitation of TGFβ mRNA level in vector-, HαA- or HαB-crystallin-transfected MiaPaCa cells. C. Quantitation of TGFβ receptor 3 mRNA level in vector-, αA- or αB-crystallin-transfected MiaPaCa cells. Note that αA-crystallin enhances expression of TGFβ mRNA but has little effect on TGF receptors.

Author's personal copy

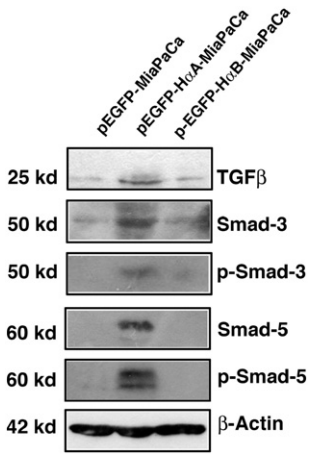

Fig. 8. αA-crystallin modulates protein expression of TGFβ and Smad3/5, as well as the phosphorylation status of Smad3/5. Western blot analysis was conducted as described in Fig. 2. Note that αA-crystallin enhances expression of TGFβ, Smad3 and Smad5. Moreover, αA-crystallin upregulates the phosphorylation status of Smad3/5.

and invasion [15]. Thus, αB-crystallin is considered as a novel oncoprotein [15].

Both αA- and αB-crystallins belong to the heat shock protein (Hsp) family [2]. Whether αA-crystallin is also in implicated in carcinogenesis remains to be explored. Compared with αB-crystallin, the limited distribution of αA-crystallin in non-lenticular tissues may restrict its function in carcinogenesis [10–14]. Nevertheless, several recent studies suggest that αA-crystallin may be also implicated in tumor development. First, in 4 cases of human sebaceous carcinoma of the eyelid examined, both αA-crystallin and αB-crystallin were found highly expressed [60]. Second, in the retinocytoma, αA-crystallin was expressed in the cytoplasm of all tumor cells and the apoptotic index was significantly higher in those cases with weak signal of αA-crystallin than in those that were strongly positive [61]. These results suggest that αA-crystallin, acting like αB-crystallin, seems to promote carcinogenesis. On the other hand, a recent study revealed that in 6 cases of retinoblastoma, preoperative chemotherapy induced strong expression of only Hsp27 and αB-crystallin but not αA-crystallin [62]. Moreover, the viable tumor cells that survived contained high levels of Hsp27 and αB-crystallin but not αA-crystallin. Therefore, these results indicate that αA-crystallin does not seem to act the same way as Hsp27 and αB-crystallin do in promoting carcinogenesis. Our present finding that in 60 different cases of pancreatic carcinoma, the expression level of αA-crystallin was consistently downregulated than that in 11 normal human pancreas samples also supports the negative regulation of carcinogenesis by αA-crystallin. In addition, our results also suggest that αA-crystallin may be used as one of the biomarkers for pancreatic cancer diagnosis.

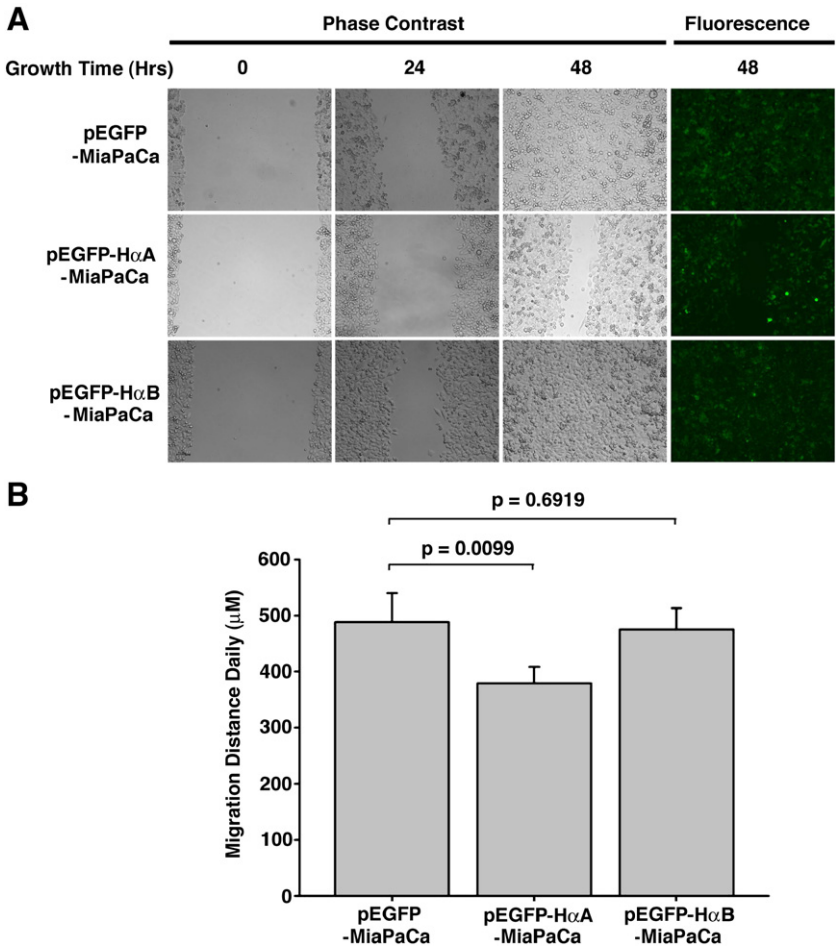

Fig. 9. Demonstration that the pancreatic cancer cell line, MiaPaCa, expressing the exogenous HαA-crystallin display retarded cell migration. The stable transfected cell lines, pEGFP-MiaPaCa, pEGFP-HαA-MiaPaCa or pEGFP-HαB-MiaPaCa cells were seeded in 6-well plates and grown until 95% confluent. Then, two straight scratches were made by using a 1 ml blue pipette tip to simulate the wound healing in each well. After PBS washing for 2 times, new DMEM medium was added for a continuous growth of another 48 h. The wound healing process was recorded daily using the Leica Inverted Phase Contrast Fluorescence Microscopy with a 10× objective. Note that the pEGFP-HαA-MiaPaCa cells display slower healing process than pEGFP-MiaPaCa and pEGFP-HαB-MiaPaCa cells, suggesting both slower cell migration and proliferation of pEGFP-HαA-MiaPaCa cells.

Author's personal copy

4.3. αA-crystallin may negatively regulate development of pancreatic tumors

Pancreatic malignancy develops from intraepithelial neoplasia (PanIN), progressing through PanIN-1a, PanIN-1b, PanIN-2, and PanIN-3 to ductal adenocarcinomas (PDAC) [63,64]. During this process, key oncogenes and tumor suppressors such as Ki-RAS, $p16^{INK4a}$, P53, DPC/SMAD4, and BRCA2 play very important roles [20–22,65–68]. The carcinogenesis signals are mediated by major signaling pathways including MAPK pathways, sonic hedgehog and notch signaling pathways, and also TGFβ signaling pathways [20–22,65–68]. In the present study, we present several lines of evidence to show that αA-crystallin seems to negatively regulate development of pancreatic tumors. First, we demonstrate that compared with the physiological level in normal human pancreas, αA-crystallin is significantly downregulated in 60 cases of pancreatic carcinomas of various types. Second, we show that pancreatic cancer cells expressing αA-crystallin display retarded cell migration. Finally, we show that pancreatic cancer cells expressing αA-crystallin have enhanced expression levels of c-Jun and c-Fos, increased phosphorylation of c-Jun oncoprotein, and elevated level of AP-1 activities in both DNA binding and transactivation, which is derived from enhanced activity of the ERK2 kinase promoted by αA-crystallin (Fig. 6). As a result, αA-crystallin positively regulates TGFβ signaling pathway (Figs. 7 and 8) through MAP kinase, and thus negatively regulate development of pancreatic malignancy.

Acknowledgements

We thank Drs. J. Horvitz for the αA/αB-crystallin antibodies and Dr. Tom Curran for the C-Jun antibody. This work is supported in part by the NIH grants 1R01 EY018380, and 1R01 EY015765, and the Lotus Scholar Program Funds from Hunan Province Government and Hunan Normal University, and the Changjiang Scholar Team Award from the National Education Ministry of China to DWL.

Appendix A. Supplementary data

Supplementary data associated with this article can be found, in the online version, at doi:10.1016/j.bbadis.2010.04.004.

References

[1] R. Benndorf, M.J. Welsh, Shocking degeneration, Nat. Genet. 36 (2004) 547–548.
[2] Y. Sun, T.H. MacRae, The small heat shock proteins and their role in human disease, FEBS J. 272 (2005) 2613–2627.
[3] F. Bennardini, A. Wrzosek, M. Chiesi, Alpha B-crystallin in cardiac tissue. Association with actin and desmin filaments, Circ. Res. 71 (1992) 288–294.
[4] D.W. Li, L. Gong, M. Deng, J.P. Liu, M. Liu, Y.W. Mao. The two lens structural proteins, αA- and αB-crystallins, prevent stress-induced apoptosis through regulation of multiple signaling transduction pathways. In: Arrigo, Simon (eds). Small Stress Proteins and Human Diseases. Nova Science Publisher, Inc NY, USA. chapter 1.3, pp. 27–57.
[5] I.J. Benjamin, Y. Guo, S. Srinivasan, S. Boudina, R.P. Taylor, N.S. Rajasekaran, R. Gottlieb, E.F. Wawrousek, E.D. Abel, R. Bolli, CRYAB and HSPB2 deficiency alters cardiac metabolism and paradoxically confers protection against myocardial ischemia in aging mice, Am. J. Physiol. Heart Circ. Physiol. 293 (2007) H3201–H3209.
[6] M. Sherman, G. Multhoff, Heat shock proteins in cancer, Ann. N. Y. Acad. Sci. 1113 (2007) 192–201.
[7] C. Didelot, D. Lanneau, M. Brunet, A.L. Joly, A. De Thonel, G. Chiosis, C. Garrido, Anti-cancer therapeutic approaches based on intracellular and extracellular heat shock proteins, Curr. Med. Chem. 14 (2007) 2839–2847.
[8] D.R. Ciocca, S.K. Calderwood, Heat shock proteins in cancer: diagnostic, prognostic, predictive, and treatment implications, Cell Stress Chaperones 10 (2005) 86–103.
[9] G.B. Reddy, P.A. Kumar, M.S. Kumar, Chaperone-like activity and hydrophobicity of alpha-crystallin, IUBMB Life 58 (2006) 632–641.
[10] M.L. Robinson, P.A. Overbeek, Differential expression of alpha A- and alpha B-crystallin during murine ocular development, Investig. Ophthalmol. Vis. Sci. 37 (1996) 2276–2284.
[11] J. Piatigorsky, Lens crystallins and their genes: diversity and tissue-specific expression, FASEB J. 3 (1989) 1933–1940.
[12] S.P. Bhat, C.N. Nagineni, alpha B subunit of lens-specific protein alpha-crystallin is present in other ocular and non-ocular tissues, Biochem. Biophys. Res. Commun. 158 (1989) 319–325.
[13] R.A. Dubin, E.F. Wawrousek, J. Piatigorsky, Expression of the murine alpha B-crystallin gene is not restricted to the lens, Mol. Cell. Biol. 9 (1989) 1083–1091.
[14] S. Kase, J.G. Parikh, N.A. Rao, Expression of alpha-crystallin in retinoblastoma, Arch. Ophthalmol. 127 (2009) 187–192.
[15] J.V. Moyano, J.R. Evans, F. Chen, M. Lu, M.E. Werner, F. Yehiely, L.K. Diaz, D. Turbin, G. Karaca, E. Wiley, T.O. Nielsen, C.M. Perou, V.L. Cryns, AlphaB-crystallin, is a novel oncoprotein that predicts poor clinical outcome in breast cancer, J. Clin. Invest. 116 (2006) 261–270.
[16] K. Kato, H. Shinohara, N. Kurobe, S. Goto, Y. Inaguma, K. Ohshima, Immunoreactive alpha A crystallin in rat non-lenticular tissues detected with a sensitive immunoassay method, Biochim. Biophys. Acta 1080 (1991) 173–180.
[17] M.B. Ujiki, M.S. Talamonti, Surgical management of pancreatic cancer, Semin. Radiat. Oncol. 15 (2005) 218–225.
[18] J.E. Niederhuber, M.F. Brennan, H.R. Menck, The National Cancer Data Base report on pancreatic cancer, Cancer 76 (1995) 1671–1677.
[19] R. Pezzilli, Pancreatic ductal carcinoma: from the bench to the bedside, JOP 7 (2006) 508–510.
[20] A.F. Hezel, A.C. Kimmelman, B.Z. Stanger, N. Bardeesy, R.A. Depinho, Genetics and biology of pancreatic ductal adenocarcinoma, Genes Dev. 20 (2006) 1218–1249.
[21] N. Bardeesy, R.A. DePinho, Pancreatic cancer biology and genetics, Nat. Rev. Cancer 2 (2002) 897–909.
[22] A.K. Rustgi, The molecular pathogenesis of pancreatic cancer: clarifying a complex circuitry, Genes Dev. 20 (2006) 3049–3053.
[23] Y.-W. Mao, J.P. Liu, H. Xiang, D.W.-C. Li, Human alphaA- and alphaB-crystallins bind to Bax and Bcl-X(S) to sequester their translocation during staurosporine-induced apoptosis, Cell Death Differ. 11 (2004) 512–526.
[24] L. Xiao, L.-L. Gong, D. Yuan, M. Deng, J.-P. Liu, L.-L. Chen, L. Zhang, S.-M. Sun, J. Liu, X.-H. Hu, H.-L. Ma, C.-B. Zheng, H. Fu, P.-Q. Chen, J.-Q. Zhao, S.-S. Xie, X.-M. Zeng, L.–J. Zou, Y.-M. Xiao, W.-B. Liu, J. Zhang, Y. Liu, D. W.-C. Li (in press). Protein phosphatase-1 regulates Akt1 signaling pathway to control gene expression, cell survival and differentiation. Cell Death Differ. doi:10.1038/cdd.2010.16.
[25] M. Marinov, A. Ziogas, O.E. Pardo, L.T. Tan, T. Dhillon, F.A. Mauri, H.A. Lane, N.R. Lemoine, U. Zangemeister-Wittke, M.J. Seckl, A. Arcaro, AKT/mTOR pathway activation and BCL-2 family proteins modulate the sensitivity of human small cell lung cancer cells to RAD001, Clin. Cancer Res. 15 (2009) 1277–1287.
[26] Y.-M. Xiao, L. Chen, J. Liu, L.-J. Zou, W.-B. Liu, H.G. Chen, Y. Liu, D.W.-C. Li, JNK1 downregulation is associated with sex reversal of the ricefield eel, J. Exp. Zool. B. MOl. Dev. Evol. 314 (2010) 242–256.
[27] H. Feng, H. Xiang, Y.-W. Mao, J. Wang, J.-P. Liu, X.Q. Huang, Y. Liu, S.-J. Liu, C. Luo, X.-J. Zhang, Y. Liu, D.W.-C. Li, Human Bcl-2 activates RAF/MEK/ERK pathway and regulates AP-1 activity and downstream genes in rabbit Lens epithelial cells, Oncogene 23 (2004) 7310–7321.
[28] J.-C. Qin, H.-G. Chen, Q. Yan, M. Deng, J.-P. Liu, S. Doerge, W.-Y. Ma, Z. Dong, D.W.-C. Li, Protein phosphatase-2A is a target of epigallocatechin-3-gallate and modulates the p53-Bak apoptotic pathway, Cancer Res. 68 (11) (2008) 4150–4162.
[29] H.-G. Chen, W.-J. Han, M. Deng, J. Qin, D. Yuan, J.-P. Liu, L. Xiao, L. Gong, S. Liang, J. Zhang, Y. Liu, D.W.-C. Li, Transcriptional regulation of PP2A-A alpha is mediated by multiple factors including AP-2alpha, CREB, ETS-1, and SP-1, PLoS One 4 (2009) e7019.
[30] D.W.-C. Li, J.R. Kuszak, K. Dunn, R.-R. Wang, W.-C. Ma, G.-M. Wang, A. Spector, M. Leib, A.M. Cotliar, M. Weiss, J. Espy, G. Howard, R.L. Farris, J. Auran, A. Donn, A. Hofeldt, C. Mackay, J. Merriam, R. Mittl, T.R. Smith, Lens epithelial cell apoptosis appears to be a common cellular basis for non-congenital cataract formation in humans and animals, J. Cell Biol. 130 (1995) 169–181.
[31] D.W.-C. Li, Jin-Ping Liu, J. Wang, Y.-W. Mao, Li-Hui Hou, Protein expression patterns of the signaling molecules for MAPK pathways in human, bovine and rat lenses, Investig. Ophthalmol. Vis. Sci. 44 (2003) 5277–5286.
[32] D.W.-C. Li, J.-P. Liu, Y.W. Mao, H. Xiang, J. Wang, W.-Y. Ma, Z. Dong, H.M. Pike, Rhoderick E. Brown, J.C. Reed, Calcium-activated RAF/MEK/ERK pathway mediates p53-dependent apoptosis and is abrogated by αB-crystallin through inhibition of Ras activation, Mol. Biol. Cell 16 (2005) 4437–4453.
[33] D. Chelouche-Lev, H.M. Kluger, A.J. Berger, D.L. Rimm, J.E. Price, alphaB-crystallin as a marker of lymph node in breast carcinoma, Cancer 100 (2004) 2543–2548.
[34] A.N. Srinivasan, C.N. Nagineni, S.P. Bhat, αA-Crystallin is expressed in non-ocular tissues, J. Biol. Chem. 267 (1992) 23337–23341.
[35] G.L. Vegh, V. Fulop, Y. Liu, S.W. Ng, Z.S. Tuncer, D.R. Genest, P. Paldi-Haris, J. Foldi, S.C. Mok, R.S. Berkowitz, Differential gene expression pattern between normal human trophoblast and choriocarcinoma cell lines: downregulation of heat shock protein-27 in choriocarcinoma in vitro and in vivo, Gynecol. Oncol. 75 (1999) 391–396.
[36] K. Ou, K. Yu, D. Kesuma, M. Hooi, N. Huang, W. Chen, S.Y. Lee, X.P. Goh, L.K. Tan, J. Liu, S.Y. Soon, S. Bin Abdul Rashid, T.C. Putti, H. Jikuya, T. Ichikawa, O. Nishimura, M. Salto-Tellez, P. Tan, Novel breast cancer biomarkers identified by integrative proteomic and gene expression mapping, J. Proteome Res. 7 (2008) 1518–1528.
[37] S.K. Gruvberger-Saal, R. Parsons, Is the small heat shock protein alphaB-crystallin an oncogene? J. Clin. Invest. 116 (2006) 30–32.
[38] T. Curran, B.R. Franza Jr., Fos and Jun: the AP-1 connection, Cell 55 (1988) 395–397.
[39] J.L. Imler, B. Wasylyk, AP1, a composite transcription factor implicated in abnormal growth control, Prog. Growth Factor Res. 1 (1989) 69–77.
[40] H.E. Varmus, Oncogenes and transcriptional control, Science 238 (1987) 1337–1339.
[41] M. Durchdewald, P. Angel, J. Hess, The transcription factor Fos: a Janus-type regulator in health and disease, Histol. Histopathol. 24 (2009) 1451–1461.

Author's personal copy

[42] M. Karin, E. Gallagher, From JNK to pay dirt: jun kinases, their biochemistry, physiology and clinical importance, IUBMB Life 57 (2005) 283–295.
[43] D.A. Leonard, N. Rajaram, T.K. Kerppola, Structural basis of DNA bending and oriented heterodimer binding by the basic leucine zipper domains of Fos and Jun, Proc. Natl. Acad. Sci. U. S. A. 94 (1997) 4913–4918.
[44] G. Gutierrez-Venegas, R. Castillo-Aleman, Characterization of the transduction pathway involved in c-fos and c-jun expression induced by *Aggregatibacter actinomycetemcomitans* lipopolysaccharides in human gingival fibroblasts, Int. Immunopharmacol. 8 (2008) 1513–1523.
[45] D.B. Chen, J.S. Davis, Epidermal growth factor induces c-fos and c-jun mRNA via Raf-1/MEK1/ERK-dependent and -independent pathways in bovine luteal cells, Mol. Cell. Endocrinol. 200 (2003) 141–154.
[46] M. Cavigelli, F. Dolfi, F.X. Claret, M. Karin, Induction of c-fos expression through JNK-mediated TCF/Elk-1 phosphorylation, EMBO J. 14 (1995) 5957–5964.
[47] P. Monje, M.J. Marinissen, J.S. Gutkind, Phosphorylation of the carboxyl-terminal transactivation domain of c-Fos by extracellular signal-regulated kinase mediates the transcriptional activation of AP-1 and cellular transformation induced by platelet-derived growth factor, Mol. Cell. Biol. 23 (2003) 7030–7043.
[48] G.J. Babu, M.J. Lalli, M.A. Sussman, J. Sadoshima, M. Periasamy, Phosphorylation of elk-1 by MEK/ERK pathway is necessary for c-fos gene activation during cardiac myocyte hypertrophy, J. Mol. Cell. Cardiol. 32 (2000) 1447–1457.
[49] A.P. Arrigo, S. Simon, B. Gibert, C. Kretz-Remy, M. Nivon, A. Czekalla, D. Guillet, M. Moulin, C. Diaz-Latoud, P. Vicart, Hsp27 (HspB1) and alphaB-crystallin (HspB5) as therapeutic targets, FEBS Lett. 581 (2007) 3665–3674.
[50] S. Kostenko, U. Moens, Heat shock protein 27 phosphorylation: kinases, phosphatases, functions and pathology, Cell. Mol. Life Sci. 66 (2009) 3289–3307.
[51] F.K. Storm, K.W. Gilchrist, T.F. Warner, D.M. Mahvi, Distribution of Hsp-27 and HER-2/neu in in situ and invasive ductal breast carcinomas, Ann. Surg. Oncol. 2 (1995) 43–48.
[52] W. Porter, F. Wang, R. Duan, C. Qin, E. Castro-Rivera, K. Kim, S. Safe, Transcriptional activation of heat shock protein 27 gene expression by 17beta-estradiol and modulation by antiestrogens and aryl hydrocarbon receptor agonists, J. Mol. Endocrinol. 26 (2001) 31–42.
[53] D.R. Ciocca, A.O. Stati, M.M. Amprino de Castro, Colocalization of estrogen and progesterone receptors with an estrogen-regulated heat shock protein in paraffin sections of human breast and endometrial cancer tissue, Breast Cancer Res. Treat. 16 (1990) 243–251.
[54] D.R. Ciocca, L.A. Puy, D.P. Edwards, D.J. Adams, W.L. McGuire, The presence of an estrogen-regulated protein detected by monoclonal antibody in abnormal human endometrium, J. Clin. Endocrinol. Metab. 60 (1985) 137–143.
[55] D. Navarro, J.J. Cabrera, L. León, R. Chirino, L. Fernández, A. López, J.F. Rivero, P. Fernández, O. Falcón, P. Jiménez, et al., Endometrial stromal sarcoma expression of estrogen receptors, progesterone receptors and estrogen-induced srp27 (24K) suggests hormone responsiveness, J. Steroid Biochem. Mol. Biol. 41 (1992) 589–596.
[56] S.P. Langdon, G.J. Rabiasz, G.L. Hirst, R.J. King, R.A. Hawkins, J.F. Smyth, W.R. Miller, Expression of the heat shock protein HSP27 in human ovarian cancer, Clin. Cancer Res. 1 (12) (Dec 1995) 1603–1609.
[57] C.S. Foster, A.R. Dodson, L. Ambroisine, G. Fisher, H. Møller, J. Clark, G. Attard, J. DeBono, P. Scardino, V.E. Reuter, C.S. Cooper, D.M. Berney, J. Cuzick, Hsp-27 expression at diagnosis predicts poor clinical outcome in prostate cancer independent of ETS-gene rearrangement, Br. J. Cancer 101 (2009) 1137–1144.
[58] T. Iwaki, J. Tateishi, Immunohistochemical demonstration of alphaB-crystallin in hamartomas of tuberous sclerosis, Am. J. Pathol. 139 (1991) 1303–1308.
[59] M. Takashi, S. Katsuno, T. Sakata, S. Ohshima, K. Kato, Different concentrations of two small stress proteins, alphaB crystallin and HSP27 in human urological tumor tissues, Urol. Res. 26 (1998) 395–399.
[60] P.K. Rigas, S. Kase, N.A. Rao, Expression of alpha-crystallins in human sebaceous carcinoma of the eyelid, Eur. J. Ophthalmol. 19 (2009) 702–707.
[61] S. Kase, J.G. Parikh, N.A. Rao, Expression of alpha-crystallin in retinoblastoma, Arch. Ophthalmol. 127 (2009) 187–192.
[62] S. Kase, J.G. Parikh, N.A. Rao, Expression of heat shock protein 27 and alpha-crystallins in human retinoblastoma after chemoreduction, Br. J. Ophthalmol. 93 (2009) 541–544.
[63] R.H. Hruban, N.V. Adsay, J. Albores-Saavedra, C. Compton, E.S. Garrett, S.N. Goodman, S.E. Kern, D.S. Klimstra, G. Klöppel, D.S. Longnecker, J. Lüttges, G.J. Offerhaus, Pancreatic intraepithelial neoplasia: a new nomenclature and classification system for pancreatic duct lesions, Am. J. Surg. Pathol. 25 (2001) 579–586.
[64] A.J. Aguirre, N. Bardeesy, M. Sinha, L. Lopez, D.A. Tuveson, J. Horner, M.S. Redston, R.A. DePinho, Activated Kras and Ink4a/Arf deficiency cooperate to produce metastatic pancreatic ductal adenocarcinoma, Genes Dev. 17 (2003) (2003) 3112–3126.
[65] S.C. Abraham, T.T. Wu, D.S. Klimstra, L.S. Finn, J.H. Lee, C.J. Yeo, J.L. Cameron, R.H. Hruban, Distinctive molecular genetic alterations in sporadic and familial adenomatous polyposis-associated pancreatoblastomas: frequent alterations in the APC/-catenin pathway and chromosome 11p, Am. J. Pathol. 159 (2001) 1619–1627.
[66] N. Bardeesy, K.-H. Cheng, J.H. Berger, G.C. Chu, J. Pahler, P. Olson, A.F. Hezel, J. Horner, G.Y. Lauwers, D. Hanahan, et al., *Smad4* is dispensable for normal pancreas development yet critical in progression and tumor biology of pancreas cancer, Genes Dev. 20 (2006) (2006) 3130–3146.
[67] H. Ijichi, A. Chytil, A.E. Gorska, M.E. Aakre, Y. Fujitani, S. Fujitani, C.V.E. Wright, H.L. Moses, Aggressive pancreatic ductal adenocarcinoma in mice caused by pancreas-specific blockade of transforming growth factor-signaling in cooperation with active Kras expression, Genes Dev. 20 (2006) 3147–3160.
[68] M. Pasca di Magliano, S. Sekine, A. Ermilov, J. Ferris, A.A. Dlugosz, M. Hebrok, Hedgehog/Ras interactions regulate early stages of pancreatic cancer, Genes Dev. 20 (2006) (2006) 3161–3173.

Cell Death and Differentiation (2010) 17, 1448–1462
© 2010 Macmillan Publishers Limited All rights reserved 1350-9047/10 $32.00
www.nature.com/cdd

Protein phosphatase-1 regulates Akt1 signal transduction pathway to control gene expression, cell survival and differentiation

L Xiao[1,2,4], L-L Gong[1,4], D Yuan[1,2,4], M Deng[1,4], X-M Zeng[2], L-L Chen[2], L Zhang[2], Qin Yan[1], J-P Liu[1], X-H Hu[2], S-M Sun[2], J Liu[2], H-L Ma[2], C-B Zheng[2], H Fu[2], P-C Chen[2], J-Q Zhao[2], S-S Xie[2], L-J Zou[2], Y-M Xiao[2], W-B Liu[2], J Zhang[*,2], Y Liu[2] and DW-C Li[*,1,2,3]

AKT pathway has a critical role in mediating signaling transductions for cell proliferation, differentiation and survival. Previous studies have shown that AKT activation is achieved through a series of phosphorylation steps: first, AKT is phosphorylated at Thr-450 by JNK kinases to prime its activation; then, phosphoinositide-dependent kinase 1 phosphorylates AKT at Thr-308 to expose the Ser-473 residue; and finally, AKT is phosphorylated at Ser-473 by several kinases (PKD2 and others) to achieve its full activation. For its inactivation, the PH-domain containing phosphatases dephosphorylate AKT at Ser-473, and protein serine/threonine phosphatase-2A (PP-2A) dephosphorylates it at Thr-308. However, it remains unknown regarding which phosphatase dephosphorylates AKT at Thr-450 during its inactivation. In this study, we present both *in vitro* and *in vivo* evidence to show that protein serine/threonine phosphatase-1 (PP-1) is a major phosphatase that directly dephosphorylates AKT to modulate its activation. First, purified PP-1 directly dephosphorylates AKT *in vitro*. Second, immunoprecipitation and immunocolocalization showed that PP-1 interacts with AKT. Third, stable knock down of PP-1α or PP-1β but not PP-1γ, PP-2Aα or PP-2Aβ by shRNA leads to enhanced phosphorylation of AKT at Thr-450. Finally, overexpression of PP-1α or PP-1β but not PP-1γ, PP-2Aα or PP-2Aβ results in attenuated phosphorylation of AKT at Thr-450. Moreover, our results also show that dephosphorylation of AKT by PP-1 significantly modulates its functions in regulating the expression of downstream genes, promoting cell survival and modulating differentiation. These results show that PP-1 acts as a major phosphatase to dephosphorylate AKT at Thr-450 and thus modulate its functions.
Cell Death and Differentiation (2010) **17,** 1448–1462; doi:10.1038/cdd.2010.16; published online 26 February 2010

Protein dephosphorylation at the serine and threonine residues of various proteins, similar to their cognate phosphorylation, has important roles in regulating various cellular processes, such as cell differentiation and apoptosis.[1,2] In eukaryotes, ~98% of dephosphorylation occurs at the serine/threonine residues and two major protein phosphatases, namely phosphatase-1 (PP-1) and phosphatase-2A (PP-2A)[3,4] contribute >90% of serine/threonine phosphatase activity. In this regard, we have recently shown that both PP-1 and PP-2A have important roles in modulating apoptosis.[5,6] PP-1 promotes survival through its negative regulation of p53, which is a master regulator of apoptosis. It directly dephosphorylates p53 at Ser-15 and Ser-37 to attenuate its transcriptional and apoptotic activities.[5] PP-2A is also found to modulate the phosphorylation status of p53 at these sites to suppress stress-induced apoptosis.[6,7] In this study, we present the first evidence to show that PP-1 has a critical role during the activation process of Akt1 signaling pathway.

The Akt/protein kinase B consists of three family members (Akt1, Akt2 and Akt3) and has an important role in regulating the survival of most cells.[8,9] It does so through regulation of the functions of various transcription factors that control both proapoptotic and antiapoptotic genes.[9,10] Examples of such genes include the those encoding IKKβ, BAD and GSK.[8,9] Deregulation of the Akt signaling pathway leads to the formation of cancer.[11–14]

In response to growth factors and various stimuli, Akt becomes activated through a series of phosphorylation events. Among the three members, activation of Akt1 is well studied.[8,14] First, a recent study has shown that Akt1 is primed through phosphorylation at Thr-450 in the cytosol by the stress-activated protein kinase, JNK1/2, under certain conditions.[15,16] Second, after activation by the ligand-regulated receptor-tyrosine kinases, the phosphoinositide-3 kinase (PI3K) generates phosphoinositol-3,4,5-triphosphate (PIP3), the lipid secondary messenger that recruits phosphoinositide-

[1]Department of Biochemistry and Molecular Biology, University of Nebraska Medical Center, Omaha, Nebraska 68198-5870, USA; [2]Key Laboratory of Protein Chemistry and Developmental Biology of Educational Ministry of China, College of Life Sciences, Hunan Normal University, Changsha, Hunan 410081, China and [3]Department of Ophthalmology and Visual Sciences, University of Nebraska Medical Center, Omaha, Nebraska 68198-5540, USA
*Corresponding authors: DW-C Li, Department of Biochemistry and Molecular Biology, University of Nebraska Medical Center, 668 S 41th Street, Omaha, Nebraska 68198-5870, USA. Tel: +402 559 5073; Fax: +402 559 6650; E-mail: dwli1688@hotmail.com or J Zhang, College of Life Sciences, Hunen Normal University, Changsha, Hunen 410081, China. Tel: +0731 8887 2792; Fax: +0731 8887 2792; E-mail: zhangijan@hunnu.edu.cn
[4]These authors contributed equally to this work.
Keywords: PP-1; dephosphorylation; Akt1; apoptosis; differentiation
Abbreviations: ARPE-19, retinal pigmental epithelial cells; bFGF, basic fibroblast growth factor; CA, Calyculin A; HLE or HLECs, human lens epithelial cells; JNK1/2/3, c-Jun terminal kinase 1/2/3; PKD1/2, phosphoinositide-dependent kinase 1/2; PHLPPs, PH-domain phosphatases; PIP3, phosphoinositol-3,4,5-triphosphate; PP-1, protein serine/threonine phosphatase-1; PP-2A, protein serine/threonine phosphatase-2A; OA, okadaic acid; S or Ser, serine residue; T or Thr, threonine residue
Received 04.11.09; revised 21.12.09; accepted 25.1.10; Edited by H Ichijo; published online 26.2.10

dependent kinase 1 (PDK1) and Akt1 to the membrane through its PH domain.[8,9] PDK1 thus phosphorylates Akt1 at Thr-308, causing a confirmation change of Akt1 to expose its C-terminal hydrophobic motif.[17,18] Finally, after the configuration change, Akt1 may either undergo autophosphorylation at Ser-473,[19,20] or become phosphorylated by a second kinase referred to as PDK2[21] or other kinases[22,23] at Ser-473 to achieve its full activation.

Akt signaling is terminated by the lipid phosphatase PTEN through dephosphorylation of PIP3.[24,25] The later event leads to dephosphorylation of Akt1 by the PH-domain phosphatases (PHLPPs) at Ser-473.[26,27] Dephosphorylation of Akt1 at Thr-308 is mediated by PP-2A.[28,29] On the other hand, dephosphorylation of Akt1 at Thr-450 remains unknown. In this study, we present both *in vitro* and *in vivo* evidence to show that PP-1 is a major phosphatase dephosphorylating Akt1 at Thr-450. Through this action, PP-1 thus modulates AKT signaling pathway functions in regulating gene expression, cell survival and differentiation.

Results

Inhibition of PP-1 but not PP-2A induces hyperphosphorylation of Akt1 at Thr-450. Recent studies have shown that JNK1/2 are involved in priming Akt1 by phosphorylating Thr-450 for further activation by PDK1 and other kinases during hypoxia/reoxygenation-induced injury of cardiomyocytes under both *in vitro* and *in vivo* conditions.[15,16] To confirm that JNKs also phosphorylate AKT1 at Thr-450, we treated human lens epithelial cells (HLECs) with 1 μM of SP600125 to inhibit JNK-1, JNK-2 and JNK-3.[30] As shown in Supplementary Figure 1A, after inhibition of JNKs for 48 h, the basic phosphorylation of AKT1 at Thr-450 was significantly decreased. Next, to explore which phosphatases may dephosphorylate Akt1 at Thr-450, we treated HLECs with okadaic acid (OA) at 0, 10 and 200 nM to inhibit either PP-2A (10 nM) or PP-1 (200 nM). PP-2A is 100 times more sensitive to OA than PP-1 because of the unique structure of the catalytic subunit.[31] At these OA concentrations, the activities of JNKs showed little changes (Supplementary Figure 1B). On the other hand, although the inhibition of PP-2A by 10 nM OA did not lead to significant change on Akt phosphorylation at Thr-450, inhibition of PP-1 by 200 nM OA led to more than two-fold increases in Akt phosphorylation at Thr-450 (bottom diagram of Figure 1a). The enhanced phosphorylation induced by 200 nM OA is not derived from changed JNK activity as pretreatment of HLE with 1 μM SP600125 did not show significant effect on Akt phosphorylation at Thr-450 (Figure 1b). Similar results were also obtained from another cell line, the human retina pigment epithelial cells (ARPE-19) (Figure 1c and d). To further confirm that inhibition of PP-1 but not PP-2A causes hyperphosphorylation of Akt1 at Thr-450, we treated the two types of cells with calyculin A, which has the same IC_{50} to both PP-1 and PP-2A. As shown in Supplementary Figure 2, calyculin A treatment led to dose-dependent hyperphosphorylation of Akt1 at Thr-450 in both types of cells. These results suggest that PP-1 but not PP-2A seems to be the major phosphatase responsible for dephosphorylation of Akt1 at Thr-450.

PP-1 can dephosphorylate Akt1 at Thr-450 *in vitro*. To show that PP-1 is the major phosphatase that could dephosphorylate Akt at Thr-450, we conducted *in vitro* dephosphorylation assays using purified PP-1 (obtained from New England Biolabs, Ipswich, MA, USA) and PP-2A (from Calbiochem, Gibbstown, NJ, USA). To prepare the dephosphorylation substrates, the GST full-length Akt1 protein and its mutant form (Akt1-T450A) were prepared (Figure 2a), further purified by GST columns (Figure 2b) and then cleaved with thrombin to yield purified Akt1 and Akt1-T450A proteins without GST, which were labeled with JNK1/2 in the presence of ^{32}P-γ-ATP. The labeled proteins were used as substrates for the *in vitro* dephosphorylation assays by purified PP-1 and PP-2A. After dephosphorylation, the free ^{32}P released from substrate proteins by PP-1 or PP-2A was measured in a scintillation counter. As shown in Figure 2c, *in vitro* enzyme concentration-dependent assays showed that PP-1 was more efficient than PP-2A in dephosphorylating the labeled substrate with the same amount of enzyme (PP-1 and PP-2A activities were calibrated as described previously[5,6]). Similarly, time-dependent assays with 1 Unit of PP-1 or PP-2A showed that the free ^{32}P released by PP-1 was much more prominent than PP-2A (Figure 2d). Dephosphorylation of the labeled mutant Akt1-T450A by PP-1 or PP-2A produced just background levels of free ^{32}P (Figure 2c and d). Together, these results suggest that although both PP-1 and PP-2A can dephosphorylate Akt1 at Thr-450 *in vitro*, PP-1 is a more efficient phosphatase to dephosphorylate Akt1 at Thr-450.

The catalytic subunits of PP-1 form a complex with Akt1. To show that PP-1 dephosphorylates Akt1 at Thr-450 under physiological conditions, we first examined whether the catalytic subunit for PP-1 could form an interacting complex with Akt1. To do so, total proteins extracted from HLECs were subjected to coimmunoprecipitation assays. When the proteins coimmunoprecipitated (Co-IP) by goat anti-PP-1α/β were probed with either the antibody against Akt1 or PP-1α/β isoforms of the catalytic subunits, it was found that a clear band of Akt1 was brought down by anti-PP-1α/β (Figure 3a). In the reverse Co-IP assay, it was also found that a clear band of PP-1α/β was bound to Akt1 (Figure 3a). Thus, PP-1 and Akt1 form a strong interacting complex in HLECs. Similar results were obtained using ARPE-19 cells (Figure 3b). Together, immunoprecipitation assays confirmed that in both HLECs and ARPE-19, PP-1 and Akt1 can form an interacting complex. Our results also showed that PP-2A interacts with Akt1 (data not shown). This is not surprising as previous studies have shown that PP-2A dephosphorylates Akt1 at Thr-308.[28,29] Immunocytochemistry analysis showed that both PP-1 and Akt1 displayed partial overlapping in both the cytoplasm and the nucleus within the HLECs (Figure 3c–f) and ARPE-19 cells (Figure 3g–j). In summary, our results showed that PP-1 can dephosphorylate Akt1 at Thr-450.

Knockdown of PP-1α/β but not PP-1γ or PP-2Aα/β leads to significant hyperphosphorylation of Akt1 at Thr-450. To confirm that PP-1 is the major phosphatase dephosphorylating Akt1 at Thr-450 under physiological conditions, we established stable clones to knock down each of the 3 PP-1 catalytic subunits (α, β and γ) and two

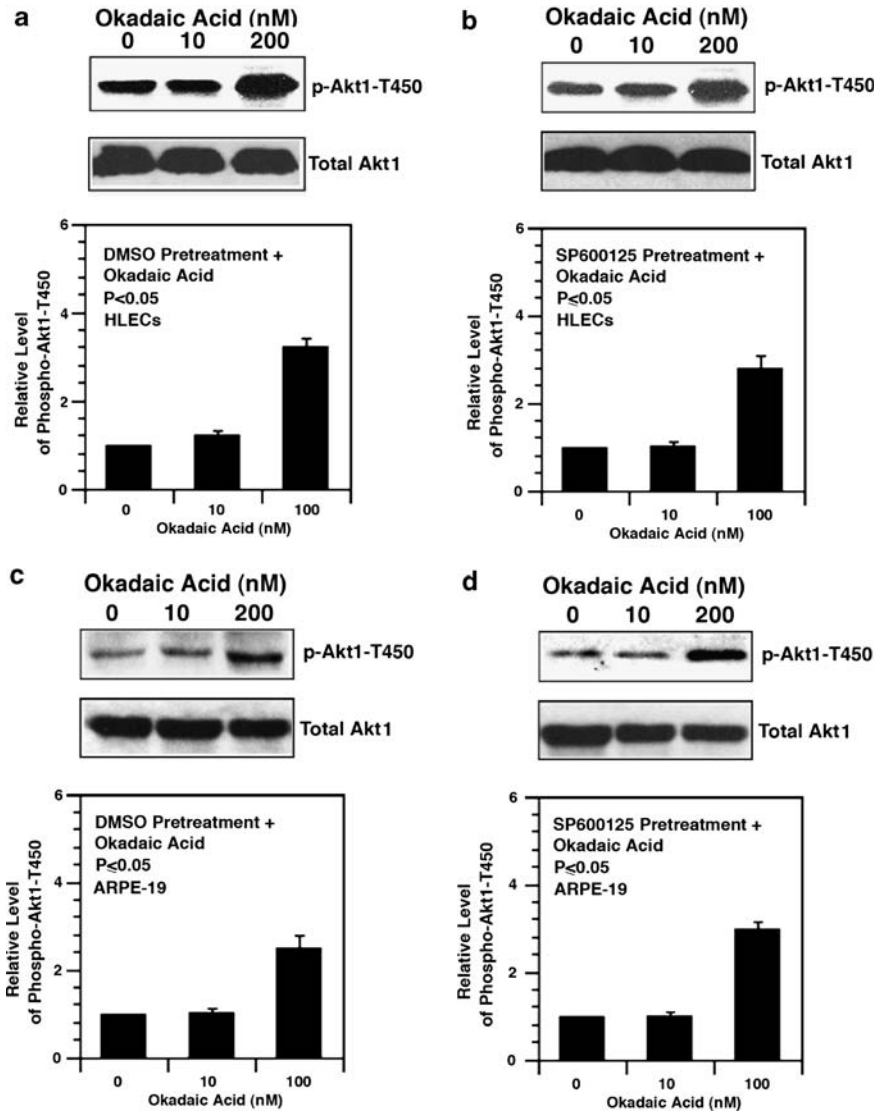

Figure 1 Inhibition of PP-1 but not PP-2A by okadaic acid induces hyperphosphorylation of Akt1 at Thr-450. (**a**, **b**) Human lens epithelial cells (HLECs) or (**c**, **d**) retinal pigment epithelial cells (ARPE-19) were grown to 95% confluence, then pretreated with 0.01% DMSO (panels a and c) or with 1 μM SP600125 ($IC_{50} = 40$ nM for inhibition of JNK1/2) (panels b and d), followed by treatment with 0, 10 or 200 nM okadaic acid for 3 h. By the end of the treatment, the cells were harvested for extraction of total proteins that were separated by SDS-PAGE. The blots were then probed with antibodies against either total Akt1 or specific phospho-Akt1 at Thr-450 (Cell Signaling Inc.) overnight. After washing three times with TBST, the blots were further blotted with donkey anti-rabbit IgG for 45 min. After washing, the blots were visualized using GE Healthcare (GE Healthcare, Piscataway, NJ, USA) reagents. The western blots were scanned, and the relative level of pixel density between phospho-Akt1 at T450 and total Akt1 was quantitated. The results are shown in the bottom of the a–d panels. It must be noted that inhibition of PP-1 (by 200 nM okadaic acid) but not PP-2A (by 10 nM okadaic acid) as previously determined[5] induces hyperphosphorylation of Akt1 at Thr-450, which is hardly affected by the inhibition of JNK1/2 with SP600125. These results suggest that PP-1 but not PP-2A seems to be involved in dephosphorylation of Akt1 at Thr-450. The *P*-value was calculated by comparing the pixel density value from each okadaic acid-treated sample with that from the mock-treated sample

PP-2A catalytic subunits (α and β) using shRNA expression constructs obtained from Open Biosystems Inc., Huntsville, AL, USA (see section 'Experimental Procedures' for details). As shown in Figure 4a and c, knockdown of PP-1α/β in HLECs leads to substantial hyperphosphorylation of Akt1 at Thr-450. However, knockdown of PP-1γ or PP-2Aα/β only caused barely detectable or no enhancement of Akt1 phosphorylation at Thr-450 (Supplementary Figure 3). The dephosphorylation pattern under knockdown of each catalytic subunit of PP-1 or PP-2A displayed no significant change after inhibition of JNK1/2/3 by 1 μM of SP600125 (Figure 4b and d). Although establishment of the stable knockdown clones with ARPE-19 cells was unsuccessful (all cells died through apoptosis), transient transfection with knockdown shRNA plasmids for various catalytic subunits of PP-1 and PP-2A showed similar results (data not shown). Together, these results clearly show that PP-1α/β but not PP-1γ and PP-2Aα/β are the major phosphatase isoforms that dephosphorylate Akt1 at Thr-450 in HLECs and ARPE-19 cells.

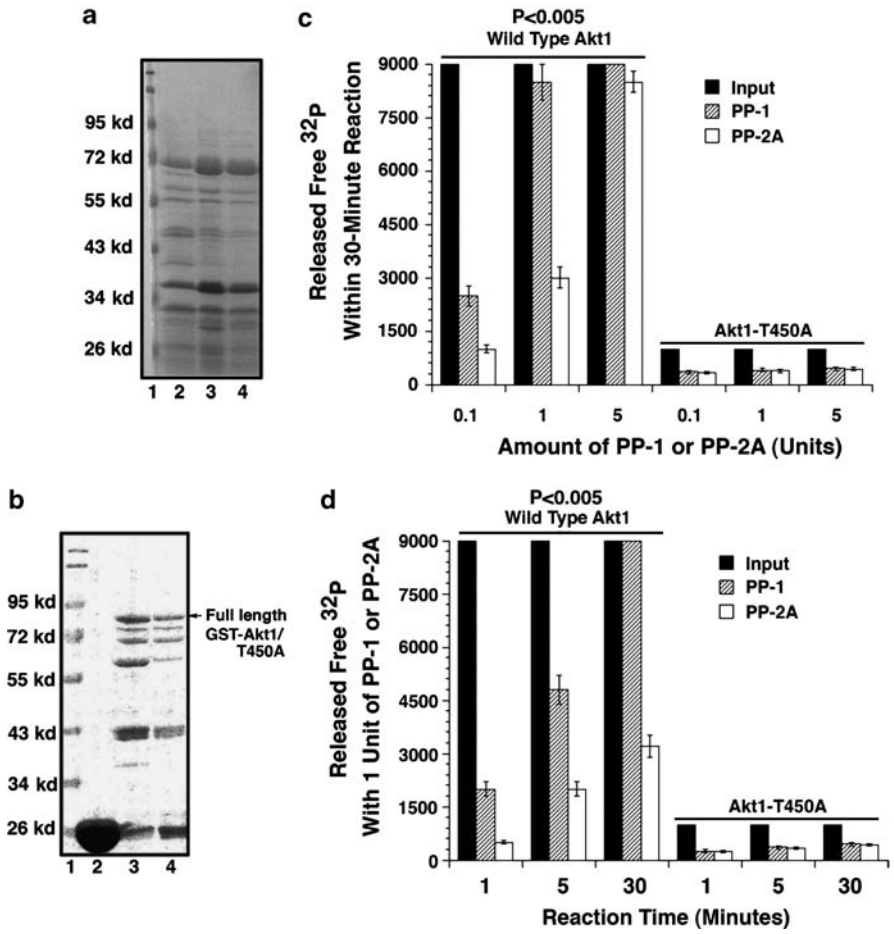

Figure 2 Demonstration that PP-1 dephosphorylates Akt1 at Thr-450 more efficiently than PP-2A does *in vitro*. (**a**) Coomassie staining of total GST, GST-Akt1 and GST-Akt1-T450A fusion proteins. (**b**) Coomassie staining of purified GST, GST-Akt1 and GST-Akt1-T450A fusion proteins. The GST-Akt1 and GST-Akt1-T450A fusion proteins were cleaved with thrombin protease, and Akt1 and Akt1-T450A were further purified and then labeled with JNK1/2, which were used as substrates for the dephosphorylation assays described in **c** and **d**. (panel c) Phosphatase concentration-dependent dephosphorylation by PP-1 and PP-2A. The labeled wild-type Akt-1 (1 μg) and mutant Akt1 (Akt1-T450A, 1 μg) were incubated with 0.1, 1 or 5 Units of PP-1 (New England Biolabs) or PP-2A (Calbiochem) at 30°C in 1 $\times$ dephosphorylation buffer for 30 min. By the end of dephosphorylation, the released free ^{32}P was recovered and measured in a scintillation counter as described previously.[5,54] It must be noted that the amount of free ^{32}P released from labeled Akt1 at each enzyme concentration point by PP-1 was significantly more than that by PP-2A. However, the amount of free ^{32}P released from labeled Akt1-T450A at each enzyme concentration point was similar by PP-1 and PP-2A, which is equal to the blank background level (the blank data were not shown). (Panel d) Time-dependent dephosphorylation assays by PP-1 and PP-2A using 1 μg substrate and 1 Unit of PP-1 or PP-2A. The dephosphorylation reactions lasted for 1, 5 or 30 min. By the end of dephosphorylation, the released free ^{32}P was recovered and measured in a scintillation counter. It must be noted that the amount of free ^{32}P released from labeled Akt1 at each time point by PP-1 was significantly more than that by PP-2A. However, the amount of free ^{32}P released from labeled Akt1-T450A at each time by PP-1 or PP-2A was similar to that from the blank background level (the blank data were not shown). The *P*-value was calculated by comparing the free ^{32}*P*-value from each PP-1 or PP-2A reaction with the input

Overexpression of PP-1α/β but not PP-2Aα/β attenuates Akt1 phosphorylation at Thr-450. To further confirm that PP-1α/β are the major isoform phosphatases that dephosphorylate Akt1 at Thr-450, we overexpressed each of the five catalytic subunits of PP-1 and PP-2A in HLECs. As shown in Figure 5a and c, overexpression of PP-1α/β caused clear hypophosphorylation of Akt1 at Thr-450. In contrast, overexpression of PP-1γ or PP-2Aα/β caused little or no change in the Akt1 phosphorylation status (Supplementary Figure 4). Inhibition of JNK1/2/3 activity by 1 μM of SP600125 had little effect on the Akt1 phosphorylation status at Thr-450 after PP-1 overexpression (Figure 5b and d, Supplementary Figure 4). Similar results were obtained in ARPE-19 cells with transient overexpression of the same catalytic subunits. Together, our results further confirm that that PP-1α/β isoforms act as major phosphatases dephosphorylating Akt1 at Thr-450.

PP-1 dephosphorylation of Akt1 at Thr-450 modulates its regulation of gene expression. Previous studies have shown that Akt1 can indirectly activate NF-κB through activation of IKKs to phosphorylate IκB for its degradation.[8,9] In addition, Akt1 also modulates GSK to regulate downstream genes (Figure 6a). To explore whether PP-1 dephosphorylation of Akt1 at Thr-450 may affect its function, we first examined the modulation of Akt1 regulation of gene expression when PP-1 or PP-2A was inhibited under different OA concentrations. As shown in Figure 6b, when the reporter gene, pNF-κB-Luc and pCI-Akt1 were cotransfected into HLECs, and then treated with either 10 or 100 nM OA,

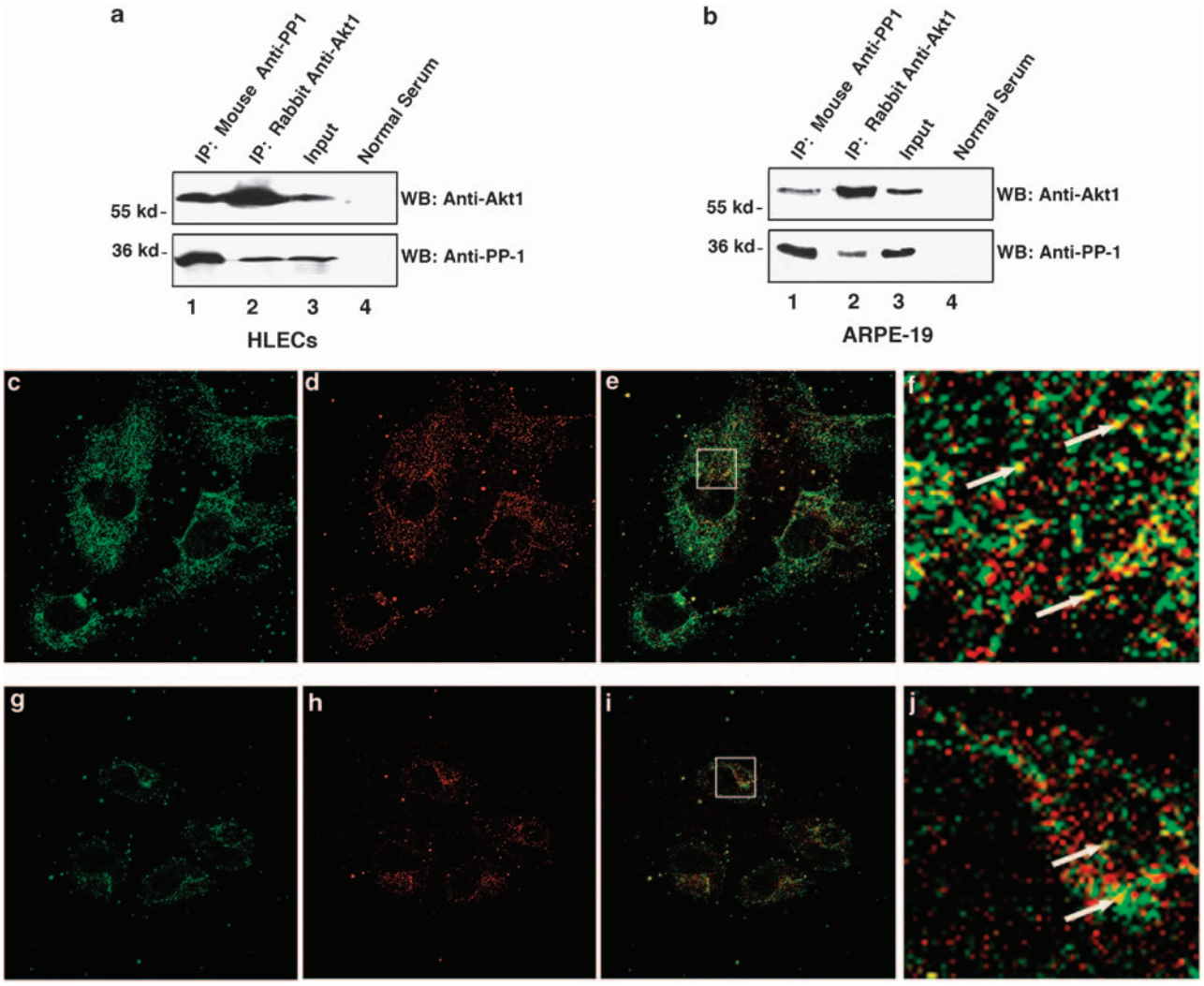

Figure 3 PP-1 interacts with Akt1 within (**a**, and **c**–**f**) human lens epithelial cells (HLECs) and (**b**, and **g**–**j**) retinal pigment epithelial cells (ARPE-19). (Panel a) Coimmunoprecipitation between Akt1 and PP-1 in HLECs. (Panel b) Coimmunoprecipitation between Akt1 and PP-1 in ARPE-19 cells. (Panel c–f) Confocal immunocytochemistry to detect colocalization of Akt1 and PP-1 in HLECs. (Panel c) FITC from anti-Akt1. (Panel d) Texas Red from anti-PP-1α. (Panel e) Merged image from both FITC and Texas Red signals. (Panel f) The stroked region in Figure 3e shows the overlapping of Akt1 and PP-1α (yellow color, arrows). (Panels g–j) Colocalization of Akt1 and PP-1 in ARPE-19 cells. (Panel g) FITC from anti-Akt1. (Panel h) Texas Red from anti-PP-1α. (Panel i) Merged image from both FITC and Texas Red signals. (Panel j) The stroked region in Figure 3i showing the overlapping of Akt1 and PP-1α (yellow color, arrows)

reporter gene activity assays showed that inhibition of PP-1 (by 100 nM OA) but not PP-2A (by 10 nM OA) substantially increased luciferase activity, indicating enhancement of Akt1 activity. To further confirm this result, we cotransfected the pNF-κB-Luc reporter gene with the empty vector pCI-Neo, or the construct expressing wild-type Akt1, or its mutants, imitating either constant dephosphorylation (Akt1-T450A) or constant phosphorylation (Akt1-T450D) in HLECs. The different Akt1 constructs were all expressed in HLECs with similar mRNA levels (data not shown) and protein levels (top panel of Figure 6c). When the luciferase activity was analyzed in each case, it was found that overexpression of either Akt1 or Akt1-T450D doubled the luciferase activity (Figure 6d). However, Akt1 mutation at Thr-450 from threonine to alanine abolished exogenous Akt1 function (Figure 6d). The phosphorylation status of the downstream target, GSK-3β at Ser-9, also confirmed a similar conclusion (Figure 6c). These results indirectly show that dephosphorylation of Akt1 at Thr-450 by PP-1 significantly modulates Akt1 function in regulating gene expression.

Overexpression of PP-1 blocks the positive regulation of gene expression by Akt1. To further confirm that PP-1 modulates Akt1 ability in regulating expression of the downstream genes, we established stable lines expressing Akt1, Akt1-T450A and Akt1-T450D in ARPE-19 cells. We then cotransfected pNF-κB-Luc with pCI-Neo, pCI-PP-1α or pCI-PP2Aα into the stable clones of ARPE-19 cells. As shown in Figure 7a, overexpression of PP-1α leads to hypophosphorylation of Akt1 at Thr-450, and also negatively affected the phosphorylation of Akt1 at T-308 and S-473. As a result, phosphorylation of GSK-3β is significantly downregulated. In contrast, overexpression of PP-2A caused a slight decrease in the phosphorylation of Akt1 at

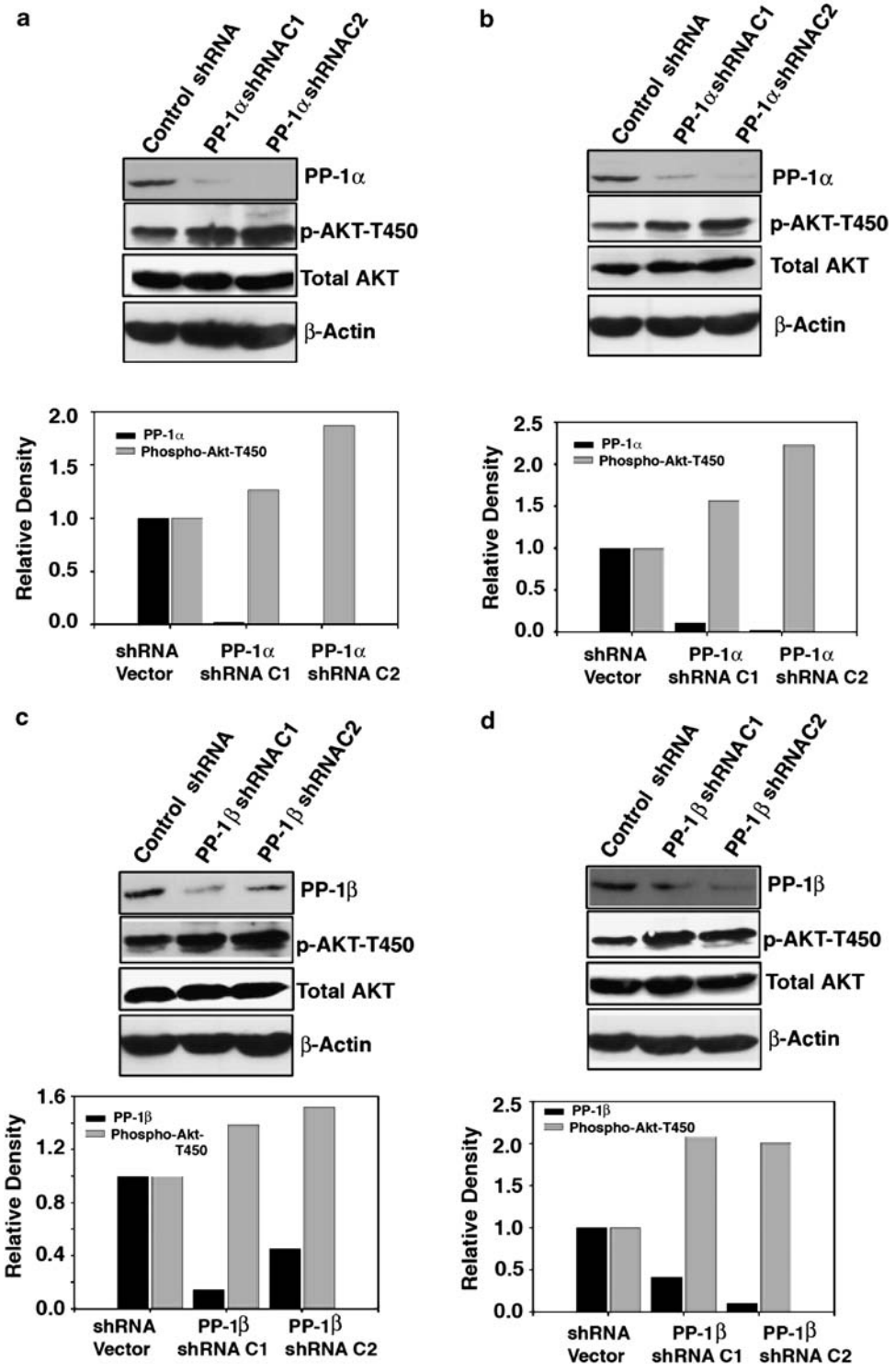

Figure 4 (**a**, **b**) Silence of PP-1α and (**c**, **d**) PP-1β by specific shRNAs enhances hyperphosphorylation of Akt1 at Thr-450 in HLECs without (panels a, c) or with (panels b, d) inhibition of JNK1/2 by 1 μM SP600125 ($IC_{50} = 40$ nM for both JNK1 and JNK2). Two clones (C1 and C2) from each catalytic subunit silence group were selected for comparison with the mock knockdown. The different silence constructs were obtained from Open Biosystems Inc. and amplified. The different constructs were then transfected into HLEC cells, and stable clones expressing shRNA for each catalytic subunit of PP-1 and PP-2A were established under screening by puromycin (250 ng/ml) for 4–6 weeks. The stable clones were first verified by RT-PCR and western blot. It must be noted that knockdown of PP-1α (panels a, b) and PP-1β (panels c, d) leads to hyperphosphorylation of Akt1 at Thr-450, which was not affected by SP600125 treatment. The relative silence of PP-1α and PP-1β, as well as the relative enhancement of Akt1 phosphorylation at Thr-450 under each silence condition, was quantitated by determining the relative levels of pixel density. The results are shown at the bottom of a–d panels

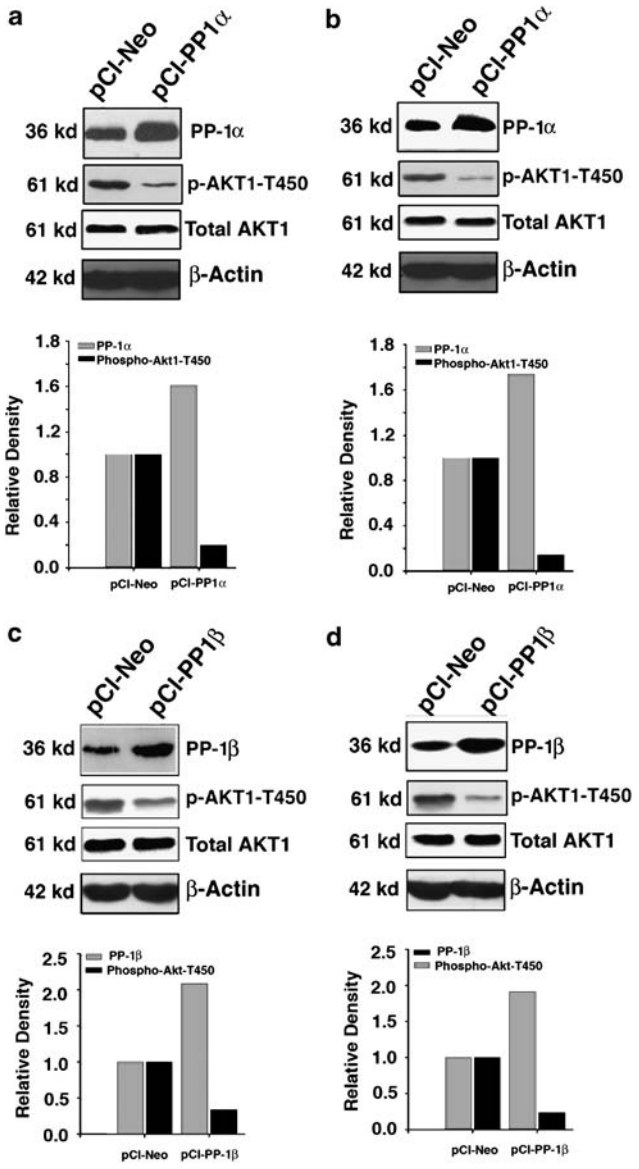

Figure 5 (**a**, **b**) Overexpression of PP-1α and (**c**, **d**) PP-1β in HLECs without (panels a, c) or with (panels b, d) treatment by 1 μM of SP600125 ($IC_{50} = 40$ nM for JNK1/2) causes hypophosphorylation of Akt1 at Thr-450. One clone from each catalytic subunit overexpression was selected for comparison with the vector-transfected clone. The overexpression constructs were prepared as described in the section 'Experimental Procedures'. Different constructs were then transfected into HLECs, and stable clones expressing each catalytic subunit of PP-1 and PP-2A were established under screening by G418 (400 μg/ml) for 4–6 weeks. The stable clones were first verified by RT-PCR and western blot before experimentation. It must be noted that overexpression of PP-1α (panels a, b) and PP-1β (panels c, d) leads to hypophosphorylation of Akt1 at Thr-450, which was not affected by SP600125 treatment. The relative level of overexpression of PP-1α and PP-1β, or the relative decrease in Akt1 phosphorylation at Thr-450 under each overexpression condition was quantitated by scanning the relative pixel level of each band. The quantitative results are shown at the bottom of panels a–d

Thr-450. However, its role in dephosphorylating Akt1 at T-308[29] also leads to hypophosphorylation of Akt1 at S-473 in comparison with vector-transfected cells. When the luciferase activity was measured (Figure 7b), it was found that in the Akt1 stable clone expressing PP-1α transiently, a $>50\%$ decrease in luciferase activity was observed. In the Akt1 stable clone expressing PP-2Aα transiently, $\sim 30\%$ decrease in luciferase activity (Figure 7b) was also observed owing to the fact that PP-2A dephosphorylates Akt1 at T-308 and thus negatively affects the full activation of Akt1 at S-473 (Figure 7a).

Mutation imitating constant dephosphorylation of Akt1 at Thr-450 changes its ability to promote cell survival. It is a well-established fact that the Akt signaling pathway has a very important role in promoting cell survival.[8,9,32–34] Active Akt1 phosphorylates a panel of antiapoptotic and proapoptotic regulators.[8–10] To show that PP-1-mediated dephosphorylation of Akt1 at Thr-450 modulates its survival-promotion ability, we treated Akt1-, Akt1-T450A- and Akt1-T450D-transfected HLECs and ARPE-19 cells with 100 nM staurosporine and examined the viability of the different types of cells (Supplementary Figure 5). As shown in Figure 8a, expression of the exogenous Akt1 enhanced $\sim 30\%$ viability in HLECs. Expression of the mutant Akt1 imitating constant dephosphorylation, Akt1-T450A, significantly abolished the survival-promotion ability of Akt1. In contrast, expression of the mutant Akt1 imitating constant phosphorylation at Thr-450 (Akt1-T450D) enhanced an additional 24% more survival than Akt1 expression cells. Similar results were observed with ARPE-19 cells (Figure 8b). Together, these results showed that dephosphorylation of Akt1 by PP-1 at Thr-450 negatively regulates its survival-promotion ability.

Differential Akt1 expression and activity were observed during mouse eye development. To examine the possible role of active Akt1 in regulating eye development, we examined the expression levels of total Akt1 and phospho-Akt1 at Thr-450, Thr-308 and Ser-473. As shown in Figure 9 (the red fluorescence in row 3), confocal immunofluorescence showed that during mouse eye development, expression of Akt1 was clearly detected in the retina, lens and cornea from 14.5 to 19.5 ED. The expression level became slightly increased in the corresponding eye tissues as development moved from 14.5 to 19.5 ED. Phosphorylation of Akt1 at Thr-450 (green fluorescence in row 5 of Figure 9), Thr-308 (green fluorescence in row 6 of Figure 9) and Ser-473 (green fluorescence in row 7 of Figure 9) is the highest at 14.5 ED and became slightly decreased from 14.5 to 17.5 ED. At 19.5 ED, although phosphorylation of Akt1 at Thr-450 was still detectable, the signals of phosphorylation fluorescence at Thr-308 and Ser-473 became much weaker (Figure 9). Together, our results showed that both the expression and phosphorylation status of Akt1 are developmentally regulated, suggesting its role in regulating eye tissue differentiation.

Akt1 mutation imitating constant dephosphorylation at Thr-450 (Akt1-T450A) abolishes FGF-induced differentiation. Previous studies have shown that bFGF induces lens differentiation under both *in vitro* and *in vivo* conditions.[35–40] To show that PP-1-mediated dephosphorylation may modulate the differentiation-promotion

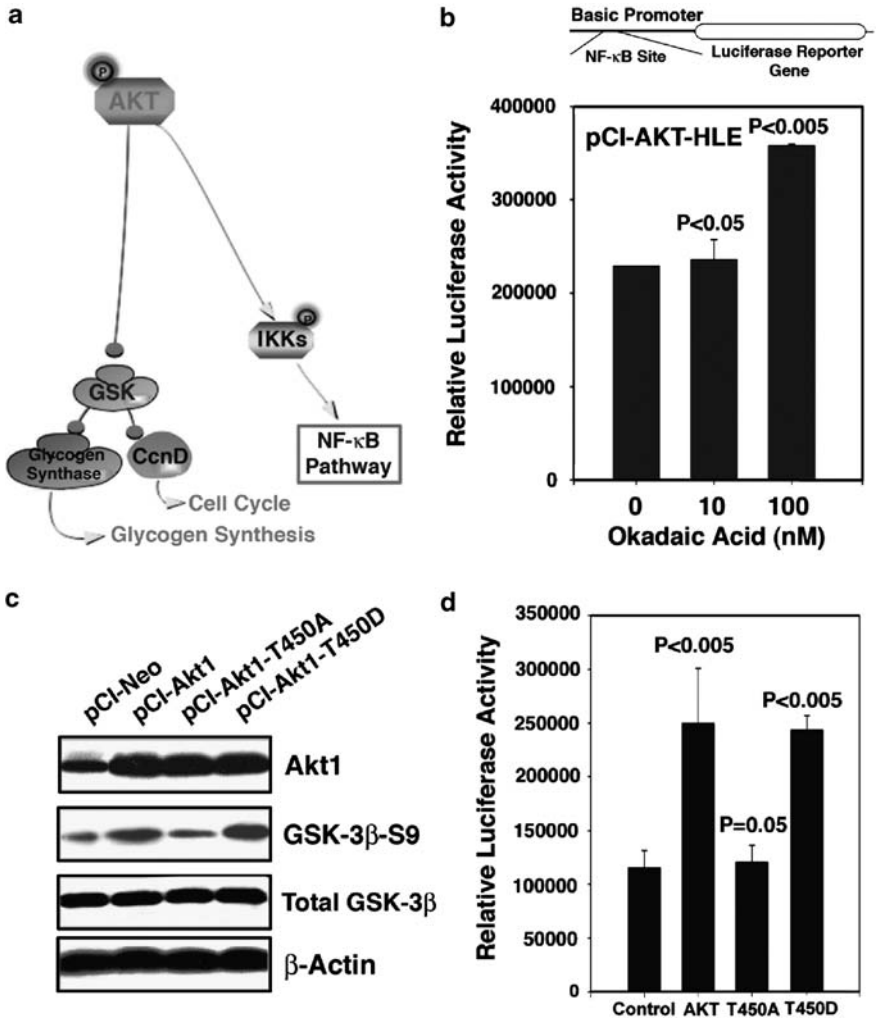

Figure 6 Inhibition of PP-1 by (**b**) okadaic acid or (**c** and **d**) overexpression of Akt1 or Akt1 mutant imitating constant phosphorylation at Thr-450 in HLECs positively modulates Akt1 function in regulating gene expression. (**a**) Diagram showing two downstream pathways subjected to Akt1 regulation. (Panel b) Treatment of HLECs with 100 nM okadaic acid (inhibiting PP-1 and PP-2A) substantially enhances the reporter gene activity driven by a mini-promoter containing an NF-κB binding site. In contrast, inhibition of PP-2A alone by 10 nM okadaic acid only slightly enhances the luciferase reporter gene activity. Inhibition of PP-1 caused hyperphosphorylation of Akt1 at Thr-450, priming Akt1 for further activation by PDK1 and other kinases. Activated Akt1 activates IKKβ to phosphorylate IκB and thus releases NF-κB for translocation into the nucleus to activate the reporter gene expression. (Panel c) Western blot analysis of the expression levels of pCI-Neo vector, pCI-Akt1, pCI-Akt1-T450A and pCI-Akt1-T450D and also the phospho-GSK-3β at Ser-9 in HLECs. It must be noted that the overexpression of wild-type Akt1 or Akt1-T450D enhanced phosphorylation of GSK-3β at Ser-9. (Panel d) Overexpression of Akt1 distinctly enhanced the reporter gene activity compared with expression of the empty vector. Overexpression of the mutant Akt1, Akt1-T450A, imitating constant dephosphorylation of Akt1 at Thr-450, abolished Akt1 function in positively regulating gene expression because of the absence of exogenous Akt1 activation. In contrast, overexpression of Akt1-T450D, imitating constant phosphorylation of Akt1 at Thr-450, also upregulates the luciferase reporter gene activity as did the wild-type Akt1. *P*-value was calculated by comparing the luciferase activity from okadaic acid-treated samples with the DMSO-treated sample (panel b), or that from Akt1, Akt1-T450A or Akt1-T450D overexpression samples with the pCI-neo vector-transfected sample (panel d)

ability of Akt1, we treated Akt1-, Akt1-T450A- and Akt1-T450D-transfected HLECs with 50 ng/ml bFGF for 0, 2 and 5 days, respectively. As shown in Figure 10a, bFGF induced lentoid formation in both Akt1- and Akt1-T450D-transfected cells but not in T450A-transfected cells. Western blot analysis further showed that T450A mutation suppressed bFGF-induced activation of Akt1 (Figure 10b), and also abolished expression of the differentiation marker, β-crystallin, or significantly attenuated expression of N-cadherin, another differentiation marker in lens. Thus, a mutant imitating constant dephosphorylation of Akt1 at Thr-450 by PP-1 abolishes its role of promoting differentiation.

PP-1 modulates Akt1-mediated FGF regulation of lens cell differentiation. To further confirm that the PP-1 dephosphorylation of Akt1 at Thr-450 modulates cell differentiation in the Akt1 stable clone, we transiently expressed PP-1α and then explored the PP-1α effect on FGF-induced differentiation. To do so, both pCI-AKT1/pCI-Neo-αTN4-1 and pCI-AKT1/pCI-PP-1α-αTN4-1 cells were treated with 50 ng/ml bFGF for 0–5 days and the differentiation status was examined. As shown in Figure 11c, FGF induced lentoid formation of the Akt1-expressing cells within 5 days; however, in both Akt1 and PP-1α coexpression cells, bFGF treatment did not induce lentoid formation

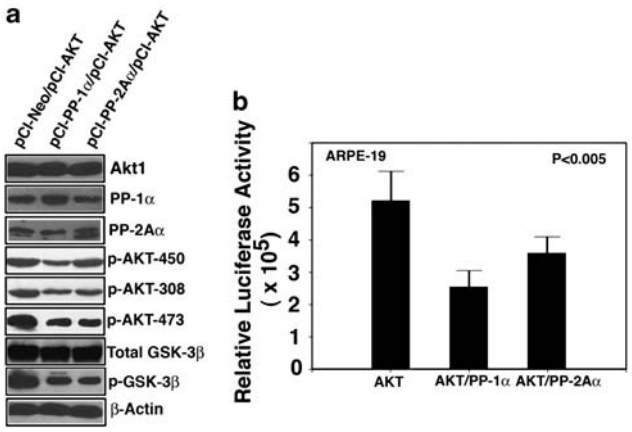

Figure 7 PP-1 dephosphorylation of Akt1 also affects its ability to regulate gene expression in ARPE-19 cells. Coexpression of wild-type Akt1 with pCI-Neo or pCI-PP-1α or pCI-PP-2Aα changes the phosphorylation patterns of Akt1 at Thr-450, Thr-308 and Ser-473, and (**a**) the downstream target GSK-3β phosphorylation status at Ser-9 residue and (**b**) the profile of the luciferase reporter gene activity. In the case of coexpression of wild-type Akt1 with pCI-Neo, pCI-PP1α or pCI-PP2Aα, both PP-1 and PP-2A downregulate GSK-3β phosphorylation status and also reporter gene activity with differential mechanisms. Expression of PP-1 attenuates Akt1 phosphorylation at Thr-450 and thus negatively regulates Akt1 activation by PDK1 and other kinases. However, expression of PP-2A inactivates Akt1 through dephosphorylation at Thr-308. The *P*-value was calculated by comparing the luciferase activity from cotransfection of Akt1 and PP-1α, or Akt1 and PP-2Aα with that from the cotransfection of Akt1 plus the pCI-neo vector (panel b)

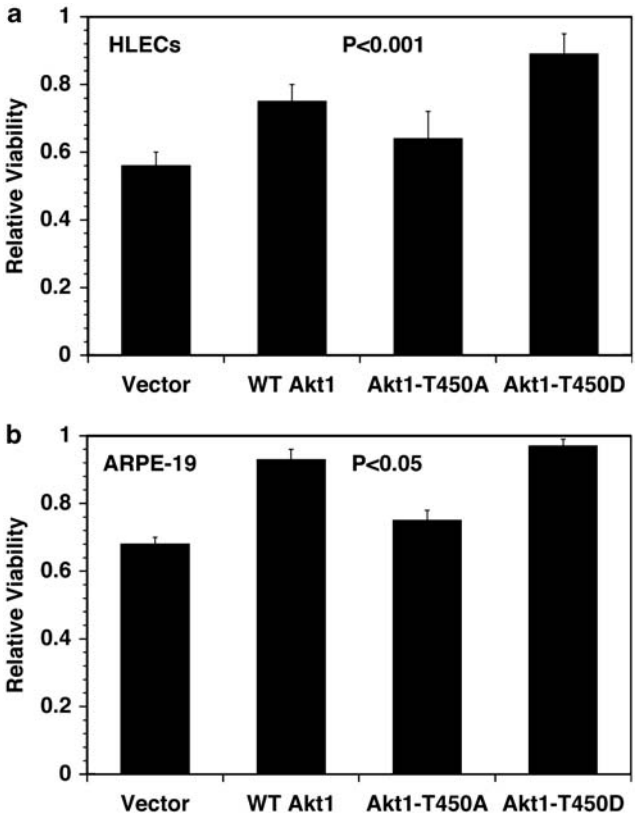

Figure 8 Mutant Akt1, Akt1-T450A, imitating constant dephosphorylation by PP-1 lost most of the survival-promotion ability of wild-type Akt1. (**a**) Stable HLECs and (**b**) ARPE-19 clones expressing pCI-Neo vector, pCI-AKT1, pCI-AKT1-T450A or pCI-AKT1-T450D were treated with a single dose of 100 nM staurosporine for 6 h and then harvested for cell flow cytometry analysis as described previously (also see Supplementary Figure 4).[6,63] It must be noted that AKT1-T450D-transfected cells showed the highest level of survival. In contrast, the AKT1-T450A-transfected cells displayed a level of apoptosis similar to vector-transfected cells, suggesting that Akt1-T450A lost most of the survival-promotion functions of AKT1. *P*-value was calculated by comparing the viability of wild-type Akt1 or mutant Akt1(T450A or T450D)-transfected cells with that of vector-transfected cells

(Figure 11d). Western blot analysis of the proteins extracted from the two types of cells treated by bFGF for 0, 1, 24, 48 and 120 h showed consistent results. As shown in Figure 11e, bFGF induced Akt1 activation and a relatively constant level of αB-crystallin expression during the whole treatment period and also β-crystallin expression on days 4 and 5 in pCI-AKT1/pCI-Neo-αTN4-1 cells, confirming the differentiation status induced by bFGF. In contrast, in pCI-AKT1/pCI-PP-1α-αTN4-1 cells, expression of PP-1α blocked Akt1 activation and also suppressed expression of β-crystallin. These results suggest that by negatively regulating Akt1 activation, PP-1 prevents bFGF-induced lens cell differentiation.

Discussion

In this study, we showed the following: (1) PP-1 is more efficient than PP-2A in dephosphorylating Akt1 at Thr-450 in the *in vitro* dephosphorylation assays; (2) PP-1 and Akt1 can form an interacting complex within HLECs and ARTPE-19 cells; (3) Inhibition of PP-1 but not PP-2A leads to hyperphosphorylation of Akt1 at Thr-450; (4) knockdown of PP-1α/β but not PP-1γ or PP-2Aα/β results in hyperphosphorylation of Akt1 at Thr-450; (5) Overexpression of PP-1α/β but not PP-1γ or PP-2Aα/β causes hypophosphorylation of Akt1 at Thr-450; (6) Mutation imitating constant dephosphorylation of Akt1 at Thr-450 or coexpression of PP-1 and Akt1 leads to down-regulation of Akt1 function in promoting gene expression, cell survival and differentiation. These results confirm that PP-1 but not PP-2A directly dephosphorylates Akt1 at Thr-450 in both HLECs and retinal pigment epithelial cells. Dephosphorylation of Akt1 by PP-1 modulates its functions in regulating gene expression, cell survival and differentiation (Figure 12).

PP-1 is a major phosphatase that dephosphorylates Akt1 at Thr-450. The Akt/PKB signaling pathway has a very important role in promoting cell proliferation, survival and differentiation.[8,9,14] On action by various growth factors, the receptor-tyrosine kinase becomes activated and then activates two important pathways. First, the JNK kinase pathway is activated,[41] which can prime the Akt1 kinase by phosphorylating Thr-450.[15,16] At the same time, the PI3K kinase pathway is activated that converts PIP2 into PIP3.[8,9] PIP3 recruits both Akt1 and PDK1 to the plasma membrane through the PH domain. PDK1 then phosphorylates Akt1 at Thr-308 to partially activate Akt1. After phosphorylation, the C terminal of the Akt1 kinase becomes unfolded and exposes the Ser-473 residue of Akt1, which can be phosphorylated by the putative PDK2 kinase or several other kinases[21,23] to achieve its full activation. When the growth factors are withdrawn, inactivation of the Akt pathway occurs at two

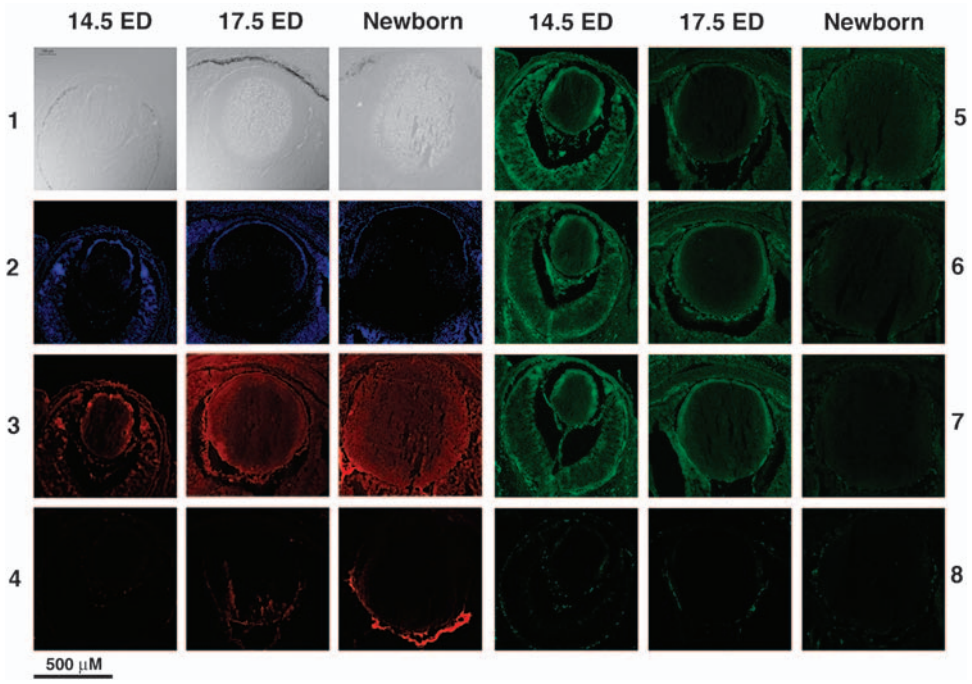

Figure 9 Confocal immunocytochemistry analysis of total and phospho-AKT1 during the development of mouse eye. The mouse eye tissues were fixed and sectioned as described in the section 'Experimental Procedures'. The sections were washed and blocked with 500 μl of 5% normal goat serum (Sigma) in PBS for 1 h at room temperature and then incubated overnight in 400 μl of diluted antibodies (1 : 100) in a humidified chamber at 4°C. The sections were then washed, followed by incubation in 400 μl of secondary antibodies linked to Texas Red (total Akt1, panel 3) or FITC (phospho-Akt1 at Thr-450 (panel 5), phospho-Akt1 at Thr-308 (panel 6), and phospho-Akt1 at Ser-473 (panel 7)) from Vector Laboratories at 1 : 1000 dilution in blocking solution for 1 h in the absence of visible light. After incubation, sections were washed and then observed under a Zeiss confocal fluorescence microscope. For negative controls, the sections were treated in the same manner, except that the primary antibody was replaced by normal serum (row 4, control for total Akt1; or row 8, control for phospho-Akt1). Row 1 shows morphology of bright field image; row 2 displays nuclei from Hoechst staining. It must be noted that from 14.5 to 19.5 ED, the signal for total Akt1 was slightly increased. The phospho-Akt1 signals, regardless at T450, T308 or Ser-473, were gradually decreased from 14.5 to 17.5 ED. At 19.5 ED, however, the signal for phospho-Akt1 at Thr-450 is relatively stronger than that at Thr-308 and Ser-473; consistent with this, phosphorylation of Akt1 at Thr-450 is important for its further activation through phosphorylation at Thr-308 and Ser-473 by PDK1 and other kinases[15,16,21–23]

levels. First, the PTEN tyrosine phosphatase will convert PIP3 into PIP2 to prevent further activation of the PDK kinases.[24,25] Second, the PH domain phosphatases will dephosphorylate Akt1 at Ser-473 and possibly at Thr-308.[26,27] In addition, recent studies have shown that PP-2A directly dephosphorylates Akt1 at Thr-308 to further inactivate Akt1.[16,28,29] For Akt1 to become completely inactivated, the Thr-450 of Akt1 needs to be dephosphorylated. In this study, we have presented both *in vitro* and physiological evidence to show that PP-1 is the major phosphatase that dephosphorylates Akt1 at Thr-450. First, PP-1 and Akt1 form a complex and are colocalized in both the cytoplasm and the nucleus. Second, inhibition or knockdown of PP-1 but not PP-2A leads to hyperphosphorylation of Akt1 at Thr-450. Third, overexpression of PP-1α/β but not PP-2Aα/β causes hypophosphorylation of Akt1 at Thr-450. Thus, in both lens epithelial cells and retina pigment epithelial cells, PP-1 is the major phosphatase that dephosphorylates Akt1 at Thr-450 to completely inactivate it. Among the three different catalytic subunits, our data also showed that the α- and β-isoforms but not the γ-isoform are mainly involved in dephosphorylation of Akt1at Thr-450 (Figures 4 and 5). Dephosphorylation of Akt1 at Thr-450 by PP-1 has significant effects on Akt1 functions that are discussed below.

PP-1 dephosphorylation of Akt1 at Thr-450 modulates the functions of the Akt1 signaling pathway. Previous studies have shown that the Akt signaling pathway has an important role in regulating gene expression.[8,9] Akt1 does so through modulation of the functions of multiple transcription factors, including FKHR, AFX and NF-κB, etc.[8] For example, by activating IKKβ through phosphorylation, Akt1 indirectly removes the inhibitory subunit IκB from the nuclear factor NF-κB complex and thus allows its nuclear translocation to positively regulate the expression of target genes. In this study, we used a luciferase reporter gene driven by a mini-promoter containing an NF-κB binding site to explore modulation of Akt1-regulated gene expression by PP-1. We show that inhibition of PP-1 activity by OA or mutation of Akt1 imitating constant phosphorylation at Thr-450 significantly enhanced the luciferase reporter gene activity (Figures 6 and 7). In contrast, overexpression of PP-1α or the mutation imitating constant dephosphorylation of Akt1 at Thr-450 significantly downregulates activity of the luciferase reporter gene (Figures 6 and 7). In addition, expression of the mutant imitating constant dephosphorylation (pCI-AKT1-T450A) also distinctly attenuates Ser-9 phosphorylation of GSK-3β (Figure 6c). Together, these results show that dephosphorylation of Akt1 at Thr-450 by PP-1 significantly modulates its function in regulating gene expression. In this

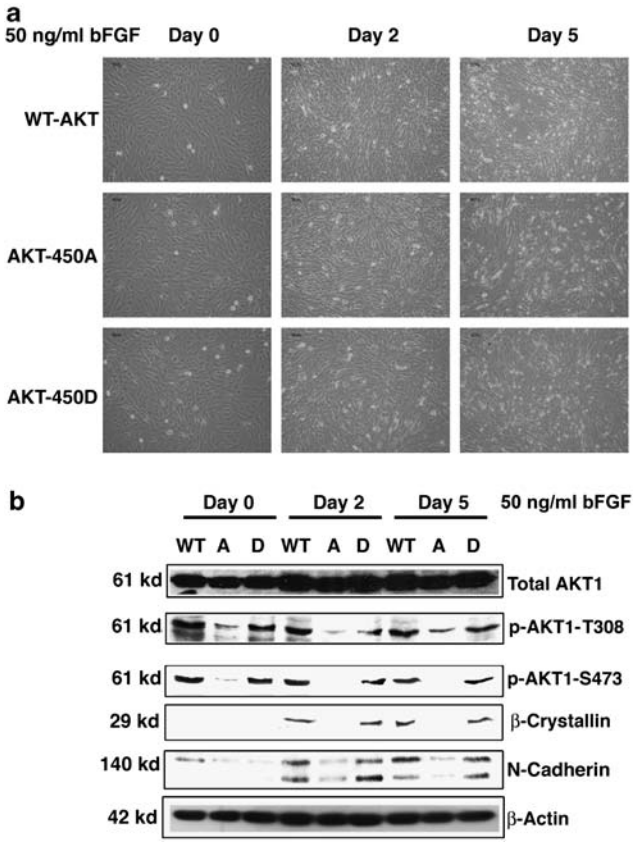

Figure 10 Mutant Akt1, Akt1-T450A, imitating constant dephosphorylation by PP-1 suppresses Akt1-mediated cell differentiation. Stable HLEC clones expressing pCI-AKT1, pCI-AKT1-T450A or pCI-AKT1-T450D were treated with 50 ng/ml bFGF for 0, 2 and 5 days, and the morphology of each group of cells was monitored with light microscopy. At the same time, the treated cells at different stages were harvested for extraction of total proteins that were used for analysis of Akt expression level and phosphorylation status, and also expression of the differentiation markers β-crystallin and N-cadherin. It must be noted that both AKT1- and AKT1-T450D-transfected cells can form lentoid after bFGF induction. (**a**) This is suppressed in the AKT1-T450A-transfected cells. (**b**) Western blot analysis showed that in AKT1 and AKT1-T450D-transfected cells, Akt1 was fully activated and the differentiation markers β-crystallin and N-cadherin were clearly detected. In contrast, in AKT1-T450A-transfected cells, activation of AKT1 was largely suppressed and expression of the differentiation markers was also inhibited. These results suggest that mutation imitating constant dephosphorylation by PP-1 interferes with Akt1-mediated promotion of differentiation

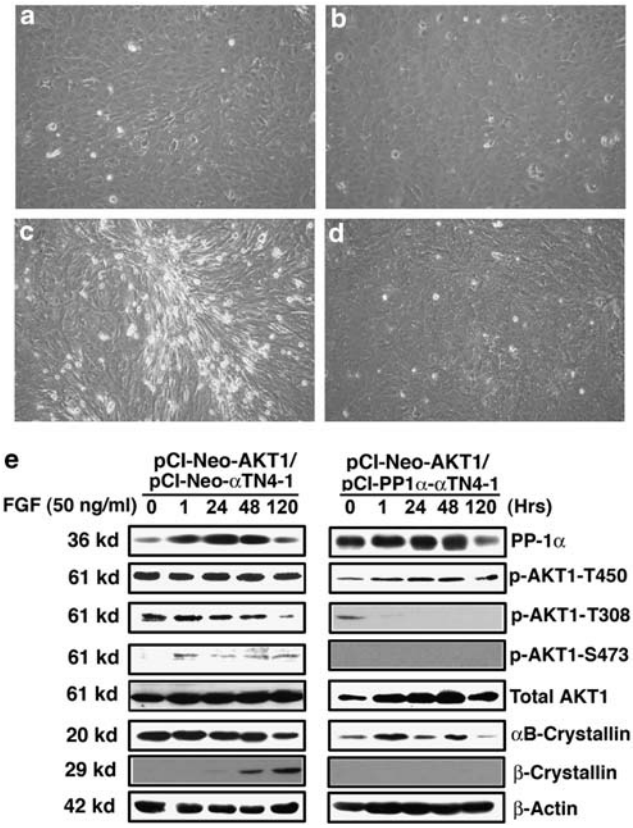

Figure 11 PP-1 modulates Akt1 function in mediating bFGF-induced cell differentiation. The pCI-AKT1/pCI-neo or pCI-AKT1/pCI-PP-1α co-transfected stable clones were treated with 50 ng/ml bFGF for 0–5 days. (**a**) Confluent pCI-Akt1/pCI-Neo-αTN4-1 cells after bFGF treatment for 0 day. (**b**) Confluent pCI-Akt1/pCI-PP-1α-αTN4-1 cells after bFGF treatment for 0 day. (**c**) Confluent pCI-Akt1/pCI-Neo-αTN4-1 cells after bFGF treatment for 5 days. (**d**) Confluent pCI-Akt1/pCI-PP-1α-αTN4-1 cells after bFGF treatment for 5 days. (**e**) pCI-Akt1/pCI-Neo-αTN4-1 cells (left panels) and pCI-Akt1/pCI-PP-1α-αTN4-1 cells (right panels) were treated with 50 ng/ml bFGF for 0, 1, 24, 48 and 120 h and then harvested for extraction of total proteins that were then subjected to western blot analysis as described in the section 'Experimental Procedures'. It must be noted that in pCI-Akt1/pCI-Neo-αTN4-1 cells, bFGF induced lentoid formation within 5 days of treatment (panel c), and the differentiation nature was confirmed by expression of the lens differentiation marker, β-crystallin (left panels of e). However, expression of PP-1α suppressed bFGF-induced lentoid formation (panel d) and β-crystallin expression because of the lack of Akt1 activation (right panels of e)

study, we also observed that although overexpression of PP-2A does not contribute much to the phosphorylation status of Akt1 at Thr-450 (Figure 5), it also downregulates the reporter gene activity to some degree as PP-1 does. The downregulations observed in both cases are derived from different mechanisms. In the case of PP-1α overexpression, it dephosphorylates Akt1 at Thr-450 to block Akt1 activation. In contrast, overexpression of PP-2A dephosphorylates Akt1 at Thr-308 to inactivate it.[16,28,29]

The Akt signaling pathway has a key role in promoting cell survival.[8,9,16,32–34] Dephosphorylation of Akt1 at Thr-450 by PP-1 also affects its survival-promotion ability. In this study, we show that in both lens epithelial cells and retinal pigment epithelial cells, Akt1 mutation imitating constant dephosphorylation at Thr-450 significantly attenuated its ability to resist on staurosporine-induced apoptosis (Supplementary Figure 5 and Figure 8). On the other hand, in these cells, Akt1 mutation imitating constant phosphorylation at Thr-450 enhances its ability to prevent staurosporine-induced apoptosis. Our results are consistent with those of earlier studies.[16] Thus, dephosphorylation of Akt1 at Thr-450 by PP-1 negatively regulates its survival-promotion activity.

The Akt1 signaling pathway is known to mediate cell differentiation.[35,36,42–45] In this study, we also show that during mouse eye development, both the expression and phosphorylation of Akt1 at Thr-450, Thr-308 and Ser-473 are clearly detected at 14.5 and 17.5 ED. At 19.5 ED, although expression and phosphorylation of Akt1 at Thr-450 are still

clearly detectable, phosphorylation of Akt1 at Thr-308 and Ser-473 at 19.5 ED becomes less obvious. This is not surprising considering that the Akt pathway is important for protecting tissue cells during rapid growth of the embryonic eye. Consistent with the role of Akt1 mediating ocular tissue differentiation is our *in vitro* results that FGF-induced differentiation of mouse lens epithelial cells requires Akt1 signaling (Figures 10 and 11). Overexpression of the mutant Akt1, Akt1-T450A in HLECs or overexpression of PP-1α in Akt1-expressing mouse lens epithelial cells prevents both Akt1 activation and also lens cell differentiation induced by FGF (Figures 10 and 11). Thus, through dephosphorylation of Akt1 at Thr-450, PP-1 also modulates Akt1 function in mediating cell differentiation.

Together, our results show that PP-1 negatively modulates Akt1 functions in regulating gene expression, cell survival and differentiation through dephosphorylation at Thr-450.

PP-1 can regulate multiple signaling pathways to control cell death and differentiation. As discussed earlier, accumulated evidence shows that protein dephosphorylation at the serine and threonine residues on proteins has important roles in regulating both cell death and cell differentiation.[1,2] PP-1 regulates these cellular processes through the regulation of several major signaling transduction pathways. First, as we have shown in this study, PP-1, through its engagement in dephosphorylation of Akt at Thr-450, can regulate Akt activity and also its downstream targets, both GSK-3β and IKK, to suppress differentiation but promote apoptosis (Figure 12). Second, the Wnt/β-catenin signaling pathway has a pivotal role in modulating cellular proliferation, differentiation, tissue organization and embryonic development. A recent study has shown that PP-1 is involved in modulating the Wnt/β-catenin pathway.[46] PP-1 is found to interact with Axin and thus dephosphorylates it to activate the Wnt/β-catenin pathway. This activation can be blocked by the endocytic adaptor disabled (Dab2) protein through direct interaction between PP-1 and Dab2.[46] Third, PP-1 can regulate the TGFβ signaling pathway. PP-1 negatively regulates this pathway through the direct dephosphorylation of TGFβ type I receptor (TGFβRI). Under stress conditions such as UV irradiation, Smad7 is induced to interact with growth arrest and DNA damage protein, GADD34, which recruits PP-1 to TGFβRI and dephosphorylates the latter to inhibit TGFβ-induced cell-cycle arrest and mediate TGFβ resistance.[47] Fourth, PP-1 can directly modulate NF-κB activation pathway, a major pathway mediating survival and differentiation in both immune and other systems. PP-1 regulates this pathway through interactions with the CUE domain-containing 2 (CUED2) protein through GADD34, recruits PP-1 to dephosphorylate IKK and thus inactivates the NF-κB pathway.[48] Finally, PP-1 modulates the unfolded protein response (UPR) pathway. Endoplasmic reticulum stress such as the protein misfolding activates UPR, which includes dephosphorylation of the eukaryotic initiation factor 2α (eIF2α) and inhibition of overall protein synthesis. On the other hand, UPR leads to the translation of a subset of mRNAs including those coding ATF4, CHOP and BiP.[49–52] The upregulation of ATF4 induces transcription of downstream genes such as GADD34, which recruits PP-1 to dephosphorylated eIF2α and thus attenuates the UPR response.[49–52]

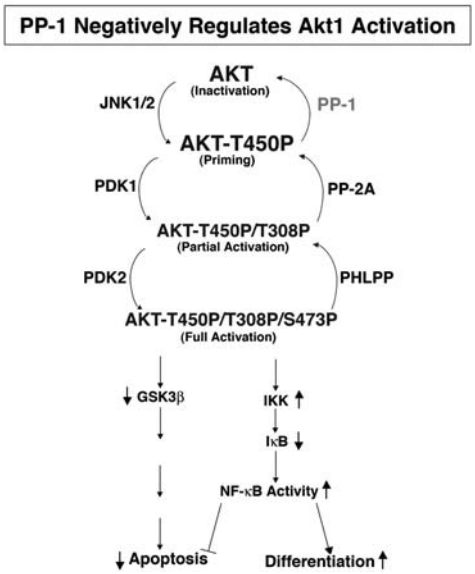

Figure 12 Diagram showing PP-1 negatively regulating Akt-1 activation. Akt1 is first primed through phosphorylation at Thr-450 in the cytosol by the stress-activated protein kinase, JNK1/2, under certain conditions. After activation by the ligand-regulated receptor-tyrosine kinases, the phosphoinositide-3-kinase (PI3K) generates phosphoinositol-3,4,5-triphosphate (PIP3), which recruits phosphoinositide-dependent kinase 1 (PDK1) and Akt1 to the membrane through its PH domain to allow PDK1 phosphorylating Akt1 at Thr-308, thus causing a confirmation change of Akt1 to expose its C-terminal hydrophobic motif. Finally, after the configuration change, Akt1 may either undergo auto-phosphorylation at Ser-473 or become phosphorylated by a second kinase referred to as PDK2 or other kinases at Ser-473 to achieve its full activation. Activated Akt1 can phosphorylate GSK-3β to inactivate its activity, and at the same time, activate IKKβ to phosphorylate IκB and release NF-κB into the nucleus. As a result of these actions, Akt1 can suppress apoptosis and promoter cell differentiation. On the other hand, Akt1 is first dephosphorylated by PHLPP at Ser-473, and later by PP-2A at Thr-308. We show here that PP-1 specifically dephosphorylates Akt1 at Thr-450 to completely inactivate Akt1

Besides the regulation of the above-mentioned major signaling pathway, PP-1 also modulates differentiation and cell death through dephosphorylation of individual molecules. For example, during myogenic differentiation of embryonic muscle cells, PP-1 has an important role. The myristoylated alanine-rich C kinase substrate (MARCKS) translocates from the cytosol to the plasma membrane when mononucleated myoblasts fuse to form multinucleated myotubes. Dephosphorylation of MARCKS by PP-1 is important for myogenic cell fusion. A mutation preventing MARCKS phosphorylation facilitates its translocation and results in the promotion of cell fusion.[53] Pax-6 is an important transcriptional factor that mediates control on both brain and eye development. Our recent study shows that PP-1 directly dephosphorylates Pax-6 to attenuate its transcriptional activity in HLECs.[54]

The two major tumor suppressors, p53 and Rb, are important in regulating cell death. p53 regulates apoptosis either through direct interaction with antiapoptotic regulators or through control of a panel of downstream apoptosis genes.[55–58] We have recently shown that PP-1 can dephosphorylate p53 at multiple sites to attenuate its transcriptional

activity and also its proapoptotic activity in both lens and non-lens cells.[5] On the other hand, dephosphorylation of Rb by PP-1 promotes its ability to bind to members of the E2F family and thus negatively regulates apoptosis.[59] Together, these results point to the conclusion that PP-1 regulates multiple signaling pathways and targets to control cell differentiation and apoptosis.

Experimental Procedures

Cell culture. The hTERT-transfected HLECs[60] and ARPE-19 cells[61] were grown in Dulbecco's modified Eagle's minimal essential medium (DMEM) (Invitrogen Life Technologies, Carlsbad, CA, USA) containing 10% fetal bovine serum and 50 Units/ml penicillin and streptomycin. All cells were kept at 37°C and 5% CO_2 gas phase. HLECs stably transfected with pCI-neo vector, pCI-AKT, pCI-AKT-T450A, pCI-AKT-T450D, pCI-PP-1α, pCI-PP-1β, pCI-PP-1γ, pCI-PP-2Aα and pCI-PP-2Aβ were grown in DMEM containing 400 μg/ml G418, 10% fetal bovine serum and 50 Units/ml penicillin and streptomycin. Similarly, ARPE-19 cells stably transfected with pCI-neo vector, pCI-AKT, pCI-AKT-T450A and pCI-AKT-T450D were also grown in DMEM containing 400 μg/ml G418, 10% fetal bovine serum and 50 Units/ml penicillin and streptomycin.

Preparation of expression constructs. The human Akt1 cDNA was obtained from ATCC (Manassas, VA, USA). The complete coding sequence for Akt1 was excised and inserted into the BamHI/SalI sites of pGEX 4T-1 vector to generate the GST fusion protein using the following primer pairs: 5′-TCCGGATCCATGAGCGACG-TG GCTATTGTGA-3′ (forward, F) and 5′-gacgtcgacTCAGGCCGTGCCG-CTGGC-3′ (reverse, R). For mutant Akt1-T450A, two primers, 5′-ATGATCACCATCGC ACCACCTGACC-3′ (F) and 5′-GGTCAGGTGGTGCG-ATGGTGATCAT-3′ (R), were used, and for mutant Akt1-T450D, 5′-ATGATCA-CCATCGACCCACC TGACC-3′ (F) and 5′-TTGGTCAGGTGGGTCGATG-GTGATC-3′ (R) were used. The mutant Akt1 expression constructs, pCI-neo-AKT-T450A and pCI-AKT-T450D were generated using PCR-linked *in vitro* mutagenesis as described previously.[5,6,61] Both wild-type and mutant constructs were cloned into pCI-neo vector at the EcoRI (5′) and SalI (3′) sites.

The human PP-1α, PP-1β, PP-1γ, PP-2Aα and PP-2Aβ catalytic subunits were purchased from ATCC. The coding sequence was excised and inserted into the pCI-neo vector as described previously.[6,54] The luciferase reporter gene driven by a mini-promoter containing a NF-κB binding site was purchased from Panomics (Fremont, CA, USA).

Stable and transient transfection. pCI-neo, pCI-AKT, pCI-AKT-T450A, pCI-AKT-T450D, pCI-PP-1α, pCI-PP-1β, pCI-PP-1γ, pCI-PP-2Aα and pCI-PP-2Aβ were amplified in DH-5α and purified using Qiagen kits (Qiagen, Valencia, CA, USA) or cesium chloride ultracentrifugation as described previously.[5,6,60,61] After treatment with RNase and extraction by phenol/chloroform, the plasmids were transfected into HLECs,[60] ARPE-19 cells[61] or αTN4-1 cells[62] using Lipofectamine 2000 (Invitrogen Life Technologies). The transfected cells were either used for experimentation or subjected to G418 (400 μg/ml) selection for 4–6 weeks. In the latter case, the individual clones for the stably transfected cell lines were established and confirmed with RT-PCR and western blot analysis.

Pretreatment by JNK1/2 inhibitor, SP600125. Parental or various silence constructs-transfected or overexpression HLEC clones were grown to 95% confluence, then pretreated with 1 μM SP600125, JNK1/2 inhibitor ($IC_{50} = 40$ nM for JNK1/2 and 90 nM for JNK3) or 0.01% DMSO (mock) for 0, 6, 24 or 48 h, as described previously,[30,63] followed by treatment with 0–100 or 200 nM OA for 3 h in DMEM (for HLECs) or no further treatment (for detection of basic AKT-Thr-450 phosphorylation level, or for various PP-1 and PP-2A knockdown or overexpression clones). After treatment, cells of different samples were harvested and then the total proteins were isolated for western blot analysis as described below.

Treatment by staurosporin, OA and calyculin A. Parental or various plasmid-transfected HLECs or ARPE-19 cells were grown to 95% confluence subjected to pretreatment or without pretreatment. A volume of 10 ml of DMEM medium containing 0.01% DMSO (control) or different concentrations of OA, calyculin A or 100 nM staurosporin was then used to replace the culture medium and the treatment was continued for 3 h. After treatment, cells of different samples were harvested and then the total proteins were isolated for western blot analysis as described below.

Silence of the five catalytic subunits of PP-1 and PP-2A. Various human shRNA expression constructs targeting the knockdown of PP-1α, PP-1β, PP-1γ, PP-2Aα and PP-2Aβ (Cat no. RHS3979-1022 to RHS3979-1080), as well as the control construct (RHS4078), were purchased from Open Biosystems Inc. Knockdown clones of stable transfection were established under screening with 0.25 μg/ml puromycin for a period of 4 weeks.

Flow cytometry analysis. The apoptosis rate of the pCI-neo-, pCI-AKT-, pCI-AKT-T450A- and pCI-AKT-T450D-transfected stable clones were determined using an Annexin V-FITC Apoptosis Detection kit (BD Biosciences, San Jose, CA, USA) as described previously.[63] Briefly, the treated cells were trypsinized, washed twice with ice-cold Dulbecco's phosphate-buffered saline and incubated at room temperature for 15 min in the dark with Annexin V-conjugated FITC and propidium iodide in the binding buffer provided. Stained cells were analyzed by flow cytometry using FACSCalibur (BD Biosciences, San Jose, CA, USA).

Protein preparation and western blot analysis. Total proteins from either treated or non-treated cells were extracted as described previously.[5,6] Total proteins were extracted from various types of cells as specified in the figure legends. The protein concentration was determined as described previously.[5,6] In all, 50 or 100 μg of total proteins were used for each lane of loaded sample. The protein blots were blocked with 5% milk in TBS buffer overnight at 4°C and then incubated for 1 h or overnight with antibodies against total Akt1, phospho-Akt1 at Thr-308, Thr-450 and Ser-473 (Cell Signaling Inc., Danvers, MA, USA), α-crystallin (a kind gift from Dr. Joseph Horvitz, UCLA), PP-1$\alpha/\beta/\gamma$, PP-2Aα/β, β-crystallin and N-cadherin (Santa Cruz Biotechnology Inc., Santa Cruz, CA, USA) and β-actin antibody (Sigma, St. Louis, MO, USA) at a dilution of 1 : 200–3000. The secondary antibody was anti-mouse IgG, anti-rabbit IgG or anti-goat IgG (Habersham Biosciences, Piscataway, NJ, USA) or anti-goat IgG (Santa Cruz Biotechnology Inc.) at a dilution of 1 : 1000–3000. Immunoreactivity was detected as described previously.[60–63]

Immunoprecipitation. Immunoprecipitation of total proteins from normal HLECs and ARPE-19 cells was conducted as described previously.[5,6]

***In vitro* phosphorylation of the purified Akt1 and Akt1-T450A proteins.** The fusion proteins of GST-Akt1, GST-Akt1-T450A were prepared as described previously.[5,6,54] The fusion protein was further purified by GST column and then cleaved by thrombin protease. Finally, purified Akt1 or Akt1-T450A without GST was used as substrate for the *in vitro* phosphorylation by JNK1/2. To prepare active JNK1/2 kinases, 10 μg of mouse anti-JNK antibody was added to 1 mg of total proteins extracted from HLECs or ARPE-19 cells. After vortexing for 10 s, the mixtures were incubated on ice for 1 h. A volume of 100 μl of protein A/G plus agarose beads was then added to each protein solution, and the protein solutions were subjected to rotation at 4°C overnight. Pellets were collected by centrifugation and washed four times with washing buffer as described previously.[5,6,54] After washing, the pellets of the precipitated HLECs or ARPE-19 proteins were left in 50 μl of 1 × kinase buffer (50 mM Tris 7.5, 10 mM $MgCl_2$, 1 mM EGTA, 2 mM DTT, 0.01% Brij35, 0.02% BSA) and used for labeling the purified Akt1 and Akt1-T450A, which were used as dephosphorylation substrates.

***In vitro* dephosphorylation assays.** The *in vitro* dephosphorylation assays were conducted as described previously.[5,6,54]

Basic FGF induction of differentiation. The pCI-AKT1-αTN4-1, pCI-AKT1-T450A-αTN4-1, pCI-AKT1-T450D-αTN4-1, pCI-AKT1/pCI-αTN4-1 and pCI-AKT1/pCI-PP1α-αTN4-1 cells were starved of serum overnight, followed by 50 μg/ml bFGF (Sigma) treatment from 0 to 5 days without changing the medium.

Analysis of transient gene expression. The Promega dual-luciferase reporter assay system (Promega, Madison, WI, USA) was used in our analysis. For transient luciferase assays, 2.5 μg luciferase reporter gene (pNF-κB-Luc) together with 3.5 μg pCI-AKT1, pCI-AKT1-T450A, pCI-AKT1-T450D alone or 3.5 μg each plus 1.5 μg pCI-PP-1α, or 1.5 μg pCI-PP-2Aα and 0.2 μg control plasmid Renilla luciferase pRL-SV40-Luc (Cat. no. E2231) were cotransfected into HLECs or ARPE-19 cells using the Lipofectamine 2000 kit from Invitrogen Life Technologies. After 36 h, the transfected cells were harvested for luciferase assays according to the company

instruction manual. The luciferase activity was determined using the Luminoskan RS microplate reader from Thermo Labsystems Corporation (Waltham, MA, USA).

Confocal immunohistochemistry analysis of the total and active AKT1 in developing mouse eye. The mouse eye tissues were fixed with 4% paraformaldehyde in PBS, pH 7.4 and embedded in O.C.T. component (Tissue-Tek, Sakura Finetek USA Inc., Torrance, CA, USA, Cat no. 4583) on dry ice. Sections of 5-μm thickness were cut in a Leica CM1950 Cyrostate (Leica, Allendale, NJ, USA) and adhered to the Superfrost/plus microscope slides (Fisher Scientific, Pittsburgh, PA, USA). The sections were washed three times with PBS. For nonspecific blocking, each section was incubated in 500 μl of 5% normal goat serum (Sigma) in PBS for 1 h at room temperature and then incubated overnight in 400 μl of diluted antibodies (1 : 100) in a humidified chamber at 4°C. The sections were then washed three times (5 min each) with PBS, followed by incubation in 400 μl of secondary antibodies linked to FITC or Texas Red (Vector Laboratories, Barlingame, CA, USA) of 1 : 1000 dilution in blocking solution for 1 h in the absence of visible light. After incubation, sections were washed six times (5 min each) with PBS at room temperature and then observed under a Zeiss confocal fluorescence microscope (Zeiss, Thornwood, NY, USA). For negative controls, the sections were treated in the same manner, except that the primary antibody was replaced by normal serum.

Quantitation and statistical analysis. The western blot gels were analyzed using the UN-SCAN-IT software from Silk Scientific Corporation (Orem, UT, USA). Total pixel data were averaged from three or more different groups of samples of each species after normalization against the background. The total pixels from the target band were divided by the total pixels from the corresponding β-actin or total Akt1 (the reference band as specified in each figure legend).

In this study, all data presented are derived from at least three experiments. During data analysis, statistical analysis was conducted for all sets of data when necessary. The means, S.D. and *P*-value were calculated and included in the figures.

Conflict of interest

The authors declare no conflict of interest.

Acknowledgements. This study is supported in part by the National Institute of Health Grants 1 R01EY15765 and 1 R01EY18380, the Changjiang Scholar Team Award Funds from Education Ministry of China, the Lotus Scholar Program Funds from Hunan Province Government and the Special Honorary Professorship Funds from Hunan Normal University.

1. Moorhead GBG, Trinkle-Mulcahy L, Ulke-Lemée A. Emerging roles of nuclear protein phosphatases. *Nat Rev Mol Cell Biol* 2007; **8**: 234–244.
2. Yan Q, Mao Y-W, Li DW. Protein serine/threonine phosphatases in the nerve system. In: Binder, Hirokawa, Windhorst (eds). *Encyclopedia of Neuroscience*. Springer: Heidelberg, 2009, pp 3325–3329.
3. Cohen P. The structure and regulation of protein phosphatases. *Annu Rev Biochem* 1989; **58**: 453–508.
4. Mumby MC, Walter G. Protein serine/threonine phosphatases: structure, regulation, and functions in cell growth. *Physiol Rev* 1993; **73**: 673–699.
5. Li DW-C, Liu J-P, Schmid PC, Schelosser R, Feng H, Liu W-B *et al.* Protein serine/threonine phosphatase-1 dephosphorylates p53 at Ser-15 and Ser-37 to modulate its transcriptional and apoptotic activities. *Oncogene* 2006; **25**: 3006–3022.
6. Qin J-C, Chen H-J, Yan Q, Deng M, Liu J-P, Doerge S *et al.* Protein phosphatase-2A is a target of epigallocatechin-3-gallate and regulates p53-Bak apoptotic pathway. *Cancer Res* 2008; **68**: 4150–4162.
7. Dohoney KM, Guillerm C, Whiteford C, Elbi C, Lambert PF, Hager GL *et al.* Phosphorylation of p53 at Serine 37 is important for transcriptional activity and regulation in response to DNA damage. *Oncogene* 2004; **23**: 49–57.
8. Scheid MP, Woodgett JR. PKB/AKT: functional insights from genetic models. *Nat Rev Mol Cell Biol* 2001; **2**: 760–768.
9. Datta SR, Brunet A, Greenberg ME. Cellular survival: a play in three Akts. *Genes Dev* 1999; **13**: 2905–2927.
10. Franke TF, Kaplan DR, Cantley LC. PI3K: downstream AKTion blocks apoptosis. *Cell* 1997; **88**: 435–437.
11. Black JD. Protein kinase C-mediated regulation of the cell cycle. *Front Biosci* 2000; **5**: D406–D423.
12. Lawlor MA, Alessi DR. PKB/Akt: a key mediator of cell proliferation, survival and insulin responses? *J Cell Sci* 2001; **114**: 2903–2910.
13. Nicholson KM, Anderson NG. The protein kinase B/Akt signalling pathway in human malignancy. *Cell Signal* 2002; **14**: 381–395.
14. Vivanco I, Sawyers CL. The phosphatidylinositol 3-kinase AKT pathway in human cancer. *Nat Rev Cancer* 2002; **2**: 489–501.
15. Shaw J, Kirshenbaum JA. Prime time for JNK-mediated Akt reactivation in hypoxia-reoxygenation. *Circ Res* 2006; **98**: 7–9.
16. Shao Z, Bhattacharya K, Hsich E, Park L, Walters B, Germann U *et al.* c-Jun N-terminal kinases mediate reactivation of Akt and cardiomyocyte survival after hypoxic injury *in vitro* and *in vivo*. *Circ Res* 2006; **98**: 111–118.
17. Alessi DR, Andjelkovic M, Caudwell B, Cron P, Morrice N, Cohen P *et al.* Mechanism of activation of protein kinase B by insulin and IGF-1. *EMBO J* 1996; **15**: 6541–6551.
18. Stephens L, Anderson K, Stokoe D, Erdjument-Bromage H, Painter GF, Holmes AB *et al.* Protein kinase B kinases that mediate phosphatidylinositol 3,4,5-trisphosphate-dependent activation of protein kinase B. *Science* 1998; **279**: 710–714.
19. Behn-Krappa A, Newton AC. The hydrophobic phosphorylation motif of conventional protein kinase C is regulated by autophosphorylation. *Curr Biol* 1999; **9**: 728–737.
20. Toker A, Newton AC. Akt/protein kinase B is regulated by autophosphorylation at the hypothetical PDK-2 site. *J Biol Chem* 2000; **275**: 8271–8274.
21. Leslie NR, Biondi RM, Alessi DR. Phosphoinositide-regulated kinases and phosphoinositide phosphatases. *Chem Rev* 2001; **101**: 2365–2380.
22. Sarbassov DD, Guertin DA, Ali SM, Sabatini DM. Phosphorylation and regulation of Akt/PKB by the rictor-mTOR complex. *Science* 2005; **307**: 1098–1101.
23. Jacinto E, Facchinetti V, Liu D, Soto N, Wei S, Jung SY *et al.* SIN1/MIP1 maintains rictor-mTOR complex integrity and regulates Akt phosphorylation and substrate specificity. *Cell* 2006; **127**: 125–137.
24. Maehama T, Dixon JE. The tumor suppressor, PTEN/MMAC1, dephosphorylates the lipid second messenger, phosphatidylinositol 3,4,5-trisphosphate. *J Biol Chem* 1998; **273**: 13375–13378.
25. Wishart MJ, Dixon JE. PTEN and myotubularin phosphatases: from 3-phosphoinositide dephosphorylation to disease. *Trends Cell Biol* 2002; **12**: 579–585.
26. Gao T, Furnari F, Newton AC. PHLPP: a phosphatase that directly dephosphorylates Akt, promotes apoptosis, and suppresses tumor growth. *Mol Cell* 2005; **18**: 13–24.
27. Brognard J, Sierecki E, Gao T, Newton AC. PHLPP and a second isoform, PHLPP2, differentially attenuate the amplitude of Akt signaling by regulating distinct Akt isoforms. *Mol Cell* 2007; **25**: 917–931.
28. Andjelkovic M, Jakubowicz T, Cron P, Ming XF, Han JW, Hemmings BA. Activation and phosphorylation of a pleckstrin homology domain containing protein kinase (RAC-PK/PKB) promoted by serum and protein phosphatase inhibitors. *Proc Natl Acad Sci USA* 1996; **93**: 5699–5704.
29. Kuo Y-C, Huang K-Y, Yang C-H, Yang Y-S, Lee W-Y, Chiang C-W. Regulation of phosphorylation of Thr-308 of Akt, cell proliferation, and survival by the B55alpha regulatory subunit targeting of the protein phosphatase 2A holoenzyme to Akt. *J Biol Chem* 2008; **283**: 1882–1892.
30. Han Z, Boyle DL, Chang L, Bennett B, Karin M, Yang L *et al.* c-Jun N-terminal kinase is required for metalloproteinase expression and joint destruction in inflammatory arthritis. *J Clin Invest* 2001; **108**: 73–81.
31. Xing Y, Xu Y, Chen Y, Jeffrey PD, Chao Y, Zheng L *et al.* Structure of protein phosphatase 2A core enzyme bound to tumor-inducing toxins. *Cell* 2006; **127**: 341–352.
32. Liu JP, Schlosser R, Ma WY, Dong Z, Feng H, Lui L *et al.* Human alphaA- and alphaB-crystallins prevent UVA-induced apoptosis through regulation of PKCalpha, RAF/MEK/ERK and AKT signaling pathways. *Exp Eye Res* 2004; **79**: 393–403.
33. Fujio Y, Nguyen T, Wencker D, Kitsis RN, Walsh K. Akt promotes survival of cardiomyocytes *in vitro* and protects against ischemia-reperfusion injury in mouse heart. *Circulation* 2000; **101**: 660–667.
34. Matsui T, Tao J, del Monte F, Lee KH, Li L, Picard MH *et al.* Akt activation preserves cardiac function and prevents injury after transient cardiac ischemia *in vivo*. *Circulation* 2001; **104**: 330–335.
35. McAvoy JW, Chamberlain CG. Growth factors in the eye. *Prog Growth Factor Res* 1990; **2**: 29–43.
36. Lang RA. Which factors stimulate lens fiber cell differentiation *in vivo*? *Invest Ophthalmol Vis Sci* 1999; **40**: 3075–3078.
37. Govindarajan V, Overbeek PA. Secreted FGFR3, but not FGFR1, inhibits lens fiber differentiation. *Development* 2001; **128**: 1617–1627.
38. Lovicu FJ, McAvoy JW. FGF-induced lens cell proliferation and differentiation is dependent on MAPK (ERK1/2) signalling. *Development* 2001; **128**: 5075–5084.
39. Le AC, Musil LS. A novel role for FGF and extracellular signal-regulated kinase in gap junction-mediated intercellular communication in the lens. *J Cell Biol* 2001; **154**: 197–216.
40. Ochi H, Ogino H, Kageyama Y, Yasuda K. The stability of the lens-specific Maf protein is regulated by fibroblast growth factor (FGF)/ERK signaling in lens fiber differentiation. *J Biol Chem* 2003; **278**: 537–544.
41. Pearson G, Robinson F, Beers Gibson T, Xu BE, Karandikar M, Berman K *et al.* Mitogen-activated protein (MAP) kinase pathways: regulation and physiological functions. *Endocr Rev* 2001; **22**: 153–183.
42. Chandrasekher G, Sailaja D. Phosphatidylinositol 3-kinase (PI-3K)/Akt but not PI-3K/p70 S6 kinase signaling mediates IGF-1-promoted lens epithelial cell survival. *Invest Ophthalmol Vis Sci* 2004; **45**: 3577–3588.
43. Gotoh N, Ito M, Yamamoto S, Yoshino I, Song N, Wang Y *et al.* Tyrosine phosphorylation sites on FRS2alpha responsible for Shp2 recruitment are critical for induction of lens and retina. *Proc Natl Acad Sci USA* 2004; **101**: 17144–17149.

44. James C, Collison DJ, Duncan G. Characterization and functional activity of thrombin receptors in the human lens. *Invest Ophthalmol Vis Sci* 2005; **46**: 925–932.
45. Iyengar L, Patkunanathan B, Lynch OT, McAvoy JW, Rasko JE, Lovicu FJ. Aqueous humour- and growth factor-induced lens cell proliferation is dependent on MAPK/ERK1/2 and Akt/PI3-K signalling. *Exp Eye Res* 2008; **83**: 667–678.
46. Jiang Y, Luo W, Howe PH. Dab2 stabilizes Axin and attenuates Wnt/beta-catenin signaling by preventing protein phosphatase 1 (PP1)-Axin interactions. *Oncogene* 2009; **28**: 2999–3007.
47. Shi W, Sun C, He B, Xiong W, Shi X, Yao D *et al.* GADD34-PP1c recruited by Smad7 dephosphorylates TGFbeta type I receptor. *J Cell Biol* 2004; **164**: 291–300.
48. Li HY, Liu H, Wang CH, Zhang JY, Man JH, Gao YF *et al.* Deactivation of the kinase IKK by CUEDC2 through recruitment of the phosphatase PP1. *Nat Immunol* 2008; **9**: 533–541.
49. Novoa I, Zeng H, Harding HP, Ron D. Feedback inhibition of the unfolded protein response by GADD34-mediated dephosphorylation of eIF2alpha. *J Cell Biol* 2001; **53**: 1011–1022.
50. Jousse C, Oyadomari S, Novoa I, Lu P, Zhang Y, Harding HP *et al.* Inhibition of a constitutive translation initiation factor 2alpha phosphatase, CReP, promotes survival of stressed cells. *J Cell Biol* 2003; **163**: 767–775.
51. Connor JH, Weiser DC, Li S, Hallenbeck JM, Shenolikar S. Growth arrest and DNA damage-inducible protein GADD34 assembles a novel signaling complex containing protein phosphatase 1 and inhibitor 1. *Mol Cell Biol* 2001; **21**: 6841–6850.
52. Lee YY, Cevallos RC, Jan E. An upstream open reading frame regulates translation of GADD34 during cellular stresses that induce eIF2alpha phosphorylation. *J Biol Chem* 2009; **284**: 6661–6673.
53. Kim SS, Kim JH, Lee SH, Chung SS, Bang OS, Park D *et al.* Involvement of protein phosphatase-1-mediated MARCKS translocation in myogenic differentiation of embryonic muscle cells. *J Cell Sci* 2002; **115** (Pt 12): 2465–2473.
54. Yan Q, Liu W-B, Qin J, Liu J-P, Chen H-G, Huang X *et al.* Protein phosphatase-1 dephosphorylates Pax-6, a transcription factor controlling brain and eye development. *J Biol Chem* 2007; **282**: 13954–13965.
55. Miyashita T, Krajewski S, Krajewska M, Wang HG, Lin HK, Liebermann DA *et al.* Tumor suppressor p53 is a regulator of bcl-2 and bax gene expression *in vitro* and *in vivo*. *Oncogene* 1994; **9**: 1799–1805.
56. Mihara M, Erster S, Zaika A, Petrenko O, Chittenden T, Pancoska P *et al.* p53 has a direct apoptogenic role at the mitochondria. *Mol Cell* 2003; **11**: 577–590.
57. Leu JI, Dumont P, Hafey M, Murphy ME, George DL. Mitochondrial p53 activates Bak and causes disruption of a Bak–Mcl1 complex. *Nat Cell Biol* 2004; **6**: 443–450.
58. Bode AM, Dong ZG. Post-translational modification of p53 in tumorigenesis. *Nat Rev Cancer* 2004; **4**: 793–805.
59. Kim TH, Goodman J, Anderson KV, Niswander L. Phactr4 regulates neural tube and optic fissure closure by controlling PP1-, Rb-, and E2F1-regulated cell-cycle progression. *Dev Cell* 2007; **13**: 87–102.
60. Xiang H, Wang J, Mao Y, Liu M, Reddy VN, Li DW. Human telomerase accelerates growth of lens epithelial cells through regulation of the genes mediating RB/E2F pathway. *Oncogene* 2002; **21**: 3784–3791.
61. Mao YW, Liu JP, Xiang H, Li DW. Human alphaA- and alphaB-crystallins bind to Bax and Bcl-X(S) to sequester their translocation during staurosporine-induced apoptosis. *Cell Death Differ* 2004; **11**: 512–526.
62. Chen H-G, Han W-J, Deng M, Qin J-C, Yuan D, Liu J-P *et al.* Transcriptional regulation of PP2A-Aα is mediated by multiple factors including AP-2α, CREB, ETS, and SP-1. *PLoS ONE* 2009; **4**: e7019.
63. Li DW-C, Liu J-P, Mao YW, Xiang H, Wang J, Ma W-Y. *et al.* Calcium-activated RAF/MEK/ERK pathway mediates p53-dependent apoptosis and is abrogated by αB-crystallin through inhibition of Ras activation. *Mol Biol Cell* 2005; **16**: 4437–4453.

Supplementary Information accompanies the paper on Cell Death and Differentiation website (http://www.nature.com/cdd)

Chapter 1.3

THE TWO LENS STRUCTURE PROTEINS, αA-CRYSTALLIN (HSPB4) AND αB-CRYSTALLIN (HSPB5), CONTROL APOPTOSIS THROUGH REGULATION OF MULTIPLE SIGNALING TRANSDUCTION PATHWAYS

David W. Li[1, 2, 3*], Lili Gong[1], Mi Deng[1], Jinping Liu[1], Mugen Liu[4], and Ying-Wei Mao[5, 6]

[1]Department of Biochemistry & Molecular Biology, College of Medicine, University of Nebraska Medical Center, 985870 Nebraska Medical Center, Omaha, NE 68198-5870

[2]Key Laboratory of Protein Chemistry & Developmental Biology of the Ministry of Education, College of Life Sciences, Hunan Normal University, Changsha, P.R. China

[3]Department of Ophthalmology & Visual Sciences, College of Medicine, University of Nebraska Medical Center, 985870 Nebraska Medical Center, Omaha, NE 68198-5870

[4]Key Laboratory of Molecular Biophysics of the Ministry of Education, College of Life Science and Technology and Center for Human Genome Research, Huazhong University of Science and Technology, Wuhan, P.R. China

[5]Howard Hughes Medical Institute

[6]Picower Institute for Learning and Memory, Department of Brain and Cognitive Sciences, Massachusetts Institute of Technology, Cambridge, MA 02139, USA

---

[*] Corresponding Author David Li
University of Nebraska Medical Center
College of Medicine
Department of Biochemistry and Molecular Biology
Department of Ophthalmology and Visual Science
985870 Nebraska Medical Center
Omaha, Nebraska 68198-5870, USA
dwli1688@hotmail.com

ABSTRACT

α-Crystallins are major lens structural proteins, belonging to the family of the small heat shock proteins (HSPs). α-Crystallins consist of two polypeptides, αA and αB that share 55% amino acid sequence identity. The two 20-kDa subunits form soluble aggregates with an average molecular mass of 600-800 kDa and can be isolated from lens fiber cells as a heteroaggregate containing αA- and αB-peptides in a ratio of 3 to 1. αA-crystallin (HspB4) is predominantly expressed in the ocular lens with small amounts present in spleen and thymus. In contrast, αB-crystallin (HspB5) is expressed mainly in the lens but also expressed outside of the lens in a number of tissues such as skeletal and cardiac muscle and to lesser extent in skin, brain, and kidney. Besides their structural role, α-crystallins are important chaperones in the ocular lens, act as autokinases, and also play important roles in suppressing both developmental and stress-induced apoptosis to guard the lens differentiation and prevent pathogenesis in the lens as well as several other tissues. In this chapter, we will focus the current knowledge regarding the molecular mechanisms by which αA- and αB-crystallins suppress apoptosis in both lens and non-lens tissues.

INTRODUCTION

αCrystallins are major lens proteins which have structural roles in maintaining lens transparency [1]. Various mutations identified in α-crystallins have been shown to cause congenital cataracts and also other human diseases (Table 1) [2-11]. α-Crystallins consist of two isoforms: αA and αB, which share 55% amino acid sequence identity [12]. While αA-crystallin is largely expressed in the lens with a small amount in the pancrease and spleen [13], αB-crystallin has been found in the lens and heart with relatively abundant level, and also in several other tissues including spinal chord, skin, muscle, brain and kidney in relatively small amount [14-16]. The two α-crystallins share a homologous C-terminal domain of about 80 amino acid residues with numerous other proteins and this feature characterizes them into a special group named small heat shock protein family [17-18]. Besides their structural roles in the lens, studies in the past two decades have revealed that α-crystallins have extraordinary non-structural functions.

Table 1. Mutations in the two α-crystallins causing cataracts and other human diseases

Crystallin	Mutations	Diseases	References
αA	W9X	Cataract	2
	R49C	Cataract	3
	R116C	Cataract	4
	R116H	Cataract	5
	G98R	Cataract	6
αB	R120G	Desmin-Related Myopathy	7
	450delA[a]	Cataract	8
	Q151X	Myofibrillar myopathy	9
	464delCTX[b]	Myofibrillar myopathy	9
	D140N	Cataract	10
	P20S	Cataract	11

[a]450delA: nucleotide deletion at position 450 that resulted in a framshift in codon 150 and produced an _Berrant protein consisting 184 residues.
[b]464CTX, 2bp nucleotide deletion at position 464 (464delCT) that generates eight missense codons (RAHHSHHP) followed by a stop codon.

The first non-structural role of α-crystallins was demonstrated by Horwitz in 1992 [19]. Using a simple light scattering assay at 360 nm to measure interactions between α-crystallins and other proteins, he demonstrated that the purified bovine α-crystallins can prevent heat-induced protein aggregation of numerous substrates that include alcohol dehydrogenase, β_L-crystallin and total lens soluble proteins. Since his pioneering study, the chaperone function of α-crystallins has been extensively studied by many laboratories [20-26] and several chapters in this book address this subject.

Soon after the discovery of the chaperone function, Kantorow and Piatigorsky [27] showed that both αA- and αB-crystallins can act as autokinases to phosphorylate themselves. Autophosphorylation of α-crystallins may have important effects in their functions, which wait to be further elucidated.

Ubiquitin/proteasome-mediated protein degradation plays essential roles in many cellular processes [28-29]. αB-Crystallin is found playing a critical role in regulating protein degradation. It binds to certain components of the 20S proteasome both in vitro and in vivo [30-34]. For example, αB-crystallin binds to an F-box containing protein, FBX-4, a component of the ubiquitin-protein isopeptide ligase SCF (SKP1/CUL1/F-box), translocates FBX-4 to the detergent-insoluble faction and stimulates the ubiquitin/proteasome pathway, which is required for cyclinD1 degradation [31].

Another important function of α-crystallins is their ability to regulate cell death in different systems through various mechanisms. This chapter will summarize the current knowledge on the anti-apoptotic function of α-crystallins with the emphasis on the mechanistic aspects. Before we discuss the anti-apoptotic role of α-crystallins and the related

molecular mechanisms, we will briefly describe the biology of the ocular lens and the role of apoptosis in lens development and pathology (involvement of sHsps in cataracts is also treated in chapter 2-2).

1. THE BIOLOGY OF THE OCULAR LENS

The lens of the vertebrate eye is a nonvascularized, noninnervated transparent organ. It contains only a single layer of epithelial cells covering its anterior surface. The remainder of the lens is principally composed of enucleated and non-organelle fiber cells [35-36]. The single layer of epithelial cells is primarily responsible for maintenance of the homeostasis of the entire lens and detoxification of noxious components in the ocular lens environment throughout life [37]. During embryonic development, the ectoderm cells destined to become the ocular lens are determined through multiple steps, initiated in the gastrula and early neurula, and completed when the cells make contact with the optic vesicle [38-39]. These ectoderm cells located in the forebrain region are further induced by the optic vesicle and become thickened into lens placodes [38-39]. The lens placode cells invaginate into a lens vesicle and finally they become separated from the neighboring ectoderm and form a complete lens vesicle [35-36, 38-39]. In the developing human lens, it takes about 8 days to form a complete lens vesicle [40]. Lens differentiation begins when the posterior cells of the lens vesicle become elongated, filling the lumen of the lens vesicle and moving towards the anterior epithelium. During mouse embryonic development, α-crystallin genes are turned on at very early stage and αB-crystallin is detected in the lens placode at E9.5, and αA-crystallin detected in the lens cup at E10 and E10.5 [41]. The elongated cells form the primary lens fiber cells through an extensive differentiation process, which culminates by denucleation, a process called pycnosis [42-43]. At the same time, the anterior lens epithelial cells divide, migrate, and differentiate into secondary lens fiber cells in the equatorial region [35-36, 38-39]. Both growth and differentiation of the ocular lens are regulated by different growth factors [44]. The lens continues to grow throughout life, building up layers of new fiber cells from the equatorial region [45]. During lens development and morphogenesis, controlled cell death through apoptosis is an important aspect, which is described in the next section.

2. APOPTOSIS AND CATARACTOGENESIS IN THE OCULAR LENS

Apoptosis is programmed cellular suicide and differs from necrotic cell death [46-47]. Necrotic cell death is a pathological form of cell death resulting from acute cellular injury, which is typified by rapid cell swelling and lysis, leading to the release of cytoplasmic materials, which often trigger an inflammatory response [47]. In contrast, apoptotic cell death is characterized by controlled autodigestion of the dying cell [46-47]. The apoptotic cells often break into small fragments called apoptotic bodies, which are phagocytosed and digested by macrophages or neighboring cells. The genetic control of apoptotic death was initially explored in *C. elegans*. Horvitz and his associates have now elucidated the genetic program and discovered that more than a dozen of regulators mediate the apoptotic death of 129 cells in *C. elegans* [48]. In mammals, apoptosis is controlled by several different families

of genes including those coding for members of death-domain-containing protein family, the Bcl-2 family, and the caspase family. The regulators of these families are assembled into two major death pathways: the extrinsic death pathway and intrinsic death pathway [49-51].

Apoptosis is a fundamental feature of animal development and occurs in many different tissues [49-50]. Apoptosis is also closely associated with diseases, which are derived from either increased apoptosis (such as AIDS) or inhibited apoptosis (such as cancer) [52].

Apoptosis plays an important role in lens development. In the developing rat lens, Gluckmann [53] documented cell death in two prominent regions: the lens vesicle ectoderm connecting to the determined corneal ectoderm and the lens stalk region. About two-decade later, Silver and Hughes reported in more details the cell death in the lens and other compartments of the rat eye [54]. Using Hoechst staining, Ishizaki *et al.* [55] confirmed that apoptotic cells were frequently observed in rat embryonic lens and also in postnatal rat lenses. These studies have recently been further confirmed during development of murine and human lenses [56-58].

Cataract, referring to any opacification in the ocular lens, is a disease that accounts for 22% of all cases of blindness and thus causes an important health problem. Cataract can develop at any time in life due to inherited mutations (congenital cataracts such as α-crystallin gene mutations described in table 1) or non-inherited conditions (non-congenital cataracts) [59].

Several line of evidence points to the conclusion that stress-induced apoptosis of lens epithelial cells leads to non-congenital cataractogenesis in animal and human. First, during development, apoptosis induced by gene mutations, expression of exogenous genes, stress factors, or mechanical damage all causes microphthalmia or cataractogenesis (see Ref. 60 for a detail summary). One of the most striking examples came from the study of CREB-2 knockout mice [61]. Normal lens development occurs between EDs 12.5 and 14.5 in CREB-2(-/-) mice. These mice displayed normal formation of the early lens vesicle, normal elongation of posterior primary fiber cells, and normal formation of the anterior lens epithelial cells. However, the anterior lens epithelial cells and their direct descendants at the equatorial poles of the lens underwent massive and synchronous p53-dependent apoptosis between EDs14.5 and 16.5. The complete loss of these cells accounts directly for the embryonic lens degeneration seen in these animals [61]. Mutation of the FoxE3 gene also induced abnormal lens epithelial cell apoptosis in the anterior epithelium of the lens vesicle and led to absence of secondary lens fibers and formation of a dysplastic, cataractous lens [62]. Introduction of a number of exogenous genes into lenses also causes lens cell apoptosis followed by cataractogenesis [63-70]. Suppression of the lens stalk cell apoptosis at the lens vesicle stage by hyaluronic acid led to faulty separation of the lens vesicle, resulting in abnormal lens formation [56]. Second, we previously demonstrated that in the in vitro rat lens organ culture, stress factors such as hydrogen peroxide, calcimycin, and UVB all induce lens epithelial cell apoptosis followed by development of lens opacification [71-73]. In vitro organ culture study by Menko and her associates demonstrated that inhibition of Src kinase pathway led to cataract formation which was initiated by apoptosis of lens epithelial cells in the treated lens [74-75]. Third, in the *in vivo* animal model studies with rat and rabbit, several laboratories have demonstrated that UV irradiation [76-78], diabetic condition [79-80], selenite [81], and N-methyl-N-nitrosourea [82] all induced early apoptosis of lens epithelial cells followed by cataractogenesis. In a recent report, Wolf and his associates demonstrated that death of lens epithelial cells is directly related to aging-related cataractogenesis [83]. Fourth, in human

cataractous lenses, we have previously observed that varying levels of apoptotic cells were present in the capsular epithelia from cataractous patients [71]. These results have been confirmed by numerous laboratories [84-87] but in contrast to one report [88]. In a recent study [87], Charakidas A et al. reported that TUNEL staining was observed in 25 (92.6%) specimens of cataractous lenses, whereas cells undergoing apoptosis were identified only in 2 (8%) of the epithelia from non-cataractous lenses. This group concluded that the accumulation of small-scale epithelial cell losses during lifetime may induce alterations in lens fiber formation and homeostasis and result in loss of lens transparency. Apoptosis is also closely associated with human polar cataracts [89-90]. Finally, recent studies have revealed that ER stresses cause cataractogenesis. In exploring the mechanism, it was found that apoptosis induced by ER stress plays an important role in ER stress-induced cataractgenesis [91].

The ocular lens is immersed in the aqueous humor and constantly faces the challenges from various stress conditions. To avoid stress-induced death of the single layer of lens epithelial cells through apoptosis and thus cataractogenesis, the lens must carry the strong defense system to guard the apoptotic process. Two of the most important guardians in the ocular lens are the lens structural proteins, αA- and αB-crystallins. We now turn to the discussion of the anti-apoptotic function of these two crystallins.

3. Discovery of the Anti-apoptotic Role of α-Crystallins

The protective role of α-crystallin was initially explored in NIH 3T3 fibroblast by Klemenz group who found that ectopic expression of αB-crystallin cDNA or induced expression of αB-crystallin by the synthetic glucocorticoid hormone dexamethasone renders NIH 3T3 cells thermoresistant [92]. Around the same time, Arrigo and his associates used a murine fibrosarcoma cell line L929 to express various members of the small heat shock proteins including *Drosophila* hsp27, human hsp27, and human αB-crystallin and then tested their functions in conferring the transfected stable lines of L929 clones the ability to resist on different stress conditions such as heat, oxidative stress, tumor necrosis factor and kinase inhibitor treatments [93-94]. During these studies, they elegantly demonstrated that αB-crystallin, like hsp27, displays strong ability to resist apoptosis induced by Fas/Fas ligand, TNF-α and staurosporine [95]. This pioneering work was soon followed by numerous laboratories and the anti-apoptotic role of α-crystallins in development and stress-induced pathology has been vigorously explored in different systems [96-124].

4. α-Crystallins Prevents Developmental and Stress-Induced Apoptosis

The direct evidence that α-crystallins prevent developmental apoptosis came from the study by Moorozov and Waurousek [114]. These authors demonstrated that knockout of the αA- and αB-crystallins caused elevated apoptosis of the cortical lens fiber cells, leading to microphthalmia and cataractogenesis. Ousman et al. [118] reported that the αB(-/-) astrocytes

showed more cleaved caspase-3 and more TUNEL staining, and thus increased apoptosis. In addition, αB-crystallin is an important regulator of tubular morphogenesis and survival of endothelial cell during tumor angiogenesis [119]. Tumor grown in αB(-/-) mice are significantly less vascularized than wild-type tumors and displayed increased areas of apoptosis/necrosis [119].

In the in vitro cultured epithelial cells derived from human and rabbit lenses, we have shown that the two α-crystallins can prevent apoptosis induced by staurosporine (a general kinase inhibitor), okadaic acid and calyculin A (the protein serine/threonine phosphatases-1 and 2A inhibitors) or oxidative stress [101-102, 108]. Andley et al. [97] demonstrated that the αA(-/-) lens epithelial cells are 40 times more sensitive to UVA damage than the wild type mouse lens epithelial cells. Introduction of the exogenous αA-crystallin into cultured lens epithelial cells enhanced the resistance of the transfected cells against UVA-induced apoptosis. The same group also compared the relative antiapoptotic abilities of the αA- and αB-crystallins under treatment of UVA irradiation, TNFα and staurosporine, and concluded that αA-crystallin is a stronger antiapoptotic regulator than αB-crystallin does [98]. However, when the two α-crystallins were overexpressed in *E. coli* and tested for their ability against cold or other stress conditions, an opposite conclusion was obtained [99]. We also tested the possible differential anti-apoptotic abilities of the two α-crystallins against stress-induced apoptosis in three different cell lines: the human lens epithelial cell line (HLE) which contains virtually undetectable endogenous crystallins; the human retina pigment epithelial cells (ARPE-19) and the rat embryonic myocardium cell line (H9c2), both of which expresses endogenous αB-crystallin [108]. The expression of the endogenous αB-crystallin in ARPE-19 and H9c2 cells makes them much more resistant to staurosporine-induced apoptosis in the absence of exogenous α-crystallin expression. Regardless absence or presence of the endogenous α-crystallin, expression of HαA and HαB in these cells provides additional protections. Under treatment of 100 nM staurosporine, 10 μM etoposide or 400 mM sorbitol (generating osmotic stress), HαA and HαB consistently show similar protections against a given stress condition in HLE, ARPE-19 or H9c2 cells. The inconsistence of the results from different laboratories may reflect the difference of the physiological conditions of the transfected cells used for the comparative analysis. On the other hand, αA and αB-crystallins, as we will discuss below, can regulate different signaling pathways, and thus provide the possibility of differential antiapoptotic abilities depending upon the physiological environment of the tested cells.

As mentioned above, α-crystallins are expressed in retinal pigment epithelial cells [108]. Recent studies have shown that the protection conferred by α-crystallins in this tissue is very important for retinal functions [117, 120].

Outside the ocular tissues, Martin et al. [96] first reported that αB-crystallin can protect cardiac myocytes from ischemic injury soon after Arrigo's pioneering study in L929 cells [95]. This in vitro work was soon followed by the in vivo studies carried out by Das's group who showed that overexpression of αB-crystallin confers simultaneous protection against cardiomyocyte apoptosis and necrosis during myocardial ischemia and reperfusion [100].

The dominant mutant, R116C in αA-crystallin and R120G in αB-crystallin displayed diminished antiapoptotic functions as tested in both lens epithelial cells [105,108] and

cardiomyocytes [112]. The possible explanation for this phenomenon is discussed later is this chapter.

5. α-CRYSTALLINS SUPPRESS APOPTOSIS THROUGH REGULATION OF MEMBERS OF THE CASPASE FAMILY

To explore the possible mechanism by which α-crystallins prevent apoptosis, we initially made an expression construct in which the mouse αB-crystallin cDNA was inserted into the green fluorescence expression vector, pEGFPC3 and then this construct, pEGFP-mαB and the corresponding vector were introduced into rabbit lens epithelial cells, N/N1003A. When the two types of cells were treated with okadaic acid (inhibitor of protein phosphatase-1 and –2A) or DMSO (mock), it was found that mouse αB-crystallin protects the transfected N/N1003A cells from okadaic acid-induced apoptosis. To determine the possible mechanism by which mouse αB-crystallin inhibits apoptosis, we examined the caspase-3 activity in both types of cells after okadaic acid treatment. It was found that caspase-3 activity was up-regulated by okadaic acid about 5-fold in non-transfected and vector-transfected N/N1003A cells. In contrast, only 1.5-fold up-regulation of caspase-3 activity was observed in mouse αB-crystallin-transfected N/N1003A cells after okadaic acid treatment. Thus, the protection against okadaic acid-induced apoptosis by mouse αB-crystallin is associated with its ability to suppress caspase-3 activation. This is the initial discovery that αB-crystallin regulates caspase-3 activity [101]. To explore how αB-crystallin suppresses caspase-3 activation, we then conducted immunoprecipitation-linked Western blot analysis [102]. Our results demonstrated that mouse αB-crystallin can interact with procaspase-3 and partially processed procaspase-3 to prevent stress-induced apoptosis [102].

Our discovery, that αB-crystallin interacts with procaspase-3 and partially processed caspase-3 to prevent caspase-3 activation, has been confirmed in several other types of cells. DePinho and his associates [122-123] recently found that the Bcl-2 like 12 gene (*bcl2L12*) is universally overexpressed in the primary glioblastoma multiforme (GBM) and functions to block post-mitochondrial apoptosis signaling by neutralizing effector caspase-3 and caspase-7 maturation. They found that while Bcl2L12 can prevent caspase-7 maturation through direct interaction between Bcl2L12 and procaspase-7, neutralization of caspase-3 maturation by Bcl2L12 occurs through an indirect mechanism in which Bcl2L12 induces transcriptional upregulation of the small heat shock protein, αB-crystallin, which binds to procaspase-3 and its cleavage intermediates *in vitro* and *in vivo*. In rat cardiomyocyte H9c2 cells, Aggeli et al. [121] reported that in responding to oxidative stress insult, αB-crystallin became phosphorylated by p38-MAPK/MSK1 in the presence of intracellular free calcium and the phosphorylated αB-crystallin interacted with procaspase-3 to block its cleavage and subsequent activation.

Around the same time when we used co-immunoprecipitation to reveal the interaction between αB-crystallin and procaspase/partially processed procaspase-3, Cryns' group [103] demonstrated that αB-crystallin interacted with the cleavage intermediate of the procaspase-3 using in vitro interaction-linked cleavage assays.

The importance of the interactions between αB-crystallin and the procaspase-3/partially processed caspase-3 is recently demonstrated *in vivo* by Waurousek's group [114], who found that knockout of both α-crystallins leads to upregulation of caspase-3 and caspase-6 activities in the fiber cell zone of mouse lens where secondary lens fiber cell disintegration occurs, suggesting that the elevated levels of caspase-3 and caspase-6 activities are probably causing the observed fiber cell disintegration, and the eventual cataractogenesis. The same group also demonstrated that αA-crystallin directly interacts with caspase-6 through co-immunoprecipitation-linked western blot analysis [114].

Using surface plasmon resonance (SPR) analysis, we have recently found that both αA- and αB-crystallins can interact with caspase-3 (Gong et al., in preparation). We found that caspase-3 exhibited a stronger binding to αB-crystallin (K_D=155 nM) than that to αA-crystallin (K_D=240 nM). These results are somewhat different from a recent report [125] where a protein pin array was used to explore the interactions between αB-crystallin and other proteins. The oligo peptide with a few amino acids from αB-crystallin had little affinity to caspase-3. The plausible explanation for the difference is that the oligos in protein pin array assay chops αB-crystallin into small fragments with a few amino acids and thus break down the binding domain or binding site in αB-crystallin response for the interaction with procaspase-3/caspase-3.

6. α-CRYSTALLINS PREVENT APOPTOSIS THROUGH CONTROL OF MEMBERS OF THE BCL-2 FAMILY

To explore whether αA- and αB-crystallins are able to prevent apoptosis at the mitochondrial level, upstream of caspase-3 activation, we cloned human αA- and αB-crystallin cDNAs from human eye lenses and generated the in frame constructs expressing fusion proteins of human αA- and αB-crystallins (HαA and HαB) with green fluorescence protein (GFP). These expression constructs (pEGFP-HαA and pEGFP-HαB) and the vector (pEGFP-neo) were transfected into the human lens epithelial cells and the st _Ble clones expressing only GFP from the vector (pEGFP-HLE), GFP-HαA (pEGFP-HαA-HLE) or GFP-HαB (pEGFP-H_B-HLE) were establish in the presence of G418 selection.

Using these stable cell lines, we demonstrated that both αA- and αB-crystallins can prevent staurosporine-induced apoptosis. Staurosporine, a potent apoptosis inducer demonstrated in a broad spectrum of cells activates apoptosis through the mitochondrial death pathway [126-130]. The pro-apoptotic members of the Bcl-2 family play a critical role in staurosporine-induced apoptosis [129-130]. Cells lacking both Bax and Bak are known to be completely resistant to multiple apoptotic stimuli including staurosporine [131-132]. Analysis of cell death in Bax- or Bak-deficient cell lines indicates that both regulators are necessary for staurosporine-induced apoptosis [133-134]. Consistent with these studies, we found that in human lens epithelial cells staurosporine regulates both Bak and Bax at different ways.

Staurosporine was found to upregulate Bak expression up to 5-fold in vector-transfected human lens epithelial cells, and the upregulated Bak was accumulated into mitochondria of the vector-transfected cells. In the GFP-HαA- and GFP-HαB-transfected cells, however, Bak upregulation was different. First, expression of HαA and HαB slightly enhanced Bak

expression in unknown mechanism. On the other hand, expression of HαA- and HαB prevented staurosporine-induced additional Bak upregulation [108]. Since cells lacking both Bax and Bak are completely resistant to staurosporine [132-133], inhibition of additional Bak upregulation by HαA and HαB, to some degree, contributed to their antiapoptotic abilities against staurosporine-induced apoptosis. Bak upregulation is also observed in human colonic adenoma AA/C1 cells during butyrate-induced apoptosis [135], and in human stomach epithelial cells during bacterium–induced apoptosis [136].

Staurosporine did not induce Bax upregulation in the vector or α-crystallin-transfected cells. This kinase inhibitor, however, promoted Bax translocation from cytosol into mitochondria in vector-transfected cells. The death signal-induced Bax conformation change followed by its insertion into mitochondrial membrane is an important step for Bax to promote apoptosis [137-140]. Thus, staurosporine-induced translocation of Bax turned on the death program in human lens epithelial cells. This process was largely abrogated in cells expressing either GFP-HαA or GFP-HαB. Both αA- and αB-crystallins can directly bind to Bax as demonstrated by GST pulldown assay and co-immunoprecipitation [108].

In addition, our results also demonstrated the regulation of another proapoptotic member of the Bcl-2 family by the two alpha-crystallins. Staurosporine stimulated translocation of Bcl-X_S from cytosol into mitochondria in vector-transfected pEGFP-HLE cells. Again, HαA and HαB directly bind to Bcl-X_S and prevent its translocation into mitochondria [108].

The two major mutants, R116C in HαA and R120G in HαB, cause cataractogenesis in the lens [4, 7]. Consistent with these observations, the chaperone-like ability of R116C and R120G was found substantially decreased [141-142]. These mutants apparently displayed much weaker antiapoptotic ability [105, 108, 112]. The attenuated antiapoptotic abilities were derived from their weak interactions with Bax and Bcl-X_S and thus decreased abilities to sequester translocation of Bax and Bcl-X_S from cytosol into mitochondria induced by staurosporine treatment [108].

In vector-transfected cells, once the pro-apoptotic members, Bax and Bcl-X_S, were mobilized into mitochondria, the integrity of mitochondria was interrupted as evidenced by the release of cytochrome c, followed by activation of executioner caspase, caspase-3 and degradation of PARP. These downstream events induced by staurosporine in vector-transfected human lens epithelial cells were similar to those reported in other cell lines [127-129]. In either HαA- or HαB-transfected cells, the staurosporine-induced downstream events were largely turned off [108]. Thus, these results demonstrate that the two α-crystallins can regulate Bcl-2 family members to prevent stress-induced apoptosis.

Besides the two α-crystallins, Hsp60 has also been shown to directly bind to Bax to halt its pro-apoptotic role [143].

7. α-CRYSTALLIN ACTIVATES AKT PATHWAY TO RESIST ON STRESS-INDUCED APOPTOSIS

c-Akt is the cellular homolog of the transforming oncogene of the AKT retrovirus [144-147]. Simultaneous with the identification of c-Akt, the protein kinase B and a kinase related to A- and C-Protein kinases were cloned [148-149]. c-Akt1, PKB and RAC-PK were found to

be encoded by the same gene (herein referred to as Akt). The Akt family contains two other members: c-Akt2 and c-Akt3 [150-153]. Akt family proteins contain a central kinase domain with specificity for serine or threonine residues in substrate proteins. In addition, the amino terminus of Akt includes a pleckstrin homology (PH) domain, which mediates lipid-protein and/or protein-protein interactions [154-156]. Phosphorylation of Akt at Thr-450 is sometimes necessary to prime it for activation [157]. Growth factor stimulation of PI3K leads to increased intracellular level of IP3. Binding of IP3 to the Akt PH domain results in Akt translocation from the cytoplasm to the plasma membrane. In addition, the interaction of the PH domain with the lipid products of PI3K causes a conformational change in Akt, allowing its activation through phosphorylation at Thr-308 and Ser-473 by PDK-1 and other kinases [158-162].

AKT signaling pathway components are highly expressed in the ocular tissues [Lan Zhang et al. in preparation]. Our recent results also demonstrated that at both mRNA and protein levels, AKT-1 are a major surviving kinase in all the four ocular tissues examined. Compared with AKT-1, AKT-2 is much reduced in all the tissues examined and AKT-3 is only expressed in the retina [Zhang et al. in preparation].

AKT signaling pathway plays an important role in lens differentiation and survival [163-168]. In our previous study of the UVA-induced apoptosis, we found that irradiation of both vector- and human αA-transfected HLE cells with a dose of 150 KJ/m^2 induced activation of both ERK1 and ERK2 [109]. In contrast, UVA-induced activation of ERK1/2 was suppressed in human αB-crystallin-transfected cells [109]. Thus, UVA-induced apoptosis was associated with activation of ERK1/2 and human αB but not αA suppresses UVA-induced activation of ERK1/2 and apoptosis of HLE. Since HαA was unable to suppress UVA-induced activation of the RAF/MEK/ERK pathway, one possibility would be that human αA may be involved in regulation of other pathways. The possible activation of Akt kinase in the three types of stably transfected cells was examined. As expected, UVA-irradiation with a dose of 150 KJ/m^2 induced exclusive activation of Akt-1 in human αA-transfected cells but not observed in the vector- and human αB-transfected cells. In addition, UVA irradiation led to some down-regulation of Akt-1 protein in the vector- and human αB-transfected cells but visible up-regulation in the human αA-transfected cells [109]. Thus, under UVA irradiation, human αA upregulates and activates Akt to counteract UVA-induced apoptosis. To further confirm that activation of AKT is important for human αA-crystallin to prevent UVA-induced apoptosis, we inhibited AKT-1 activation. When αA-crystallin-regulated AKT-1 activation by UVA was blocked, the protection against UVA-induced apoptosis by αA-crystallin was significantly attenuated [109].

To explore how αA-crystallin may activate Akt pathway, we examined its possible interaction with Akt-1. First, we performed the surface plasmon resonance (SPR) analysis between αA, or αB and Akt-1 using BIACORE 3000 with research grade CM5 sensor chips and purified Akt-1, αA and αB crystallins [Gong et al., submitted]. αA- and αB-crystallins were covalently coupled to individual flow cell surfaces of a carboxymethyldextran-coated BIAcore sensor chip CM5 using amine-coupling chemistry. To determine the kinetics of the interactions between Akt-1 and αA-/αB-crystallins, Akt-1 with five different concentrations (50, 100, 250, 500, 1000 nM) was passed over the surfaces of both αA- and αB-crystallin chips at 30 μl/min. A buffer injection was used as a negative control. The association rates, dissociation rates, and affinity constants were calculated with BIA evaluation 4.1 software

(Biacore αB, Uppsala, Sweden). Our results suggest that Akt-1 only binds to αA-crystallin (Kd=5.6 μM) but not αB-crystallin [Gong et al., submitted].

To further explore the interaction between αA and Atk-1, co-immunoprecipitation was conducted and the obtained results showed that αA and Akt-1 form *in vivo* interacting complex in mouse lens [Gong et al., submitted]. Immunocytochemistry revealed that Akt1 and αA-crystallin were co-localized in both epithelium and fiber cells of mouse eye lens [Gong et al., submitted]

Activation of Akt pathway by αA-crystallin was further confirmed by in vivo studies [Gong et al., submitted]. An examination of the phosphorylation status of Akt-1 at Ser-473 in normal, αA-/-, and αA-/αB- DKO mice revealed that the normal Akt-1 activity detected in wild type mouse was dropped more than 50% in both αA-/-, and αA-/αB- DKO mice. These results clearly indicate that αA-crystallin displays strong regulation on Akt-1 activity.

While the details regarding how αA-crystallin activates Akt-1 remains to be worked out, the regulation of Akt activation by Hsp27 provides important hint. Hsp 27 is found in the same signaling complex with p38 MAPK, MAPK-activated protein kinase 2 (MAPKAPK-2), and Akt [161, 169-171]. Moreover, in polymorphonuclear leukocyte, Hsp27 activates Akt by scaffolding MAPKAPK-2 to Akt signal complex [171]. Deletion of the Hsp27 binding site in Akt (amino acids 117-128) results in loss of its interactions with Hsp27 and MAPKAPK-2 but not with Hsp90 as demonstrated by co-immunoprecipitation and GST pulldown studies [171]. On the other hand, phosphorylation of Hsp27 at Ser-82 by Akt induces dissociation of Hsp27 from Akt1 [171]. In addition, Hsp 90 can directly interact with Akt and help it to stay in its active status [172].

8. αB-CRYSTALLIN SUPPRESSES ERK PATHWAY TO INHIBIT STRESS-INDUCED APOPTOSIS

The mitogen-activated protein kinases (MAPKs) are actively involved in mediation of stress-induced apoptosis [173-174]. In the ocular lens, all of the three types of MAP kinases are expressed [175]. These kinases play important role in lens development and pathogenesis [176-186]. During stress-induced apoptosis of lens epithelial cells, activation of ERK1/2 is necessary for calcimycin-induced apoptosis [110] and for UVA-induced apoptosis [109]. This property distinguishes lens epithelial cells from most other tissue cells and also explains why the ocular lens never develops natural tumor [110]. Considering that the ERK pathway is normally involved in promotion of surviving in most other tissues and that oncogenic RAS persistently activates the ERK1 and ERK2 pathways, which contributes to the increased proliferative rate of tumor cells [187], lack of natural tumor in the ocular lens may partially be due to the fact that in the lens epithelial cells (the only cells that have complete sets of cellular organelles including nuclei in the lens organ), the RAF/MEK/ERK pathway mediates stress-induced apoptosis. Upon DNA damages induced by various stress factors, activation of the RAF/MEK/ERK pathway, instead of promoting survival of the cells with genetic lesions, signals apoptosis of the damaged cells. In this way, the cells bearing the genetic damages are removed in a timely manner and thus tumor development is avoided [110].

αB-crystallin can prevent both calcimycin- and UVA-induced apoptosis [109-110]. To understand the possible mechanism, we tested whether αB-crystallin could abrogate calcimycin-induced activation of ERK1/2. Western blot analysis revealed that ERK1/2 activity became downregulated during calcimycin treatment in pEGFP-mαB-N/N1003A cells [110]. Similarly, the activity of the p38 kinase became steady downregulated during calcimycin treatment. αB-crystallin also prevented the calcimycin-induced transient activation of JNK2 [110]. These results indicate that the mechanism for αB-crystallin to prevent calcimycin-induced apoptosis is derived from its suppression of calcimycin-induced activation of ERK1/2. The fact that in αB-crystallin expression cells, calcimycin-induced activation of ERK1/2, p38 and JNK2 (Figure 4) was all inhibited indicates that αB-crystallin may act on the initial steps of RAS/RAF/MEK/ERK signaling pathway. For this reason, we investigated the effect of αB-crystallin on Ras activation.

Both pEGFP-N/N1003A and pEGFP-mαB-N/N1003A cells were labelled with ^{32}P-orthophosphate and then treated with DMSO and 5μM calcimycin. Cell extracts were prepared from labeled and treated cells, and the RAS protein in each sample was immunoprecipitated. After that, the levels of GTP-bound RAS and GDP-bound RAS were determined with thin-layer chromatography. While DMSO treatment of both vector and αB-crystallin expression cells only induced background levels of RAS activation [110], treatment of the vector-transfected cells with 5 μM calcimycin induced substantially activation of RAS. However, such activation of RAS was not observed in the αB-crystallin expression cells. Thus, αB-crystallin blocks Ras activation to suppress activation of the downstream MAP kinases after treatment by calcimycin [110]. To explore how αB-crystallin may block the activation of RAS, we examined the upstream regulators of RAS. The RAS small GTPases are normally activated by the quanine nucleotide exchange factors (GEFs), which induce the dissociation of GDP to allow association of GTP [188]. Upon response to growth factor stimulation, two common RAS GEFs, son-of-sevenless 1 (Sos 1) and 2 (Sos 2), are activated to transfer from cytosol to the plasma membrane and there they activate RAS [189]. However, under calcium treatment, RAS is activated by other factors, the RAS-guanine-nucleotide-releasing factor 1 (RAS-GRF1) and 2 (RAS-GRF2) [188]. Because RAS-GRF1 is mainly expressed in the nerve system and RAS-GRF2 is widely expressed in many tissues [190-191], we therefore examined the activation of RAS by RAS-GRF2 after calcimycin treatment. After calcimycin treatment, the 135 kd RAS-GRF2 was transferred from cytosol to plasma membrane. In the αB-crystallin expression cells, however, the translocation of the RAS-GRF2 from cytosol to plasma membrane was largely inhibited [110]. These results and also the cross-linking experiments demonstrated that in N/N1003A cells, calcimycin activated RAS mainly through RAS-GRF2 and αB-crystallin negatively regulates activation of RAS through suppression of RAS-GRF2 translocation [110].

A recent study reported that the total and phospho-ERK1/2 and p38 were much enhanced in the astrocytes of the αB(-/-) mice than in those from normal mice with the same genetic background [119]. These results are consistent with our observation that αB-crystallin negatively regulates RAS/RAF/MEK/ERK signaling pathway. On the other hand, in breast cancer cells, Cryns et al [192] reported that overexpression of αB-crystallin constitutively activated the MEK/EKR signaling pathway and transformed the immortalized human mammary epithelial cells. The mechanism underlining this function of αB-crystallin remains

to be elucidated. Thus, depending upon the types of cells, αB-crystallin may have differential effects on the MAPK pathway.

9. α CRYSTALLINS REGULATE DNA DAMAGING PATHWAY TO CONTROL STRESS-INDUCED APOPTOSIS

In eukaryotes, DNA damage induces rapid response of the damaging signaling transduction pathway. The major components of this pathway include the upstream kinases, ATM and ATR, the intermediate kinases CHK1 and CHK2, and the G1 checkpoint substrates, p53 and Mdm2; S phase and G2/M checkpoint substrates [193-194]. UV or ionizing radiation (IR) induces activation of ATM through autophosphorylation, and the activated ATM then regulate the downstream G1 checkpoint substrates p53, Mdm2 and CHK2 [195]. Recent studies have revealed that α-crystallins can regulated the DNA damaging pathway components. Andley and her associates first reported that the primary cultures of the lens epithelial cells derived from αB-/- mice display genomic instability and undergo hyperproliferation. This property is at least partially related to the upregulated expression of the functionally impaired p53 [196]. Xiao and his associates [197] demonstrated that in mouse myogenic C2C12 cells, hydrogen peroxide induced apoptosis of the treated cells. During hydrogen peroxide treatment, p53 in the C2C12 cells was found translocated from cytoplasm into mitochondria. Overexpression of αB-crystallin in the C2C12 cells prevented hydrogen peroxide-induced apoptosis. The mechanism mediating this protection was largely related to the interaction between αB-crystallin and p53, which blocked p53 translocation from cytosol into mitochondria. We recently found that UVA irradiation induced hyperphosphorylation of p53 at several residues in human lens epithelial cells. Both αA- and αB-crystallins distinctly attenuated p53 hyperphosphorylation at these sites (Liu et al., in preparation). Furthermore, the two α-crystallins seemed to interfere with the activation of several p53 upstream kinases (Liu et al., in preparation).

10. MODULATION OF THE ANTI-APOPTOTIC ABILITY OF αB-CRYSTALLIN BY PHOSPHORYLATION

Early studies have shown that α-crystallins are phosphoproteins [198]. Phosphorylation of αB-crystallin at Ser-59 is important for its function against apoptosis in cardiac myocytes. Hoover et al. [99] demonstrated that MKK6-activated p38 MAP kinase can phosphorylate αB-crystallin at Ser-59, which seems to provide maximal protection of cardiac myocytes from apoptosis [99, 199]. A recent study [200] demonstrated that phosphorylation of αB-crystallin occurred after its translocation from cytosol into mitochondria. Once αB-crystallin is phosphorylated at Ser-59 in mitochondria, it stabilizes mitochondrial membrane potential and thus inhibits apoptosis.

Although it has not be examined weather phosphorylation of αB-crystallin at Ser-19 has a role in modulating its antiapoptotic ability, analysis of the P20S mutant αB-crystallin provides some hint. The immunofluorescence confocal microscopy revealed that wild-type

αB-crystallin was localized mainly in the cytoplasm and surrounded the cell nucleus, whereas mutant P20S αB-crystallin was present in both the cytoplasm and nucleus. To investigate whether mutation P20S of αB-crystallin acquires any detrimental function to cellular homeostasis, we examined the cytotoxic effect of mutation P20S. HLE cells with stable expression of wild-type αB-crystallin or mutant P20S αB-crystallin were stained using Hoechst 33342 in order to study the changes in nuclear morphology. The stable expression of P20S αB-crystallin increased chromatin condensation and fragmentation compared with cells with stable expression of wild-type αB-crystallin or cells transfected with empty vector only [124]. These results demonstrate that the P20S mutation increases apoptosis of human lens epithelial cells. Thus, phosphorylation modulates the antiapoptotic function of α-crystallins.

CONCLUSION

Both *in vitro* and *in vivo* studies have shown that α-crystallins act as strong anti-apoptotic regulators. In lens and retina of the eye, cardiac myocytes of the heart, and neuron and glial cells of the brain, α-crystallins are important guardians preventing apoptosis triggered by stress factors and pathological conditions and thus protect these tissues from running into various diseases such as cataract, retina degeneration, heart failure, and various brain diseases. α-crystallins prevent stress-induced apoptosis through regulating members of the Bcl-2 and caspase families. In addition, αA-crystallin can help to activate the Akt survival pathway to suppress apoptosis, while αB-crystallin can intervened the Ras/Raf/MEK/ERK signaling pathway to inhibit apoptosis, displaying differential anti-apoptotic mechanisms dependent upon the stress conditions implicated. The two α-crystallins can also modulate the DNA damaging pathway to halt apoptosis. Together, these results demonstrate that the two α-crystallins can regulate multiple signaling transduction pathways to regulate apoptosis (Figure 1). It is expected that in the near future, the detail mechanisms regarding how α-crystallins regulate these different signaling transduction pathways to halt apoptosis will be elucidated.

ACKNOWLEDGEMENTS

This work is supported in part by the National Institute of Health Grants 1 R01EY15765 and 1R01EY018380 (DWL), the University of Nebraska Medical Center startup funds (DWL), the Changjiang Scholar Team Award Funds from Education Ministry of China (DWL), National Science Foundation Funds of China (ML), National Key Laboratory Funds of China (DWL), the Lotus Scholar Program Funds from Hunan Province Government (DWL) and the Special Honorary Professorship Funds from Hunan Normal University (DWL). We apologize to those colleagues whose valuable publications could not be cited here due to space limitation.

REFERENCE

[1] Bloemendal, H. (1982). Lens proteins. *CRC Crit. Rev. Biochem.* 12:1-38.

[2] Pras E, Frydman M, Levy-Nissenbaum E, Bakhan T, Raz J, Assia EI et al. (2000). A nonsense mutation (W9X) in CRYAA causes autosomal recessive cataract in an inbred Jewish Persian family. Invest Ophthalmol Vis Sci 41: 3511–3515.

[3] Mackay DS, Andley UP, Shiels A. (2003). Cell death triggered by a novel mutation in the alphaA-crystallin gene underlies autosomal dominant cataract linked to chromosome 21q. Eur J Hum Genet 11: 784–793.

[4] Litt M, Kramer P, LaMorticella DM, Murphey W, Lovrien EW, Weleber RG. (1998). Autosomal dominant congenital cataract associated with a missense mutation in the human alpha crystallin gene CRYAA. Hum Mol Genet 7: 471–474.

[5] Gu F, Luo W, Li X, Wang Z, Lu S, Zhang M et al. (2008). A novel mutation in AlphaA-crystallin (CRYAA) caused autosomal dominant congenital cataract in a large Chinese family. Hum Mutat 29: 769.

[6] Santhiya ST, Soker T, Klopp N, Illig T, Prakash MV, Selvaraj B et al. (2006). Identification of a novel, putative cataract-causing allele in CRYAA (G98R) in an Indian family. Mol Vis 12: 768–773.

[7] Vicart P, Caron A, Guicheney P, Li Z, Prevost MC, Faure A et al. (1998). A missense mutation in the alph _B-crystallin chaperone gene causes a desmin-related myopathy. Nat Genet 20: 92–95.

[8] Berry V, Francis P, Reddy MA, Collyer D, Vithana E, MacKay I et al. (2001). Alpha-B crystallin gene (CRY _B) mutation causes dominant congenital posterior polar cataract in humans. Am J Hum Genet 69: 1141–1145.

[9] Selcen D, Engel AG. (2003). Myofibrillar myopathy caused by novel dominant negative alpha B-crystallin mutations. Ann Neurol 54: 804–810.

[10] Liu M, Ke T, Wang Z, Yang Q, Chang W, Jiang F et al. (2006a). Identification of a CRY _B mutation associated with autosomal dominant posterior polar cataract in a Chinese family. Invest Ophthalmol Vis Sci 47: 3461–3466.

[11] Liu Y, Zhang X, Luo L, Wu M, Zeng R, Cheng G et al. (2006b). A novel alph _B-crystallin mutation associated with autosomal dominant congenital lamellar cataract. Invest Ophthalmol Vis Sci 47: 1069–1075.

[12] Andley, UA. (2007). Crystallins in the eye: Function and pathology. *Progress in Retinal and Eye Research* 26: 78–98.

[13] Kato K, Shinohara H, Kurobe N, Goto S, Inaguma Y, Ohshima K. (1991). Immunoreactive alpha A crystallin in rat non-lenticular tissues detected with a sensitive immunoassay method. *Biochim Biophys Acta.* 1080: 173-180.

[14] Bhat SP, Nagineni CN. (1989). _B subunit of lens specific protein a-crystallin is present in other ocular and non-ocular tissues. *Biochem. Biophys. Res. Commun.* 158: 319-325.

[15] Iwaki T, Kume-Iwaki A, Liem RKH, Goldman JE. (1989). _B-crystallin is expressed in non lenticular tissues and accumulates in Alexander's disease brain. *Cell.* 57: 71-78.

[16] Dubin RA, Wawrousek EF, Piatigorsky J. (1989). Expression of the murine _B-crystallin gene is not restricted to lens. *Mol. Cell. Biol*. 9: 1083-1091.

[17] Ingolia TD, Craig EA. (1982). Four small Drosophila heat shock proteins are related to each other and to mammalian a-crystallin. *Proc. Natl. Acad. Sci. USA.* 79, 2360-2364.

[18] Klemenz R, Frohli E, Steiger RH, Schafer R, and Aoyama A (1991). Alpha B-crystallin is a small heat shock protein. . *Proc. Natl. Acad. Sci. USA.* 88:3652-3656.

[19] Horwitz J. (1992). a-Crystallin can function as a molecular chaperone. *Proc. Natl. Acad. Sci. USA.* 89:10449-10453.

[20] Rao PV, Horwitz J, Zigler JS Jr. (1993). Alpha-crystallin, a molecular chaperone, forms a st _Ble complex with carbonic anhydrase upon heat denaturation. *Biochem Biophys Res Commun*. 190:786-793.

[21] Kelley MJ, David LL, Iwasaki N, Wright J, Shearer TR. (1993). alpha-Crystallin chaperone activity is reduced by calpain II in vitro and in selenite cataract. *J Biol Chem.* 268:18844-18849.

[22] Boyle D, Takemoto L. (1994). Characterization of the alpha-gamma and alpha-beta complex: evidence for an *in vivo* functional role of alpha-crystallin as a molecular chaperone. *Exp Eye Res*. 58:9-15.

[23] Nicholl ID, Quinlan RA. (1994). Chaperone activity of alpha-crystallins modulates intermediate filament assembly. *EMBO J.* 13:945-53.

[24] Clark JI, Huang QL. (1996). Modulation of the chaperone-like activity of bovine alpha-crystallin. *Proc Natl Acad Sci U S A*. 93:15185-15189.

[25] Sun TX, Das BK, Liang JJ. (1997). Conformational and functional differences between recombinant human lens alphaA- and alph _B-crystallin. *J Biol Chem.* 272:6220-6225.

[26] Reddy GB, Das KP, Petrash JM, Surewicz WK. (2000). Temperature-dependent chaperone activity and structural properties of human alphaA- and alph _B-crystallins. *J Biol Chem*. 275:4565-4570.

[27] Kantorow M and Piatigorsky J (1994). Alpha-crystallin/small heat shock protein has autokinase activity. *Proc. Natl. Acad. Sci. USA* 91: 3112-3116.

[28] Arrigo AP, Tanaka K, Goldberg AL, Welch WJ. (1988). Identity of the 19S 'prosome' particle with the large multifunctional protease complex of mammalian cells (the proteasome). *Nature.* 331(6152), 192-4.

[29] Finley D, Ciechanover A, Varshavsky A. (2004). Ubiquitin as a central cellular regulator. *Cell*. S116, S29–S32.

[30] den Engelsman J, Keijsers V, de Jong WW, Boelens WC. (2003). The small heat-shock protein alpha B-crystallin promotes FBX4-dependent ubiquitination. *J Biol Chem.* 278(7), 4699-704.

[31] Lin DI, Barbash O, Kumar KG, Weber JD, Harper JW, Klein-Szanto AJ, Rustgi A, Fuchs SY, Diehl JA. (2006). Phosphorylation-dependent ubiquitination of cyclin D1 by the SCF(FBX4-alph _B crystallin) complex. *Mol Cell.* 24(3), 355-66.

[32] Barbash O, Lin DI, Diehl JA. (2007). SCF Fbx4/alph _B-crystallin cyclin D1 ubiquitin ligase: a license to destroy. *Cell Div.* 2, 2.

[33] Lin DI, Lessie MD, Gladden _B, Bassing CH, Wagner KU, Diehl JA. (2008). Disruption of cyclin D1 nuclear export and proteolysis accelerates mammary carcinogenesis. *Oncogene.* 27(9),1231-42.

[34] Barbash O, Diehl JA. (2008). SCF(Fbx4/alph _B-crystallin) E3 ligase: when one is not enough. *Cell Cycle.* 7(19):2983-6.

[35] McAvoy, J.W. (1980). Induction of the eye lens. *Differentiation* 17,137-149.
[36] Piatigorsky J. (1981). Lens differentiation in vertebrates. A review of cellular and molecular features. *Differentiation.* 19, 134-153.
[37] Spector A. (1995). Oxidative stress-induced cataract: mechanism of action. *FASEB J.* 9, 1173-1182.
[38] Grainger RM. (1992). Embryonic lens induction: shedding light on vertebrate tissue determination. *Trends Genet.* 8, 349-355.
[39] Wride, M.A. (1996). Cellular and molecular features of lens differentiation: a review of recent advances. *Differentiation*. 61, 77-93.
[40] O'Rahilly, R. The early development of the eye in staged human embryos. *Contrib. Embryo. Carneg. Inst*. 38,1-42.
[41] Robinson, M.L., Overbeek, P.A., 1996. Differential expression of alpha A- and alpha B-crystallin during murine ocular development. *Invest. Ophthalmol. Vis. Sci*. 37, 2276–2284.
[42] Kuw _Bara, T., and Imaizumi, M. (1974). Denucleation process of the lens. *Invest. Ophthalmol. Vis. Sci.* 13, 973-981.
[43] Bassnett S, Mataic D. (1997). Chromatin degradation in differentiating fiber cells of the eye lens. J. Cell Biol. 137, 37-49.
[44] Lang RA. (1999). Which factors stimulate lens fiber cell differentiation in vivo? *Invest Ophthalmol Vis Sci.* 40, 3075-3078.
[45] Harding JJ, Cr _Bbe JC. (1984). The lens: development, proteins, met _Bolism and cataract. In "*The Eye*". (ed. Davison, H.). pp 207-492. Academic press, New York.
[46] Kerr, J.F.R., Wyllie, A.H., and Currrie, A.R. (1972). Apoptosis: a basic biological phenomenon with wide-ranging implications in tissue kinetics. *Br. J. Cancer.* 26, 239-257.
[47] Arends, M. J. and Wyllie, A. H. (1991). Apoptosis: mechanisms and roles in pathology. *Int. Rev. Exp. Path.* 32, 223-254.
[48] Horvitz, H.R., Shaham, S. and Hengartner, M.O. (1994) The genetics of programmed cell death in the nematode *Caenorh _Bditis elegans*. *Cold Spring Harbor Symp Quant Biol* 59:377-385.
[49] Vaux, D.L., Korsmeyer, S.J. (1999). Cell death in development. *Cell*. 96(2), 245-254.
[50] Gross, A., McDonnell, J.M., Korsmeyer, S.J. (1999). BCL-2 family members and the mitochondria in apoptosis. *Genes Dev.* 13:1899-1911.
[51] Danial NN, Korsmeyer SJ (2006). Cell Death: Critical Control Points. *Cell*. 116, 205–219.
[52] Thompson, C. B. (1995). Apoptosis in the pathogenesis and treatment of disease. *Science.* 267:1456-1462.
[53] Glucksmann, A. (1951). Cell deaths in normal vertebrate ontogeny. *Biol. Rev.* 26:59-86.
[54] Silver J, AFW Hughes (1973). The role of cell death during morphogenesis of the mammalian eye. *J. Morph.* 140:159-170.
[55] Ishizaki, Y., Voyvodic, J.T., Burne, J.F., and Raff, M.C. (1993). Control of lens epithelial cell survival. *J. Cell Biol.* 121:899-908.
[56] Ozeki H, Ogura Y, Hir _Bayashi Y, Shimada S. (2001). Suppression of lens stalk cell apoptosis by hyaluronic acid leads to faulty separation of the lens vesicle. *Exp Eye Res*. 72:63-70.

[57] Bozanic D, Tafra R, Saraga-B _Bic M.(2003). Role of apoptosis and mitosis during human eye development. *Eur J Cell Biol*. 82:421-429.

[58] Mohamed YH, Amemiya T. (2003). Apoptosis and lens vesicle development. *Eur J Ophthalmol*. 13(1):1-10.

[59] Harding, J.J. and Cr _Bbe, J.C. (1984) The lens: development, proteins, met _Bolism and cataract. In: Davison, H. (ed.): The Eye. Academic press, New York

[60] Yan, Q., Liu, J-P and Li, D. W-C. (2006) Apoptosis in lens development and pathology. *Differentiation.* 74, 195-211.

[61] Hettmann T, Barton K, Leiden JM. (2000). Microphthalmia due to p53-mediated apoptosis of anterior lens epithelial cells in mice lacking the CREB-2 transcription factor. *Dev. Biol.* 222:110-123.

[62] Blixt A, Mahlapuu M, Aitola M, Pelto-Huikko M, EneRback S, Carlsson P. (2000). A forkhead gene, FoxE3, is essential for lens epithelial proliferation and closure of the lens vesicle. *Genes Dev*. 14:245-254.

[63] Fromm L, Shawlot W, Gunning K, Butel JS, OveRbeek PA. (1994). The retinoblastoma protein-binding region of simian virus 40 large T antigen alters cell cycle regulation in lenses of transgenic mice. *Mol Cell Biol*. 14:6743-6754.

[64] Pan H, Griep AE.(1995). Temporally distinct patterns of p53-dependent and p53-independent apoptosis during mouse lens development. *Genes Dev*. 9:2157-2169.

[65] Morgenbesser SD, Schreiber-Agus N, Bidder M, Mahon KA, OveRbeek PA, Horner J, DePinho RA. (1995). Contrasting roles for c-Myc and L-Myc in the regulation of cellular growth and differentiation in vivo. *EMBO J.* 14:743-756.

[66] Nakamura T, Pichel JG, Williams-Simons L, Westphal H. (1995). An apoptotic defect in lens differentiation caused by human p53 is rescued by a mutant allele. *Proc Natl Acad Sci U S A*. 92:6142-6146.

[67] Robinson ML, MacMillan-Crow LA, Thompson JA, OveRbeek PA. (1996). Expression of a truncated FGF receptor results in defective lens development in transgenic mice. *Development.* 121:3959-3967.

[68] Gomez Lahoz E, Liegeois NJ, Zhang P, Engelman JA, Horner J, Silverman A, Burde R, Roussel MF, Sherr CJ, Elledge SJ, DePinho RA. (1997). Cyclin D- and E-dependent kinases and the p57(KIP2) inhibitor: cooperative interactions in vivo. *Mol Cell Biol.* 19:353-363.

[69] McCaffrey J, Yamasaki L, Dyson NJ, Harlow E, Griep AE. (1999). Disruption of retinoblastoma protein family function by human papillomavirus type 16 E7 oncoprotein inhibits lens development in part through E2F-1. *Mol Cell Biol*. 19:6458-68.

[70] de Iongh RU, Lovicu FJ, OveRbeek PA, Schneider MD, Joya J, Hardeman ED, McAvoy JW. (2001). Requirement for TGFbeta receptor signaling during terminal lens fiber differentiation. *Development.*128:3995-4010.

[71] Li WC, Kuszak JR, Dunn K, Wang RR, Ma W, Wang GM, Spector A, et al. (1995). Lens epithelial cell apoptosis appears to be a common cellular basis for non-congenital cataract development in humans and animals. *J Cell Biol*. 130:169-181.

[72] Li W-C, Kuszak JR, Wang G-M, Wu Z-Q, Spector A. (1995). Calcimycin-induced lens epithelial cell apoptosis contributes to cataract formation. *Exp. Eye Res.* 61:89-96.

[73] Li W-C, Spector A. (1996). Lens epithelial cell apoptosis is an early event in the development of UVB-induced cataract. *Free Radic Biol Med.* 20:301-311.

[74] Menko S and Zhou J (2004). Src kinase signaling formation of cataract through a mechanism involving caspase activation, cadherin cleavage and the induction of apoptosis. *Invest Ophthalmol Vis Sci.* 45 (supplement): _Bstract #3507.

[75] Zhou J, Leonard M, Van Bockstaele E, Menko AS. (2007).Mechanism of Src kinase induction of cortical cataract following exposure to stress: dest _Bilization of cell-cell junctions. *Mol Vis.* 13:1298-310.

[76] Michael R, Vrensen GF, van Marle J, Gan L, SodeRberg PG. (1998). Apoptosis in the rat lens after *in vivo* threshold dose ultraviolet irradiation. *Invest Ophthalmol Vis Sci*. 39, 2681-2687.

[77] Michael, R., Vrensen, G.F., van Marle, J., Lofgren, S., Soderberg, P.G. (2000). Repair in the rat lens after threshold ultraviolet radiation injury. *Invest Ophthalmol Vis Sci.* 41(1),204-212.

[78] Ayala M, Strid H, Jacobsson U, Söderberg PG. (2007). p53 Expression and Apoptosis in the lens after ultraviolet radiation exposure. *Invest Ophthalmol Vis Sci.*, 48(9):4187-4191.

[79] Takamura Y, Kubo E, Tsuzuki S, Akagi Y. (2003). Apoptotic cell death in the lens epithelium of rat sugar cataract. *Exp Eye Res*. 77:51-57.

[80] Murata M, Ohta N, Sakurai S, Alam S, Tsai J, Kador PF, Sato S. (2001). The role of aldose reductase in sugar cataract formation: aldose reductase plays a key role in lens epithelial cell death (apoptosis). *Chem Biol Interact.* 130-132(1-3):617-25.

[81] Tamada Y, Fukiage C, Nakamura Y, Azuma M, Kim YH, Shearer TR. (2000). Evidence for apoptosis in the selenite rat model of cataract. *Biochem Biophys Res Commun*. 275, 300-306.

[82] Yoshizawa K, Oishi Y, Nambu H, Yamamoto D, Yang J, Senzaki H, Miki H, Tsubura A. (2000). Cataractogenesis in neonatal Sprague-Dawley rats by N-methyl-N-nitrosourea. *Toxicol Pathol.* 28, 555-564.

[83] Wolf N, et al. 2005. Age-related cataract progression in five mouse models for anti-oxidant protection or hormonal influence. *Exp Eye Res*. 81:276-85

[84] Nishi O, Nishi, K. (1998). Apoptosis in lens epithelial cells of human cataracts. *Journal of Eye (In Japanese).* 15:1309-1313.

[85] Takamura, Y., Sugimoto, Y., Kubo, E., Takahashi, Y. and Akagi,Y. (2001) Immunohistochemical study of apoptosis of lens epithelial cells in human and di _Betic rat cataracts. *Jpn J Ophthalmol* 45:559–563.

[86] Okamura, N., Ito, Y., Shibata, M.A., Ikeda, T. and Otsuki, Y. (2002) Fas-mediated apoptosis in human lens epithelial cells of cataracts associated with di _Betic retinopathy. *Med Electron Microsc.* 35:234–241.

[87] Charakidas A. Kalogeraki A, Tsilimbaris M, Koukoulomatis P, Brouzas D, Delides G. (2005). Lens epithelial apoptosis and cell proliferation in human age-related cortical cataract. *Eur J Ophthalmol.* 15(2):213-20.

[88] Harocopos GJ, Alvares KM, Kolker AE, Beebe DC. (1998). Human age-related cataract and lens epithelial cell death. *Invest Ophthalmol Vis Sci*. 39:2696-2706.

[89] Mihara E, Miyata H, Nagata M, Ohama E., (2000). Lens epithelial cell damage and apoptosis in atopic cataract-histopathologcal and immunohistochemical studies. *Jpn J Ophthalmol*. 44:695-696.

[90] Lee, J.H., Wan, L., Song, J., Kang, J.J., Chung, W., Lee, E.H. and Kim, E.K. (2002) TGF-b-induced apoptosis and reduction of Bcl-2 in human lens epithelial cells in vitro. *Curr Eye Res* 25, 147-153.

[91] Mulhern ML, Madson CJ, Danford A, Ikesugi K, Kador PF, Shinohara T. (2006). The unfolded protein response in lens epithelial cells from galactosemic rat lenses. *Invest Ophthalmol Vis Sci.* 47(9):3951-3959.

[92] Aoyama A, Frohli E, Schafer R, Klemenz R. (1993). Alpha B-crystallin expression in mouse NIH 3T3 fibroblasts: glucocorticoid responsiveness and involvement in thermal protection. *Mol Cell Biol.* 13:1824-1835.

[93] Mehlen P, Preville X, Chareyron P, Briolay J, Klemenz R, Arrigo AP.(1995). Constitutive expression of human hsp27, Drosophila hsp27, or human alpha B-crystallin confers resistance to TNF- and oxidative stress-induced cytotoxicity in st _Bly transfected murine L929 fibroblasts. *J Immunol.* 154:363-374.

[94] Mehlen P, Kretz-Remy C, Preville X and Arrigo A-P (1996) Human hsp27, Drosophila hsp27 and human alph _B-crystallin expression-mediated increase in glutathione is essential for the protective activity of these proteins against TNFalpha-induced cell death. *EMBO J*. 15:2695-2706.

[95] Mehlen P, Schulze-Osthoff K, Arrigo AP. (1996). Small stress proteins as novel regulators of apoptosis. Heat shock protein 27 blocks Fas/APO-1- and staurosporine-induced cell death. *J Biol Chem.* 271(28), 16510-4.

[96] Martin JL, Mestril R, Hilal-Dandan R, Brunton LL, Dillmann WH. (1997). Small heat shock proteins and protection against ischemic injury in cardiac myocytes. *Circulation.* 96(12):4343.

[97] Andley UP, Song Z, Wawrousek EF, Bassnett S. (1998). The molecular chaperone alphaA-crystallin enhances lens epithelial cell growth and resistance to UVA stress. *J Biol Chem*. 273:31252-61.

[98] Andley UP, Song Z, Wawrousek EF, Fleming TP, Bassnett S. (2000). Differential protective activity of alpha A- and alph _B-crystallin in lens epithelial cells. *J Biol Chem*. 275:36823-31.

[99] Hoover HE, Thuerauf DJ, Martindale JJ, Glembotski CC. (2000). alpha B-crystallin gene induction and phosphorylation by MKK6-activated p38. A potential role for alpha B-crystallin as a target of the p38 branch of the cardiac stress response. *J Biol Chem*. 275: 23825-33.

[100] Ray PS, Martin JL, Swanson EA, Otani H, Dillmann WH, Das DK. (2001). Transgene overexpression of alph _B crystallin confers simultaneous protection against cardiomyocyte apoptosis and necrosis during myocardial ischemia and reperfusion. *FASEB J.* 15:393-402.

[101] Li DW-C, Xiang H, Mao Y-W, Wang J, Fass U, Zhang X-Y, and Xu C. (2001). Caspase-3 is actively involved in okadaic acid-induced lens epithelial cell apoptosis. *Exp. Cell Res*. 266:279-291.

[102] Mao Y-W, Xiang H, Wang J, Korsmeyer S, Reddan J, Li D W-C. (2001). Human Bcl-2 gene attenuates the _Bility of r _Bbit lens epithelial cells against H_2O_2-induced apoptosis through downregulation the alpha B crystallin gene. *J. Biol. Chem.* 27: 43435-43445.

[103] Kamradt MC, Chen F, Cryns VL. (2001). The small heat shock protein alpha B-crystallin negatively regulates cytochrome c- and caspase-8-dependent activation of caspase-3 by inhibiting its autoproteolytic maturation. *J Biol Chem.* 276:16059-63.

[104] Kamradt MC, Chen F, Sam S, Cryns VL. (2002). The small heat shock protein alpha B-crystallin negatively regulates apoptosis during myogenic differentiation by inhibiting caspase-3 activation. *J Biol Chem*. 277:38731-38736.

[105] Andley UP, Patel HC, Xi JH. (2002). The R116C mutation in alpha A-crystallin diminishes its protective _Bility against stress-induced lens epithelial cell apoptosis. *J Biol Chem*. 277:10178-10186.

[106] Alge CS, Priglinger SG, Neubauer AS, Kampik A, Zillig M, Bloemendal H, Welge-Lussen U. (2002). Retinal pigment epithelium is protected against apoptosis by alph _B-crystallin. Invest Ophthalmol Vis Sci. 43(11):3575-82.

[107] Morrison LE, Hoover HE, Thuerauf DJ, Glembotski CC. (2003). Mimicking phosphorylation of alph _B-crystallin on serine-59 is necessary and sufficient to provide maximal protection of cardiac myocytes from apoptosis. *Circ Res*. 92(2):203-11.

[108] Mao, Y-W., Liu, J-P., Xiang, H., and Li, D. W-C. (2004). Human aA- and _B-crystallins bind to Bax and Bcl-XS to sequester their translocation during staurosporine-induced apoptosis. *Cell Death and Differ.* 11:512-526.

[109] Liu, J-P., R. Schlosser, W-Y. Ma, Z. Dong, H. Feng, L. Liu, X.-Q. Huang, Y. Liu, and D.W-C. Li. (2004). Human aA- and _B-crystallins prevent UVA-induced apoptosis through regulation of PKCa, RAF/MEK/ERK and AKT signaling pathways. *Exp. Eye Res.* 79:393-403.

[110] Li, D. W-C., J-P., Liu, Mao, Y-W., H. Xiang, J. Wang, Z. Dong and J. Reed (2005). Calcium-activated RAF/MEK/ERK signaling pathway mediates p53-dependent apoptosis and is _Brogated by alph _B-crystallin through inhibition of RAS activation. *Mol. Biol. Cell.* 16:4437-4453.

[111] Liu B, Bhat M, Nagaraj RH. (2004). Alph _B-crystallin inhibits glucose-induced apoptosis in vascular endothelial cells. *Biochem Biophys Res Commun*. 321(1):254-8.

[112] Maloyan A, Sanbe A, Osinska H, Westfall M, Robinson D, Imahashi K, Murphy E, Robbins J. (2005). Mitochondrial dysfunction and apoptosis underlie the pathogenic process in alpha-B-crystallin desmin-related cardiomyopathy. *Circulation.* 112:3451-61.

[113] Kamradt MC, Lu M, Werner ME, Kwan T, Chen F, Strohecker A, Oshita S, Wilkinson JC, Yu C, Oliver PG, Duckett CS, Buchsbaum DJ, LoBuglio AF, Jordan VC, Cryns VL. The small heat shock protein alpha B-crystallin is a novel inhibitor of TRAIL-induced apoptosis that suppresses the activation of caspase-3. *J Biol Chem.* 280:11059-66.

[114] Moorozov, V., Wawrousek, E.F. (2006). Caspase-dependent secondary lens fiber cell disintegration in aA/ _B-crystallin double knockout mice. *Development.* 133:813-821.

[115] Ikeda R, Yoshida K, Ushiyama M, Yamaguchi T, Iwashita K, Futagawa T, Shibayama Y, Oiso S, Takeda Y, Kariyazono H, Furukawa T, Nakamura K, Akiyama S, Inoue I, Yamada K. (2006). The small heat shock protein alph _B-crystallin inhibits differentiation-induced caspase 3 activation and myogenic differentiation. *Biol Pharm Bull.* 29(9):1815-9.

[116] Kadono T, Zhang XQ, Srinivasan S, Ishida H, Barry WH, Benjamin IJ. (2006). CRY _B and HSPB2 deficiency increases myocyte mitochondrial perme _Bility transition and mitochondrial calcium uptake. *J Mol Cell Cardiol.* 40:783-9.

[117] Yaung J, Jin M, Barron E, Spee C, Wawrousek EF, Kannan R, Hinton DR. (2007). alpha-Crystallin distribution in retinal pigment epithelium and effect of gene knockouts on sensitivity to oxidative stress. *Mol Vis.* 13:566-77.

[118] Ousman S, Beren H. Tomooka, Johannes M. van Noort, Eric F. Wawrousek, Kevin C. O'Connor, David A. Hafler, Raymond A. Sobel, William H. Robinson & Lawrence Steinman. (2007). Protective and therapeutic role for _B-crystallin in autoimmune demyelination. *Nature.* 448:474-479.

[119] Dimberg A, Rylova S, Dieterich LC, Olsson AK, Schiller P, Wikner C, Bohman S, Botling J, Lukinius A, Wawrousek EF, Claesson-Welsh L. (2008). alph _B-crystallin promotes tumor angiogenesis by increasing vascular survival during tube morphogenesis. *Blood*. 111(4):2015-23.

[120] Whiston EA, Sugi N, Kamradt MC, Sack C, Heimer SR, Engelbert M, Wawrousek EF, Gilmore MS, Ksander BR, Gregory MS. (2008). alph _B-crystallin protects retinal tissue during Staphylococcus aureus-induced endophthalmitis. *Infect Immun*. 76(4):1781-90.

[121] Aggeli IK, Beis I, Gaitanaki C. (2008). Oxidative stress and calpain inhibition induce alpha B crystallin phosphorylation via p38-MAPK and calcium signalling pathways in H9c2 cells. *Cell Signal.* 20 (7):1292-302. Erratum in: *Cell Signal.* 2008. 20(9):1695.

[122] Stegh AH, Kesari S, Mahoney JE, Jenq HT, Forloney KL, Protopopov A, Louis DN, Chin L, DePinho RA.(2008). Bcl2L12-mediated inhibition of effector caspase-3 and caspase-7 via distinct mechanisms in glioblastoma. *Proc Natl Acad Sci U S A.* 105(31):10703-8.

[123] Stegh AH, Chin L, Louis DN, DePinho RA. (2008). What drives intense apoptosis resistance and propensity for necrosis in glioblastoma? A role for Bcl2L12 as a multifunctional cell death regulator. Cell Cycle. 7(18):2833-9.

[124] Li H, Li C, Lu Q, Su T, Ke T, Li DW-C, Yuan M, Liu J, Ren X, Zhang Z, Zeng S, K Q. Wang Q and M Liu (2008). Cataract mutation P20S of _B-crystalline impairs chaperone activity of _A-crystalline and induces apoptosis of human lens epithelial cells. *Biophy. Biochem. Acta-Human Diseases*. 1782, 303-309.

[125] Ghosh JG, Shenoy AK Jr, Clark JI. (2007). Interactions between important regulatory proteins and human alph _B crystallin. *Biochemistry.* 46(21):6308-17.

[126] Vander Heiden MG, Chandel NS, Williamson EK, Schumacker PT and Thompson CB (1997) Bcl-xL regulates the membrane potential and volume homeostasis of mitochondria. *Cell* 91, 627-637.

[127] Bossy-Wetzel E, Newmeyer DD and Green DR (1998) Mitochondrial cytochrome c release in apoptosis occurs upstream of DEVD-specific caspase activation and independently of mitochondrial transmembrane depolarization. *EMBO J.* 17, 37-49.

[128] Deshmukh M and Johnson EM Jr (2000) Staurosporine-induced neuronal death: multiple mechanisms and methodological implications. *Cell Death. Differ*. 7: 250-261.

[129] Murphy KM, Ranganathan V, Farnsworth ML, Kavallaris M and Lock RB (2000) Bcl-2 inhibits Bax translocation from cytosol to mitochondria during drug-induced apoptosis of human tumor cells. *Cell Death Differ.* 7: 102-111.

[130] Kashkar H, Kronke M and Jurgensmeier JM (2002) Defective Bax activation in Hodgkin B-cell lines confers resistance to staurosporine-induced apoptosis. *Cell Death Differ.* 9: 750-757.

[131] Wei MC, Zong WX, Cheng EH, Lindsten T, Panoutsakopoulou V, Ross AJ, Roth KA, MacGregor GR, Thompson CB and Korsmeyer SJ (2001) Proapoptotic BAX and BAK: a requisite gateway to mitochondrial dysfunction and death. *Science* 292: 727-730.

[132] Cheng EH, Wei MC, Weiler S, Flavell RA, Mak TW, Lindsten T and Korsmeyer SJ (2001) BCL-2, BCL-X(L) sequester BH3 domain-only molecules preventing BAX- and BAK-mediated mitochondrial apoptosis. *Mol. Cell*. 8: 705-11.

[133] Wang GQ, Gastman BR, Wieckowski E, Goldstein LA, Gambotto A, Kim TH, Fang B, R _Binovitz A, Yin XM and R _Binowich H (2001) A role for mitochondrial Bak in apoptotic response to anticancer drugs. *J. Biol. Chem.* 276: 34307-34317.

[134] Theodorakis P, Lomonosova E and Chinnadurai G (2002) Critical requirement of BAX for manifestation of apoptosis induced by multiple stimuli in human epithelial cancer cells. *Cancer Res.* 62: 3373-3376.

[135] Hague A, Diaz GD, Hicks DJ, Krajewski S, Reed JC and Paraskeva C (1997) Bcl-2 and Bak may play a pivotal role in sodium butyrate-induced apoptosis in colonic epithelial cells; however overexpression of bcl-2 does not protect against bak-mediated apoptosis. *Int. J. Cancer.* 72: 898-905.

[136] Chen G, Sordillo EM, Ramey WG, Reidy J, Holt PR, Krajewski S, Reed JC, Blaser MJ and Moss SF (1997) Apoptosis in gastric epithelial cells is induced by Helicobacter pylori and accompanied by increased expression of BAK. *Biochem. Biophys. Res. Commun*. 239: 626-32.

[137] Goping IS, Gross A, Lavoie JN, Nguyen M, Jemmerson R, Roth K, Korsmeyer SJ and Shore GC (1998) Regulated Targeting of BAX to Mitochondria. *J. Cell Biol.* 143: 207-215.

[138] Nechushtan A, Smith CL, Hsu YT and Youle RJ (1999) Conformation of the Bax C-terminus regulates subcellular location and cell death. *EMBO J.* 18: 2330-2341.

[139] Wang K, Gross A, Waksman G and Korsmeyer SJ (1998) Mutagenesis of the BH3 domain of BAX identifies residues critical for dimerization and killing. *Mol. Cell. Biol.* 18: 6083–6089.

[140] Suzuki M, Youle RJ and Tjandra N (2000) Structure of Bax: coregulation of dimer formation and intracellular localization. *Cell* 103: 645–654.

[141] Shroff NP, Cherian-Shaw M, Bera S, _Braham EC. (2000). Mutation of R116C results in highly oligomerized alpha A-crystallin with modified structure and defective chaperone-like function. *Biochemistry*. 39(6):1420-1426.

[142] Bova MP, Yaron O, Huang Q, Ding L, Haley DA, Stewart PL, Horwitz J. (1999). Mutation R120G in alph _B-crystallin, which is linked to a desmin-related myopathy, results in an irregular structure and defective chaperone-like function. *Proc Natl Acad Sci U S A.* 96(11):6137-42.

[143] Kirchhoff SR, Gupta S, Knowlton AA. (2002). Cytosolic heat shock protein 60, apoptosis and myocardial injury. *Circulation*. 105,2899-2904.

[144] Staal, S.P. (1987). Molecular cloning of the *akt* oncogene and its human homologs *Akt1* and *Akt2*: Amplification of *Akt1* in a primary human gastric adenocarcinoma. *Proc. Natl. Acad. Sci.* 84:5034-5037.

[145] Staal, S.P., J.W. Hartley, and W.P. Rowe. (1977). Isolation of transforming murine leukemia viruses from mice with a high incidence of spontaneous lymphoma. *Proc. Natl. Acad. Sci.* 74:3065-3067.

[146] Bellacosa, A., J.R. Testa, S.P. Staal, and P.N. Tsichlis. (1991). A retroviral oncogene, *akt*, encoding a serine threonine kinase containing an SH2-like region. *Science* 254:274-277.

[147] Bellacosa, A., T.F. Franke, M.E. Gonzalez-Portal, K. Datta, T. Taguichi, J. Gardner, J.Q. Cheng, J.R. Testa, and P.N. Tsichlis. (1993). Structure, expression and chromosomal mapping of *c-akt*: Relationship to *v-akt* and its implications. *Oncogene* 8:745-754.

[148] Coffer, P.J. and J.R. Woodgett. (1991). Molecular cloning and characterization of a novel putative protein-serine kinase related to the cAMP-dependent and protein kinase C families. *Eur. J. Biochem.* 201:475-481.

[149] Jones, P.F., T. Jakubowicz, F.J. Pitossi, F. Maurer, and B.A. Hemmings. (1991). Molecular cloning and identification of a serine/threonine protein kinase of the second messenger subfamily. *Proc. Natl. Acad. Sci.* 88:4171-4175.

[150] Cheng, J.Q., B. Ruggeri, W.M. Klein, G. Sonoda, D.A. Altomare, D.K. Watson, and J.R. Testa. 1996. Amplification of AKT2 in human pancreatic cancer cells and inhibition of AKT2 expression and tunorigeneicity by antisense RNA. *Proc. Natl. Acad. Sci.* 93:3636-3641.

[151] Konishi, H., S. Kuroda, M. Tanaka, H. Matsuzaki, Y. Ono, K. Kameyama, T. Haga, and U. Kikkawa. 1995. Molecular cloning and characterization of a new member of the RAC protein kinase family: Association of the pleckstrin homology domain of three types of RAC protein kinase with protein kinase C subspecies and beta gamma subunits of G proteins. *Biochem. Biophys. Res. Comm.* 216:526-534.

[152] Brodbeck, D., P. Cron, and B.A. Hemmings. 1999. A human protein kinase B with regulatory phosphorylation sites in the acitvation loop and in the C-terminal hydrophobic domain. *J. Biol. Chem.* 274: 9133-9136.

[153] Nakatani, K., H. Sakaue, D.A. Thompson, R.J. Weigel, and R.A. Roth. 1999. Identification of a human Akt3 (protein kinase B) which contains the regulatiory serine phosphorylation. *Biochem. Biophys. Res. Comm.* 257:906-910.

[154] Mayer, B.J., R. Ren, K.L. Clark, and D. Baltimore. 1993. A putative modular domain present in diverse signalling proteins. *Cell* 73:629-630.

[155] Musacchio, A., T. Gibson, P. Rice, J. Thompson, and M. Saraste. 1993. The PH domain: A common piece in the structural pathwork of signaling proteins. *Trends Biochem. Sci.* 18:343-348.

[156] Datta, K., T.F. Franke, T.O. Chan, A. Makris, S.-I. Yang, D.R. Kaplan, D.K. Morrison, E.A. Golemis, and P.N. Tsichlis. 1995. AH/PH domain-mediated interaction between Akt molecules and its potential role in Akt regulation. *Mol. Cell. Biol.* 15:2304-2310.

[157] Shao Z, Bhattacharya K, Hsich E, Park L, Walters B, Germann U, Wang Y-M, Kyriakis J, Mohanlal R, Kuida K, Namchuk M, Salituro F, Yao Y-M, Hou W-M, Chen X, Aronovitz M, Tsichlis PN, Bhattacharya S, Force T, Kilter H. *Circ Res.* **98,** 111–118.

[158] Datta SR, Brunet A, Greenberg ME. (1999). Cellular survival: a play in three Akts. *Genes Dev.*13:2905-2927.

[159] Vivanco I, Sawyers CL. (2002). The phosphatidylinositol 3-Kinase AKT pathway in human cancer. *Nat Rev Cancer*. 2:489-501.

[160] Michael P. Scheid and James R.Woodgett (2001). PKB/AKT: functional insight from genetic models. *Nat. Rev. Mol. Cell. Biol.* 2:760-768

[161] Zheng C, Lin Z, Zhao ZJ, Yang Y, Niu H, Shen X. (2006). MAPK-activated protein kinase-2 (MK2)-mediated formation and phosphorylation-regulated dissociation of the signal complex consisting of p38, MK2, Akt, and Hsp27. *J Biol Chem.* 281(48):37215-26.

[162] Viniegra JG, Martinez N, Modirassari P, Losa JH, Parada Cobo C, Lobo VJ, Luquero CI, Alvarez-Vallina L, Ramon y Cajal S, Rojas JM, Sanchez-Prieto R. (2005). Full activation of PKB/Akt in response to insulin or ionizing radiation is mediated through ATM. *J Biol Chem.* 280(6):4029-36.

[163] Chandrasekher G, Sailaja D. (2003). Differential activation of phosphatidylinositol 3 kinase signaling during proliferation and differentiation of lens epithelial cells. *Invest Ophthalmol Vis Sci.* 44(10):4400-11.

[164] Chandrasekher G, Sailaja D. (2004) Phosphatidylinositol 3-kinase (PI-3K)/Akt but not PI-3K/p70 S6 kinase signaling mediates IGF-1-promoted lens epithelial cell survival. *Invest Ophthalmol Vis Sci.* 45(10):3577-88.

[165] Gotoh N, Ito M, Yamamoto S, Yoshino I, Song N, Wang Y, Lax I, Schlessinger J, Shibuya M, Lang RA. (2004). Tyrosine phosphorylation sites on FRS2alpha responsible for Shp2 recruitment are critical for induction of lens and retina. Proc *Natl Acad Sci U S A.* 101(49):17144-9.

[166] James C, Collison DJ, Duncan G. (2005) Characterization and functional activity of thrombin receptors in the human lens.*Invest Ophthalmol Vis Sci.* 46(3):925-32.

[167] Iyengar L, Patkunanathan B, Lynch OT, McAvoy JW, Rasko JE, Lovicu FJ. Aqueous humour- and growth factor-induced lens cell proliferation is dependent on MAPK/ERK1/2 and Akt/PI3-K signalling. *Exp Eye Res.* 83(3):667-78.

[168] Weber GF, Menko AS. (2006). Phosphatidylinositol 3-kinase is necessary for lens fiber cell differentiation and survival. *Invest Ophthalmol Vis Sci.* 47(10):4490-9.

[169] Madhavi J. Rane, Patricia Y. Coxon, Dave W. Powell, Rose Webster, Jon B. Klein, William Pierce, Peipei Ping, and Kenneth R. McLeish (2001). p38 Kinase-dependent MAPKAPK-2 Activation Functions as 3-Phosphoinositide-dependent Kinase-2 for Akt in Human Neutrophils. *J. Biol. Chem.* 276, 3517-3523.

[170] Madhavi J. Rane, Yong Pan, Saur _Bh Singh, David W. Powell , Rui Wu, Timothy Cummins, Qingdan Chen, Kenneth R. McLeish, and Jon B. Klein. (2003). Heat Shock Protein 27 Controls Apoptosis by Regulating Akt Activation. *J. Biol. Chem*. 278, 27828-27836.

[171] Rui Wu, Hina Kausar, Paul Johnson, Diego E. Montoya-Durango, Michael Merchant, and Madhavi J. Rane. (2007). Hsp27 Regulates Akt Activation and Polymorphonuclear Leukocyte Apoptosis by Scaffolding MK2 to Akt Signal Complex. *J. Biol. Chem.* 282, 21598-21608.

[172] Saori Sato, Naoya Fujita, and Takashi Tsuruo (2000). Modulation of Akt kinase activity by binding to Hsp90. *Proc. Natl. Acad. Sci. USA*,. 97, 10832-10837.

[173] Xia Z, Dickens M, Raingeaud J, Davis RJ, Greenberg ME.(1995). Opposing effects of ERK and JNK-p38 MAP kinases on apoptosis. *Science*. 270:1326-1331.

[174] Ballif BA, Blenis J. (2001). Molecular mechanisms mediating mammalian mitogen-activated protein kinase (MAPK) kinase (MEK)-MAPK cell survival signals. *Cell Growth Differ*. 12:397-408.

[175] Li, D. W-C., Jin-Ping Liu, J. Wang, Mao, Y-W., and Li-Hui Hou. (2003). Protein expression patterns of the signaling molecules for MAPK pathways in human, bovine and rat lenses. *Invest. Ophthalmol. Vis. Sci.* 44:5277-5286.

[176] Gong X, Wang X, Han J, Niesman I, Huang Q, Horwitz J. (2001). Development of cataractous macrophthalmia in mice expressing an active MEK1 in the lens. *Invest Ophthalmol Vis Sci.* 42:539-548.

[177] Zatechka SD Jr, Lou MF. (2002). Studies of the mitogen-activated protein kinases and phosphatidylinositol-3 kinase in the lens. 1. The mitogenic and stress responses. *Exp Eye Res.* 74(6):703-17.

[178] Zatechka SD Jr, Lou MF. (2002). Studies of the mitogen-activated protein kinases and phosphatidylinositol-3 kinase in the lens. 2. The intercommunications. *Exp Eye Res.* 75(2):177-92.

[179] Govindarajan V, Overbeek PA. (2001). Secreted FGFR3, but not FGFR1, inhibits lens fiber differentiation. *Development.* 128:1617-27.

[180] Lovicu FJ, McAvoy JW. (2001). FGF-induced lens cell proliferation and differentiation is dependent on MAPK (ERK1/2) signalling. *Development.* 128:5075-5084.

[181] Le AC, Musil LS. (2001). A novel role for FGF and extracellular signal-regulated kinase in gap junction-mediated intercellular communication in the lens. *J Cell Biol*. 154:197-216.

[182] Le AC, Musil LS. (2001). FGF signaling in chick lens development. *Dev Biol.* 233:394-411.

[183] Seth RK, Haque MS, Zelenka PS. (2001). Regulation of c-fos induction in lens epithelial cells by 12(S)HETE-dependent activation of PKC. *Invest Ophthalmol Vis Sci.* 42(13):3239-3246.

[184] Zhou J, Fariss RN, Zelenka PS. (2003). Synergy of epidermal growth factor and 12(s)-hydroxyeicosatetraenoate on protein kinase C activation in lens epithelial cells. *J Biol Chem.* 278:5388-98.

[185] Benkhelifa S, Provot S, N _Bais E, Eychene A, Calothy G, Felder-Schmittbuhl MP. (2001). Phosphorylation of MafA is essential for its transcriptional and biological properties. *Mol Cell Biol*. 21:4441-4452.

[186] Ochi H, Ogino H, Kageyama Y, Yasuda K. (2003). The st _Bility of the lens-specific Maf protein is regulated by fibroblast growth factor (FGF)/ERK signaling in lens fiber differentiation. *J Biol Chem*. 278:537-44.

[187] Johnson GL, Lapadat R. (2002). Mitogen-activated protein kinase pathways mediated by ERK, JNK, and p38 protein kinases. *Science.* 298, 1911-1912.

[188] Cullen, P.J. and Lockyer, P.J. (2002). Integration of calcium and Ras signalling. *Nat. Rev. Mol. Cell Biol. 3*:339–348.

[189] Campbell SL, Khosravi-Far R, Rossman KL, Clark GJ, Der CJ. 1998. Increasing complexity of Ras signaling. *Oncogene.* 17:1395-413.

[190] Farnsworth, C.L., Freshney, N.W., Rosen, L.B., Ghosh, A., Greenberg, M.E. and Feig, L.A. 1995. Calcium activation of Ras mediated by neuronal exchange factor Ras-GRF. *Nature 376*:524–527.

[191] Fam, N.P., Fan, W.T., Wang, Z.X., Zhang, L.J., Chen, H. and Moran, M.F. 1997. Cloning and characterization of Ras-GRF2, a novel guanine nucleotide exchange factor for Ras. *Mol. Cell. Biol*. *17*: 1396–1406.

[192] Moyano JV, Evans JR, Chen F, Lu M, Werner ME, Yehiely F, Diaz LK, Turbin D, Karaca G, Wiley E, Nielsen TO, Perou CM, Cryns VL. (2006). _B-crystallin is a novel oncoprotein that predicts poor clinical out come in breast cancer. J. Clin. Invest. 116, 261-270.

[193] Hartwell, L. H. & Kastan, M. B. (1994). Cell cycle control and cancer. *Science* 266, 1821–1828.

[194] Kastan MB, Lim D-S. (2000). The many substrates and functions of ATM. *Nature Rev. Mol. Cell Biol.* 1, 179–186.

[195] Bakkenist CJ, Kastan MB (2003). DNA damage activates ATM through intermolecular autophosphorylation and dimmer dissociation *Nature.* 421, 499-506.

[196] Bai F, Xi JH, Wawrousek EF, Fleming TP, and Andley UP. (2003). Hyperproliferation and p53 status of lens epithelial cells derived from _B-crystallin knockout mice. *J. Biol. Chem.* 278, 36876-36886.

[197] Liu S, Li J, Tao Y, Xiao X. (2007). Small heat shock protein _B-crystallin binds to p53 to sequester its translocation to mitochondria during hydrogen peroxide-induced apoptosis. *Biochem. Biophy. Res. Commun.* 354, 109–114.

[198] Spector, A., Chiesa, R., Sredy, J. & Garner, W. (1985). cAMP-dependent phosphorylation of bovine lens alpha-crystallin. *Proc. Natl. Acad. Sci. USA* 82, 4712-4716.

[199] Morrison LE, Hoover HE, Thuerauf DJ, Glembotski CC. (2003). Mimicking phosphorylation of alph _B-crystallin on serine-59 is necessary and sufficient to provide maximal protection of cardiac myocytes from apoptosis. *Circ Res*. 92(2):203-11.

[200] Whittaker R, Glassy MS, Gude N, Sussman MA, Gottlieb RA, Glembotski CC. (2009). Kinetics of the Translocation and Phosphorylation of _B-crystallin in mouse heart mitochondria during ex vivo ischemia. *Am J Physiol Heart Circ Physiol.* 2009 Feb 27. [Epub ahead of print] PMID: 19252088.

Cell Death and Differentiation (2004) 11, 512–526
© 2004 Nature Publishing Group All rights reserved 1350-9047/04 $25.00
www.nature.com/cdd

Human αA- and αB-crystallins bind to Bax and Bcl-X_S to sequester their translocation during staurosporine-induced apoptosis

Y-W Mao[1,4], J-P Liu[2], H Xiang[1,5] and D W-C Li*[,1,2,3]

[1] Department of Molecular Biology, University of Medicine and Dentistry of New Jersey, Stratford, NJ, USA
[2] Hormel Institute, University of Minnesota, Austin, MN, USA
[3] College of Life Sciences, Hunan Normal University, Changsha, Hunan, China
[4] Current address: Department of Pharmacology, University of Michigan, Ann Arbor, MI 48109, USA
[5] Current address: State Key Laboratory of Microbial Resources and Center for Molecular Microbiology, Institute of Microbiology, Chinese Academy of Sciences, Beijing 100080, PR China
* Corresponding author: D W-C Li, Hormel Institute, University of Minnesota, 801 16th Avenue NE, Austin, MN 55912, USA. Tel: +507-437-9636; Fax: +507-437-9606; E-mail: dwcli@hi.umn.edu

Received 25.7.03; revised 14.11.03; accepted 19.11.03; published online 30.1.04
Edited by Dr M Piacentini

Abstract

αA- and αB-crystallins are distinct antiapoptotic regulators. Regarding the antiapoptotic mechanisms, we have recently demonstrated that αB-crystallin interacts with the procaspase-3 and partially processed procaspase-3 to repress caspase-3 activation. Here, we demonstrate that human αA- and αB-crystallins prevent staurosporine-induced apoptosis through interactions with members of the Bcl-2 family. Using GST pulldown assays and coimmunoprecipitations, we demonstrated that α-crystallins bind to Bax and Bcl-X_S both *in vitro* and *in vivo*. Human αA- and αB-crystallins display similar affinity to both proapoptotic regulators, and so are true with their antiapoptotic ability tested in human lens epithelial cells, human retina pigment epithelial cells (ARPE-19) and rat embryonic myocardium cells (H9c2) under treatment of staurosporine, etoposide or sorbitol. Two prominent mutants, R116C in αA-crystallin and R120G, in αB-crystallin display much weaker affinity to Bax and Bcl-X_S. Through the interaction, α-crystallins prevent the translocation of Bax and Bcl-X_S from cytosol into mitochondria during staurosporine-induced apoptosis. As a result, α-crystallins preserve the integrity of mitochondria, restrict release of cytochrome *c*, repress activation of caspase-3 and block degradation of PARP. Thus, our results demonstrate a novel antiapoptotic mechanism for α-crystallins.

Cell Death and Differentiation (2004) **11,** 512–526.
doi:10.1038/sj.cdd.4401384
Published online 30 January 2004

Keywords: αA-crystallin; R116C; αB-crystallin; R120G; Bax; Bcl-X_S

Abbreviations: α-crystallin, alpha-crystallin; GFP, green fluorescence protein; HαA, human αA-crystallin; HαB, human αB-crystallin; GFP-HαA, green fluorescence and human αA-crystallin fusion protein; GFP-HαB, green fluorescence and human αB-crystallin fusion protein; MEM, Eagle's minimal essential medium; PAGE, polyacrylamide gel electrophoresis; PBS, phosphate-buffered saline; PMSF, phenylmethylsufonyl fluoride; HLE, human lens epithelial cells; SDS, sodium dodecylsulfate; TBS, tris-buffered saline; TBS-T, tris-buffered saline with tween-20.

Introduction

Apoptosis is one of the major causes for ocular diseases. [1–3] In lens system, our previous work[4–6] has suggested that induced lens epithelial cell apoptosis appears to be a common cellular mechanism mediating stress-induced, noncongenital cataractogenesis. Subsequently, several laboratories have reported that lens epithelial cell apoptosis is indeed actively involved in lens pathogenesis as demonstrated from *in vivo* animal model studies.[7–12] In addition, both overexpression of various exogenous genes and disruption of certain endogenous genes also lead to lens cell apoptosis followed by abnormal lens formation during lens development.[13–18]

Apoptosis is regulated by a series of positive and negative regulators. The balance of these regulators controls the determination of apoptosis. Among these various apoptotic regulators, members of Bcl-2 family and heat-shock proteins play an important role.[19–21]

So far, members of the Bcl-2 family are the most well-characterized apoptotic regulators and are generally classified into two functional groups.[21] Members of the first group, including Bcl-2 and Bcl-X_L, possess antiapoptotic ability, while members of the second group such as Bak, Bax and Bcl-X_S have been shown to promote apoptosis.[21] The functions of Bcl-2 family members could be regulated by their subcellular localization. Bcl-2 and Bcl-X_L are localized on the mitochondrial membrane, endoplasmic reticulum (ER) and nuclear membrane.[21,22] In contrast, a substantial fraction of Bax is found in the cytosol and loosely attached to the mitochondrial membrane prior to induction of cell death.[23] In the absence of death stimuli, the N-terminus of Bax helps to maintain the inactive status of Bax by restraining the C-terminal transmembrane (TM) domain in the cytosol.[24] Lack of the N-terminus of Bax or replacement of the TM domain of Bax with the corresponding domain of Bcl-2 permits the integration of Bax into the mitochondrial membrane.[25] The C-terminal TM domain of Bax is critical for its targeting to mitochondrial membrane. Deletion and point mutations of the C-terminal hydrophobic region severely damage the ability of Bax to integrate into the mitochondrial membrane and kill cells.[26] During apoptosis, Bax undergoes a conformational change that enables it to insert into the mitochondrial outer membrane.[24] Stimulated by death signals, the C-terminal domain

of Bax changes its conformation and the C-terminal α-helix is removed from the BH3 domain, which allows the BH3 domain to interact with other antiapoptotic Bcl-2 family members.[27,28] Caspase[25] and p38 MAP kinase[29] may stimulate the translocation of Bax upon apoptotic stimulus. After Bax inserts into the mitochondrial membrane, Bax can directly induce the release of cytochrome *c*[30,31] or form permeability transition pore.[32]

Bcl-X_S is a proapoptotic regulator with only the BH3, BH4 and TM domains.[33] Several reports have demonstrated that overexpression of Bcl-X_S selectively induces tumor cells to undergo apoptosis.[34–35] Moreover, overexpression of Bcl-X_S in the skin of transgenic mice results in extreme sensitivity to UV-induced cell death.[36] Bcl-X_S has been suggested to stimulate apoptosis through inactivation of antiapoptotic Bcl-2 family members, such as Bcl-2 and Bcl-X_L,[33] or repression of the binding of Bcl-X_L to cytochrome *c*.[37] The endogenous Bcl-X_S is distributed in the cytosol, but is translocated to the mitochondrial membrane upon overexpression. Its proapoptotic ability can be inhibited by Bcl-2 and Bcl-X_L.[38]

Another important group of apoptosis regulators are heat-shock proteins that include alpha-crystallins (α-crystallins),[39–46] Hsp27,[39–40, 47–52] Hsp70,[53–57] Hsp90[58] and Hsp60.[59–60] While Hsp60 appears to enhance apoptosis by promoting maturation of procaspase-3,[59,60] the majority of these factors seems to protect cells from induced apoptosis through different mechanisms. Hsp90 is able to inhibit apoptosome formation.[58] Hsp70 can interact with BAG-1[57,58] and inhibit apoptosis by preventing recruitment of procaspase-9 to the Apaf-1 apoptosome complex.[53] Hsp70 is also capable of functioning downstream of caspase activation.[54] Hsp27 prevents cell death at multiple signaling steps. First, it interacts with cytochrome *c* to prevent activation of procaspase-9.[47,48] It also binds to caspase-3 and modulates the activity of caspase-3.[49] Finally, Hsp27 can abrogate apoptotic pathway through regulation of Bid intracellular distribution and protection of F-actin integrity.[52]

Both α-crystallins and Hsp27 are closely related family members.[19–20,61] αA/B-crystallins are initially known as major lens structural proteins that play an essential role in maintaining the transparency of the ocular lens.[62] Later, α-crystallins are found to act as molecular chaperones[63–67] and also display autokinase activity.[68,69] As antiapoptotic regulators, α-crystallins are initially shown to protect cells from thermal,[70] osmotic[71] and oxidative insult.[72] More recently, α-crystallins have been shown to prevent induced apoptosis by various factors including staurosporine,[39–40,43] TNF,[39,43] UVA irradiation,[43] okadaic acid[44] and hydrogen peroxide.[45] Regarding the antiapoptotic mechanism, recent studies from our laboratory and another group have demonstrated that αB-crystallin can directly interact with the precursors of caspase-3 to suppress its activation.[45,46]

In the present study, we have explored the interactions between α-crystallins and members of the Bcl-2 family. Our results demonstrated that human αA- and αB-crystallins (HαA and HαB) can directly bind to Bax and Bcl-X_S *in vitro* and *in vivo*. The two crystallins display almost close affinity to both proapoptotic regulators, and so are true with their antiapoptotic ability tested in three different cell lines under treatment of different stress conditions. The two prominent mutants, R116C in αA-crystallin and R120G in αB-crystallin, displayed much weaker affinity to Bax and Bcl-X_S. The two crystallins markedly sequestered Bax and Bcl-X_S in the cytosol and prevented their translocation into mitochondria during staurosporine-induced apoptosis. In contrast, the two mutants only weakly sequestered Bax and Bcl-X_S in the cytoplasm. As a result of this interaction, the two crystallins preserve the integrity of mitochondria and turn off the downstream apoptotic events. Thus, our results provide a novel antiapoptotic mechanism for αA/B-crystallins.

Results

Expression of human α-crystallins in human lens epithelial (HLE) cells

To study the mechanisms by which α-crystallins protect lens epithelial cells from stress-induced apoptosis, we cloned both αA- and αB-crystallin cDNAs from human eye lenses (National Disease Research Interchange). Then, we generated the in frame constructs expressing fusion proteins of HαA and HαB with green fluorescence protein (GFP). These expression constructs (pEGFP-HαA and pEGFP-HαB) and the vector (pEGFP-neo) were transfected into the HLE cells using electroporation.[44,45] The stable expression clones of pEGFP-HLE (expressing only GFP from the vector), pEGFP-HαA-HLE (expressing GFP-HαA) and pEGFP-HαB-HLE (expressing GFP-HαB) were obtained after a 6-week selection with G418 (600 μg/ml). As shown in Figure 1, expression of GFP, green fluorescence and human αA-crystallin fusion protein (GFP-HαA) and green fluorescence and human αB-crystallin fusion protein (GFP-HαB) can be detected by fluorescence microscopy. The GFP was distributed homogeneously throughout the nucleus and cytoplasm (Figure 1a). In contrast, the GFP-HαA (Figure 1b) and GFP-HαB (Figure 1c) were localized in the cytoplasm only. Western blot analysis was conducted to further confirm the expression of these proteins. As shown in Figure 1d (top panel), the anti-αA/B-crystallin antibody recognized the GFP-HαA in pEGFP-HαA-HLE cells and GFP-HαB in pEGFP-HαB-HLE cells, respectively. Expression of the endogenous HαA or HαB was hardly detectable in all three types of cells (data not shown). When anti-GFP antibody was used to probe the same blot (the second panel from the top of Figure 1d), the same GFP-HαA and GFP-HαB were detected in pEGFP-HαA-HLE and pEGFP-HαB-HLE cells, respectively. In pEGFP-HLE cells, however, anti-GFP antibody recognized only the 27 kDa GFP protein. As a control for equal loading, the anti-β-actin antibody was used to probe the same blot and the results are shown in the third panel from the top of Figure 1d. Thus, the three different cell lines, pEGPF-HLE, pEGFP-HαA-HLE and pEGFP-HαB-HLE, were successfully established. To quantitate the expression of GFP, GFP-HαA and GFP-HαB in pEGFP-HLE, pEGFP-HαA-HLE and pEGFP-HαB-HLE cells, respectively, purified GFP protein of different concentrations was loaded into the same gel for comparison (bottom panel). After probing with anti-GFP antibody, it was determined that the clone of pEGFP-HLE cells contained about 0.5 ng GFP/μg total proteins, that the clone of pEGFP-HαA-HLE cells expressed about 0.48 ng GFP-HαA/μg total proteins and that

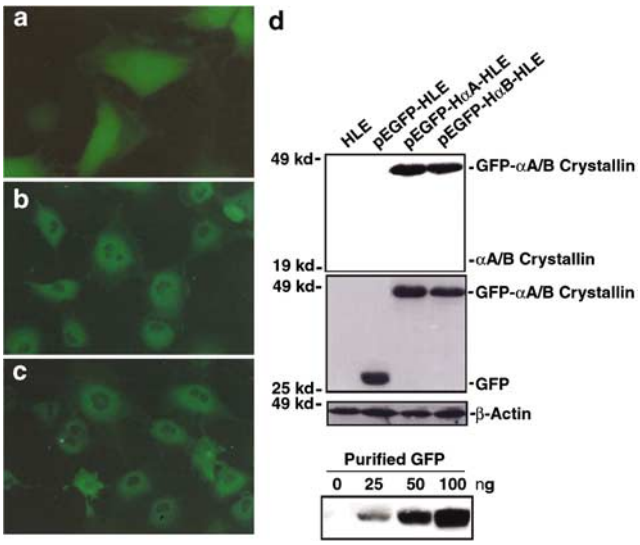

Figure 1 Overexpression of HαA or HαB in HLE cells. (**a-c**) Direct visualization of the pEGFP-HLE, pEGFP-HαA-HLE and pEGFP-HαB-HLE cells by fluorescence microscopy. Note that in the vector-transfected cells (**a**), the GFP protein is homogeneously expressed in both cytoplasm and nucleus. In contrast, in either HαA (**b**)- or HαB (**c**)-transfected cells, the fusion protein of GFP-HαA or GFP-HαB was only detected in the cytoplasm. (**d**) Western blot analysis of HαA and HαB in parental, pEGFP-HLE, pEGFP-HαA-HLE and pEGFP-HαB-HLE. Total proteins (100 μg) from the four types of cells were separated by 10% SDS polyacrylamide gel and transferred to nitrocellulose membrane. Then the membrane was blotted sequentially with anti-αA/B-crystallin antibody (top panel), anti-GFP antibody (middle panel) and anti-β-actin antibody (bottom panel) and visualized with the ECM Kit (Amersham). The purified GFP (bottom panel, from Clontech) was loaded in the same gel and used for reference to measure the concentrations of GFP, GFP-HαA and GFP-HαB in pEGFP-HLE, pEGFP-HαA-HLE and pEGFP-HαB-HLE cells, respectively. Note that the endogenous α-crystallin was hardly detectable in any of the four types of cells (top panel)

the clone of pEGFP-HαB-HLE cells had about 0.42 ng GFP-HαB/μg total proteins.

HαA- and HαB-crystallins prevent staurosporine-induced apoptosis in HLE cells

Our previous studies[44,45] have demonstrated that mouse αB-crystallin can block okadaic acid and H_2O_2-induced apoptosis in the immortalized rabbit lens epithelial cells, N/N1003A. To delineate the antiapoptotic mechanisms of αA- and αB-crystallins, we utilized our established stable clones, pEGFP-HLE, pEGFP-HαA-HLE and pEGFP-HαB-HLE. After grown to 100% confluence, these cells were subjected to treatment with 100 nM staurosporine for 3, 6, 12 and 17 h. The percentage of apoptotic cells in these samples was analyzed with a viability assay described before.[44,45] As shown in Figure 2a, after a 3 h treatment, about 30% vector-transfected cell underwent apoptosis. In contrast, less than 20% of either HαA- or HαB-transfected cells were apoptotic. A 6 h treatment led to apoptosis of more than 60% of the vector-transfected cells. However, less than 30% of pEGFP-HαA-HLE cells and 25% of pEGFP-HαB-HLE cells were found apoptotic under the same conditions. The apoptotic nature of cell death was verified by DNA fragmentation (Figure 2b). After a 6 h treatment, the DNA from vector-transfected cells displayed a clear pattern of fragmentation (Lane 3 of Figure 2b). However, the DNA samples from either HαA- or HαB-

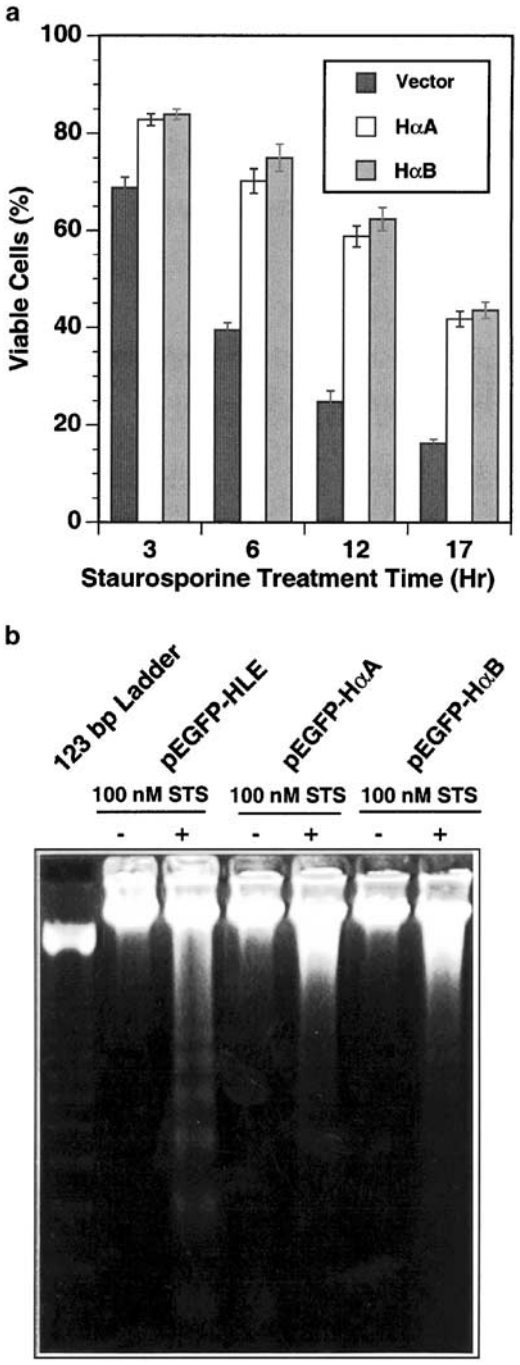

Figure 2 Analysis of the antiapoptotic ability of HαA and HαB in HLE cells. (**a**) Viability assays. pEGFP-HLE, pEGFP-HαA-HLE and pEGFP-HαB-HLE cells were grown to 100% confluence, then treated with 100 nM staurosporine for 3, 6, 12 and 17 h. Viability of the three types of cells was determined as described previously.[99] (**b**) DNA fragmentation assay. pEGFP-HLE, pEGFP-HαA-HLE and pEGFP-HαB-HLE cells were grown to 100% confluence, then treated with 100 nM staurosporine or 0.01% DMSO (control) for 6 h. Then, the cells were harvested for isolation of genomic DNA and the isolated DNA samples were analyzed with 2.0% agarose gel as described previously.[4] The 123 bp marker from Gibco BRL was shown on the left. STS: staurosporine

transfected cells displayed a much weak fragmentation (lanes 5 and 7 of Figure 2b). Thus, HαA- and HαB provide marked protection against staurosporine-induced apoptosis.

HαA- and HαB-crystallins prevent staurosporine-induced upregulation of Bak in human lens epithelial cells

As overexpression of α-crystallins significantly protected HLE cells from staurosporine-induced apoptosis, we first examined whether the antiapoptotic ability of α-crystallins was derived from their regulation of expression of Bcl-2 family members. The pEGFP-HLE, pEGFP-HαA-HLE and pEGFP-HαB-HLE cells were incubated with either 0.01% DMSO or 100 nM staurosporine for 3 h. The total proteins were extracted for Western blot analysis and the results are shown in Figure 3. The relative expression levels of GFP-αA/B-crystallin fusion proteins, Bcl-2, Bcl-X_L, Bcl-X_S, Bax and Bak, were further quantitated using an automated digitizing system from the Silk Scientific Corporation. While expression of Bcl-2, Bcl-X_L, Bcl-X_S and Bax showed only slight variations in vector- and α-crystallin-transfected cells with or without staurosporine treatment (Figure 3 and data not shown), expression of Bak was upregulated about five-fold in vector-transfected cells by staurosporine treatment. In HαA- and HαB-transfected cells, expression of either HαA or HαB enhanced expression of Bak for about 2.5-fold. However, staurosporine-induced additional upregulation was not observed in HαA- and HαB-transfected cells. Thus, HαA and HαB were able to suppress staurosporine-induced upregulation of Bak in HLE cells.

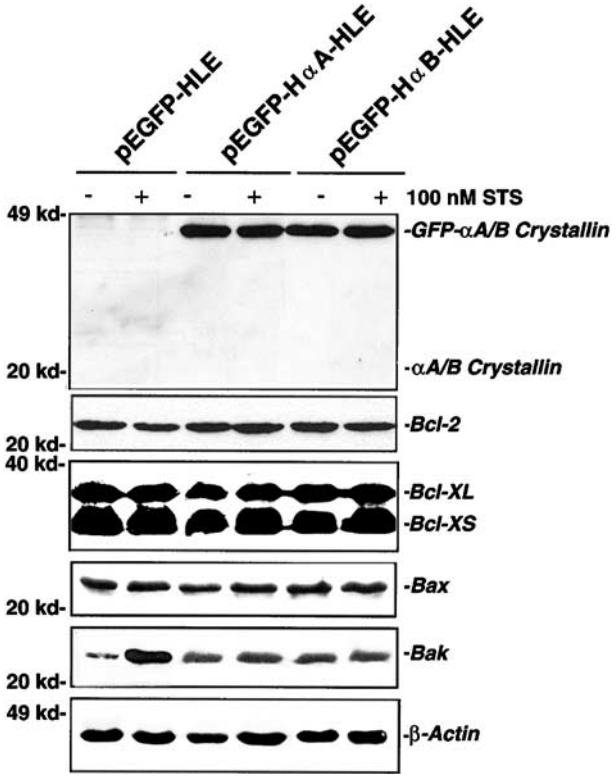

Figure 3 Expression of different Bcl-2 family members during staurosporine-induced apoptosis. The pEGFP-HLE, pEGFP-HαA-HLE and pEGFP-HαB-HLE cells were treated with either 0.01% DMSO (−STS) or 100 nM staurosporine (+STS) for 3 h. The total proteins from the differentially treated cells were extracted and analyzed by Western blot analysis with anti-αA/B-crystallin, anti-Bcl-2, anti-Bcl-$X_{S/L}$, anti-Bax, anti-Bak and anti-β-actin antibodies as described in the Material and Methods

HαA- and HαB-crystallins can interact with Bcl-X_S and Bax *in vitro* and *in vivo*

To explore whether αA- and αB-crystallins are able to prevent apoptosis at the mitochondrial level, upstream of caspase-3 activation, as part of the antiapoptotic mechanism, we conducted GST pulldown assays to identify possible interactions between HαA-crystallin as well as HαB-crystallin with members of the Bcl-2 family. The cDNAs for HαA- and HαB-crystallins were subcloned into pGEX-4T-1 vector to establish (in frame) GST-HαA- and GST-HαB-crystallin fusion protein constructs. The purified GST-HαA- and GST-HαB-crystallin fusion proteins from *Escerichia coli* BL21 were used to pull down the HαA- and HαB-crystallins-associated proteins from HLE cells. The proteins pulled down were further analyzed with antibodies against various members of the Bcl-2 family. As shown in Figure 4, both Bax (the third panel from top) and Bcl-X_S (the fourth panel from the top) were found bound to GST-HαA- and GST-HαB-crystallins, but not to the GST protein control. In contrast, the anti-Bcl-2 and anti-Bak antibodies did not crossreact with any proteins eluted from either GST-HαA or GST-HαB columns (the top two panels of Figure 4). To confirm that the interaction actually occurs *in vivo*, coimmunoprecipitates from the pEGFP-HLE, pEGFP-HαA-HLE and pEGFP-HαB-HLE cells using anti-αA/B-crystallin antibody were further probed with anti-Bcl-2, anti-Bak, anti-Bax, anti-Bcl-X_S and anti-GFP antibodies (Figure 5a). As expected, anti-Bcl-2 and anti-Bak antibodies did not cross-

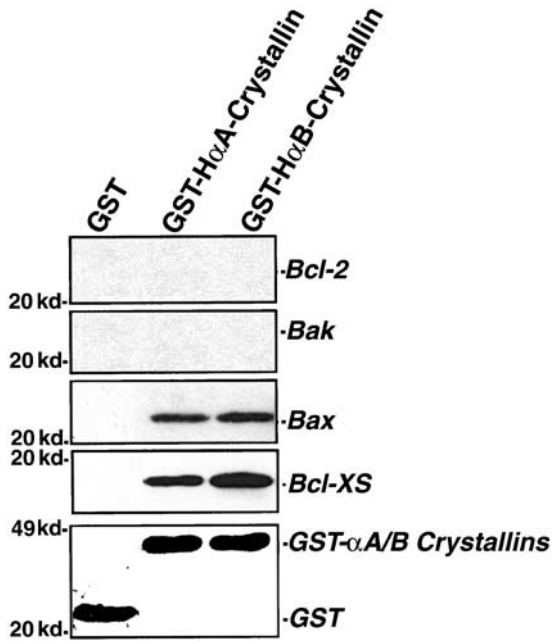

Figure 4 GST pulldown assays to demonstrate that HαA and HαB can interact with Bax and Bcl-X_S *in vitro*. The purified GST, GST-HαA and GST-HαB fusion proteins immobilized on glutathione–Sepharose beads were incubated with cell extracts from the HLE cells. After removal of nonspecific proteins by tris-buffered saline with tween-20 (TBS-T) washes, the associated proteins were eluted and separated by 10% SDS polyacrylamide gel electrophoresis (PAGE). The immunoblots were probed with the antibodies against different members of the Bcl-2 family as indicated in the figure. Only Bax and Bcl-X_S were found bound to HαA and HαB. The lower panel shows equal input of GST, GST-HαA and GST-HαB

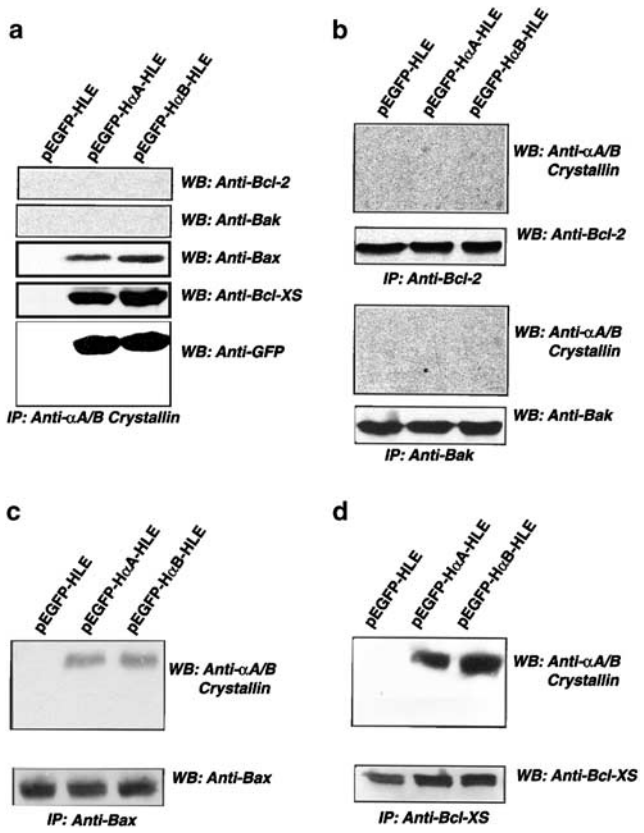

Figure 5 Coimmunoprecipitations to demonstrate that HαA and HαB can interact with Bax and Bcl-X_S *in vivo*. (**a**) The total proteins extracted from pEGFP-HLE, pEGFP-HαA-HLE and pEGFP-HαB-HLE cells were immunoprecipitated with anti-αA/B-crystallin antibody. The precipitated samples were then sequentially blotted with anti-Bcl-2, anti-Bak, anti-Bax, anti-Bcl-X_S and anti-GFP antibodies. Only Bax and Bcl-X_S were found to be brought down by anti-αA/B-crystallin antibody. (**b**) The total proteins extracted from pEGFP-HLE, pEGFP-HαA-HLE and pEGFP-HαB-HLE cells were immuoprecipitated by anti-Bcl-2 and anti-Bak antibodies. The precipitated samples were then probed with both anti-αA/B-crystallin antibody and anti-Bcl-2 (top two panels) or anti-αA/B-crystallin antibody and anti-Bax antibodies (bottom two panels). Note that there was no crossreacting protein detected with anti-αA/B-crystallin antibody in both samples brought down either by anti-Bcl-2 or by anti-Bak antibodies. (**c**) The total proteins extracted from pEGFP-HLE, pEGFP-HαA-HLE and pEGFP-HαB-HLE cells were immunoprecipitated using anti-Bax antibody. The precipitated samples were then sequentially probed with anti-αA/B-crystallin and anti-Bax antibodies. (**d**) The total proteins extracted from pEGFP-HLE, pEGFP-HαA-HLE and pEGFP-HαB-HLE cells were immuoprecipitated using anti-Bcl-X_S antibody. The precipitated samples were then sequentially blotted with anti-αA/B-crystallin and anti-Bcl-X_S antibodies

react with any proteins precipitated down by anti-αA/B-crystallin antibody (the top two panels of Figure 5a). In contrast, both Bax and Bcl-X_S were coimmunoprecipitated from pEGFP-HαA-HLE and pEGFP-HαB-HLE cells but not from pEGFP-HLE cells using anti-αA/B-crystallin antibody. HαB seemed to have slightly better affinity to Bax and Bcl-X_S than HαA did (the middle two panels of Figure 5a). Since these experiments were semiquantitative, such difference may not be significant. Analysis of Bax and Bcl-X_S left in the supernatant fraction after immunoprecipitation revealed that more than 60% of total Bax and more than 80% of total Bcl-X_S were precipitated down by the anti-αA/B-crystallin antibody (data not shown). Next, we performed the immunoprecipitations with the antibodies against Bcl-2, Bak, Bax and Bcl-X_S and the cell extract from the three types of cells. While anti-Bcl-2 and anti-Bak antibodies did not bring down either GFP-HαA or GFP-HαB (Figure 5b), anti-Bax (Figure 5c) and anti-Bcl-X_S (Figure 5d) antibodies were able to coimmunoprecipitate with GFP-HαA in pEGFP-HαA-HLE cell and GFP-HαB in pEGFP-HαB-HLE cells. In pEGFP-HLE cells, neither HαA nor HαB was detected in the immunoprecipitated proteins by anti-Bax and anti-Bcl-X_S antibodies (left lane of Figure 5c and d). These results indicate that HαA- and HαB can specifically bind to Bax and Bcl-X_S both *in vitro* and *in vivo.*

The N-terminal fragments of HαA and HαB fused with GFP did not protect the transfected cells from apoptosis and displayed no interaction with Bcl-X_S and Bax

To demonstrate that the observed protection against staurosporine-induced apoptosis of pEGFP-HαA-HLE and pEGFP-HαB-HLE cells was not derived from the action of GFP, we have created two fusion protein constructs using PCR cloning strategy. A fragment of 89 amino acids from the N-terminal of HαA was fused with GFP in frame to generate the first construct. Similarly, a fragment of 74 amino acids from the N-terminal of HαB was fused with GFP in frame to create the second construct (Figure 6a). The two constructs were introduced into HLE cells and their expressions were verified by Western blot analysis (Figure 6b) and fluorescence microscopy (Figure 6d and e). Like GFP-HαA and GFP-HαB, the two new fusion proteins, GFP-HαA-89 and GFP-HαB-74, were also distributed in the cytoplasm (Figures 6d and e). Treatment of the cells expressing these new fusion proteins with 100 nM staurosporine induced apoptosis of similar rate as found in vector-transfected cells (Figure 6f), indicating the absence of protection by these new fusion proteins. Immunoprecipitation with anti-GFP, anti-Bax and anti-Bcl-X_S antibodies on the total proteins extracted from vector- and the new constructs-transfected cells demonstrated that the two new fusion proteins did not bind to Bax and Bcl-X_S (Figure 6g). Thus, it is the HαA and HαB but not GFP that interacts with Bax and Bcl-X_S.

HαA[R116C] and HαB[R120G] showed much less protection on staurosporine-induced apoptosis and also displayed much weak interactions with Bcl-X_S and Bax

Two major mutants found in α-crystallin are R116C in HαA and R120G in HαB. Previous studies[73,74] have shown that both mutants displayed decreased protection against apoptosis induced by staurosporine and other stress conditions. To explore the possible mechanisms for the decreased protection, we have created the two mutants using wild-type HαA and HαB cDNAs and PCR amplification procedure. The two mutants were fused into the GFP expression vector to generate pEGFP-HαA[R116C] and pEGFP-HαB[R120G], which were introduced into HLE cells. Expressions of HαA[R116C] and HαB[R120G] were confirmed with Western blot analysis (Figure 7a). Their protections against stauro-

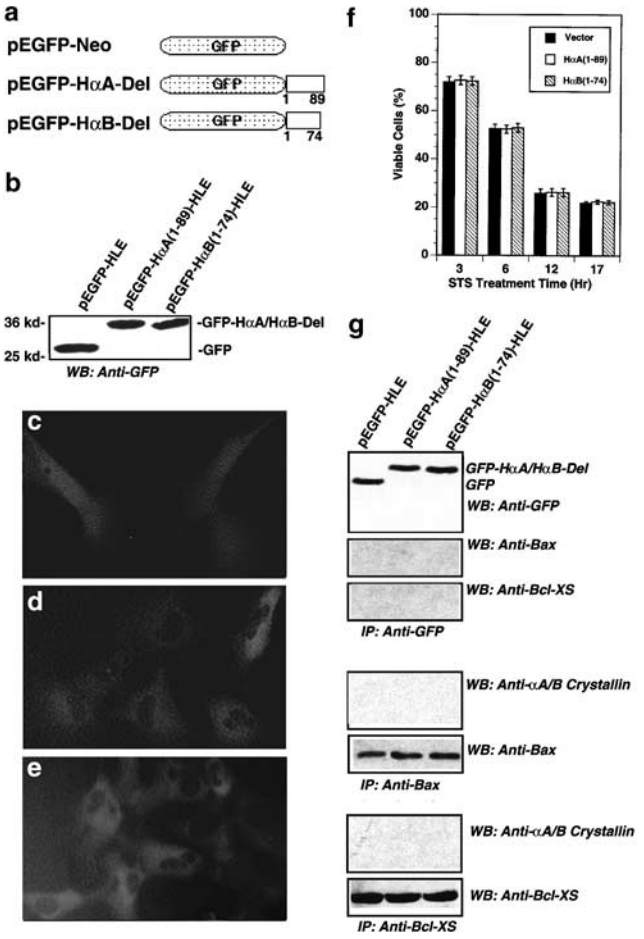

Figure 6 Demonstration that the N-terminal fragments of either HαA or HαB, when fused with GFP, was also localized in the cytoplasm but displayed no protection against staurosporine-induced apoptosis. (**a**) Diagram of the structures of pEGFP-neo, pEGFP-HαA-Del and pEGFP-HαB-Del. (**b**) Western blot analysis of expression of GFP, GFP-HαA-Del and GFP-HαB-Del. Western blot analysis was carried out as described in Figure 1. (**c–e**) Detection of GFP, GFP-HαA-Del and GFP-HαB-Del by fluorescence microscopy as described in Figure 1. (**f**). HαA-Del- and HαB-Del-transfected cells displayed similar apoptosis rate as vector-transfected cells. Viability was assayed as described in Figure 2a. (**g**) Coimmunoprecipitations revealed that these deletion mutants of HαA and HαB do not interact with Bax and Bcl-X_S. Coimmunoprecipitation was conducted as described in Figure 5.

sporine-induced apoptosis were analyzed. As shown in Figure 7b, both HαA[R116C] and HαB[R120G] displayed less protection against staurosporine-induced apoptosis as compared with wild-type HαA and HαB (Figure 2a). To explore the possible mechanism for this decreased antiapoptotic ability, we examined their interactions with Bax and Bcl-X_S. Reciprocal immunoprecipitation with anti-αA/B-crystallin, anti-Bax and anti-Bcl-X_S antibodies revealed that HαA[R116C] and HαB[R120G] had much weaker interactions with both Bax and Bcl-X_S in comparison with the corresponding wild-type proteins, HαA and HαB (Figure 7c). Thus, part of the mechanisms responsible for the decreased protection by HαA[R116C] and HαB[R120G] are derived from their aberrant interactions with the two proapoptotic members of the Bcl-2 family.

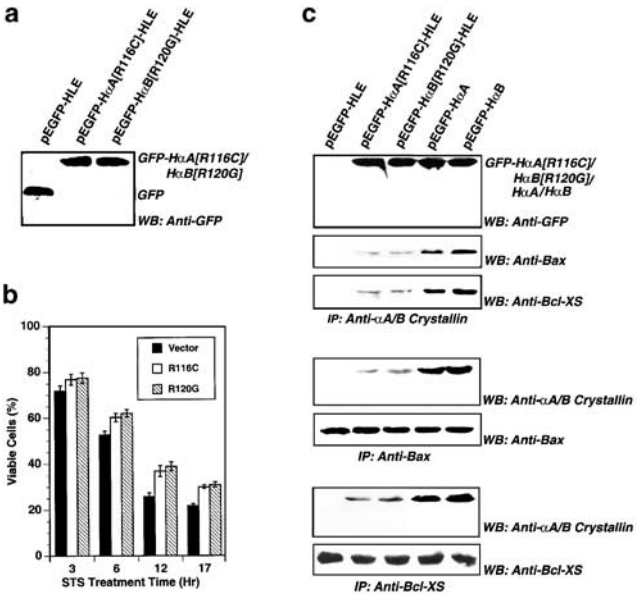

Figure 7 Demonstration that R116C and R120G, the two major mutant proteins found in HαA and HαB, have decreased ability against staurosporine-induced apoptosis and also displayed much less affinity for binding to Bax and Bcl-X_S. (**a**) Western blot analysis to detect expressions of GFP, R116C and R120G in pEGFP-HLE, pEGFP-HαA[R116C]-HLE and pEGFP-HαB[R120G]-HLE cells. Western blot analysis was conducted as described in Figure 1. (**b**) Viability assays to show the relative antiapoptotic ability of GFP-R116C and GFP-R120G. Viability assay was conducted as described in Figure 2a. (**c**) Coimmunoprecipitations to demonstrate that R116C and R120G have much lower affinity to Bax and Bcl-X_S in comparison with their wild-type proteins, HαA and HαB. Coimmunoprecipitation was conducted as described in Figure 5

Staurosporine-induced mitochondrial translocations of Bax and Bcl-X_S in pEGFP-HLE cells were blocked in pEGFP-HαA-HLE and pEGFP-HαB-HLE cells

Bcl-2 family members are the major apoptotic regulators that control the homeostasis of mitochondria. Proapoptotic Bcl-2 family members such as Bax and Bcl-X_S have been shown to be activated and translocated from the cytosol into mitochondria after apoptotic stimulation.[24,38] Since human α-crystallins were able to interact with Bax and Bcl-X_S *in vitro* and *in vivo*, we predicted that the translocation of Bax and Bcl-X_S could be affected in the presence of HαA and HαB. To test this possibility, the pEGFP-HLE, pEGFP-HαA-HLE and pEGFP-HαB-HLE cells were treated with either 0.01% DMSO or 100 nM staurosporine for 3 h and the mitochondrial-associated (M) and soluble (S) proteins were isolated from the three types of cells as described in Materials and Methods. Then, the same amounts of mitochondrial (M) and cytosolic proteins (S) were immunoblotted using the antibodies against superoxide dismutase (Mn^{2+}), Bcl-2, Bcl-X_L, Bak, Bax and Bcl-X_S. The purity of mitochondrial fraction was shown by the exclusive distribution of a mitochondria-specific protein, superoxide dismutase (Mn^{2+}) (Figure 8a). Bcl-2, Bcl-X_L and Bak were found to be associated with the mitochondrial membrane even after staurosporine treatment (Figure 8b–d). The upregulated Bak found in pEGFP-HLE cells was also accumulated in the mitochondria (Figure 8d). Bax was distributed in cytosol before staurosporine treatment in all

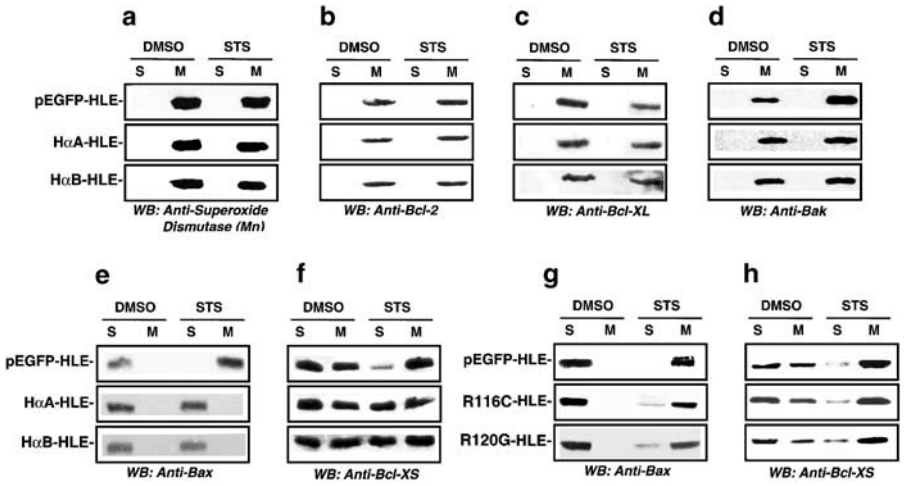

Figure 8 Demonstration that HαA and HαB prevent staurosporine-induced translocation of Bax and Bcl-X_S from the cytosol into mitochondria (**a–f**) and that the two mutants, R116C in HαA and R120 in HαB, display much weaker ability to sequester the staurosporine-induced translocation of Bax and Bcl-X_S from the cytosol into mitochondria (**g–h**). The pEGFP-HLE, pEGFP-HαA-HLE and pEGFP-HαB-HLE cells were grown to 100% confluence and then treated with 0.01% DMSO (DMSO) or 100 nM staurosporine (STS) for 3 h. These samples were then used for isolation of mitochondrial (M) and cytosolic (S) fractions. Total proteins were then extracted from the two fractions and subjected to Western blot analysis. Briefly, 50 μg of the mitochondrial protein (M) and cytosolic protein (S) from both control and treated cells were separated by 10% SDS-PAGE. The distributions of Mn-superoxide dismutase (marker for mitochondria-specific protein) (**a**), Bcl-2 (**b**), Bcl-X_L (**c**), Bak (**d**), Bax (**e**) and Bcl-X_S (**f**) were determined by Western blot analysis using the corresponding antibodies. Similarly, the pEGFP-HLE, pEGFP-HαA[R116C]-HLE and pEGFP-HαB[R120G]-HLE cells were grown to 100% confluence and then treated with 0.01% DMSO (DMSO) or 100 nM staurosporine (STS) for 3 h. These samples were then used for isolation of mitochondrial (M) and cytosolic (S) fractions. Total proteins were then extracted from the two fractions and subjected to Western blot analysis using antibody against Bax (**g**) and Bcl-X_S (**h**) as described above. Note that R116C and R120G display much weaker ability to sequester Bax (**g**) and Bcl-X_S (**h**) in the cytosol compared with the sequestration of Bax (**e**) and Bcl-X_S (**f**) by wild-type HαA and HαB

three types of cells. However, after staurosporine treatment, Bax was translocated into mitochondria in pEGFP-HLE cells but retained in cytosol of pEGFP-HαA-HLE and pEGFP-HαA-HLE cells (Figure 8e). Bcl-X_S was equally distributed in both the soluble fraction (S) and the mitochondria-associated fraction (M) before staurosporine treatment. After treatment with 100 nM staurosporine, more than 90% of Bcl-X_S was translocated into mitochondria, leading to its dominant distribution in mitochondria and much less amount in the cytosolic fraction in pEGFP-HLE cells (top panel of Figure 8f). In contrast, in pEGFP-HαA-HLE cells (middle panel of Figure 8f) and pEGFP-HαB-HLE cells (bottom panel of Figure 8f), the staurosporine-induced translocation of Bcl-X_S was largely blocked as reflected by the even distribution of Bcl-X_S in both cytosolic fraction and mitochondria with or without 100 nM staurosporine treatment. In contrast, the two prominent mutants, R116C and R120G, displayed much weaker abilities to sequester Bax (Figure 8g) and Bcl-X_S (Figure 8h) in the cytosol. These results demonstrated that HαA and HαB can prevent the translocation of Bcl-X_S and Bax into mitochondria after staurosporine stimulation.

HαA and HαB prevent staurosporine-induced cytochrome *c* release, caspase-3 activation and PARP cleavage

Earlier studies have shown that translocation of Bax directly induces release of cytochrome *c* from mitochondria and activation of caspase-3.[30–31] As HαA and HαB can interact with Bax and Bcl-X_S and prevent their translocation from the cytosol to mitochondria, we tested whether this sequestration could inhibit release of cytochrome *c* and suppress activation of caspase-3. Total proteins from both the cytosolic fraction and mitochondria of the three types of cells treated with 0.01% DMSO or 100 nM staurosporine for 0.5, 3 and 6 h were analyzed with Western blot analysis using an anti-cytochrome *c* antibody. As shown in Figure 9a, after 30-min treatment by staurosporine, no cytochrome *c* was released from either vector- or HαA- or HαB-transfected cells. As the treatment time increased to 3 h, staurosporine induced a substantial amount of cytochrome *c* released from mitochondria (M) into cytosol (S) in pEGFP-HLE cells (Figure 9b, top panel). However, the release of cytochrome *c* was hardly observed in either HαA- or HαB-transfected HLE cells (Figure 9b, middle and bottom panels). By 6 h treatment, a majority of cytochrome *c* was released into cytoplasm in vector-transfected cells (Figure 9c, top panel). In contrast, only a small amount of cytochrome *c* was released in HαA- and HαB-transfected HLE cells (Figure 9c, middle and bottom panels). Since differential release of cytochrome *c* was observed in the three types of cells, we predicted that activation of caspase-3 and downstream apoptotic events may also be different in these cells. To test this possibility, total proteins from these cells treated with either 0.01% DMSO or 100 nM staurosporine for 6 h were extracted for analysis of caspase-3 activity and cleavage of poly (ADP-ribose) polymerase (PARP), a substrate of caspase-3. As shown in Figure 10a, staurosporine treatment of pEGFP-HLE cells induced more than 17-fold activation of caspase-3 compared with DMSO treatment. In contrast, only two- to three-fold activation induced by staurosporine was observed in pEGFP-HαA-HLE and pEGFP-HαB-HLE cells in comparison with DMSO treatment. Consistent with differential caspase-3 activation, a large amount of PARP p116 was

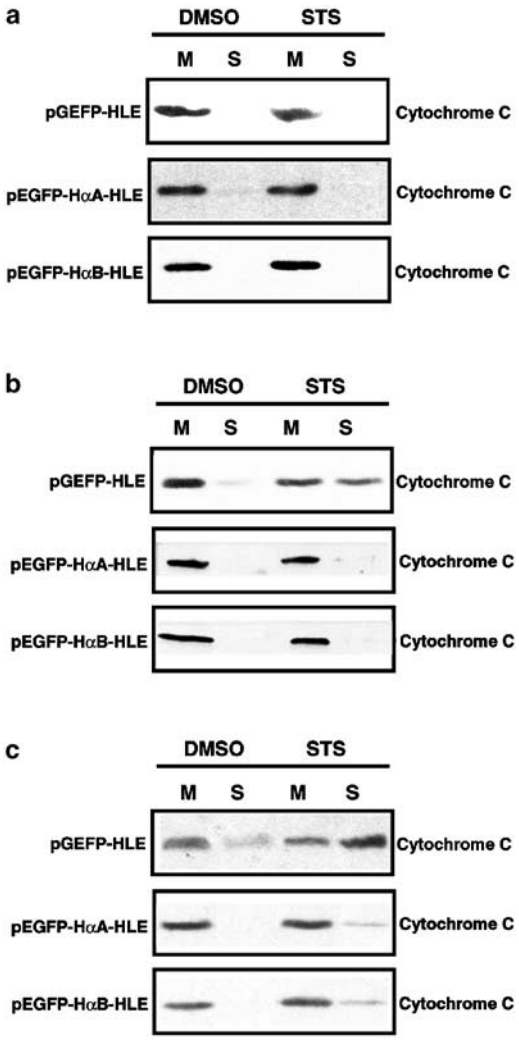

Figure 9 Demonstration that HαA and HαB prevent staurosporine-induced release of cytochrome *c*. The pEGFP-HLE, pEGFP-HαA-HLE and pEGFP-HαB-HLE cells were grown to 100% confluence and then treated with 0.01% DMSO (control) or 100 nM staurosporine (STS) for 30 min (**a**), 3 h (**b**) and 6 h (**c**). These samples were then used for isolation of mitochondrial (M) and cytosolic (S) fractions. Total proteins were then extracted from the two fractions and subjected to Western blot analysis. Briefly, 50 μg of the mitochondrial fraction (M) and cytosolic fraction (S) from the control and treated cells were separated by 10% SDS-PAGE and the immunoblots were detected with an anti-cytochrome *c* antibody

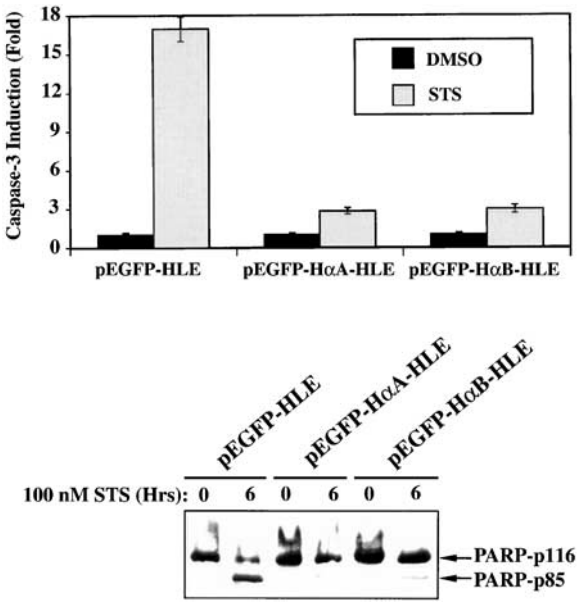

Figure 10 Demonstration that HαA and HαB prevent staurosporine-induced activation of caspase-3 and cleavage of PARP. (**a**) Caspase-3 activity in pEGFP-HLE, pEGFP-HαA-HLE and pEGFP-HαB-HLE cells after treatment with 0.01% DMSO (DMSO) or 100 nM staurosporine (STS). Caspase-3 activity was analyzed as described previously.[44,45] Note that staurosporine induced more than 17-fold increase in caspase-3 activity compared to the DMSO control in vector-transfected cells. The activation of caspase-3 in HαA- and HαB-transfected cells was substantially repressed. (**b**) Western blot analysis of the caspase-3 substrate, PARP. Nuclear proteins (100 μg) from the pEGFP-HLE, pEGFP-HαA-HLE and pEGFP-HαB-HLE cells after treatment with 0.01% DMSO (control) or 100 nM staurosporine(STS) for 6 h were separated in an 8% SDS polyacrylamide gel. The PARP cleavage was detected with an anti-PARP antibody. Note that the p85 subunit was prominent in vector-transfected cells but barely detectable in HαA- and HαB-transfected cells after 100 nM staurosporine treatment

cleaved by caspase-3 to p85 in pEGFP-HLE cells after 6 h treatment by staurosporine. On the other hand, the degraded PARP (p85) was barely detectable in pEGFP-HαA-HLE and pEGFP-HαB-HLE cells (Figure 10b). Thus, both HαA and HαB were able to block downstream apoptotic events through interactions with Bax and Bcl-X_S.

HαA and HαB-crystallins display similar protection against apoptosis induced by different stress conditions in both lens and nonlens cells

Our results with HLE cells under treatment of 100 nM staurosporine suggest that HαA and HαB display similar protection against induced apoptosis. To further confirm these results, we introduced both HαA and HαB into a retina pigment epithelial cell line, ARPE-19,[75] and a rat embryonic myocardium cell line, H9c2.[76] Different from the SV40 large T-transformed HLE cells that lack endogenous α-crystallin, both ARPE-19 and H9c2 express endogenous αB-crystallin. ARPE-19 cells expressed about 0.4 ng αB-crystallin/μg total proteins using purified αB-crystallin (Stressgen) as standard. The rat embryonic myocardium, H9c2 cells, expressed 0.21 ng αB-crystallin/μg total proteins, half of that found in ARPE-19 cells (data not shown). Accordingly, both ARPE-19 and H9c2 have much stronger resistance to staurosporine-apoptosis in comparison with HLE cells in the absence of the exogenous α-crystallin expression (see the vector-transfected cells in Figure 11a, c and e). We suggest that different expression levels of the endogenous αB-crystallin levels likely contribute to their differential antiapoptotic abilities of ARPE-19 and H9c2 cells (see the vector-transfected cells in Figure 11c and e). Expression of the exogenous GFP-HαA or GFP-HαB fusion protein in both ARPE-19 and H9c2 cells provides additional protection (Figure 11c–f). When the established stable clones of vector or human α-crystallin-transfected ARPE and H9c2 cells (those clones expressing similar levels of GFP, GFP-HαA or GFP-HαB were used) were subjected to treatment of 100 nM staurosporine (Figure 11c and e), 10 μM etoposide (Figure 11d) or 400 mM sorbitol (Figure 11f), it was

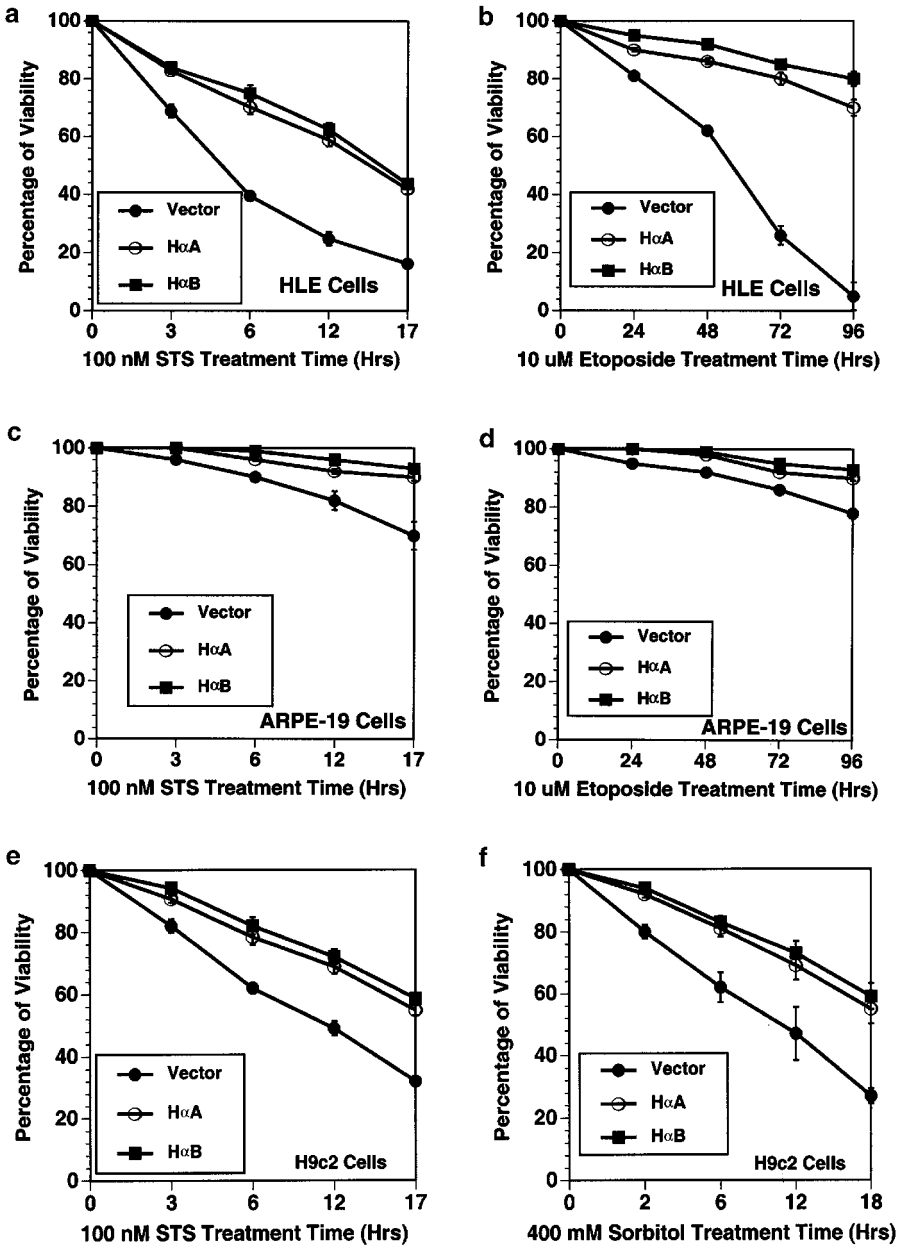

Figure 11 Comparison of the relative antiapoptotic ability of HαA and HαB in three different types of cells. pEGFP-neo, pEGFP-HαA and pEGFP-HαB were introduced into HLE (**a**, **b**), human retina pigment epithelial cells, ARPE-19 (**c, d**) and rat embryonic myocardium cells, H9c2 (**e, f**). After selection with G418 medium, stable clones expressing GFP, GFP-HαA or GFP-HαB were isolated. Their expression levels were determined by Western blot analysis. For all cells (HLE or ARPE-19 or H9c2), the clones with similar expression levels were used for analysis of the relative ability against induced apoptosis. Each stable clone was grown to 100% confluence and then subjected to treatment by 100 nM staurosporine (**a, c, e**), or 10 μM etoposide (**b**, **d**), or 400 mM sorbitol (**f**) for different length of time as indicated, the viability was then assayed as described in Figure 2a

found that both HαA and HαB displayed similar protection against all stress conditions tested (Figure 11).

Discussion

In the present study, we have demonstrated the following: (1) both GST pulldown assay and coimmunoprecipitation demonstrate that HαA and HαB binds to Bax and Bcl-X_S; (2) the two prominent mutants, R116C in HαA and R120G in HαB, display much weaker affinity to Bax and Bcl-X_S; (3) the interactions between α-crystallin and Bax as well as Bcl-X_S prevent their translocation into mitochondria during staurosporine-induced apoptosis; (4) the two prominent mutants, R116C and R120G, exhibit much attenuated sequestration of Bax and Bcl-X_S in the cytosol; (5) both HαA and HαB display similar antiapoptotic ability as tested in three different cell lines under various stress conditions; (6) through inhibition of Bax and Bcl-X_S translocation and repression of Bak upregulation, HαA and HαB prevent staurosporine-induced apoptosis. Thus, our results reveal a novel antiapoptotic mechanism for α-crystallin (Figure 12).

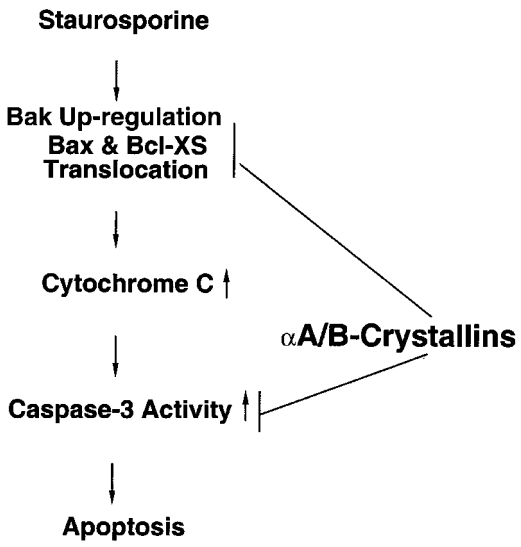

Figure 12 Diagram to show the apoptotic pathway for staurosporine-induced apoptosis in HLE cells and the protective mechanisms of HαA and HαB against staurosporine-induced apoptosis. Staurosporine induces upregulation of Bak and translocation of Bax and Bcl-X_S, leading to alteration in the permeability of mitochondria as reflected by release of cytochrome *c*, which causes activation of caspase-3 and cleavage of PARP, and eventually execution of the apoptotic program. HαA and HαB block upregulation of Bak and translocation of Bax and Bcl-X_S, and consequently suppress downstream apoptotic events

Antiapoptotic mechanisms of α-crystallins

The small heat-shock proteins have multiple functions.[39–46, 62–74] One of the most important functions is the ability to protect cell from induced apoptosis.[39–46] α-Crystallin and Hsp27 are closely related family members and protect cells from apoptosis induced by a large numbers of stress factors.[39–46] Both of them prevent stress-induced apoptosis at multiple signaling steps. However, the exact mechanism or regulating targets seem to be different. Hsp27 prevents apoptosis by interacting with caspase-3 to modulate its activity,[47–48] by interacting with cytochrome *c* to prevent procaspase-9 activation,[49] or by regulating Bid intracellular distribution and F actin integrity to block mitochondrial death pathway.[52] In contrast, α-crystallin utilizes a different mechanism to negatively regulate caspase-3 activity. Our recent study shows that αB-crystallin prevents H_2O_2-induced apoptosis through interaction with procaspase-3 and partially processed procaspase-3 to prevent caspase-3 activation.[45] Secondly, instead of regulating Bid distribution, our results presented here demonstrate that α-crystallin binds to Bax and Bcl-X_S to prevent their translocation into mitochondria induced by staurosporine, thus maintaining the integrity of mitochondria. The differential antiapoptotic mechanism was further illustrated in a recent study in which αB-crystallin but not Hsp27 was found capable of repressing differentiation-induced caspase-3 activation.[74]

The results from both GST pulldown assay (Figure 4) and coimmunoprecipication-linked Western blot analysis with antibodies against αA/B-crystallin and Bcl-X_S (Figure 5a and d) suggest that HαB seems to have slightly stronger affinity to Bax and Bcl-X_S than HαA does. However, this is not consistent with the coimmunoprecipitation-linked Western blot analysis with anti-Bax antibody (Figure 5c). Such discrepancy may be partially derived from the difference in the antibody affinity to the complexes precipitated and also partially resulted from variation from experiments to experiments (Figure 5c and Figure 7c). Since both assays are semiquantitative, the observed differential affinity to Bax and Bcl-X_S displayed by HαA and HαB need to be further explored. Nevertheless, our observation that both HαA and HαB bind to these proapoptotic regulators and sequester their translocation into mitochondria during staurosporine-induced apoptosis is important for understanding the antiapoptotic mechanisms of HαA and HαB.

The two major mutants, R116C in HαA and R120G in HαB, cause cataractogenesis in the lens.[77,78] Consistent with these observations, the chaperone-like ability of R116C and R120G was found substantially decreased.[79,80] The results reported here and also from earlier studies[73–74] reveal that the two mutants apparently display much weaker antiapoptotic ability. Our demonstration that the mutants have much less affinity to Bax and Bcl-X_S provides an explanation. Part of their attenuated antiapoptotic ability is derived from their weak interactions with Bax and Bcl-X_S and thus decreased ability to sequester translocation of Bax and Bcl-X_S from cytosol into mitochondria induced by staurosporine treatment. Why R116C and R120G display deceased affinities to Bax and Bcl-X_S remains to be further studied.

An early study[43] has suggested that αA-crystallin is more competent than αB-crystallin in preventing apoptosis induced by staurosporine, TNF-α and UVA. In the present study, we have compared the antiapoptotic ability of the two crystallins in three different cell lines: the human lens epithelial cell line (HLE) which contains virtually undetectable endogenous crystallins; the human retina pigment epithelial cells (ARPE-19) and the rat embryonic myocardium cell line (H9c2), both of which expresses endogenous αB-crystallin. The expression of the endogenous αB-crystallin in ARPE-19 and H9c2 cells makes them much more resistant to staurosporine-induced apoptosis in the absence of exogenous α-crystallin expression (Figure 11). Regardless absence or presence of the endogenous α-crystallin, expression of HαA and HαB in these cells provides additional protections. Under treatment of 100 nM staurosporine, 10 μM etoposide or 400 mM sorbitol (generating osmotic stress), HαA and HαB consistently show similar protections against a given stress condition in HLE, ARPE-19 or H9c2 cells.

Signaling pathway mediating staurosporine-induced apoptosis

Apoptosis occurs through two major signaling pathways: extrinsic or intrinsic.[81] The extrinsic pathway initiated from activation of death domain containing cell surface receptors of the tumor necrosis factor (TNF) super family leads to the recruitment and proteolytic activation of caspase-8, which results in the cleavage and activation of downstream effector caspases.[82–83] The intrinsic apoptotic signaling pathway involves mitochondria and results in the release of proapoptotic factors from mitochondria, such as cytochrome *c*. The released cytochrome *c* binds to the apoptotic protease-

activating factor-1(Apaf-1), subsequently turns on the downstream executioner caspases such as caspase-3.[84–86] Staurosporine, a potent apoptosis inducer demonstrated in a broad spectrum of cells activate apoptosis through the mitochondrial death pathway.[87–91] The proapoptotic members of the Bcl-2 family play a critical role in staurosporine-induced apoptosis. Cells lacking both Bax and Bak are known to be completely resistant to multiple apoptotic stimuli including staurosporine.[92–93] Analysis of cell death in Bax- or Bak-deficient cell lines indicates that both regulators are necessary for staurosporine-induced apoptosis.[94,95] Consistent with these studies, here we show that in HLE cells staurosporine regulates both Bak and Bax at different ways.

Staurosporine was found to upregulate Bak expression up to five-fold (Figure 3) and the upregulated Bak was accumulated into mitochondria (Figure 8) in vector-transfected cells. In the HαA- and HαB-transfected cells, Bak upregulation is different. First, expression of HαA and HαB enhances Bak expression in unknown mechanism. On the other hand, expression of HαA- and HαB prevents staurosporine-induced additional Bak upregulation (Figure 3). Since cells lacking both Bax and Bak are completely resistant to staurosporine,[92,93] inhibition of additional Bak upregulation by HαA- and HαB, to some degree, contributes to their antiapoptotic abilities against staurosporine-induced apoptosis. Bak upregulation is also observed in human colonic adenoma AA/C1 cells during butyrate-induced apoptosis,[96] and in human stomach epithelial cells during bacterium-induced apoptosis.[97]

It is well established that death signal induced conformation change followed by insertion into mitochondrial membrane is an important step for Bax to promote apoptosis.[25–28] Although staurosporine does not induce Bax upregulation, this kinase inhibitor promotes Bax translocation from cytosol into mitochondria in vector-transfected cells, thus turning on the mitochondrial death pathway. This process is largely abrogated in cells expressing either HαA or HαB (Figure 8e).

In addition, our results demonstrate that staurosporine also regulates Bcl-X_S. It also stimulates translocation of Bcl-X_S from cytosol into mitochondria in vector-transfected pEGFP-HLE cells. To our knowledge, this is the first evidence that Bcl-X_S translocation is stimulated by staurosporine. Again, HαA and HαB prevent translocation of Bcl-X_S (Figure 8f).

In vector-transfected cells, once the proapoptotic members, Bax and Bcl-X_S, were mobilized into mitochondria, the integrity of mitochondria was interrupted as evidenced by the release of cytochrome *c*, followed by activation of executioner caspase, caspase-3 and degradation of PARP. These downstream events induced by staurosporine in vector-transfected HLE cells are similar to those reported in other cell lines.[87–91] In either HαA- or HαB-transfected cells, the staurosporine-induced downstream events were largely turned off. Thus, our results provide additional evidence that both Bax and Bak are important for staurosporine-induced apoptosis. Moreover, our demonstration that staurosporine stimulates translocation of Bcl-X_S provides novel information for our understanding of staurosporine-induced signaling pathway (Figure 12).

Materials and Methods

Chemicals

Various molecular biology reagents were purchased from Invitrogen Life Technologies, Gaithersburg, MD, USA; Stratagene, La Jolla, CA, USA and Promega Biotech, Madison, WI, USA. All the oligos, DNA and protein size markers were purchased from Invitrogen Life Technologies, Gaithersburg, MD, USA. Mammalian expression vector was purchased from Clontech, Palo Alto, CA, USA. Various antibodies were obtained from Cell Signaling Technology, Boston, MA, USA; Roche Molecular Biochemicals, Indianapolis, IN, USA; Transduction Laboratories, San Diego, CA, USA and Stressgen, Vancouver, Canada. The culture medium, and most other chemicals and antibiotics were purchased from Sigma, St. Louis, MO, USA and Invitrogen Life Technologies, Gaithersburg, MD, USA.

Culture of HLE, human retina pigment epithelial cells (ARPE-19) and rat embryonic myocardium cells (H9c2)

The HLE cells, kindly provided by Dr. V Reddy, were grown in Dulbecco's modified Eagle's medium (Gibco catalog number 31600-026) containing 10% fetal bovine serum as described previously.[98] The medium was prepared in ion-exchanged double-distilled water to give an osmolarity of 300 ± 5 mosmol supplemented with 26 mM $NaHCO_3$ and 50 U/ml penicillin and streptomycin. The media and sera were sterilized by filtration through 0.22-μm filters (Corning catalog number 25942) with pH adjusted to 7.2. All cells were kept at 37°C and 5% CO_2 gas phase. The human retina pigment epithelial cells (ARPE-19)[75] and rat embryonic myocardium cells (H9c2)[76] were obtained from ATCC and grown in Eagle's minimal essential medium (MEM) (Fisher Scientific) with addition of 10% fetal bovine serum and 50 U/ml penicillin and streptomycin.

Preparation of expression constructs

The HαA and HαB cDNAs were amplified by RT-PCR from human lens mRNA using the following primers: 5′-TACCTCGAGATGGACGTGACCATCCAGC-3′ (αA-crystallin, forward), 5′-CAACCCGGGTTAGGACGAGGGAGCCGAG-3′ (αA-crystallin, reverse), 5′-TACCTCGAGATGGACATCGCCATCCAC-3′ (αB-crystallin, forward), 5′-CAACCCGGGTTCAAGAAAGGGCATCTA-3′(αB-crystallin, reverse). The cDNAs were further inserted into an enhanced green fluorescence protein expression vector, pEGFPC3, at the *Xho*I and *Sma*I sites that were created by PCR to generate in frame fusion constructs. The pGST-HαA/B-crystallin fusion constructs were created by PCR using the following primers: 5′-TACGAATTCATGGA-CGTGACCATCCAGC-3′ (αA-crystallin, forward), 5′-CAAGTCGACTTAGGACGAGGGA-GCCGAG-3′ (αA-crystallin, reverse), 5′-TACGAATTCATGGACATCGCCATCCAC-3′ (αB-crystallin, forward), 5′-CAAGTCGACTTCAAGAAAGGGCATCTA-3′(αB-crystallin, reverse). The amplified HαA and HαB cDNAs were subcloned into pGEX-4T-1 (Pharmacia Biotech), fused in frame with GST at the *Eco*RI and *Sal*I sites. pEGFP-HαA-Del and pEGFP-HαB-Del were generated using PCR and the following primers: 5′-TACCTCGAGATGGACGTGACCAT-CCAGC-3′ (HαA-Del, forward), 5′-CAAGTCGACCTAGGATCGAACCTCAGAGATG-3′ (HαA-Del, reverse); 5′-TAC-CTCGAGATGGACATCGCCATCCAC-3′ (HαB-Del, forward), 5′- CAAGTCGACC-TATGAGAGTCCAGTGTCAAAC-3′ (HαB-Del, reverse).

In vitro mutagenesis for creation of R116C and R120G mutants

The two prominent mutants R116C and R120G were created through a two-step PCR amplification procedures with the following primers: 5′-TACCTCGAGATGGACGTGA-CCATCCAGC-3′ (R116C, forward-1), 5′-AGCGGCAGTGGAACTCACGGGAAA-3′ (R116C-Reverse-1), 5′-GTTCCACTGCCGCTACCGCCTGCCG-3′ (R116C-forward-2), 5′-CAACC-CGGGTTAGGACGAGGGAGCCGAG-3′ (R116C, reverse-2); 5′-TACCTCGAGATGGACA-TCGCCATCCAC-3′ (R120G forward-1), 5′-ATTTCCCGTGGAACTCCCTGGAGA-3′ (R120G, reverse-1), 5′-GTTCCACGGGAAATACCGGATCCC-3′ (R120G, forward-2), 5′-CAACCCGGGTT-CAAGAAAGGGCATCTA-3′(R120G, reverse-2). For R116C generation, wild-type HαA was used as the template in the initial two PCR reactions. One PCR reaction was conducted with the R116C N-terminal primer pair (forward-1 and reverse-1), and the other conducted with R116 C-terminal primer pair (forward-2 and reverse-2). The products from the two PCR reactions were gel-purified to remove the initial template (HαA full-length cDNA). The recovered two partial cDNAs carrying the mutated codon (from Arg-116 to Cys-116) were first denatured and then annealed together, and the ends are filled with klenow DNA polymerase. The newly annealed mutated cDNA was used for template in the third PCR reaction in which the R116C forward-1 primer, 5′-TACCTCGAGATG-GACGTGACCATCCAGC-3′ and R116C reverse-2 primer, 5′-CAACCCGGGTTAGGACGAGGGAGCCGAG-3′ were used. The amplified cDNA was digested at the *Xho*I and *Sma*I sites and then inserted into the mammalian expression vector pEGFPC3 to produce pEGFP-HαA[R116C]. The same procedure was used to generate pEGFP-HαB[R120G] where the two pairs of R120G primers were used for the PCR reactions. Both pEGFP-HαA[R116C] and pEGFP-HαB[R120G] were sequenced to verify the correct mutation.

Establishment of stable expression cell lines

The pEGFP, pEGFP-HαA and pEGFP-HαB constructs were amplified in DH-5α and purified by two rounds of CsCl ultracentrifugation as previously described.[44,45] Transfection of HLE, ARPE-19 and H9c2 cells was performed using electroporation with a BTX Electro Cell Manipulator as described before[44,45] or with Lipofectamine™ 2000 from the Invitrogen Life Technologies, according to the company instruction manual. The transfected cells were then subjected to G418 (400–600 μg/ml) selection for 4–6 weeks and then the individual clones for the following stable transfected cell lines were established. These include pEGFP-HLE, pEGFP-ARPE-19 and pEGFP-H9c2 (expressing only the GFP from the vector); pEGFP-HαA-HLE, pEGFP-HαA-ARPE-19 and pEGFP-HαA-H9c2 (expressing the fusion protein of GFP-HαA); and pEGFP-HαB-HLE, pEGFP-HαB-ARPE-19, and pEGFP-HαB-H9c2 (expressing the fusion protein of GFP-HαB). pEGFP-HαA[R116C]-HLE, pEGFP-HαA-Del-HLE, pEGFP-HαB[R120G]-HLE and pEGFP-HαB-Del-HLE were also established in the same way using pEGFP-HαA[R116C], pEGFP-HαA-Del, pEGFP-HαB[R120G] and pEGFP-HαB-Del constructs, respectively.

Treatment by staurosporine, etoposide and sorbitol

The pEGFP-HLE, pEGFP-ARPE-19, pEGFP-H9c2, pEGFP-HαA-HLE, pEGFP-HαA[R116C]-HLE, pEGFP-HαA-Del-HLE pEGFP-HαA-ARPE-19, pEGFP-HαA-H9c2, pEGFP-HαB-HLE, pEGFP-HαB[R120G]-HLE, pEGFP-HαB-Del-HLE, pEGFP-HαB-ARPE-19, and pEGFP-HαB-H9c2 cells were grown to 100% confluence in DMEM or MEM containing 10% fetal calf serum in the presence of 400–600 μg/ml G418. Then, the media containing 10% serum plus 0.01% DMSO (control) or 100 nM staurosporine, 10 μM etoposide or 400 mM sorbitol (experiment) were used to replace the culture media for the required period of incubation as indicated. After treatment, all samples were collected for analysis of apoptosis, apoptotic pathways and protein–protein interactions.

Apoptosis assay, DNA fragmentation analysis and Hoechst staining

The percentage of apoptotic cells in DMSO or staurosporine, etoposide or sorbitol-treated samples was determined as described before.[99] The apoptotic nature of the treated cells was further verified by DNA fragmentation and Hoechst staining as previously described.[4,44,45,99]

Protein preparation and Western blotting analysis

The total proteins were prepared from the pEGFP-HLE, pEGFP-HαA-HLE, pEGFP-HαB-HLE, pEGFP-HαA[R116C]-HLE, pEGFP-HαB[R120G]-HLE, pEGFP-HαA-Del-HLE and pEGFP-HαB-Del-HLE cells treated with 0.01% DMSO or 100 nM staurosporine for 30 min–6 h using protein extraction buffer. The buffer contained 1% NP-40, 0.5% sodium deoxycholate, 0.1% SDS, 9.1 mM Na_2HPO_4, 1.7 mM NaH_2PO_4, 150 mM NaCl, 10 μl/ml phenylmethylsufonyl fluoride (PMSF) stock solution (10 mg/ml in isopropanol), 30 μl/ml aprotinin with pH of the preparation adjusted to 7.4. After homogenization by passing through a 21-gauge needle, an additional 10 μl of PMSF was added to each sample, which was incubated on ice for 30 min. After the cell lysate was centrifuged at 10 000 × *g* for 20 min at 4°C, the supernatant fraction of each sample was collected and stored in aliquots at −70°C. For each sample, the protein concentration was determined as previously described.[44,45] In total, 50 or 100 μg of total proteins in each sample were resolved by 10% SDS-polyacrylamide gel and transferred into supported nitrocellulose membranes. The protein blots were blocked with 5% nonfat milk in tris-buffered saline (TBS) (10 mM Tris HCl, pH 8.0/150 mM NaCl) overnight at 4°C, and incubated with anti-αA/B-crystallin antibody (StressGen Biotechnologies), anti-β-actin, anti-Bax, anti-Bcl-$X_{S/L}$, anti-Bcl-2 and anti-cytochrome *c* antibodies (Santa Cruz Biotechnology), anti-Bak antibody (Upstate Biotechnology), anti-PARP antibody and anti-GFP antibody (Roche Molecular Biochemicals) at a dilution of 1:500–2000 (μg/ml) in 5% milk prepared in TBS. The secondary antibody is anti-mouse IgG (for anti-GFP and anti-Bcl-2 antibodies), anti-rabbit IgG (for anti-αA/B-crystallin, anti-Bax, anti-Bcl-$X_{S/L}$, anti-cytochrome *c* and anti-Bak antibodies), or anti-goat IgG (for anti-actin) at a dilution of 1:1000 (Amersham). Immunoreactivity was detected with an enhanced chemilluminescence detection kit according to the company's instruction (ECL, Amersham Corp.).

GST pulldown assay

Human αA- and αB-crystallin cDNAs were subcloned into vector pGEX-4T-1. Both vector and expression constructs were transfected into *E.coli* BL21. When *E.coli* BL21 was grown to $OD_{600} = 0.5$ at 37°C, IPTG was added into the medium to a final concentration of 0.5 mM. The culture was continued overnight at 20°C. Thereafter, cells were harvested by centrifugation, frozen and thawed twice by immersing the tubes in dry ice and a 37°C water bath, and resuspended in 1/50 of the starting culture volume of phosphate-buffered saline (PBS), pH 7.2, 5 mM EDTA, 1 mM dithiothreitol (DTT), 2 μg/ml aprotinin, 2 mM phenylmethylsulfonyl fluoride (PMSF) and 2 mg/ml lysozyme. After 30 min on ice, Triton X-100 was

added to a final concentration of 1% and the cells were sonicated. The supernatant fraction was collected by centrifugation and incubated with the glutathione–Sepharose beads (Sigma) for 1 h. The beads were washed with 1 × PBS, 1% Triton X-100, 5 mM EDTA, 1 mM DTT, 2 μg/ml aprotinin and 1 mM PMSF four times. GST alone, GST-HαA or GST-HαB fusion proteins immobilized on glutathione–agarose beads were incubated with HLE cell lysate overnight at 4°C. The nonspecific binding proteins were washed off the beads with TBST buffer (20 mM Tris-Cl, pH 7.4; 150 mM NaCl; 2 mM EDTA; 1% Triton X-100) four times. The interacting proteins were further analyzed by Western blot using anti-Bax and anti Bcl-X_S antibodies.

Immunoprecipitation-linked Western blot analysis

The pEGFP-HLE, pEGFP-HαA-HLE and pEGFP-HαB-HLE, pEGFP-HαA[R116C]-HLE, pEGFP-HαB[R120G]-HLE, pEGFP-HαA-Del-HLE and pEGFP-HαB-Del-HLE cells were grown to 100% confluence and treated with 0.01%. DMSO or 100 nM staurosporine for 3 h as described above. The treated cells were harvested by the end of treatment and used for extraction of total proteins. The protein samples were quantitated and processed for immunoprecipitation-linked Western blot analysis as described below. First, 500 μg of total proteins from pEGFP-HLE, pEGFP-HαA-HLE and pEGFP-HαB-HLE, pEGFP-HαA[R116C]-HLE, pEGFP-HαB[R120G]-HLE, pEGFP-HαA-Del-HLE and pEGFP-HαB-Del-HLE cells were incubated with 10 μg of antibody against αA/B-crystallins, Bax, Bcl-X_S, Bcl-2 or Bak as well as 50 μl protease inhibitor cocktail for 1 h on ice. After incubation, 50 μl of protein A/G plus agarose were added into each incubated sample. These samples were then incubated overnight in a 4°C refrigerator attached to a slow motion rotator. At the end of incubation, these samples were washed three times with RIPA buffer (1 × PBS, 1% Nonidet P-40, 0.5% sodium deoxycholate, 0.1% SDS) by spinning down for 5 min at 10 000 × *g*. After final wash, the pelleted samples were subjected to Western blot analysis as described above using proper antibodies indicated in the text.

Preparation of mitochondrial and soluble proteins

Preparation of mitochondrial and cytosolic proteins was conducted as described previously.[100] Briefly, 40 dishes (100 mm) of pEGFP-HLE, pEGFP-HαA-HLE and pEGFP-HαB-HLE cells in 100% confluence were treated with 0.01% DMSO or 100 nM staurosporine for 3 h. The cells were harvested and washed twice with PBS. The cell pellets were resuspended in hypotonic buffer (10 mM NaCl, 1.5 mM $MgCl_2$, 10 mM HEPES, pH 7.5) with protease inhibitors and incubated on ice for 30 min. Then the cells were lysed with homogenizers for 20 strokes, and the 4 × MS buffer was added into cell lyses to obtain a final concentration of 1 × MS buffer (110 mM mannitol, 280 mM sucrose, 40 mM HEPES, pH 7.5, 1 mM EDTA, 0.05% BSA, plus protease inhibitors). The cell lysates were centrifuged at 1000 × *g* for 5 min at 4°C to remove nuclei and unbroken cells. The supernatant was further centrifuged at 17 000 × *g* at 4°C for 20 min to separate mitochondrial/heavy membrane fraction and soluble fraction. The mitochodrial/heavy membrane fraction was lysed in protein extraction buffer as described above. The protein concentrations in both fractions were determined as described above. Equal amounts of protein in the mitochondrial/heavy membrane fraction and soluble fraction were separated in 10% SDS-PAGE and assayed by different antibodies as described above. The nuclear proteins were further analyzed with anti-PARP antibody (Pharmingen) to detect PARP cleavage during staurosporine-induced apoptosis.

Acknowledgements

This study was supported in part by the Hormel Foundation, University of Minnesota Graduate School, and NIH Grant EY11372 (DWL). We thank Dr. Venkat Reddy for the human lens epithelial cell line and Dr. Ann Bode for a critical reading of the manuscript. We are also grateful to Ms. Andria Hansen for the editing of the manuscript.

References

1. Li DW-C (1997) The lens epithelium, apoptosis and cataract formation. Nova Acta Leopoldina 75: 81–108
2. Lolley RN (1994) The rd gene defect triggers programmed rod cell death. The Proctor Lecture. Invest. Ophthalmol. Vis. Sci. 35: 4182–4191
3. Papermaster DS and Windle J (1995) Death at an early age. Apoptosis in inherited retina degenerations. Invest Ophthalmol. Vis. Sci. 36: 977–983
4. Li WC, Kuszak JR, Dunn K, Wang RR, Ma W, Wang GM, Spector A, Leib M, Cotliar AM, Weiss M Espy J, Howard G, Farris RL, Auran J, Donn A, Hofeldt A, Mackay C, Merriam J, Mittl R and Smith TR (1995a) Lens epithelial cell apoptosis appears to be a common cellular basis for non-congenital cataract development in humans and animals. J. Cell. Biol. 130: 169–181
5. Li WC, Kuszak JR, Wang G-M, Wu Z-Q and Spector A (1995b) Calcimycin-induced lens epithelial cell apoptosis contributes to cataract formation. Exp. Eye Res. 61: 89–96
6. Li WC and Spector A (1996) Lens epithelial cell apoptosis is an early event in the development of UVB-induced cataract. Free Radic. Biol. Med. 20: 301–311
7. Michael R, Vrensen GF, van Marle J, Gan L and Soderberg PG (1998) Apoptosis in the rat lens after *in vivo* threshold dose ultraviolet irradiation. Invest. Ophthalmol. Vis. Sci. 39: 2681–2687
8. Tamada Y, Fukiage C, Nakamura Y, Azuma M, Kim YH and Shearer TR (2000) Evidence for apoptosis in the selenite rat model of cataract. Biochem. Biophys. Res. Commun. 275: 300–306
9. Yoshizawa K, Oishi Y, Nambu H, Yamamoto D, Yang J, Senzaki H, Miki H and Tsubura A (2000) Cataractogenesis in neonatal Sprague–Dawley rats by *N*-methyl-*N*-nitrosourea. Toxicol. Pathol. 28: 555–564
10. Pandya U, Saini MK, Jin GF, Awasthi S, Godley BF and Awasthi YC (2000) Dietary curcumin prevents ocular toxicity of naphthalene in rats. Toxicol. Lett. 115: 195–204
11. Ye J, Yao K, Lu D, Wu R and Jiang H (2001) Low power density microwave radiation induced early changes in rabbit lens epithelial cells. Chin. Med. J. (Engl) 114: 1290–1294
12. Takamura Y, Kubo E, Tsuzuki S and Akagi Y (2003) Apoptotic cell death in the lens epithelium of rat suger cataract. Exp. Eye Res. 77: 51–57
13. Morgenbesser SD, Schreiber-Agus N, Bidder M, Mahon KA, Overbeek PA, Horner J and DePinho RA (1995) Contrasting roles for c-Myc and L-Myc in the regulation of cellular growth and differentiation *in vivo*. EMBO J. 14: 743–756
14. Gomez Lahoz E, Liegeois NJ, Zhang P, Engelman JA, Horner J, Silverman A, Burde R, Roussel MF, Sherr CJ, Elledge SJ and DePinho RA (1997) Cyclin D- and E-dependent kinases and the p57(KIP2) inhibitor: cooperative interactions *in vivo*. Mol. Cell. Biol. 19: 353–363
15. Yoshida H, Kong YY, Yoshida R, Elia AJ, Hakem A, Hakem R, Penninger JM and Mak TW (1998) Apaf1 is required for mitochondrial pathways of apoptosis and brain development. Cell 94: 739–750
16. Blixt A, Mahlapuu M, Aitola M, Pelto-Huikko M, Enerback S and Carlsson P (2000) A forkhead gene, FoxE3, is essential for lens epithelial proliferation and closure of the lens vesicle. Genes Dev. 14: 245–254
17. Hettmann T, Barton K and Leiden JM (2000) Microphthalmia due to p53-mediated apoptosis of anterior lens epithelial cells in mice lacking the CREB-2 transcription factor. Dev. Biol. 222: 110–123
18. de Iongh RU, Lovicu FJ, Overbeek PA, Schneider MD, Joya J, Hardeman ED and McAvoy JW (2001) Requirement for TGFbeta receptor signaling during terminal lens fiber differentiation. Development 128: 3995–4010
19. Arrigo AP (1998) Small stress proteins: chaperones that act as regulators of intracellular redox state and programmed cell death. Biol. Chem. 379: 19–26

20. Xanthoudakis S and Nicholson DW (2000) Heat-shock proteins as death determinants. Nat. Cell. Biol. 2: E163–E165
21. Gross A, McDonnell JM and Korsmeyer SJ (1999) BCL-2 family members and the mitochondria in apoptosis. Genes Dev. 13: 1899–1911
22. Cory S and Adams JM. (2002) The Bcl2 family: regulators of the cellular life-or-death switch. Nat. Rev. Cancer 2: 647–656
23. Gross A, Jockel J Wei MC and Korsmeyer SJ (1998) Enforced dimerization of BAX results in its translocation, mitochondrial dysfunction and apoptosis. EMBO J. 17: 3878–3885
24. Wolter KG, Hsu YT, Smith CL, Nechushtan A, Xi XG and Youle RJ (1997) Movement of Bax from the cytosol to mitochondria during apoptosis. J. Cell Biol. 139: 1281–1292
25. Goping IS, Gross A, Lavoie JN, Nguyen M, Jemmerson R, Roth K, Korsmeyer SJ and Shore GC (1998) Regulated targeting of BAX to mitochondria. J. Cell Biol. 143: 207–215
26. Nechushtan A, Smith CL, Hsu YT and Youle RJ (1999) Conformation of the Bax C-terminus regulates subcellular location and cell death. EMBO J. 18: 2330–2341
27. Wang K, Gross A, Waksman G and Korsmeyer SJ (1998) Mutagenesis of the BH3 domain of BAX identifies residues critical for dimerization and killing. Mol. Cell. Biol. 18: 6083–6089
28. Suzuki M, Youle RJ and Tjandra N (2000) Structure of Bax: coregulation of dimer formation and intracellular localization. Cell 103: 645–654
29. Ghatan S, Larner S, Kinoshita Y, Hetman M, Patel L, Xia Z, Youle RJ and Morrison RS (2000) p38 MAP kinase mediates Bax translocation in nitric oxide-induced apoptosis in neurons. J. Cell. Biol. 150: 335–348
30. Jürgensmeier JM, Xie Z, Deveraux Q, Ellerby L, Bredesen D and Reed JC (1998) Bax directly induces release of cytochrome *c* from isolated mitochondria. Proc. Natl. Acad. Sci. USA 95: 4997–5002
31. Eskes R, Antonsson B, Osen-Sand A, Montessuit S, Richter C, Sadoul R, Mazzei G, Nichols A and Martinou JC (1998) Bax-induced cytochrome *c* release from mitochondria is independent of the permeability transition pore but highly dependent on Mg 2+ ions. J. Cell Biol. 143: 217–224
32. Pastorino JG, Tafani M, Rothman RJ, Marcinkeviciute A, Hoek JB, Farber JL and Marcineviciute A (1999) Functional consequences of the sustained or transient activation by Bax of the mitochondrial permeability transition pore. J. Biol. Chem. 274: 31734–31739
33. Boise LH, Gonzaiz-Garcia M, Postema CE, Ding L, Lindsten T, Turka LA, Mao X, Nunez G and Thompson CB (1993) bcl-x, a bcl-2-related gene that functions as a dominant regulator of apoptotic cell death. Cell 74: 597–608
34. Clarke MF, Apel IJ, Benedict MA, Eipers PG, Sumantran V, GonzaÂlez-GarcõÂa M, Doedens M, Fukunaga N, Davidson B, Dick JE, Minn AJ, Boise LH, Thompson CB, Wicha M and NuÃez G (1995) A recombinant bcl-xs adenovirus selectively induces apoptosis in cancer cells but not in normal bone marrow cells. Proc. Natl. Acad. Sci. USA 92: 11024–11028
35. Dole MG, Clarke MF, Holman P, Benedict M, Lu J, Jasty R, Eipers P, Thompson CB, Rode C, Bloch C, Nunez and Castle VP (1996) Bcl-xS enhances adenoviral vector-induced apoptosis in neuroblastoma cells. Cancer Res. 56: 5734–5740
36. Pena JC, Fuchs E and Thompson CB (1997) Bcl-x expression influences keratinocyte cell survival but not terminal differentiation. Cell. Growth. Differ. 8: 619–629
37. Kharbanda S, Pandey P, Schofield L, Israels S, Roncinske R, Yoshida K, Bharti A, Yuan ZM, Saxena S, Weichselbaum R, Nalin C and Kufe D (1997) Role for Bcl-x_L as an inhibitor of cytosolic cytochrome *c* accumulation in DNA damage-induced apoptosis. Proc. Natl. Acad. Sci. USA 94: 6939–6942
38. Lindenboim L, Yuan J and Stein R (2000) Bcl-xS and Bax induce different apoptotic pathways in PC12 cells. Oncogene 19: 1783–1793
39. Mehlen P, Kretz-Remy C, Preville X and Arrigo A-P (1996) Human hsp27, Drosophila hsp27 and human alphaB-crystallin expression-mediated increase in glutathione is essential for the protective activity of these proteins against TNFalpha-induced cell death. EMBO J. 15: 2695–2706
40. Mehlen P, Schulze-Osthoff K and Arrigo A-P (1996) Small stress proteins as novel regulators of apoptosis. Heat shock protein 27 blocks Fas/APO-1- and staurosporine-induced cell death. J. Biol. Chem. 271: 16510–16514
41. Golenhofen N, Htun P, Ness W, Koob R, Schaper W and Drenckhahn D (1999) Binding of the stress protein alpha B-crystallin to cardiac myofibrils correlates with the degree of myocardial damage during ischemia/reperfusion *in vivo*. J. Mol. Cell. Cardiol. 31: 569–580
42. Hoover HE, Thuerauf DJ, Martindale JJ and Glembotski CC (2000) Alpha B-crystallin gene induction and phosphorylation by MKK6-activated p38. A potential role for alpha B-crystallin as a target of the p38 branch of the cardiac stress response. J. Biol. Chem. 275: 23825–23833
43. Andley UP, Song Z, Wawrousek EF, Fleming TP and Bassnett S (2000) Differential protective activity of alpha A- and alphaB-crystallin in lens epithelial cells. J. Biol. Chem. 275: 36823–36831
44. Li DW-C, Xiang H, Mao Y-W, Wang J, Fass U, Zhang X-Y and Xu C (2001) Caspase-3 is actively involved in okadaic acid-induced lens epithelial cell apoptosis. Exp. Cell Res. 266: 279–291
45. Mao Y-W, Xiang H, Wang W, Korsmeyer SJ, Reddan J and Li DW-C (2001) Human bcl-2 gene attenuates the ability of rabbit lens epithelial cells against H_2O_2-induced apoptosis through down-regulation of the alpha B-crystallin gene. J. Biol. Chem. 278: 43435–43445
46. Kamradt MC, Chen F and Cryns VL (2001) The small heat shock protein alpha B-crystallin negatively regulates cytochrome *c*- and caspase-8-dependent activation of caspase-3 by inhibiting its autoproteolytic maturation. J. Biol. Chem. 276: 16059–16063
47. Bruey J, Ducasse MC, Bonniaud P, Ravagnan L, Susin SA, Diaz-Latoud C, Gurbuxani S, Arrigo AP, Kroemer G, Solary E and Garrido C (2000) Hsp27 negatively regulates cell death by interacting with cytochrome *c*. Nat. Cell Biol. 2: 645–652
48. Garrido C, Bruey JM, Fromentin A, Hammann A, Arrigo AP and Solary E (1999) HSP27 inhibits cytochrome *c*-dependent activation of procaspase-9. FASEB J. 13: 2061–2070
49. Pandey P, Farber R, Nakazawa A, Kumar S, Bharti A, Nalin C, Weichselbaum R, Kufe D and Kharbanda S (2000) Hsp27 functions as a negative regulator of cytochrome *c*-dependent activation of procaspase-3. Oncogene 19: 1975–1981
50. Tezel G and Wax MB (2000) The mechanisms of hsp27 antibody-mediated apoptosis in retina neuronal cells. J. Neurosci. 20: 3552–3562
51. Wagstaff MJ, Collaco-Moraes Y, Smith J, de Belleroche JS, Coffin RS and Latchman DS (1999) Protection of neuronal cells from apoptosis by Hsp27 delivered with a herpes simplex virus-based vector. J. Biol. Chem. 274: 5061–5069
52. Paul C, Manero F, Gonin S, Kretz-Remy C, Virot S and Arrigo AP (2002) Hsp27 as a negative regulator of cytochrome *c* release. Mol. Cell. Biol. 22: 816–834
53. Beere HM, Wolf BB, Cain K, Mosser DD, Mahboubi A, Kuwana T, Tailor P, Morimoto RI, Cohen GM and Green DR (2000) Heat-shock protein 70 inhibits apoptosis by preventing recruitment of procaspase-9 to the apaf-1 apoptosome. Nat. Cell Biol. 2: 469–475
54. Jäättelä M, Wissing D, Kokholm K, Kallunki T and Egeblad M (1998) Hsp70 exerts its anti-apoptotic function downstream of caspase-3-like proteases. EMBO J. 17: 6124–6134
55. Li C-Y, Lee J-S, Ko Y-G, Kim J-I and Seo J-S (2000) Heat shock protein 70 inhibits downstream of cytochrome *c* release and upstream of caspase-3 activation. J. Biol. Chem. 275: 25665–25671
56. Mosser DD, Caron AW, Bourget L, Denis-Larose C and Massie B (1997) Role of the human heat shock protein hsp70 in protection against stress-induced apoptosis. Mol. Cell. Biol. 17: 5317–5327
57. Takayama S, Bimston DN, Matsuzawa S, Freeman BC, Aime-Sempe C, Xie Z, Morimoto RI and Reed JC (1997) BAG-1 modulates the chaperone activity of Hsp70/Hsc70. EMBO J. 16: 4887–4896
58. Pandey P, Saleh A, Nakazawa A, Kumar S, Srinivasula SM, Kumar V, Weichselbaum R, Nalin C, Alnemri ES, Kufe D and Kharbanda S (2000) Negative regulation of cytochrome *c*-mediated oligomerization of Apaf-1 and activation of procaspase-9 by heat shock protein 90. EMBO J. 19: 4310–4322
59. Xanthoudakis S, Roy S, Rasper D, Hennessey T, Aubin Y, Cassady R, Tawa P, Ruel R, Rosen A and Nicholson DW (1999) Hsp60 accelerates the maturation of pro-caspase-3 by upstream activator proteases during apoptosis. EMBO J. 18: 2049–2056
60. Samali A, Cai J, Zhivotovsky B, Jones DP and Orrenius S (1999) Presence of a pre-apoptotic complex of pro-caspase-3, Hsp60 and Hsp10 in the mitochondrial fraction of jurkat cells. EMBO J. 18: 2040–2048
61. Ingolia TD and Craig EA (1982) Four small Drosophila heat shock proteins are related to each other and to mammalian alpha-crystallin. Proc. Natl. Acad Sci. USA 79: 2360–2364
62. Bloemendal H (1982) Lens proteins. CRC Crit. Rev. Biochem. 12: 1–38

63. Horwitz J (1992) -Crystallin can function as a molecular chaperone. Proc. Natl. Acad. Sci. USA 89: 10449–11045
64. Rao PV, Horwitz J and Zigler Jr JS (1993) Alpha-crystallin, a molecular chaperone, forms a stable complex with carbonic anhydrase upon heat denaturation. Biochem. Biophys. Res. Commun. 190: 786–793
65. Wang K and Spector A (1994) The chaperone activity of bovine alpha crystallin. Interaction with other lens crystallins in native and denatured states. J. Biol. Chem. 269: 13601–13608
66. Boyle D and Takemoto L (1994) Characterization of the alpha-gamma and alpha-beta complex: evidence for an *in vivo* functional role of alpha-crystallin as a molecular chaperone. Exp. Eye Res. 58: 9–15
67. Sun TX, Das BK and Liang JJ (1997) Conformational and functional differences between recombinant human lens alphaA- and alphaB-crystallin. J. Biol. Chem. 272: 6220–6225
68. Kantorow M and Piatigorsky J (1994) Alpha-crystallin/small heat shock protein has autokinase activity. Proc. Natl. Acad. Sci. USA 91: 3112–3116
69. Kantorow M, Horwitz J, van Boekel MA, de Jong WW and Piatigorsky J (1995) Conversion from oligomers to tetramers enhances autophosphorylation by lens alpha A-crystallin. Specificity between alpha A- and alpha B-crystallin subunits. J. Biol. Chem. 270: 17215–17220
70. Aoyama A, Frohli E, Schafer R and Klemenz R (1993) Alpha B-crystallin expression in mouse NIH 3T3 fibroblasts: glucocorticoid responsiveness and involvement in thermal protection. Mol. Cell. Biol. 13: 1824–1835
71. Dasgupta S, Hohman TC and Carper D (1992) Hypertonic stress induces alpha B-crystallin expression. Exp. Eye Res. 54: 461–470
72. Mehlen P, Preville X, Chareyron P, Briolay J, Klemenz R and Arrigo AP (1995) Constitutive expression of human hsp27, Drosophila hsp27, or human alpha B-crystallin confers resistance to TNF- and oxidative stress-induced cytotoxicity in stably transfected murine L929 fibroblasts. J. Immunol. 154: 363–374
73. Andley UP, Patel HC and Xi JH. (2002) The R116C mutation in alpha A-crystallin diminishes its protective ability against stress-induced lens epithelial cell apoptosis. J Biol Chem. 277: 10178–10186
74. Kamradt MC, Chen F, Sam S and Cryns VL. (2002) The small heat shock protein alpha B-crystallin negatively regulates apoptosis during myogenic differentiation by inhibiting caspase-3 activation. J Biol Chem. 277: 38731–38736
75. Dunn KC, Aotaki-Keen AE, Putkey FR and Hjelmeland LM (1996) ARPE-19, a human retina pigment epithelial cell line with differentiated properties. Exp. Eye Res. 62: 155–169
76. Kimes BW and Brandt BL (1976) Properties of a clonal muscle cell line from rat heart. Exp Cell Res 98: 367–381
77. Litt M, Kramer P, LaMorticella DM, Murphey W, Lovrien EW and Weleber RG (1998) Autosomal dominant congenital cataract associated with a missense mutation in the human alpha crystallin gene CRYAA. Hum. Mol. Genet. 7: 471–474
78. Vicart P, Caron A, Guicheney P, Li Z, Prevost MC, Faure A, Chateau D, Chapon F, Tome F, Dupret JM, Paulin D and Fardeau M (1998) A missense mutation in the alphaB-crystallin chaperone gene causes a desmin-related myopathy. Nat. Genet. 20: 92–95
79. Shroff NP, Cherian-Shaw M, Bera S and Abraham EC (2000) Mutation of R116C results in highly oligomerized alpha A-crystallin with modified structure and defective chaperone-like function. Biochemistry 39: 1420–1426
80. Bova MP, Yaron O, Huang Q, Ding L, Haley DA, Stewart PL and Horwitz J (1999) Mutation R120G in alphaB-crystallin, which is linked to a desmin-related myopathy, results in an irregular structure and defective chaperone-like function. Proc. Natl. Acad. Sci. USA 96: 6137–6142
81. Orrenius S, Zhivotovsky B and Nicotera P (2003) Regulation of cell death: the calcium-apoptosis link. Nat. Rev. Mol. Cell. Biol. 4: 552–565
82. Nagata S. (1997) Apoptosis by death factor. Cell 88: 355–365
83. Krueger A, Baumann S, Krammer PH and Kirchhoff S (2001) FLICE-inhibitory proteins: regulators of death receptor-mediated apoptosis. Mol. Cell. Biol. 21: 8247–8254
84. Yang J, Liu X, Bhalla K, Kim CN, Ibrado AM, Cai J, Peng TI, Jones DP and Wang X (1997) Prevention of apoptosis by Bcl-2: release of cytochrome *c* from mitochondria blocked. Science 275: 1129–1132
85. Kluck RM, Bossy-Wetzel E, Green DR and Newmeyer DD (1997) The release of cytochrome *c* from mitochondria: a primary site for Bcl-2 regulation of apoptosis. Science 275: 1132–1136
86. Green DR and Reed JC (1998) Mitochondria and apoptosis. Science 281: 1309–1312
87. Vander Heiden MG, Chandel NS, Williamson EK, Schumacker PT and Thompson CB (1997) Bcl-xL regulates the membrane potential and volume homeostasis of mitochondria. Cell 91: 627–637
88. Bossy-Wetzel E, Newmeyer DD and Green DR (1998) Mitochondrial cytochrome *c* release in apoptosis occurs upstream of DEVD-specific caspase activation and independently of mitochondrial transmembrane depolarization. EMBO J. 17: 37–49
89. Deshmukh M and Johnson Jr EM (2000) Staurosporine-induced neuronal death: multiple mechanisms and methodological implications. Cell Death Differ. 7: 250–261
90. Murphy KM, Ranganathan V, Farnsworth ML, Kavallaris M and Lock RB (2000) Bcl-2 inhibits Bax translocation from cytosol to mitochondria during drug-induced apoptosis of human tumor cells. Cell Death Differ. 7: 102–111
91. Kashkar H, Kronke M and Jurgensmeier JM (2002) Defective Bax activation in Hodgkin B-cell lines confers resistance to staurosporine-induced apoptosis. Cell Death Differ. 9: 750–757
92. Wei MC, Zong WX, Cheng EH, Lindsten T, Panoutsakopoulou V, Ross AJ, Roth KA, MacGregor GR, Thompson CB and Korsmeyer SJ (2001) Proapoptotic BAX and BAK: a requisite gateway to mitochondrial dysfunction and death. Science 292: 727–730
93. Cheng EH, Wei MC, Weiler S, Flavell RA, Mak TW, Lindsten T and Korsmeyer SJ (2001) BCL-2, BCL-X(L) sequester BH3 domain-only molecules preventing BAX- and BAK-mediated mitochondrial apoptosis. Mol. Cell 8: 705–711
94. Wang GQ, Gastman BR, Wieckowski E, Goldstein LA, Gambotto A, Kim TH, Fang B, Rabinovitz A, Yin XM and Rabinowich H (2001) A role for mitochondrial Bak in apoptotic response to anticancer drugs. J. Biol. Chem. 276: 34307–34317
95. Theodorakis P, Lomonosova E and Chinnadurai G (2002) Critical requirement of BAX for manifestation of apoptosis induced by multiple stimuli in human epithelial cancer cells. Cancer Res. 62: 3373–3376
96. Hague A, Diaz GD, Hicks DJ, Krajewski S, Reed JC and Paraskeva C (1997) Bcl-2 and Bak may play a pivotal role in sodium butyrate-induced apoptosis in colonic epithelial cells; however overexpression of bcl-2 does not protect against bak-mediated apoptosis. Int. J. Cancer 72: 898–905
97. Chen G, Sordillo EM, Ramey WG, Reidy J, Holt PR, Krajewski S, Reed JC, Blaser MJ and Moss SF (1997) Apoptosis in gastric epithelial cells is induced by *Helicobacter pylori* and accompanied by increased expression of BAK. Biochem. Biophys. Res. Commun. 239: 626–632
98. Ibaraki N, Chen SC, Lin LR, Okamoto H, Pipas JM and Reddy VN (1998) Human lens epithelial cell line. Exp. Eye Res. 67: 577–585
99. Li DW-C, Fass U, Huizar I and Spector A (1998) Okaidac acid-induced lens epithelial cell apoptosis requires inhibition of phosphatase-1 and is associated with induction of gene expression including p53 and bax. Eur. J. Biochem. 257: 351–361
100. Eskes R, Desagher S, Antonsson B and Martinou JC (2000) Bid induces the oligomerization and insertion of Bax into the outer mitochondrial membrane. Mol. Cell. Biol. 20: 929–935